

Surface Meteorology during Ocean Storms Field Program

by
Ronald W. Lindsay

Technical Report
APL-UW TR 8823
October 1988

DTIC
ELECTE
S **D**
APR 14 1989
H

Contract N00014-87-K-0004

DISTRIBUTION STATEMENT A
Approved for public release
Distribution Unlimited

ABSTRACT

A summary of the meteorological conditions in the Gulf of Alaska during the Ocean Storms experiment is presented along with a data set of the surface meteorological observations by ships of opportunity and National Data Buoy Center buoys. An optimal interpolation procedure is described and used with the surface observations to interpolate air pressure, wind speed and direction, air temperature, air-sea temperature difference, and dew point depression. Separate interpolations are made using the National Meteorological Center 2.5° grids and digitized versions of hand analyses made during the experiment. Extensive comparisons are made between these three data sets and the observations at three NDBC buoys. These are used to assess the accuracy of the interpolated fields and to suggest optimal ways to use them to compute surface winds, temperatures, and fluxes. The hand analyzed synoptic charts of the surface meteorology are included. The air stress and sensible heat flux are presented for the position of the Ocean Storms moorings. A data tape containing all the observations, interpolations, and fields is described.



Accession For	
NTIS GRA&I	<input checked="" type="checkbox"/>
DTIC TAB	<input type="checkbox"/>
Unannounced	<input type="checkbox"/>
Justification	
By <i>per letter</i>	
Distribution/	
Availability Codes	
Dist	Avail and/or Special
<i>A-1</i>	

CONTENTS

	<i>Page</i>
I. INTRODUCTION.....	1
II. SYNOPTIC SUMMARY.....	3
III. THE COMPILED MARINE OBSERVATIONS DATA SET	22
IV. OPTIMAL INTERPOLATION	25
V. METLIB FIELDS	27
VI. CORRELATIONS BETWEEN THE INTERPOLATED AND THE MEASURED FIELDS AT THE DATA BUOYS.....	29
VII. SPACE AND TIME RESOLUTION	39
VIII. AIR STRESS AND HEAT FLUX ANALYSIS	42
IX. SAMPLE DATA	44
X. RECOMMENDATIONS	48
REFERENCES	49
Appendix A. SYNOPTIC MAPS	A1
Appendix B. SURFACE METEOROLOGY DATA TAPE	B1

LIST OF FIGURES

	<i>Page</i>
Figure 1. The Ocean Storms region in the Northeast Pacific with buoys, moorings, and Metlib area marked	2
Figure 2. Mean sea level pressure maps for August 1987 through March 1988.	4
Figure 3. Storm tracks.....	6
Figure 4. Comparison of monthly averages during Ocean Storms with climatology	10
Figure 5. Time series of wind speed and direction, air pressure, and air and sea temperatures	17
Figure 6. Bar graph of the total number of observations at each hour of day in the Ocean Storms marine observations data set	24
Figure 7. Scattergram of the measured wind speed at all three data buoys vs the interpolated wind speed from the NMC wind component fields...	34
Figure 8. Scattergram of the measured wind speed at all three data buoys vs the geostrophic wind from the NMC sea level pressure fields.....	36
Figure 9. Power spectra and coherence for the measured wind speed and the interpolated wind speed from observations at three buoys.....	40
Figure 10. Power spectra and coherence for the measured wind speed and the interpolated geostrophic wind speed at the three buoys	41
Figure 11. Time series of the estimates of the wind speed and direction, air pressure, and temperature for the central Ocean Storms mooring	45
Figure 12. Time series of estimates of the stress and the sensible heat flux at the center of the Ocean Storms moored array.....	46
Figure 13. Time series of the sum of the air stress and the sensible heat flux.....	47

LIST OF TABLES

	<i>Page</i>
Table I. Data buoys in the Ocean Storms data set.....	23
Table II. Correlations of 6 hour averaged measured wind speed with interpolations for Buoy 46004	30
Table III. Interpolations from observations.....	31
Table IV. Interpolations from NMC grids.....	32
Table V. Interpolations from Metlib grids.....	38
Table B-1. Variables and format of the marine observations data set.....	B3
Table B-2. Sample of marine observations file	B3
Table B-3. Variables in the interpolated data files	B4
Table B-4. Sample of the interpolated data files	B4

I. INTRODUCTION

The Ocean Storms experiment took place in the Gulf of Alaska in the fall and winter of 1987. The purpose of the experiment was to investigate the effect of severe storms on the ocean as well as the structure and evolution of storms as they approach the coast (D'Asaro, 1985). Ocean Storms involved investigators from several universities, government laboratories, the National Weather Service, and the Canadian Atmospheric Environment Service. Figure 1 shows the locations of the Ocean Storms fixed moorings and of the National Data Buoy Center (NDBC) weather buoys in the area.

This report summarizes the surface weather conditions during the experiment and presents four data sets: (1) a compiled data set of marine observations from ships and buoys in the North Pacific, (2) interpolated values of meteorological variables for the positions of the Ocean Storms moorings and drifting buoys from the compiled surface observations, (3) interpolated values of meteorological variables from the National Meteorological Center (NMC) 2.5° grid data, and (4) grid fields based on hand analyses of synoptic charts done at the Ocean Storms Forecast Office (here called Metlib fields). Extensive comparisons are made between the interpolated values and measurements at the NDBC buoys. We show that the wind speeds from the NMC grids, after linear corrections are applied, are slightly better than those based on observations and similar in quality to those based on the Metlib fields.

Finally, a formulation for calculating the air stress is outlined and air stress calculations are presented for the site of the Ocean Storms moorings.

Recommendations concerning the use of the data are given in the concluding section.

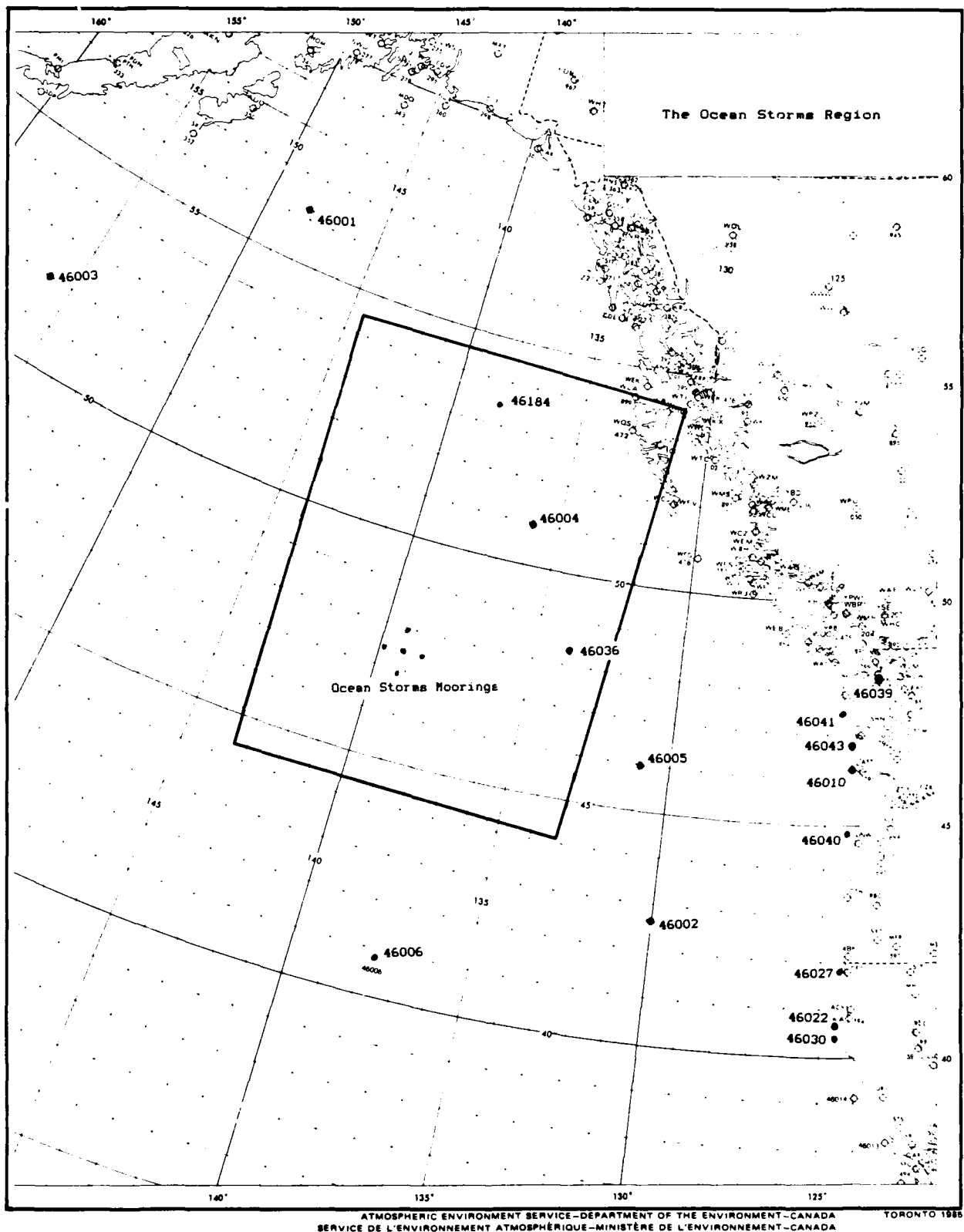


Figure 1. The Ocean Storms region in the Northeast Pacific. The positions of the NDBC buoys and the location of the Ocean Storms moorings are marked. The rectangle is the area covered by the Metlib fields.

II. SYNOPTIC SUMMARY

The weather in the North Pacific during the Ocean Storms experiment is summarized in the following brief excerpts from the Mariner's Weather Log (MWL, 1988a-c). Mean sea level pressure maps for each month are shown in Figure 2, and storm tracks for each month are shown in Figure 3.

September, 1987. The subtropical high dominated the North Pacific as usual, however its influence extended more towards Japan and the result was a +7 mb anomaly centered near 45°N, 175°E. There were negative anomalies in the Gulf of Alaska and eastern Bering Sea, reflecting a higher than normal number of Lows in these waters. South of 30°N and west of 170°E negative anomalies in the -4 to -5 mb range were apparent. In the steering level (700 mb) there was a trough over China and Korea and another extending southward from Alaska. This resulted in storms moving in general west to east with a tendency to curve northeastward toward the Gulf of Alaska east of 160°W. . . [One significant storm passed near the Ocean Storms site on the 13th.]

October, 1987. The Aleutian Low was a little stronger than average and west of its normal position in the Gulf of Alaska. The subtropical high was also more intense and its influence extended more to the northeast and west than it usually does. This resulted in a concentration of storm activity in the Bering Sea and the western Gulf of Alaska. This is supported by the 700 mb upper level steering currents, which were zonal from Asia to about 160°W where they curved northeastward. . . [and missed the Ocean Storms site. Note the small high pressure cell nearly centered on the Ocean Storms operating region in the October mean pressure map, Figure 3b. This is indicative of the light winds experienced there during the month.]

November, 1987. When the Aleutian Low and the subtropical high are more intense, or deeper, than normal, the pressure gradient between them becomes tighter and this usually results in a rough weather month. November was just such a month. The Aleutian Low was 5 to 9 mb deeper than normal while the subtropical high showed +3 to +5 mb anomalies. An additional squeeze was put on by the Arctic High, which was 8 to 9 mb deeper than average. Throw in a super typhoon and you have a not-so-Pacific Ocean. The steering currents at 700 mb were zonal from Asia to 150°W, where they bent or curved cyclonically northeastward. . . [Most systems stayed well to the northwest of Ocean Storms.]

December, 1987. This month usually features an extensive double-centered Aleutian Low with a relatively small subtropical high between Baja California and Hawaii. This year the Aleutian Low was more intense than normal with anomalies of up to -12 mb in the Bering Sea and -2 to -4 mb in the northern Gulf of Alaska. To the south high pressure extended into the western Pacific resulting in anomalies up to +8 mb. The steering currents at the 700 mb level were in general oriented from the west southwest to the east northeast. . . [More systems passed over the Ocean Storms area than earlier in the season.]

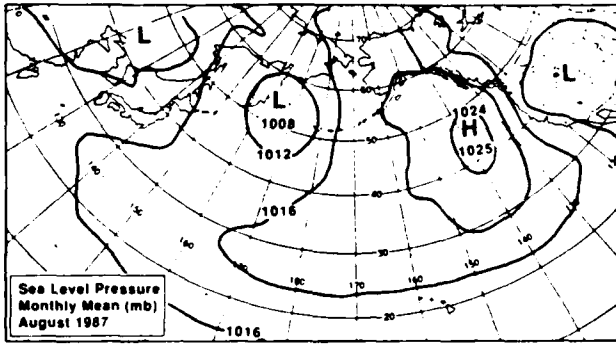


Figure 4 — The subtropical High dominates the eastern North Pacific

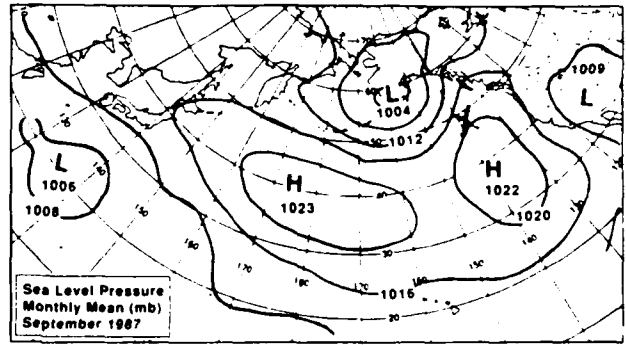


Figure 9 — The Aleutian Low makes its presence felt

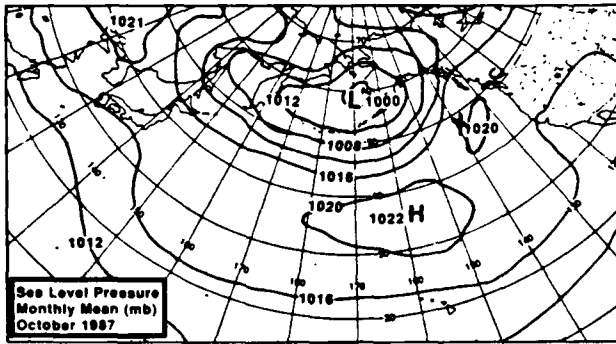


Figure 1 — October was a little more intense than normal

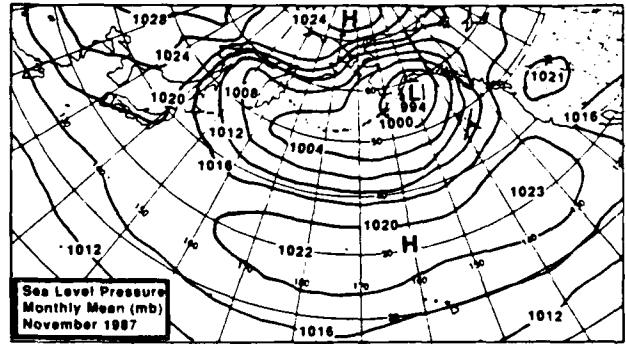


Figure 4 — All the climatic features were intensified this month

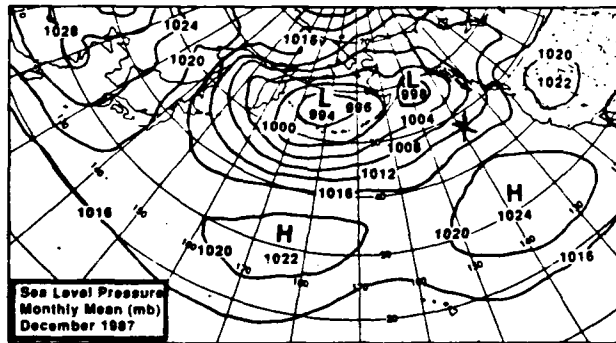


Figure 7 — This month features an intense Aleutian Low

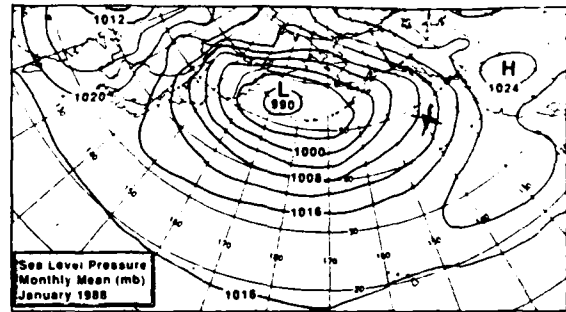


Figure 1 — An intense Aleutian Low dominates the North Pacific

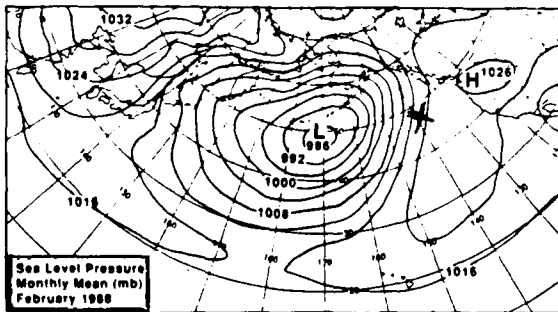


Figure 6 — An Aleutian Low that's bigger than life

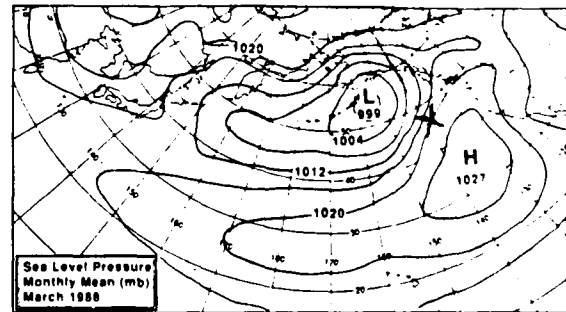


Figure 9 — Both the Aleutian Low and the subtropical high were more intense than normal

Figure 2. Mean sea level pressure maps for August 1987 through March 1988 (MWL 1988a-c). The Ocean Storms site is marked with an X.

January, 1988. The North Pacific's reflection of the winter storms, the Aleutian Low, was positioned nearly normal, but was more intense, by up to 13 mb, than usual. It can be reasonably expected that extratropical storm activity was plentiful and a look at the storm tracks for January confirms this. Steering currents at the 700 mb level were nearly zonal west of 170°E but curved cyclonically toward the northeast to the east. This means, ideally, that a storm over Tokyo would eventually cross Vancouver Island. . . [and cross the Ocean Storms site in the process. It was a stormy month at 47°N, 139°W.]

February, 1988. While the Aleutian Low dominates the February climate charts, this year it pressed the fact home with anomalies that ranged up to -17 mb near 50°N, 170°W. This was easily the most impressive feature. However, the subtropical high pushed farther to the northeast than normal and, more intense than usual, created a +8 mb anomaly in the Pacific Northwest. The steering currents at 700 mb were nearly zonal from Japan to the Dateline and then curved cyclonically northeastward over the eastern Pacific and Gulf of Alaska. This means, ideally, that a storm over Tokyo would wind up in Southeast Alaska. . . [and not over Ocean Storms. Few storms passed our area of interest.]

March, 1988. The Aleutian Low was deeper than normal and its center was displaced eastward to the Alaska Peninsula resulting in negative anomalies up to -10 mb in the Gulf of Alaska. The subtropical high was deeper and more extensive than normal resulting in a +7 mb anomaly off the coast of Washington and British Columbia and 2 to 3 mb in the central Pacific waters south of 30°N. The steering currents at the 700 mb heights were nearly zonal between 30°N and 45°N except east of 160°W where they curved sharply toward the northeastward toward the Gulf of Alaska and northwestern U. S. coast. Under ideal conditions a storm off Tokyo might end up over Vancouver Island. . . [and cross the Ocean Storms moorings. The winds pick up a little over February.]

Figure 4 compares the monthly mean and the climatological mean for various meteorological parameters at three NDBC data buoys. Included are the monthly mean wind speeds, air pressures, air temperatures, water temperatures, and wave heights. The circles denote the monthly means during the experimental period, and the squares the monthly means from climatology (NDBC, 1986); the solid lines show the standard deviations for the months during Ocean Storms, and the dashed lines the standard deviations from climatology. In general, the standard deviations for a single month are less than those from climatology because year-to-year variations are not included. The buoy closest to the Ocean Storms moorings, 46004, showed winds lower than from climatology for every month from September to April, with the wind averaging almost 3 m/s less in the month of October. Buoy 46005, farther south, was similar to 46004; Buoy 46001, to the northwest, showed wind speeds near the climatological mean. The anomalies in the pressure cited in the Mariner's Weather Log summaries are apparent in the values for air pressure. For example, in October when the subtropical high was more to the

Principal Tracks of Centers of Cyclones at Sea Level, North Pacific

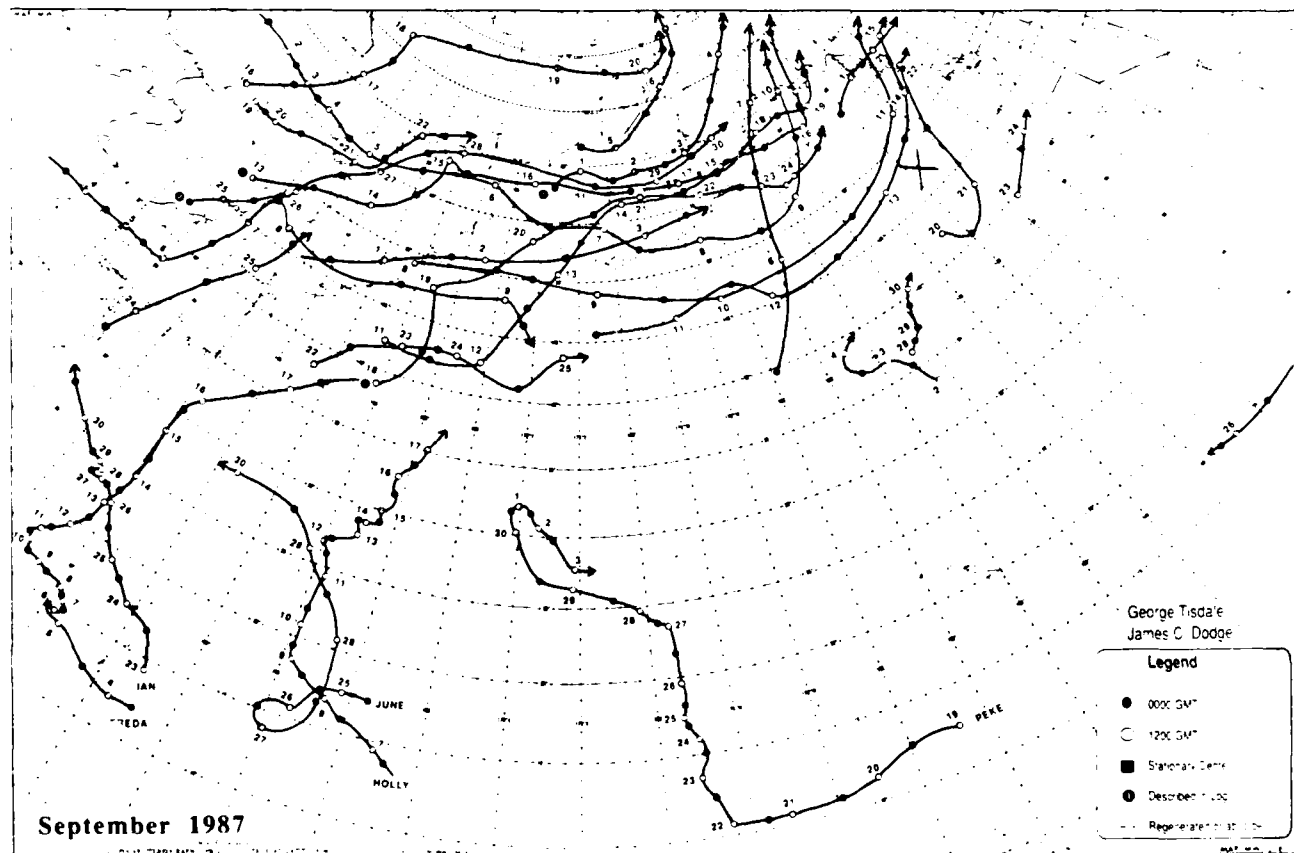
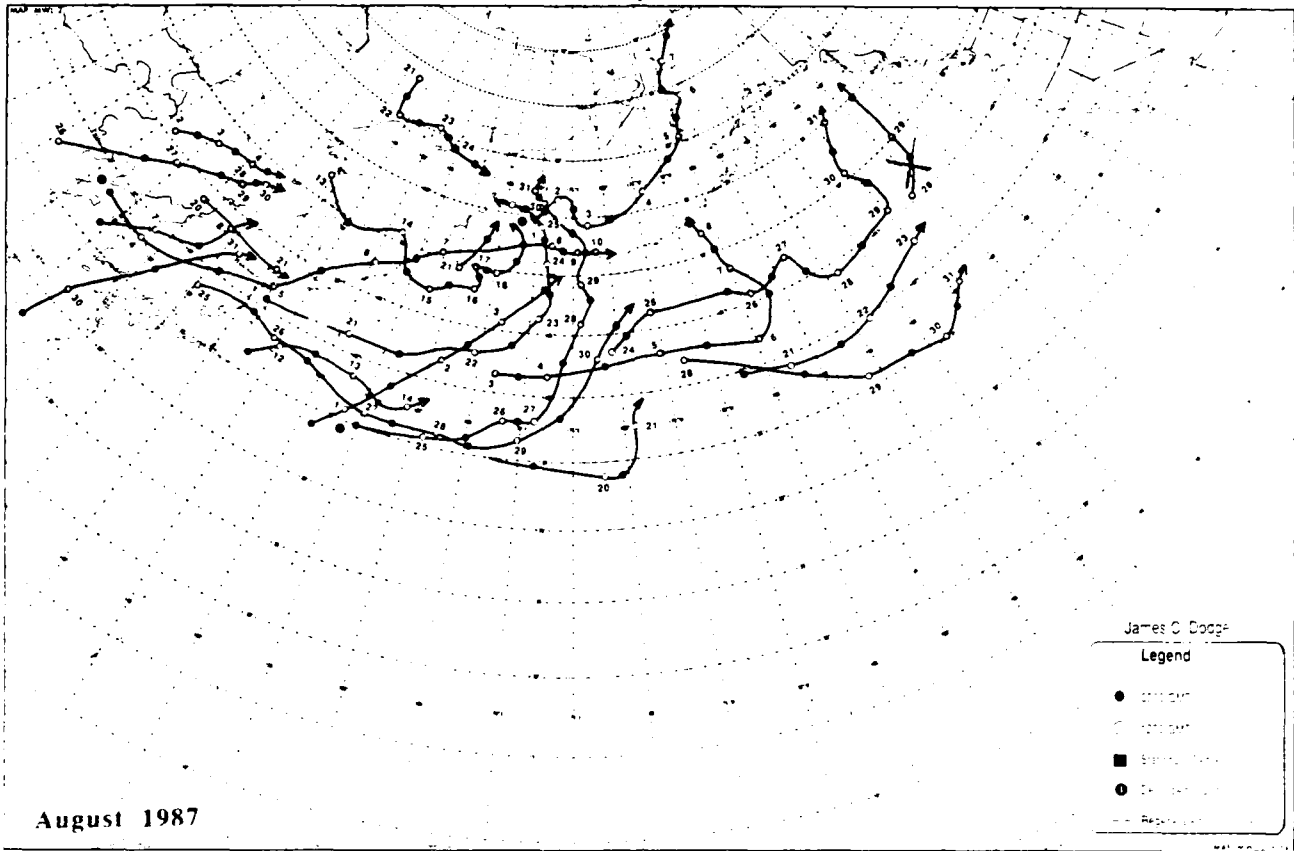


Figure 3a

Figure 3. Storm tracks (MWL 1988a-c); Ocean Storms site marked with an X.

Principal Tracks of Cyclone Centers at Sea Level, North Pacific

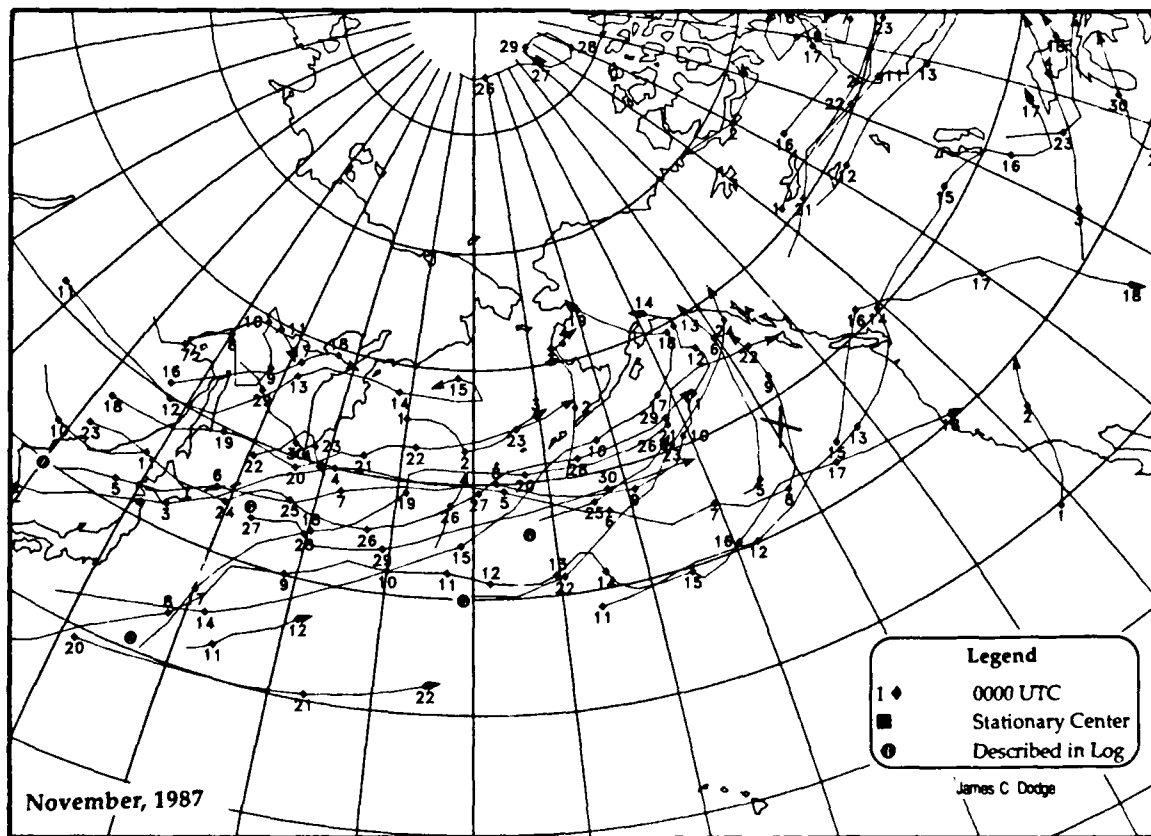
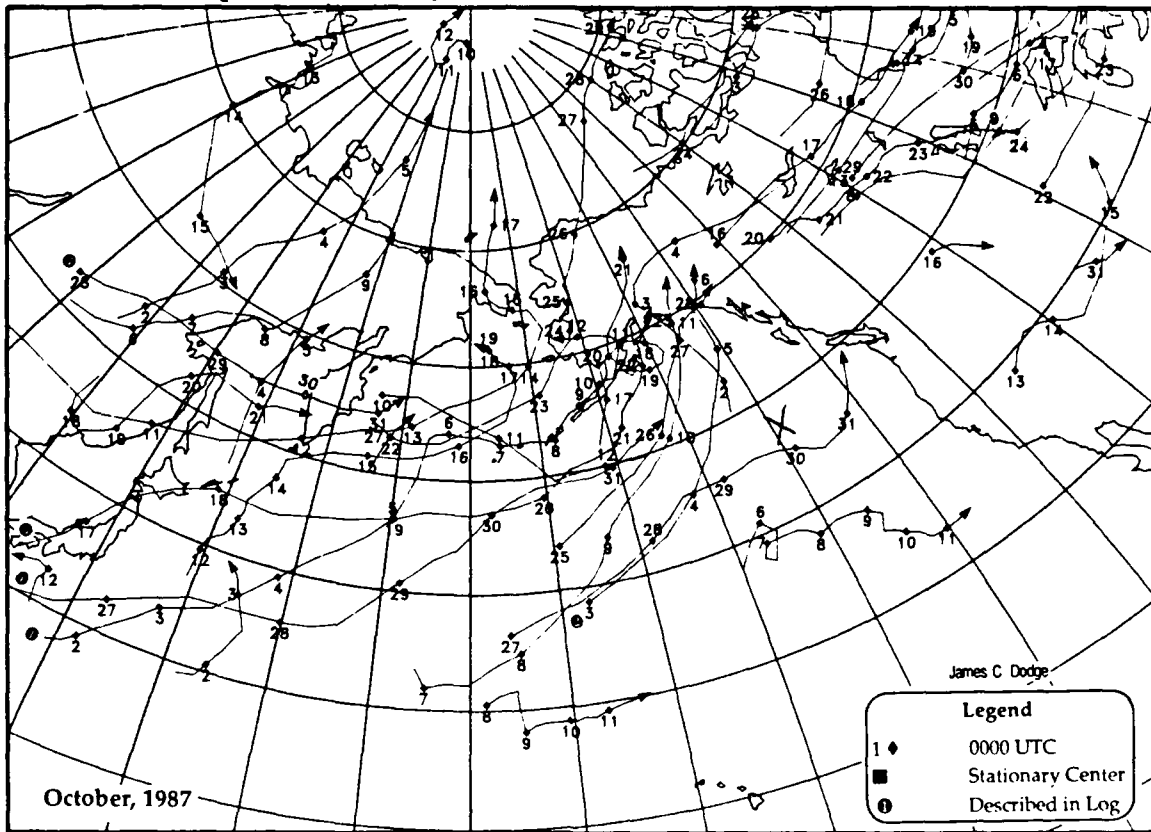


Figure 3b

Principal Tracks of Cyclone Centers at Sea Level, North Pacific

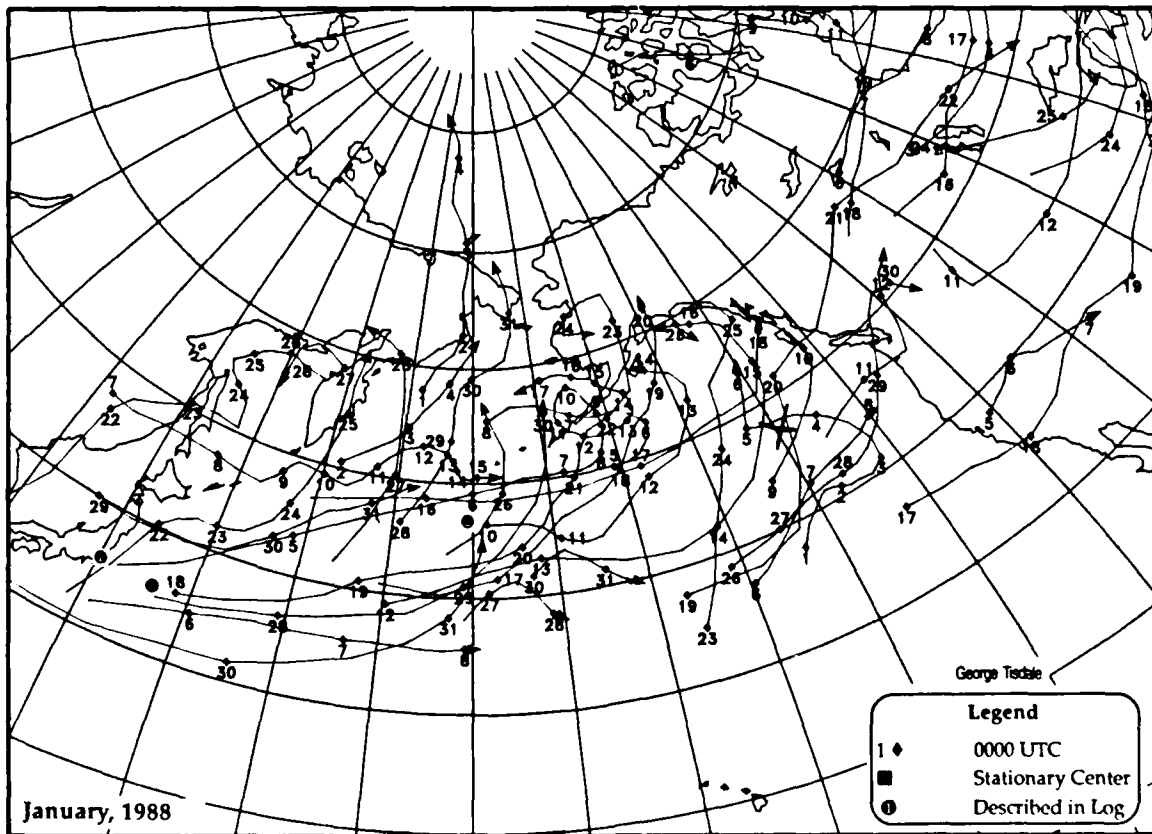
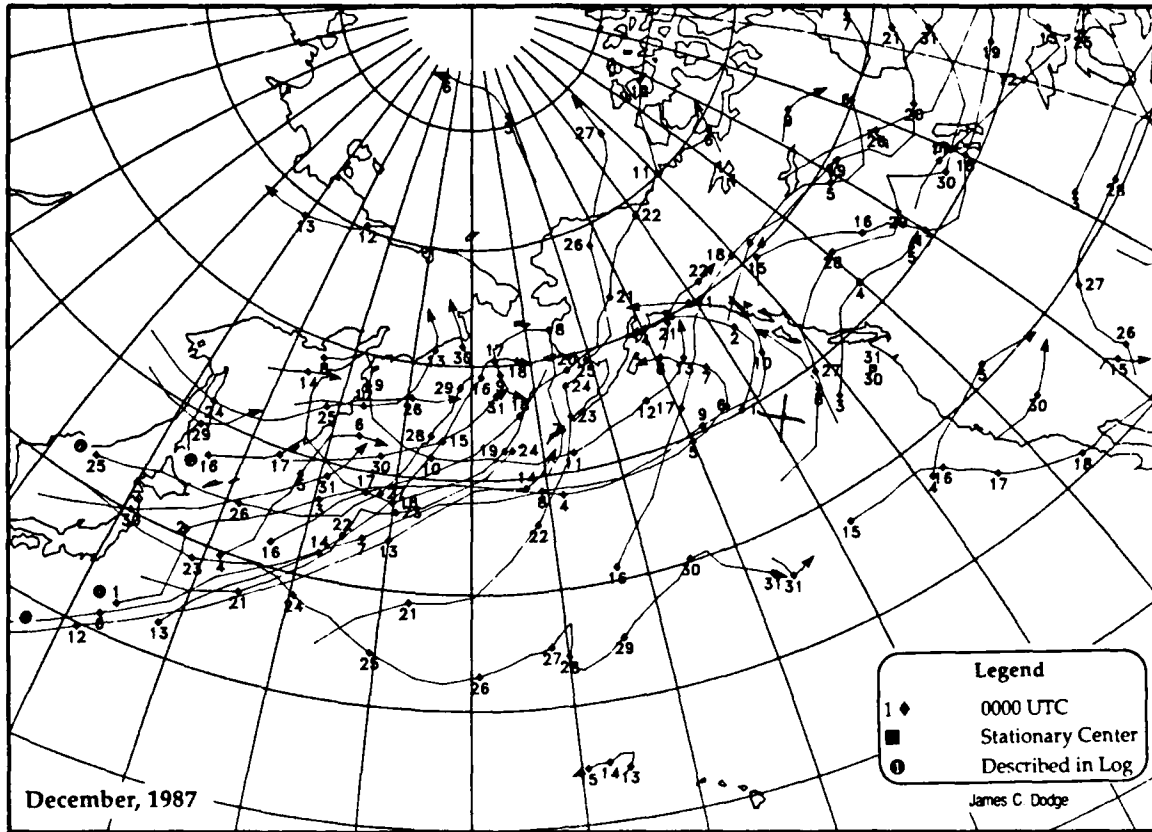


Figure 3c

Principal Tracks of Cyclone Centers at Sea Level, North Pacific

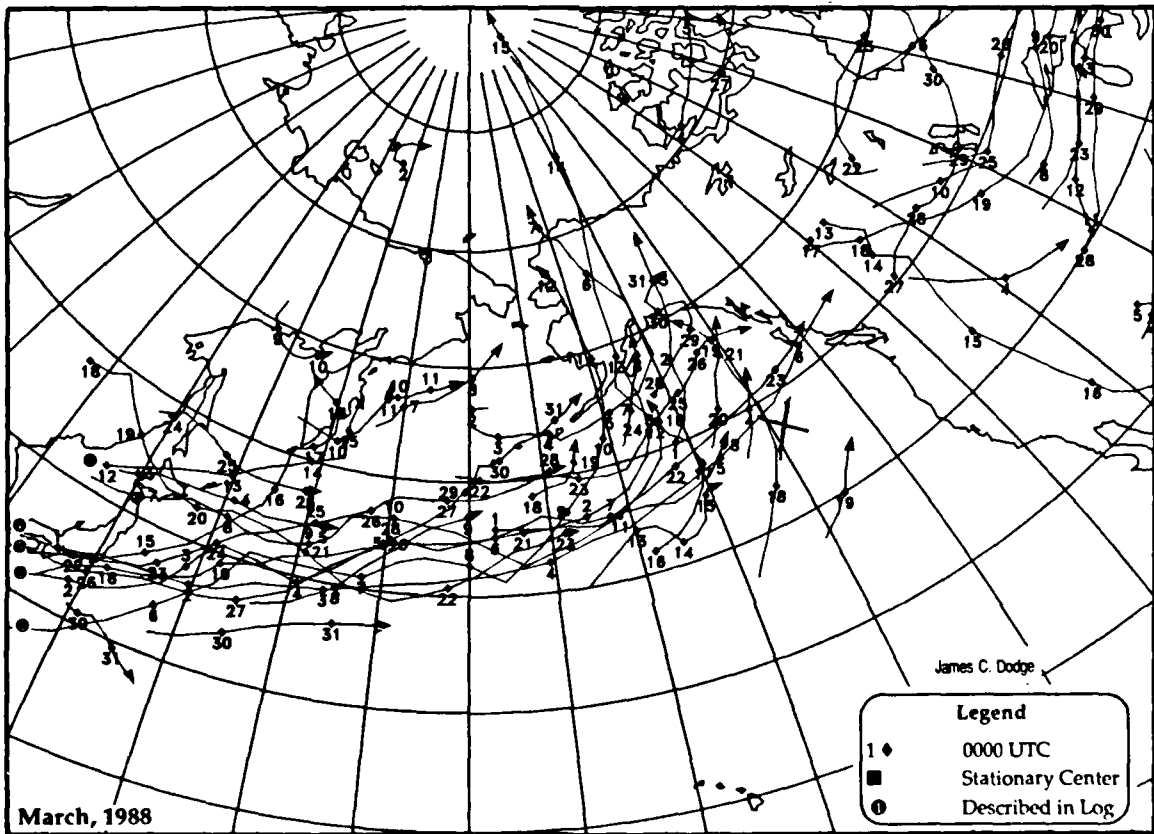
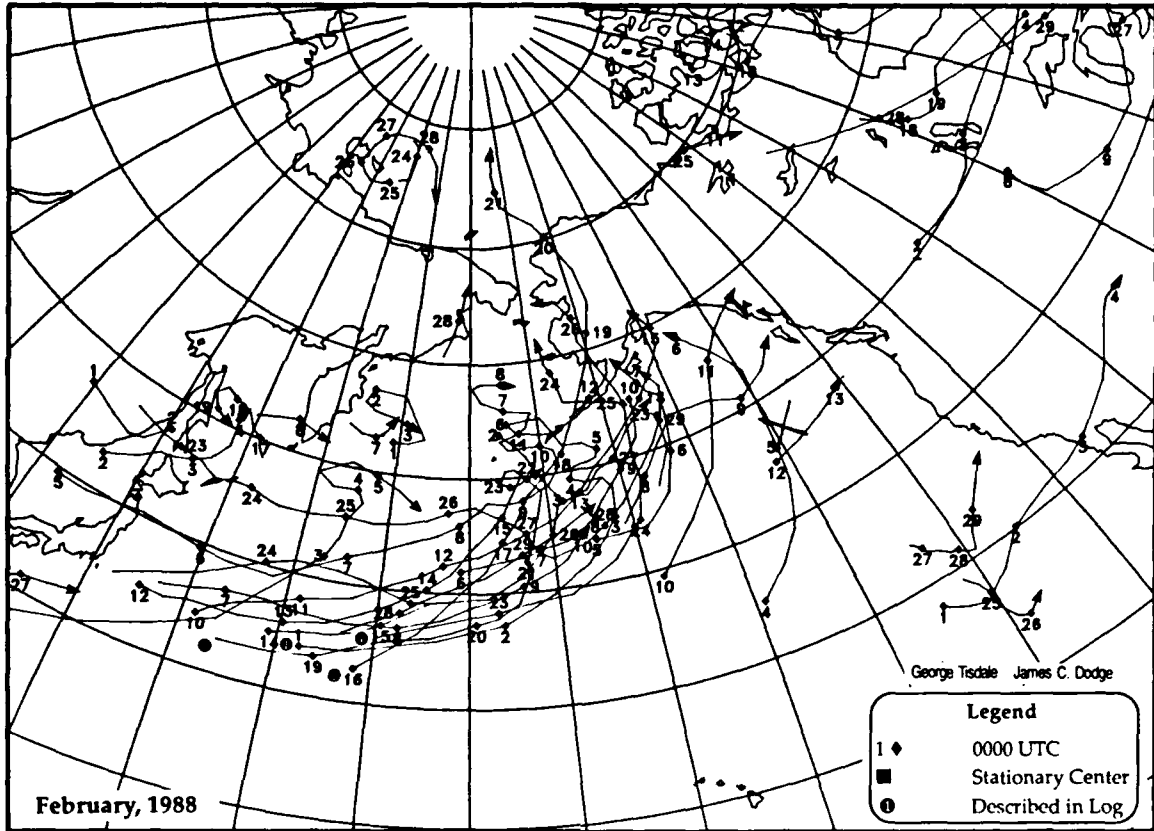


Figure 3d

WIND SPEED

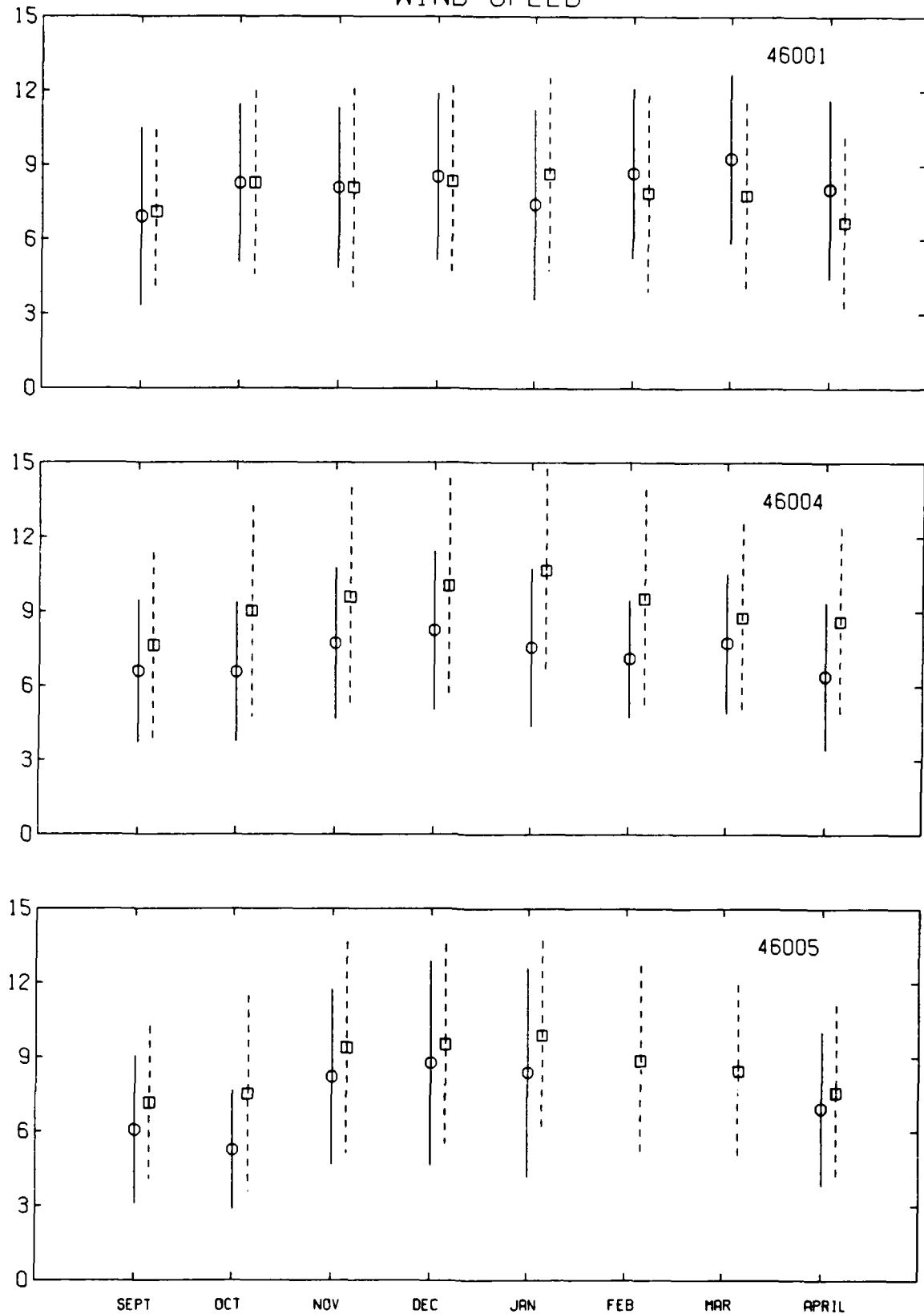


Figure 4a

Figure 4. Comparison of monthly averages during Ocean Storms with climatology. The monthly mean during Ocean Storms is shown with a circle, and the standard deviation with a solid line; the climatological mean is shown with a square, and the standard deviation with a dashed line (NDBC, 1986).

PRESSURE

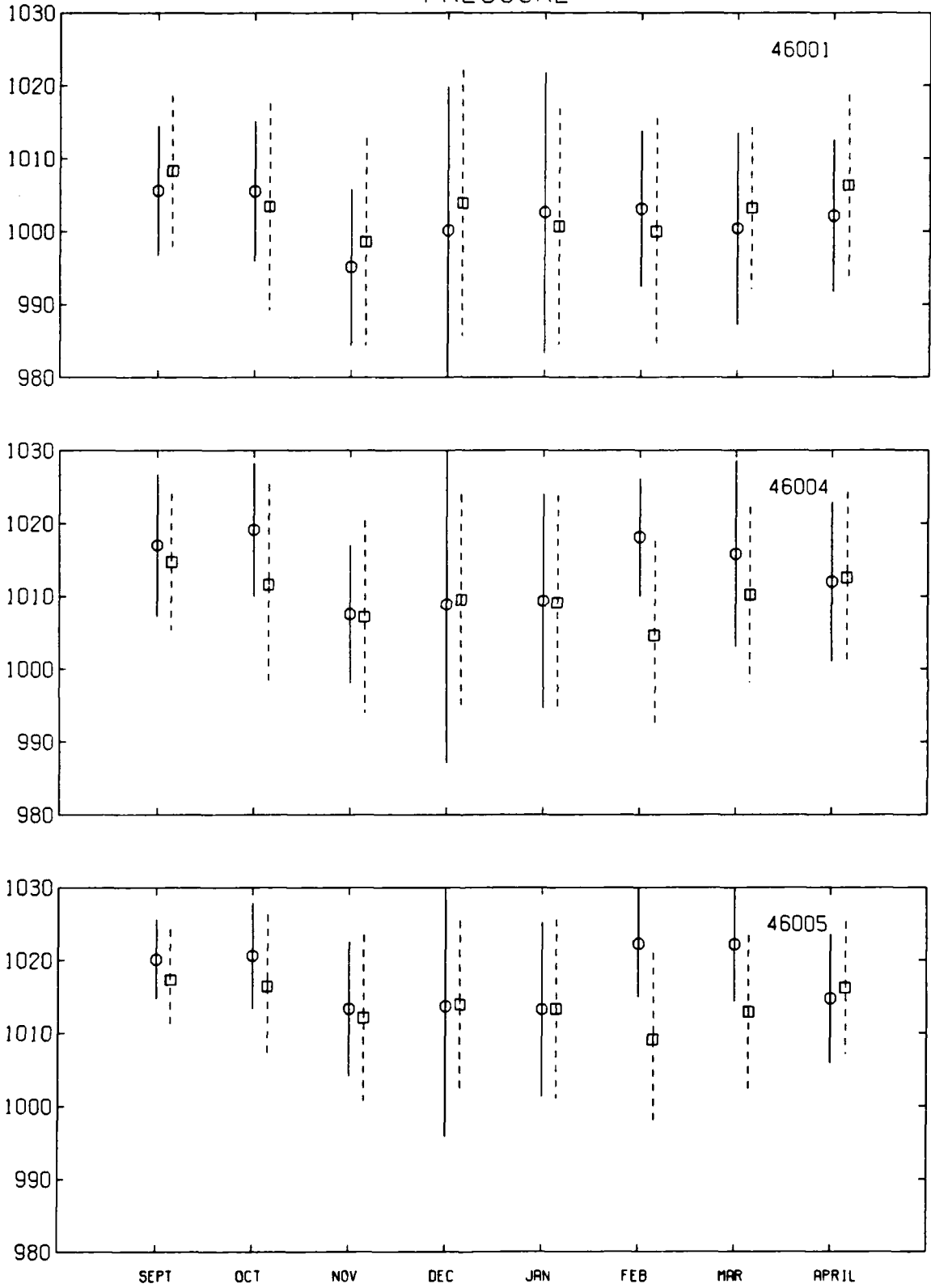


Figure 4b

AIR TEMPERATURE

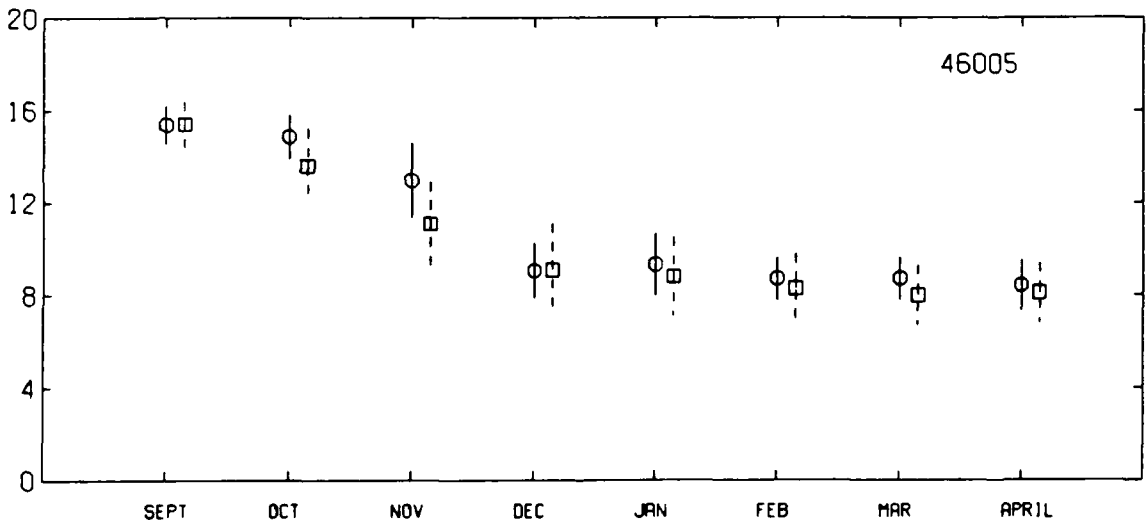
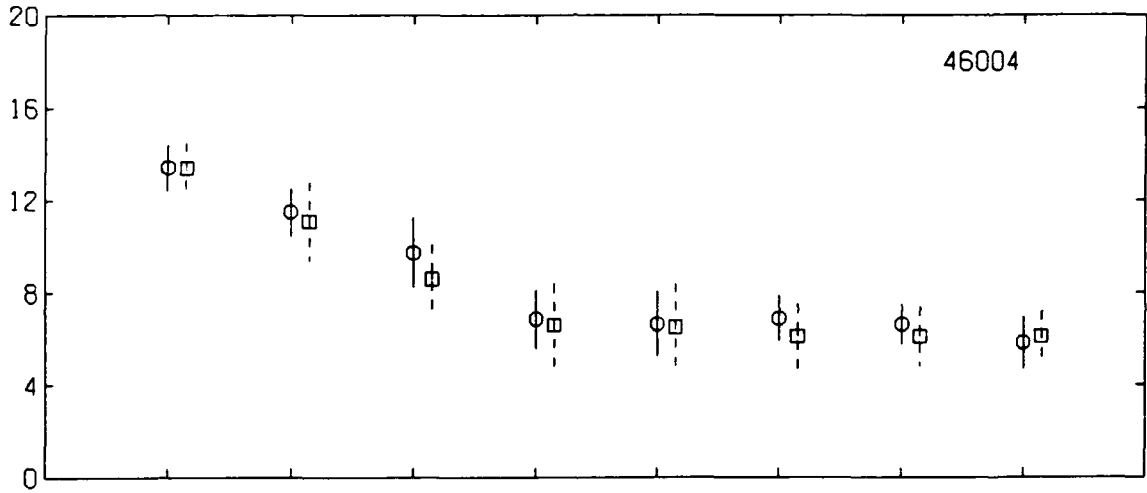
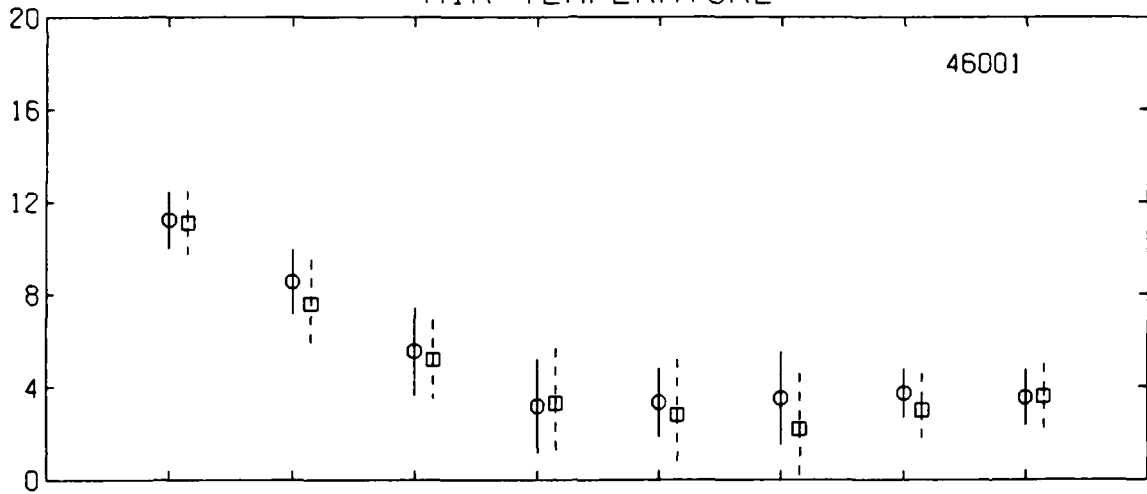


Figure 4c

SEA TEMPERATURE

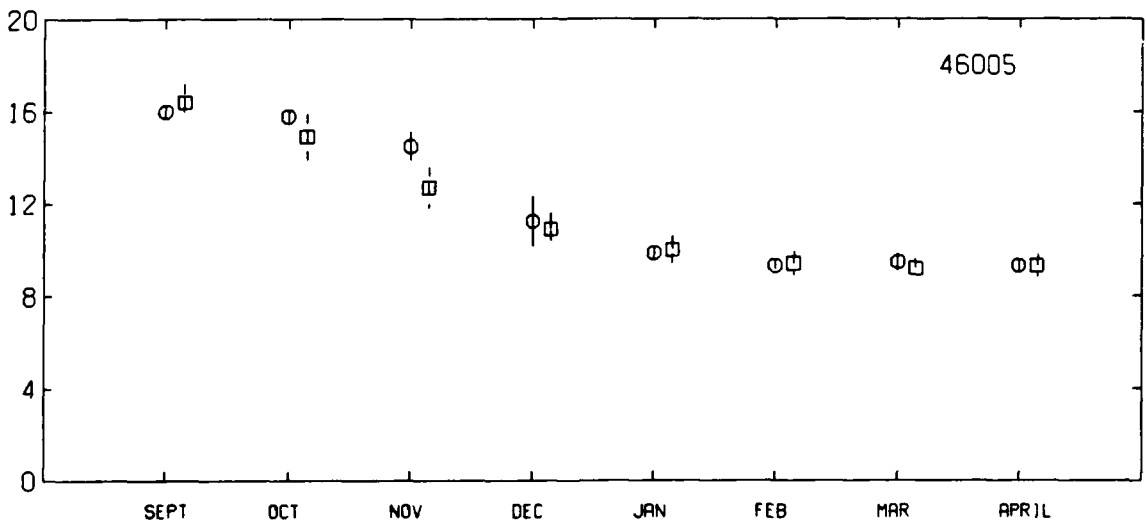
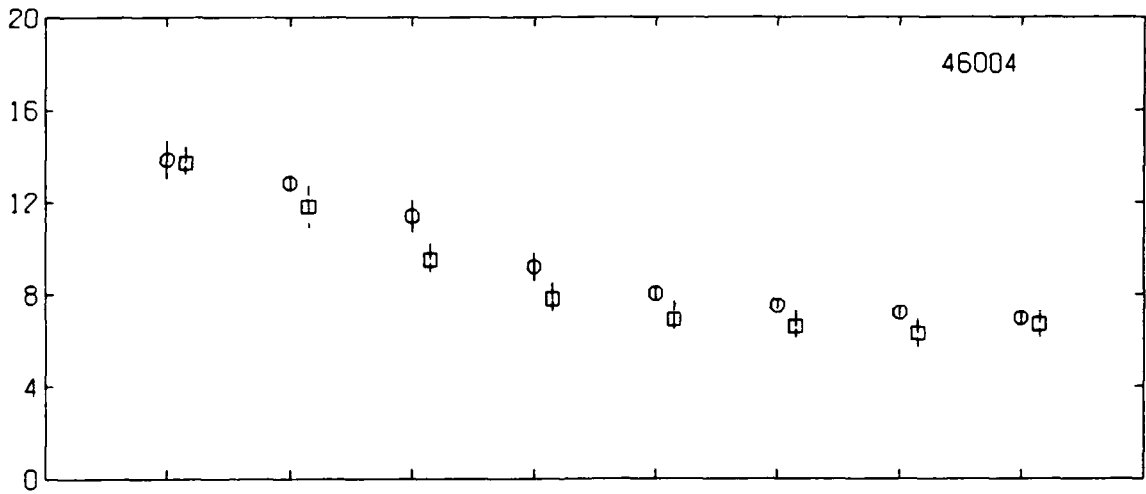
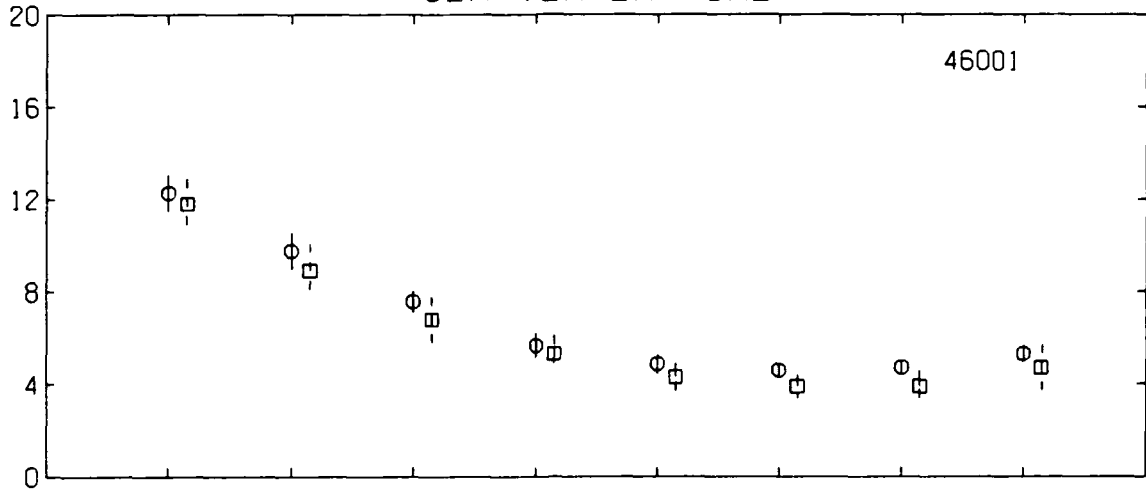


Figure 4d

AIR-SEA TEMPERATURE

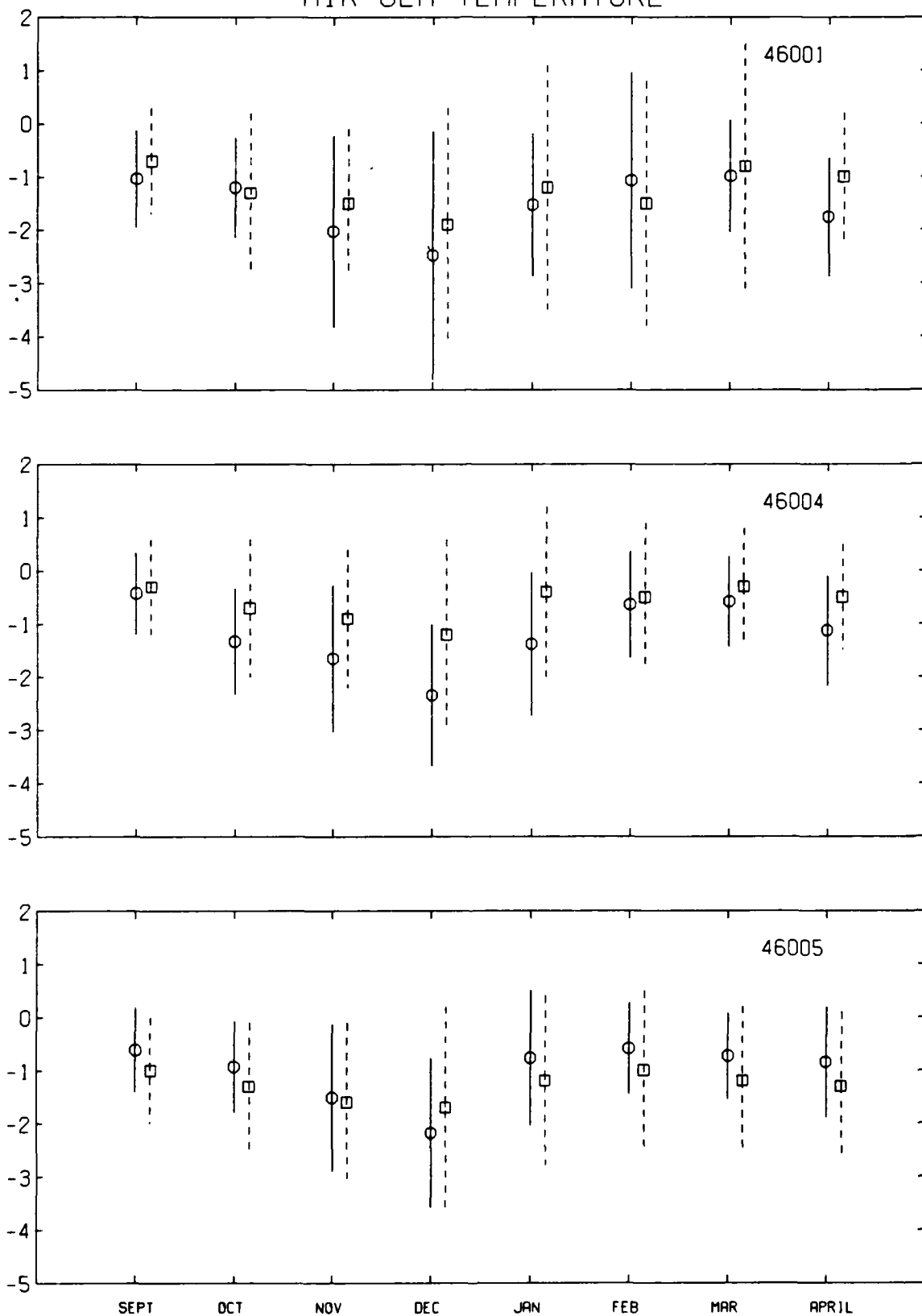


Figure 4e

WAVE HEIGHT

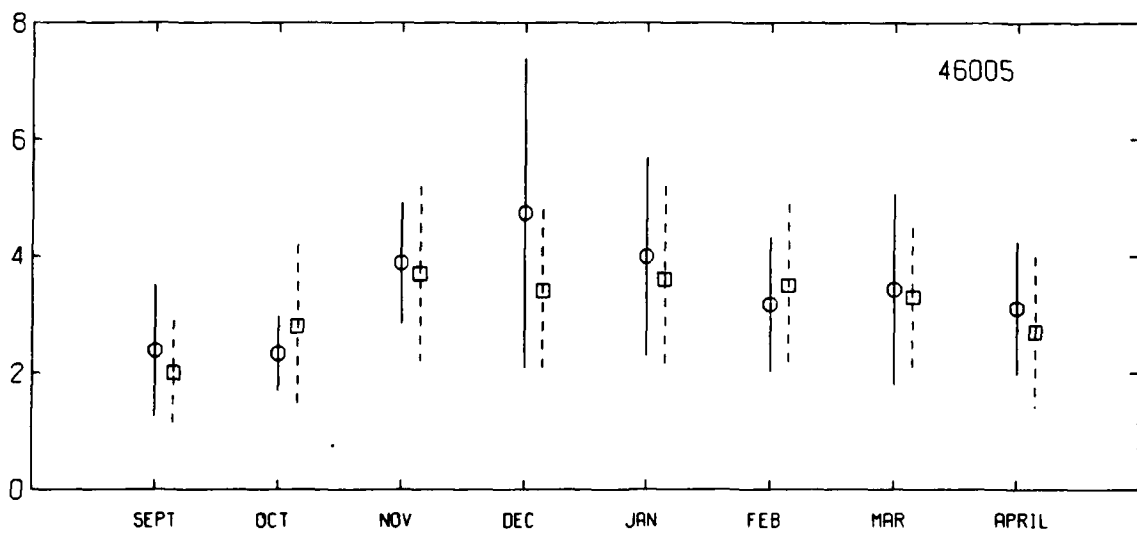
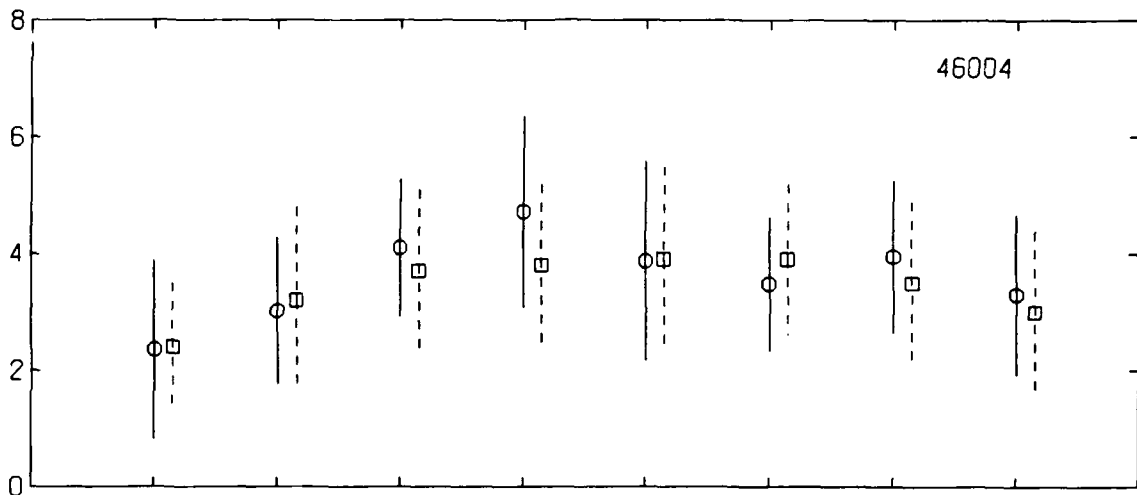
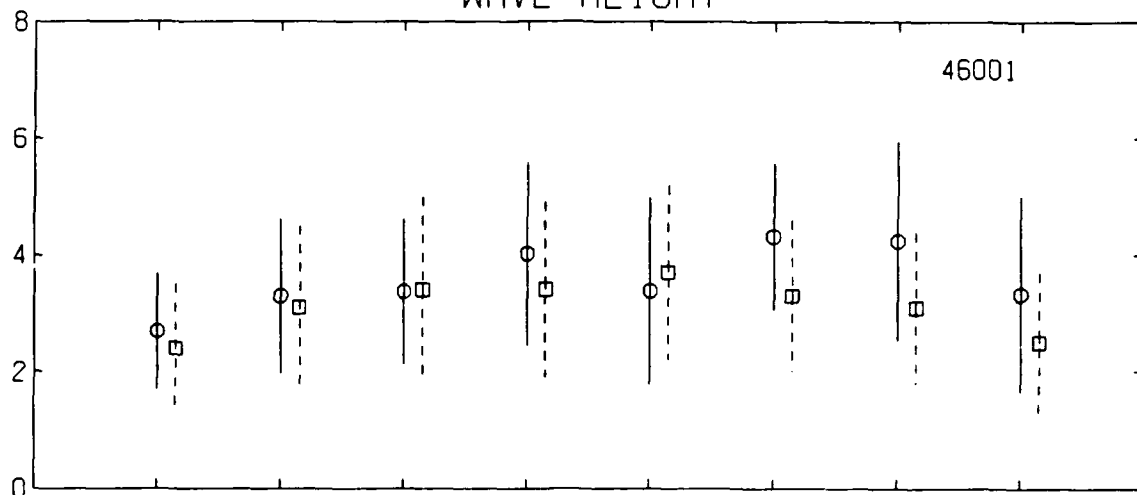


Figure 4f

northeast than usual, 46004, the middle buoy, showed an anomaly of +7.5 mb; in November, when the Aleutian Low showed a -5 to -9 mb anomaly, 46001 showed a -3.5 mb anomaly on its eastern edge.

Time series plots of the wind, pressure, and air and sea temperature are presented in Figure 5 for Buoy 46004 (400 km northeast of the Ocean Storms moored array) for the months of August 1987 through April 1988. We have hourly reports for most of the fall and reports at 3 hour intervals for the remainder of the period. Both air and sea temperatures are plotted in the bottom panel: circles for air, triangles for sea. Note the sharp drop in water temperature on 14 September, associated with an early fall storm with winds up to 18.0 m/s. Such strong winds were not recorded again at this buoy during our entire period of record, and there was no other similar drop in water temperature. In October and November the winds did not exceed 14 m/s, but in early December there were significant wind events on the 1st and the 5th, with winds to 17 m/s.

The synoptic maps in Appendix A were made at the Ocean Storms Forecast Office. Located at the Seattle Weather Service Office at Sand Point, this office was staffed by forecasters from the Atmospheric Environment Service's Pacific Weather Centre in Vancouver, Canada, and from the Seattle Weather Service Office. They made hand analyses of the synoptic charts every 6 hours and provided specialized forecasts for the aircraft operations. Included here are copies of a portion of the 0600 and 1800 GMT maps for the period 20 October to 9 December 1987. These charts are working copies used for forecasting; they were not redone for publication. The originals are currently stored at the Seattle WSO.

BUOY 46004

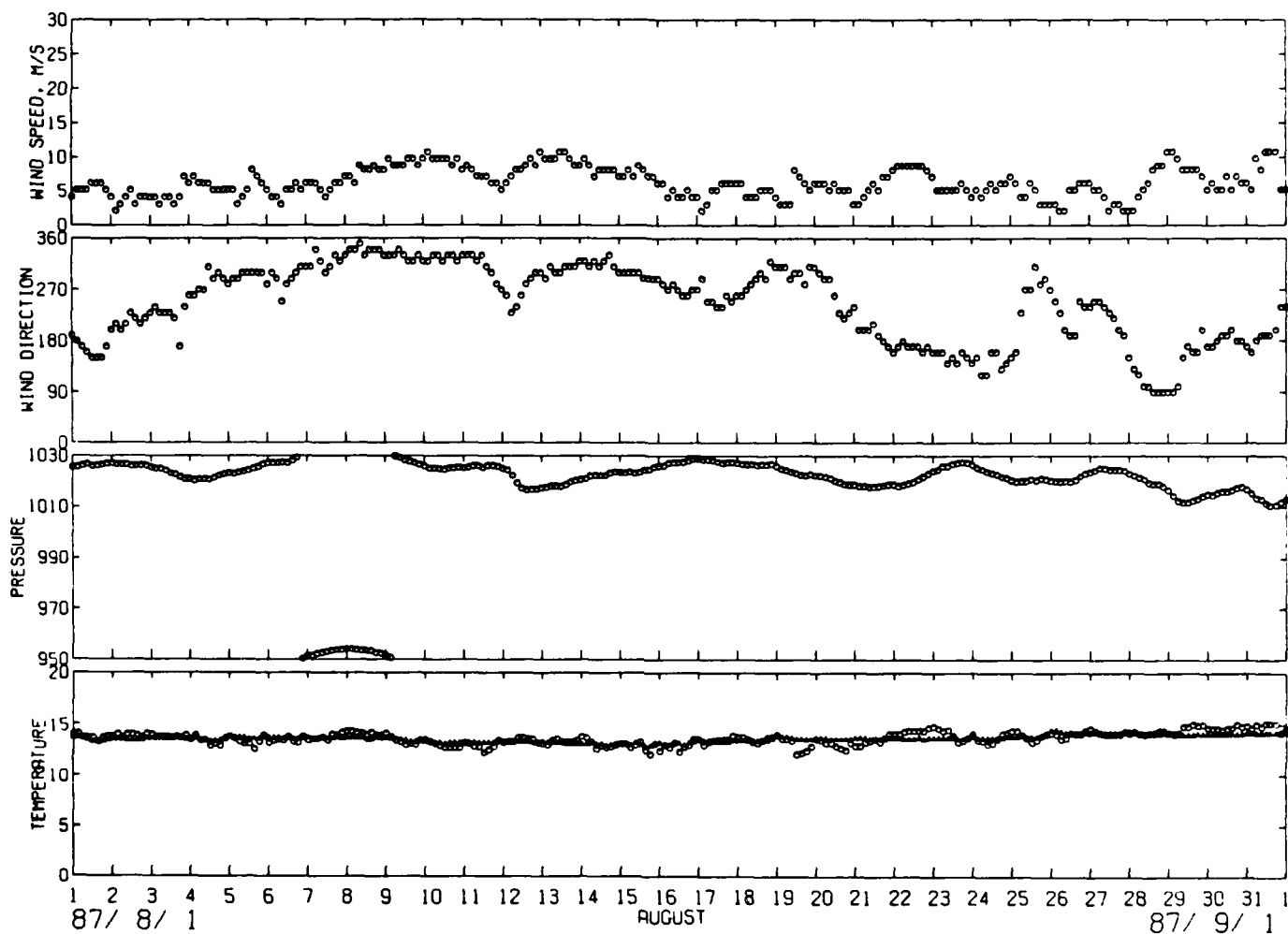
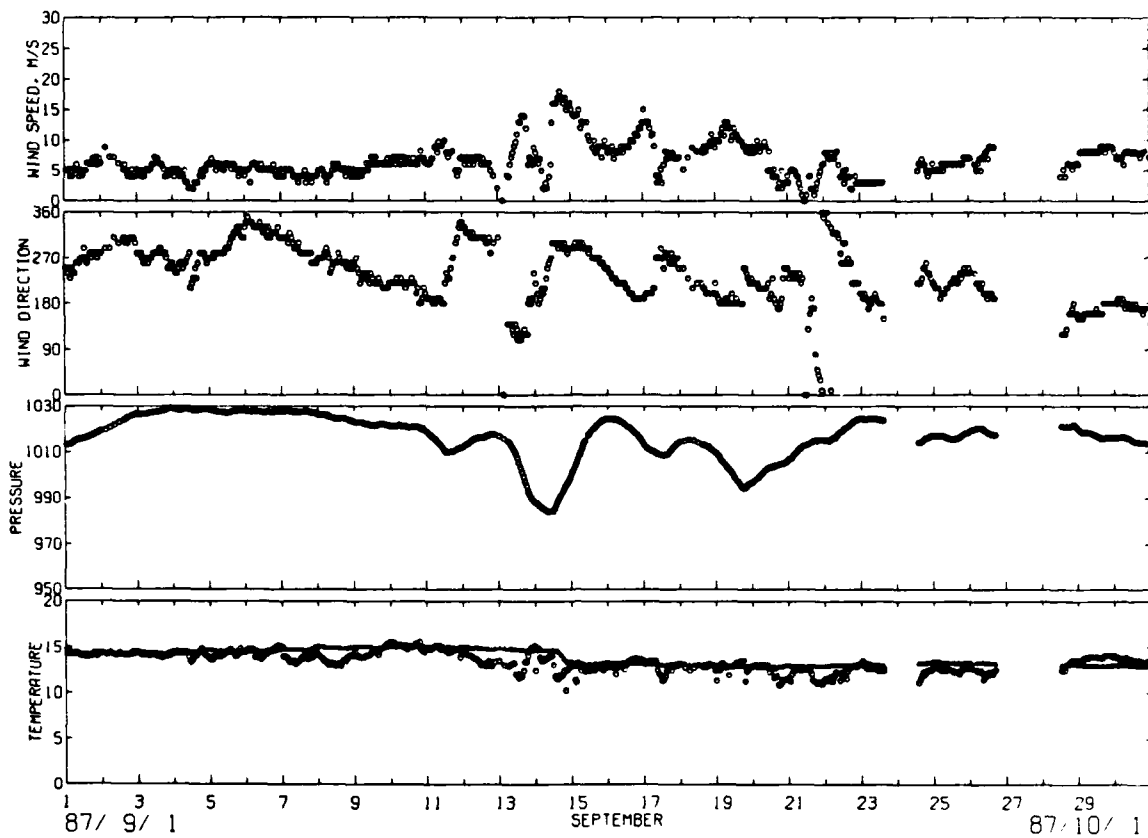


Figure 5a

Figure 5. Time series of wind speed and direction, air pressure, and air and sea temperatures from NDBC Buoy 46004, August 1987 through April 1988. In the bottom panel the air temperature (circles) shows much higher variance than the sea temperature (triangles).

BUOY 46004



BUOY 46004

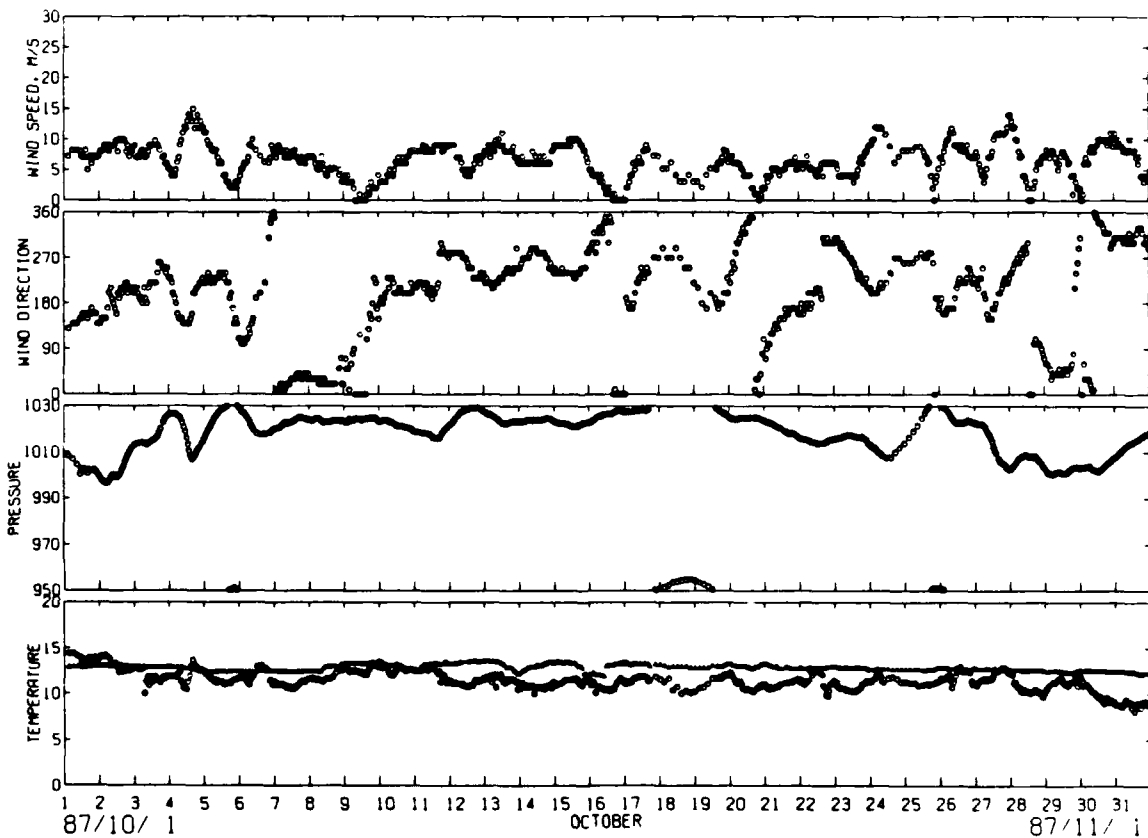
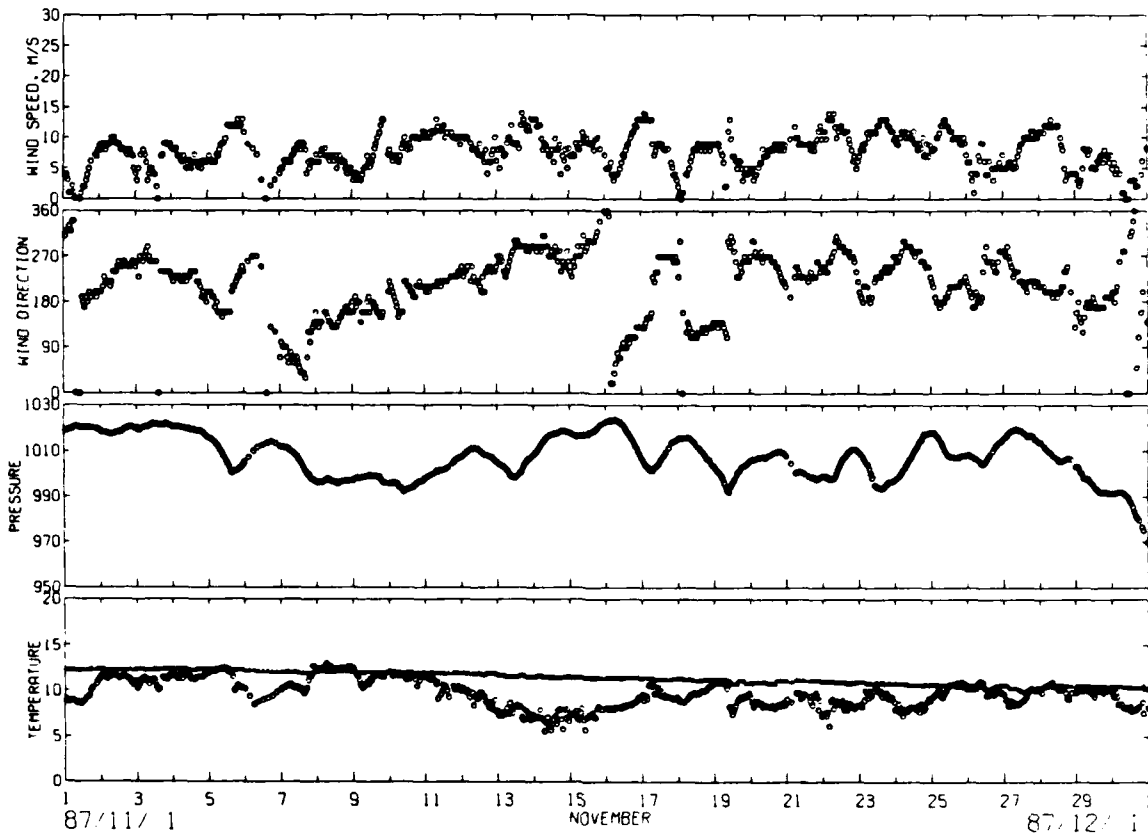


Figure 5b

BUOY 46004



BUOY 46004

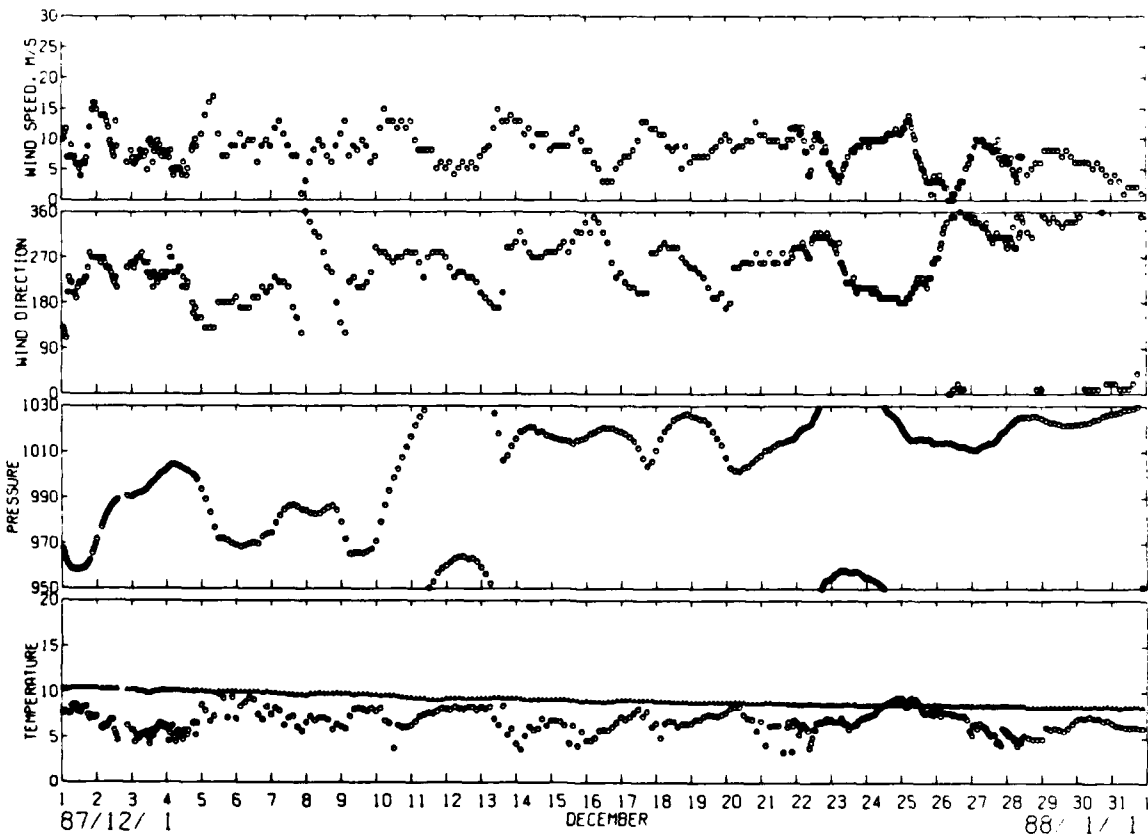
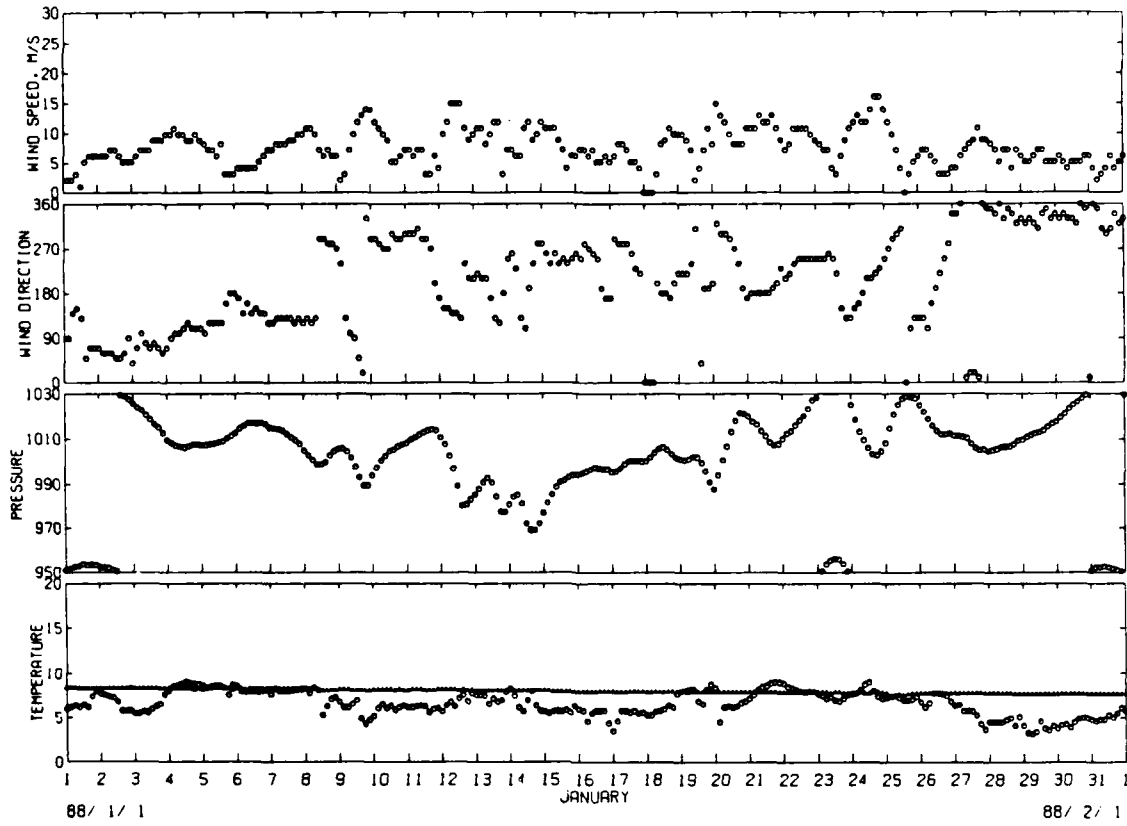


Figure 5c

BUOY 46004



BUOY 46004

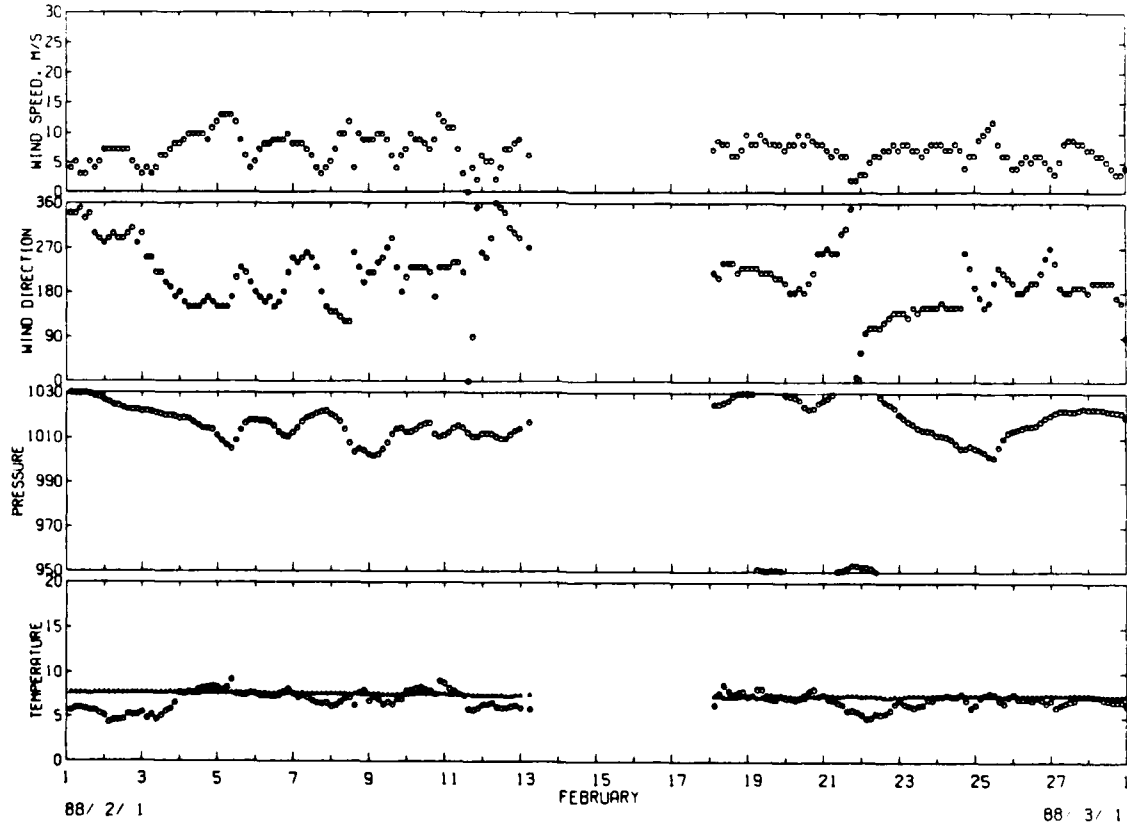
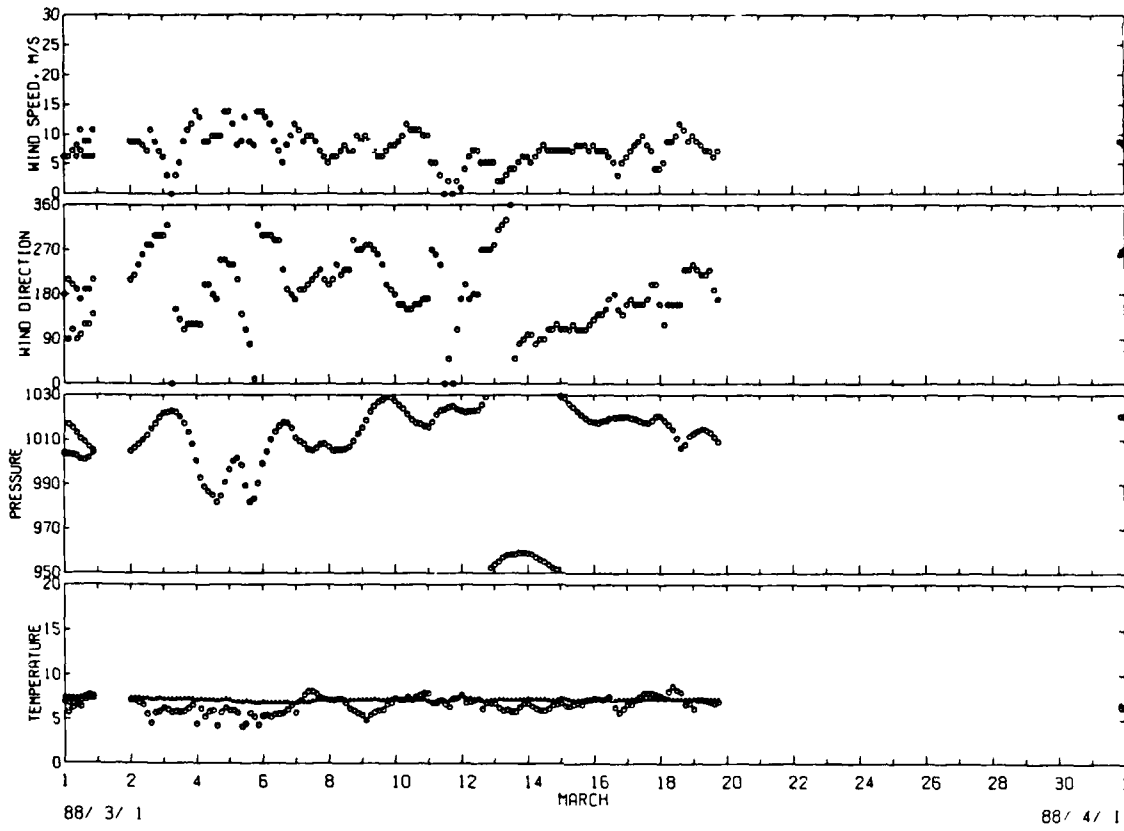


Figure 5d

BUOY 46004



BUOY 46004

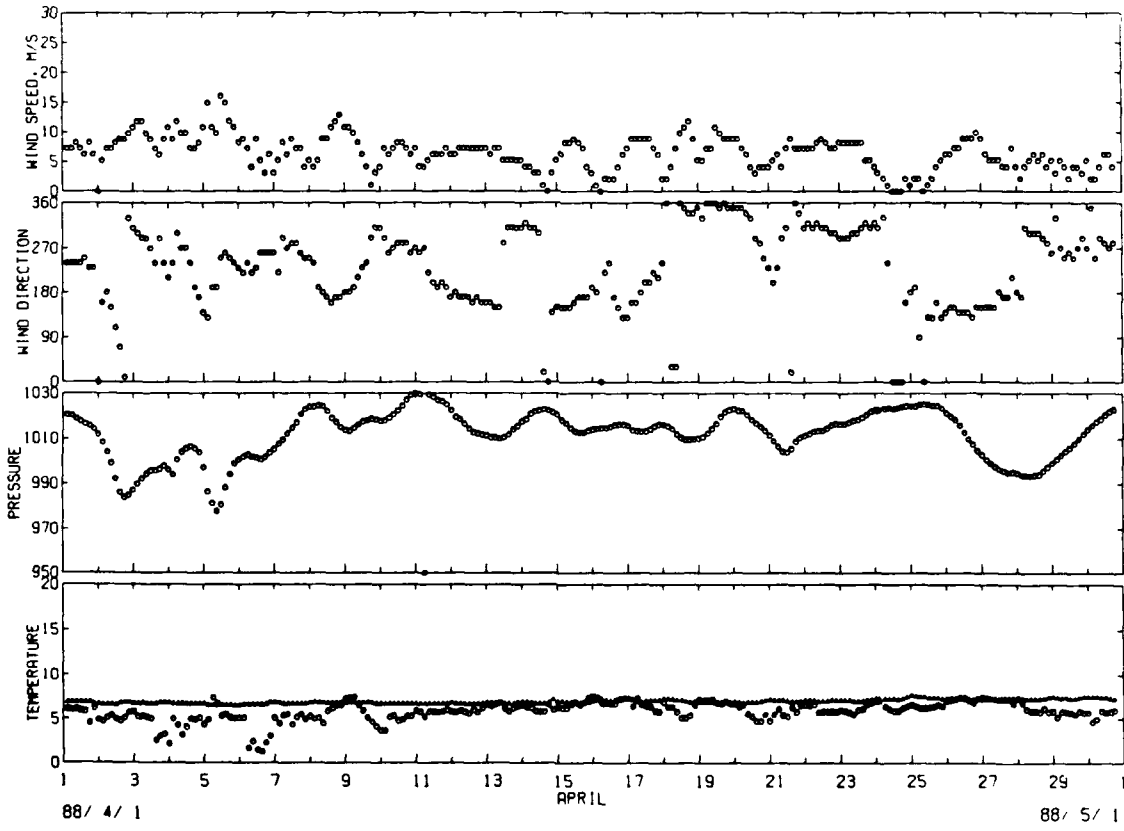


Figure 5e

III. THE COMPILED MARINE OBSERVATIONS DATA SET

A data set of surface marine observations from ships and buoys in the Gulf of Alaska was compiled for the period 20 August 1987 through 30 April 1988. The observations were obtained from two principal sources: the ship and buoy reports that were recorded on the University of Washington Department of Atmospheric Sciences Prime computer system during the intensive phase of the experiment, and reports in the Marine Surface Observations data file, TD1129, at the National Climate Data Center (NCDC). The Atmospheric Sciences Prime computer recorded weather observations in real time from several of the international weather communications circuits. We obtained all the marine observations, ships and buoys, recorded on the Prime during the period 20 August to 31 December 1987 for the North Pacific. TD1129 is an NCDC data file of marine observations received from telecommunications circuits, mailed from ships of opportunity, received from foreign governments, and sent from the National Data Buoy Center. We have observations from 20 August 1987 to 30 April 1988. Since many reports appeared in both systems, all duplicate reports from the Prime were removed. The data buoys were recorded every hour on the Prime system but were retained only every 3 hours in TD1129.

The processing of the marine surface observations began with selecting only those observations within the region 40° to 60° N and 120° to 160° W. Figure 1 shows the Ocean Storms region in the North Pacific and the locations of the moored data buoys that are included in the data set. The reports from ships, drifting buoys, and moored buoys were all decoded and put into the same format with only selected variables retained and limited quality control applied. The variables included were station identification; time; position; air pressure; wind direction and speed; air, water and dew point temperatures; significant wave height and period; visibility; and cloud cover.

The data set is contained on a magnetic tape that is fully described in Appendix B. There are 94,495 reports in the set, with an average of 370 reports recorded each day; 56,790 are from ships of opportunity and 37,705 are from data buoys, fixed and drifting. The buoys are listed in Table I, along with their positions, the type of buoy, and the number of observations recorded. The number of reports received each hour of the day is summarized in Figure 6. Ships normally report on a 6 hour interval and send fewer reports during the night hours of 0600 and 1200 GMT. Almost all the reports at the 3 hour intervals are from data buoys, and those at hourly intervals are from data buoys recorded on the Prime.

Table I. Data buoys in the Ocean Storms data set.

<u>Buoy</u>	<u>Type</u>	<u>Position</u>	<u>Number of Observations</u>
46001	6N/G	56.3, 148.3	3517
46002	6N/G	42.5, 130.4	3516
46003	6N/G	51.9, 155.9	3513
46004	6N/G	50.9, 135.9	3266
46005	6N/G	46.1, 131.0	3506
46006	12D/G	40.8, 137.6	2981
46010	LNB/D	46.2, 124.2	1556
46022	6N/G	40.7, 124.5	1558
46027	LNB/D	41.8, 124.4	1729
46030	ELB/D	40.4, 124.5	241
46036	6N/G	48.3, 133.9	1050
46039	AN/D	48.2, 123.4	1370
46040	3D/D	44.8, 124.3	3298
46041	3D/D	47.4, 124.5	3503
46043	?	46.9, 124.2	800
46184	6N/G	53.5, 138.3	383
46688	drifter	41, 158	391
46689	drifter	51, 143	554
46690	drifter	48, 156	114
46691	drifter	47, 139	545
46703	drifter	43, 157	56
46751	drifter	50, 135	254

Hull Types:

- 6N A boat-shaped hull 6 meters long and 3 meters wide with a 10 ton displacement. Anemometers and air temperature sensors are located 5 meters above the waterline. Barometers are at the water line, and surface water temperature sensors are 1 meter below.
- 12D A discus hull 12 meters in diameter with a 100 ton displacement. Anemometers and air temperature sensors are located 10 meters above the waterline. Barometers are at the waterline and surface water temperature sensors are 1 meter below.
- 3D 3 meter discus, anemometer height is 5 meters, air temperature sensor is at 4 meters.
- LNB USCG Large Navigational Buoy, anemometer height is 13.8 meters, air temperature sensor is 11.4 meters.
- ELB USCG Exposed Location Buoy, anemometer height is 7.2 meters, air temperature sensor is at 6.1 meters.
- AN USCG Aids-to-Navigation Buoy, anemometer height is 5.5 meters.

Sensor packages:

- G General Service Buoy Payload, UHF communications. Wind sensor is a vane-directed impeller, 8.5 minute averaging time.
- D Data Acquisition, Control, and Telemetry, UHF communications. Wind sensor is a vane-directed impeller, 8.0 minute averaging time.

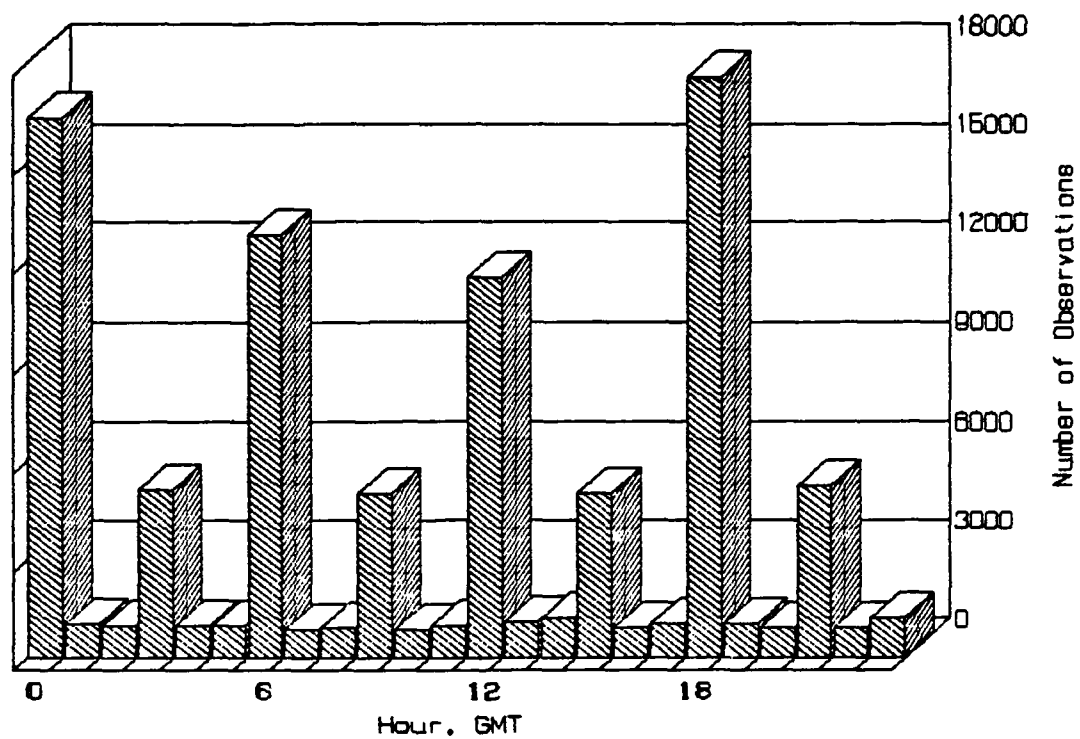


Figure 6. Bar graph of the total number of observations at each hour of day in the Ocean Storms marine observations data set.

IV. OPTIMAL INTERPOLATION

To estimate the wind, the wind stress, and the heat flux at positions of interest in the Gulf of Alaska, an optimal interpolation procedure was developed. Standard optimal interpolation techniques were used, as first developed by Gandin (1963). There are two free parameters that enter the interpolation: the autocorrelation length scale of each field to be estimated and the ratio of the measurement error to the standard deviation of the field. These two were chosen by trial and error to maximize the correlation (not minimize the difference) between the value of a parameter measured at a buoy and the value interpolated to the position of the buoy without the benefit of the buoy's observation. In the case of air pressure, the correlation between the measured wind speed and the geostrophic wind speed was maximized. The autocorrelation function was assumed to be of the form

$$R(d) = \exp - (d/L)^2$$

where L is the autocorrelation length scale. The following length scales were used: air pressure, 1500 km; wind speed, 500 km; and air temperature, air-sea temperature difference, and dew point depression, 1500 km.

The ten nearest stations were used in each interpolation. The field was assumed to approach the mean of the ten observations rather than the climatological mean when there were no observations close to the interpolation point. Thus the proper standard deviation of the field to use in the interpolation is different from that of climatology and was determined by trial and error as mentioned above. In all variables the assumed measurement error of the ships was double that of the NDBC buoys. The measurement error at the buoys and the standard deviations of the fields for each variable were as follows: air pressure, 0.5 and 12 mb; wind speed, 0.5 and 1.5 m/s; air temperature, 0.5 and 1.0°C; and air-sea temperature difference and dew point depression, 0.5 and 1.5°C.

The following variables were interpolated: air pressure; wind speed; wind direction (from interpolated components); air temperature; air-sea temperature difference; dew point depression; and a nine point, 1 km grid of air pressure in the vicinity of the location. This grid can be used to find the geostrophic wind both at the location of interest and a small distance away so that curl and divergence calculations of the stress can be made based on gradients of the geostrophic wind. The grid is described more completely in Appendix B.

Two data bases were used for the interpolations. The first consisted of the marine observations described above and the second consisted of the NMC 2.5° grid point fields.

The NMC fields for sea level pressure, air temperature, water temperature, and the U and V components of the 1000 mb wind were obtained from the National Center for Atmospheric Research (NCAR). They have a resolution of 2.5° in both latitude and longitude. The interpolation technique was similar to that used with the observations, but taking the ten grid points nearest to each interpolation location rather than the ten nearest ships or buoys. The grid point fields were for the hours of 0000 and 1200 GMT. There were no water temperatures for 1200 GMT. No dew point depression values were obtained for the NMC grid point data.

Some effort was made to check for possible errors in the pressure observations by estimating the pressure at the location of each observation (without the benefit of the observation being checked) and comparing the estimation to the reported value. If the difference divided by the estimated interpolation error was above a threshold, the report was flagged for elimination. If more than one report was flagged, a further check was made to see whether dropping any other flagged report would "save" a threatened report, thereby reducing the chance of bad reports forcing the elimination of good reports. Interpolations from the observations were performed for 0000, 0600, 1200, and 1800 GMT. The two methods will be compared in the next section.

Each data set was used to interpolate to the locations of the following: (1) the 9 Ocean Storms moorings, (2) the 6 thermistor buoys deployed by William Large of the National Center for Atmospheric Research, and (3) the 48 Lagrangian drifters deployed by Peter Niiler of the Scripps Institution of Oceanography. The results are stored in six files on the data tape described in Appendix B along with the marine observations.

V. METLIB FIELDS

The Metlib fields consist of wind, wind stress, and sensible and latent heat flux fields for the Ocean Storms region. The fields are based on the synoptic weather charts in Appendix A and cover the period 20 October to 9 December 1987. These fields were produced with the aid of the Metlib programming package (Macklin et al., 1984) using the facilities at the NOAA Pacific Marine Environmental Laboratory at Sand Point in Seattle.

The first step in producing the Metlib fields was manual digitization of the pressure fields drawn by the forecasters. The region digitized is shown in Figure 1. Two grids were used, one 900 km by 900 km for the first 19 days and a second, larger one, 900 km by 1200 km, beginning 8 November. Composed of points 100 km apart, the grid was on a stereopolarographic projection true at 60°N. The Metlib program interpolated the pressure readings to a 50 km grid—half of the initial spacing—and smoothed them with a 3 by 3 pyramid filter. The resulting fields were then dimensioned 19 by 19 or 19 by 25.

The air temperature, dew-point temperature, and air-sea temperature difference fields were also digitized, but on a coarser grid: every third point (300 km) of the pressure grid was entered. These fields were based on the limited ship or buoy reports found within the Ocean Storms region. In extrapolating the sparse reports to this coarse grid, an attempt was made to account for the presence of fronts, but the reliability of these fields is limited. The fields on the 300 km grid were interpolated to the same 50 km grid used for the pressure and smoothed in the same manner as the pressure fields. All three of these temperatures were assumed to be referenced to 10 m; no attempt was made to correct for the variable, and often unknown, heights of the thermometers on the ships and buoys.

The digitized fields were then used to calculate the 10 m wind vector, the wind stress vector at the surface, and the latent and sensible heat fluxes using the Brown Planetary Boundary Layer Model (Brown and Liu, 1982). This model is a one-dimensional Ekman layer model with a matched diabatic surface layer, parameterized secondary flow within the boundary layer, and a stratification-dependent eddy diffusivity. Starting with the geostrophic wind calculated from the surface pressure fields, the model determines the wind at the top of the boundary layer using the thermal wind equation. The surface roughness in the model is found from an empirical relation based on the surface wind speed (Kondo, 1975); the temperature and moisture roughness lengths include molecular sublayer effects as suggested by Liu et al. (1979). Finally, a diabatic wind profile is used

based on the wind speed, the air-sea temperature difference, and the humidity to calculate the air stress and the sensible and latent heat fluxes as outlined in Section VIII.

To evaluate the accuracy of the Metlib fields, the field values were compared with single measurements from Buoy 46004. A simple linear interpolation was made from the 50 km grid to the location of the buoy. The pressure as reported at the buoy was generally within 1.2 mb of the pressure recorded in the fields (field - buoy mean difference = -0.8 mb; rms difference = 1.2 mb; N = 99), indicating that the analysis and digitizing errors were small at the location of the buoy; this is to be expected since the analysts often use the buoy measurement in drawing the isobars. For the wind comparison the field winds were corrected down from a 10 m reference height to 5 m, the buoy anemometer height, using a diabatic log profile (typically a 5% correction). The corrected winds averaged 2.8 m/s too high and showed an rms difference of 4.0 m/s. This rather large error in the winds indicates that the stress and heat flux fields are also unreliable. The mean difference in wind directions was very low, 4°, but the rms difference of 32° was more substantial. A more extensive comparison between the field values and the buoy measurements is found in the next section (see Table V).

VI. CORRELATIONS BETWEEN THE INTERPOLATED AND THE MEASURED FIELDS AT THE DATA BUOYS.

We have done extensive investigations of the correlations between the parameters measured at three NDBC data buoys and the interpolated values from observations (without benefit of the buoy observation), from the NMC fields, and from the Metlib fields. The correlations were a standard least squares best fit of the line

$$V_b = A + B V_i \quad (1)$$

where V_b is the buoy observation and V_i is the interpolated value; A is the constant, and B is the gain. The root-mean-square error (rms error) of the fit is the rms difference between the observation and the value obtained from the equation. A and B are, of course, calculated to minimize the rms error.

Table II summarizes the correlations and the rms error of the linear best fit of the wind speeds (6 hour average) for the three data sets at Buoy 46004 only. The correlations are a little better for the NMC fields than for the observations or for the Metlib fields—a small surprise. The rms error of the fit is 1.45 m/s for the NMC values and 1.60 and 1.62 m/s for observations and Metlib, respectively. The NMC fields used the buoy reports, unlike the interpolations based on the observations. Consequently the fields may be more accurate at the buoy locations than at other locations and may have an unfair advantage over the observations. The NMC interpolations showed slightly better correlations with the measurements in pressure, wind speed, and air-sea temperature difference, but not in air temperature.

Also shown in Table II are correlations using both the interpolated wind speed and the geostrophic wind speed. These are based on a multiple regression of the form

$$V_b = A + B V_i + C V_g \quad (2)$$

where V_b is the buoy wind speed, V_i is the interpolated wind speed, and V_g is the geostrophic wind speed based on the interpolated pressure field. The estimates of wind speed based on observations and those from the Metlib fields are helped substantially by including the additional information from the pressure field as represented by the geostrophic wind. The rms error of the fit is reduced to 1.42 and 1.39 m/s, respectively. The estimate from the NMC fields is helped only slightly, to 1.37 m/s.

More complete comparisons between the interpolated values and the buoy measurements are given in Tables III (observations), IV (NMC), and V (Metlib). The accuracy of the interpolated estimates can be improved substantially in all cases by using an

Table II. *Correlations of 6 hour averaged measured wind speed with interpolations for Buoy 46004.*

	<u>Observations</u>	<u>NMC Grid</u>	<u>Metlib</u>
Wind Speed			
correlation	.806	.844	.806
rms error, m/s*	1.60	1.45	1.62
N	928	448	100
Wind Speed and Geostrophic Wind Speed			
correlation	.851	.863	.865
rms error, m/s*	1.42	1.37	1.39
N	926	448	100

*Root-mean-square value of the residuals

Table III. Interpolations from observations. Correlations between 6 hour average observations (dependent) and interpolated values (independent), August 1987 through April 1988.

	Buoy	46001	46004	46005	All 3
Latitude		56.3	50.9	46.1	
Longitude		148.3	135.9	131.0	
Number of Points		935	928	723	2586
Pressure					
rms difference		2.60	1.66	1.28	1.97
correlation		.982	.995	.993	.990
constant		18.18	3.71	-16.65	.57
gain		.982	.997	1.016	1.000
rms error in the fit		2.59	1.27	1.27	1.94
Air Temperature					
rms difference		1.40	.96	.91	1.13
correlation		.953	.958	.959	.970
constant		-.95	.01	.30	-.75
gain		1.01	.957	.958	1.03
rms error in the fit		1.08	.87	.88	1.00
Air - Sea Temperature Difference					
rms difference		1.43	1.10	1.06	1.22
correlation		.658	.725	.640	.675
constant		-.96	-.77	-.71	-.82
gain		.740	.71	.659	.717
rms error in the fit		1.15	.84	.86	.98
Wind Speed					
rms difference		4.32	3.92	2.70	3.78
correlation		.678	.806	.829	.759
constant		1.92	1.40	.612	1.46
gain		.548	.559	.732	.587
rms error in the fit		2.38	1.60	1.84	2.02
Buoy Wind and Geostrophic Wind Speed					
correlation		.688	.790	.823	.748
constant		4.08	3.16	2.65	3.43
gain		.254	.272	.385	.284
rms error in the fit		2.34	1.65	1.87	2.05
Buoy Wind and Both the Interpolated and the Geostrophic Wind Speeds					
correlation		.760	.851	.882	.814
constant		1.84	1.56	.87	1.58
gain for interpolated wind		.328	.336	.426	.352
gain for geostrophic wind		.163	.145	.214	.161
rms error		2.10	1.42	1.55	2.05
Complex Correlations					
Buoy Wind and Interpolated Wind					
correlation		.834	.912	.903	.864
gain		.60	.61	.71	.62
		(+-.28)	(+-.20)	(+-.25)	(+-.25)
turning		12°	-2°	0°	4°
		(+26°)	(+19°)	(+20°)	(+23°)
rms error		4.60	3.11	3.26	3.87
Buoy Wind and Geostrophic Wind					
correlation		.868	.882	.887	.864
gain		.40	.40	.51	.42
		(+-.17)	(+-.13)	(+-.18)	(+-.17)
turning		27°	13°	15°	19°
		(+25°)	(+19°)	(+21°)	(+23°)
rms error		4.37	3.10	3.42	3.82

Table IV. Interpolations from NMC grids. Correlations between 6 hour average observations (dependent) and interpolated values (independent), August 1987 through May 1988.

	Buoy	46001	46004	46005	All 3
Latitude		56.3	50.9	46.1	
Longitude		148.3	135.9	131.0	
Number of Points		451	448	346	1245
Pressure					
rms difference		1.26	1.12	1.08	1.16
correlation		.996	.997	.996	.997
constant		-14.30	-11.79	-25.81	-15.17
gain		1.014	1.012	1.025	1.015
rms error in the fit		1.22	1.03	.978	1.14
Air Temperature					
rms difference		2.72	2.50	2.44	2.57
correlation		.936	.936	.929	.957
constant		-1.80	-0.53	-.53	-1.65
gain		.921	.844	.886	.942
rms error in the fit		1.19	1.03	1.13	1.17
Air - Sea Temperature Difference					
rms difference		2.51	2.76	2.81	2.69
correlation		.738	.648	.625	.688
constant		-1.99	-1.93	-1.83	-1.96
gain		.699	.562	.488	.600
rms error in the fit		1.08	.98	.89	1.01
Wind Speed					
rms difference		3.56	4.59	3.44	3.94
correlation		.859	.844	.888	.849
constant		1.83	1.29	.46	1.28
gain		.591	.535	.673	.588
rms error in the fit		1.68	1.45	1.53	1.65
Buoy Wind and Geostrophic Wind Speed					
correlation		.837	.851	.873	.836
constant		3.11	2.97	2.59	3.06
gain		.310	.295	.419	.317
rms error in the fit		1.79	1.42	1.62	1.71
Buoy Wind and Both the Interpolated and the Geostrophic Wind Speeds					
correlation		.862	.863	.898	.861
constant		1.96	2.04	1.09	1.77
gain for geostrophic wind		.080	.170	.168	.136
gain for interpolated wind		.459	.246	.426	.361
rms error		1.66	1.37	1.47	1.59
Complex Correlations					
Buoy Wind and Interpolated Wind					
correlation		.964	.941	.963	.950
gain		.69	.60	.67	.65
		(+-.17)	(+-.14)	(+-.16)	(+-.16)
turning		7°	-1°	2°	3°
		(+14°)	(+14°)	(+14°)	(+14°)
rms error		2.81	2.41	2.41	2.65
Buoy Wind and Geostrophic Wind					
correlation		.948	.915	.944	.925
gain		.43	.43	.56	.45
		(+-.12)	(+-.11)	(+-.15)	(+-.15)
turning		22°	15°	15°	18°
		(+15°)	(+15°)	(+15°)	(+16°)
rms error		2.97	2.62	2.62	2.90

expression of the form shown in (1) or (2) to correct the estimate. These three tables provide the values of A (the constant) and B and C (the gains) in order to make the correction. This correction will account in a gross way for biases arising from different measurement heights or methods, as well as those arising from the numerical techniques used in creating the fields at NMC or with Metlib.

The rest of this section presents a few comments about each parameter compared.

Pressure: All three data sets do quite well. NMC does best with a correlation coefficient reaching 0.997 and rms errors near 1.0 mb in the linear best fit. In the observations, the interpolation at Buoy 46001 does a bit worse than at the other two (rms error 2.6 vs 1.3 mb), probably because of the reduced number of reports in the western part of the Gulf of Alaska; this difference will be seen in the rest of the parameters as well. The high correlations in air pressure come as no surprise, but they are a good check to show there are no gross errors in positioning or timing in the computational process.

Air Temperature: The Metlib fields do best (rms error of 0.6°C), but this is because the buoys were weighted very heavily in defining the air temperature field (in part, out of distrust of any ship reports). In this variable, as well as the next, the observations did better than NMC—though only slightly.

Air-Sea Temperature Difference: Metlib did best, for the reason stated above.

Wind Speed: NMC does best, with an rms error of 1.65 m/s for three buoys and 1.45 m/s for 46004 alone. Again, the NMC fields benefit from the buoy measurement but the interpolations from observations do not. The interpolated wind speeds from ship observations are usually higher than those measured at the buoy. This difference may be due to the fact that the ships' anemometers are higher than those of the buoys, which are at 5 m. There are small differences in the line of best fit from buoy to buoy that may represent regional differences in the number and composition of the reports near each buoy or may be a reflection of biases in the measurement systems of the buoys. One might ask if there is any significant difference in the corrections at the three buoys. For no wind, the constants of 1.8, 1.3, and 0.5 m/s show a spread that is comparable to the error in fit of about 1.5 m/s, and at 10 m/s the corrected wind speeds of 7.7, 6.6, and 7.2 m/s also show a comparable spread. So we can conclude that there are small but significant differences in the corrections at each buoy.

Figure 7 is a scattergram of the measured and NMC interpolated wind speeds for all three buoys with the 1:1 line added for reference. There is a clear bias of about 2 m/s at low wind speeds and a slight curvature to the points showing a tendency for the buoy to report even lower winds at high wind speeds. The bias is simply a reflection of the

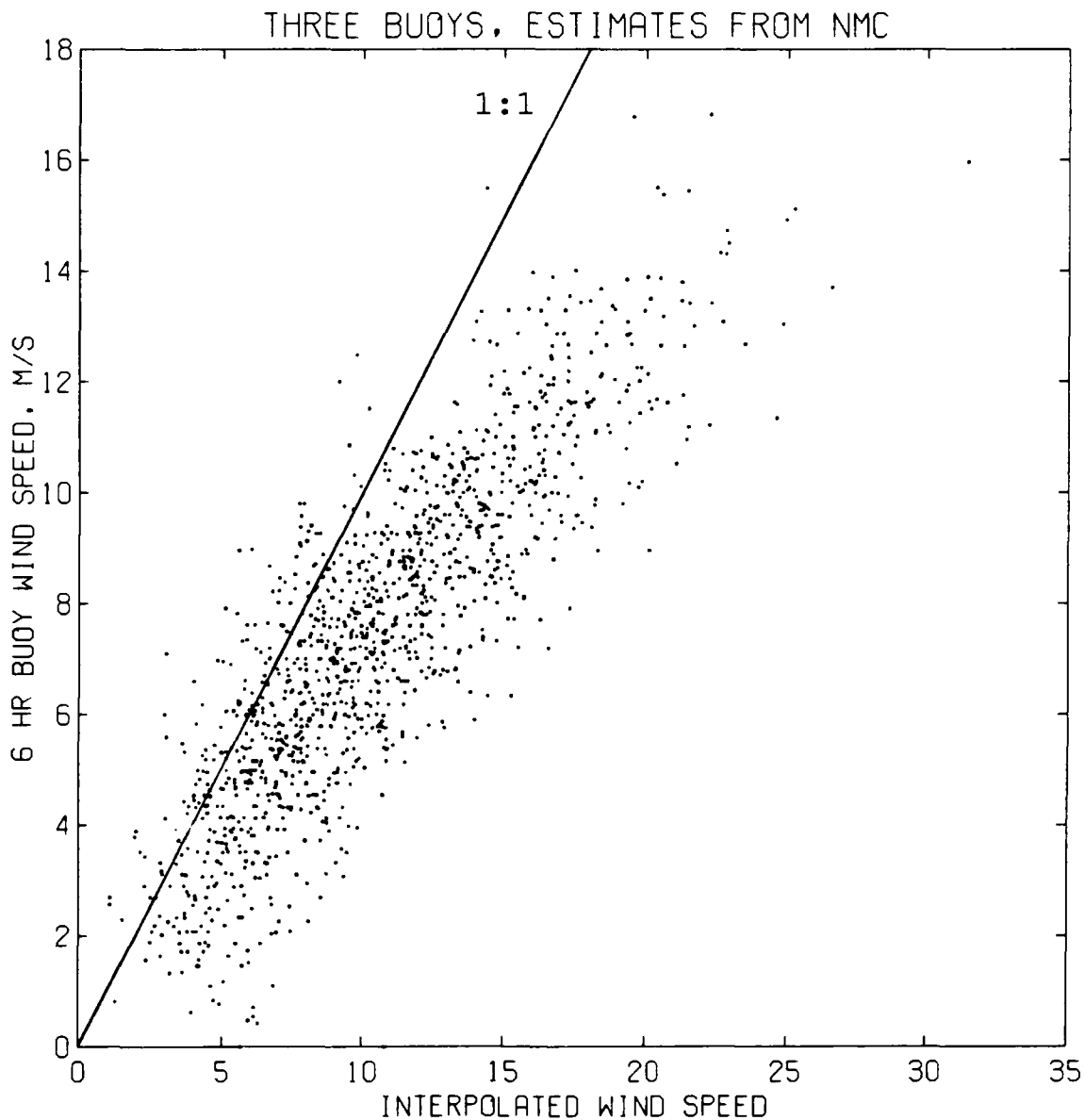


Figure 7. Scattergram of the measured wind speed (6 hour average) at all three NDBC data buoys versus the interpolated wind speed from the NMC 1000 mb wind component fields. The 1:1 line is added for reference.

numerical techniques of the NMC initialization procedures and the difference between the NMC "1000 mb wind" and the 5 m wind at the buoy. The curvature may possibly be a result of waves sheltering the buoy at high wind speeds. We will see a similar result with the geostrophic wind.

Wind Speed and Geostrophic Wind Speed: The correlation of buoy wind speed with geostrophic wind speed is roughly the same as with interpolated wind speed in all three data sets. However, it is interesting that for the Metlib fields there is a slightly better correlation of the measured wind with the geostrophic wind than with the wind calculated using the Brown Model. The linear correlation, with its two free parameters, does not give us the geostrophic reduction. The easiest way of finding this parameter, and perhaps the most accurate, is to calculate the ratio of the mean of the wind speed to the mean of the geostrophic wind speed. These ratios for all three buoys are 0.62 for the observations and 0.66 for the NMC interpolations. These values are not in good agreement with the findings of Marsden (1987), who studied the relationship between the geostrophic wind and the wind measured at Ocean Station Papa over a 30 year period. His geostrophic winds were obtained from 6 hour pressure fields from the Fleet Numerical Weather Center at Monterey. His value for the geostrophic reduction, 0.84, is much higher than ours, but is relative to the 20 m anemometer height of the Papa ships. If both our value and his are corrected to the traditional 10 m level using a neutral wind profile, we get 0.65 and 0.67 from our data sets and 0.79 for the Marsden value. These two are still different from each other, but ours is in good agreement with the value of 0.70 reported for monthly averaged winds in the North Atlantic (Thompson et al., 1983).

Figure 8 shows a scattergram of the measured wind speed versus the geostrophic wind speed for all three buoys using the NMC interpolations; the 0.7:1 line, representing a geostrophic reduction of 0.70, is added for reference. Again we see a slight curvature to the points, showing a greater geostrophic reduction at large wind speeds—perhaps more evidence of the shielding of the buoys in high winds. The story is not entirely tidy. The buoy reports wave height, but there is only a modest correlation of wave height with wind speed ($R = 0.63$) and almost none between the wave height and the geostrophic reduction ($R = -0.29$). Allowing for both first and second order terms (G and G^2) in the regression equation did not help the correlation significantly ($R = 0.84$, first order only; $R = 0.85$, second order). The smaller geostrophic reduction in high winds is also a product of the increased roughness of the sea surface at high wind speeds. The Brown planetary boundary layer model (Brown and Liu, 1982) shows a reduction in U_{10}/G from 0.81 at $G = 10$ m/s to 0.68 at $G = 30$ m/s (neutral stratification). Including the air-sea temperature difference as an additional parameter did not significantly help the correlations between the measured and the geostrophic wind speeds.

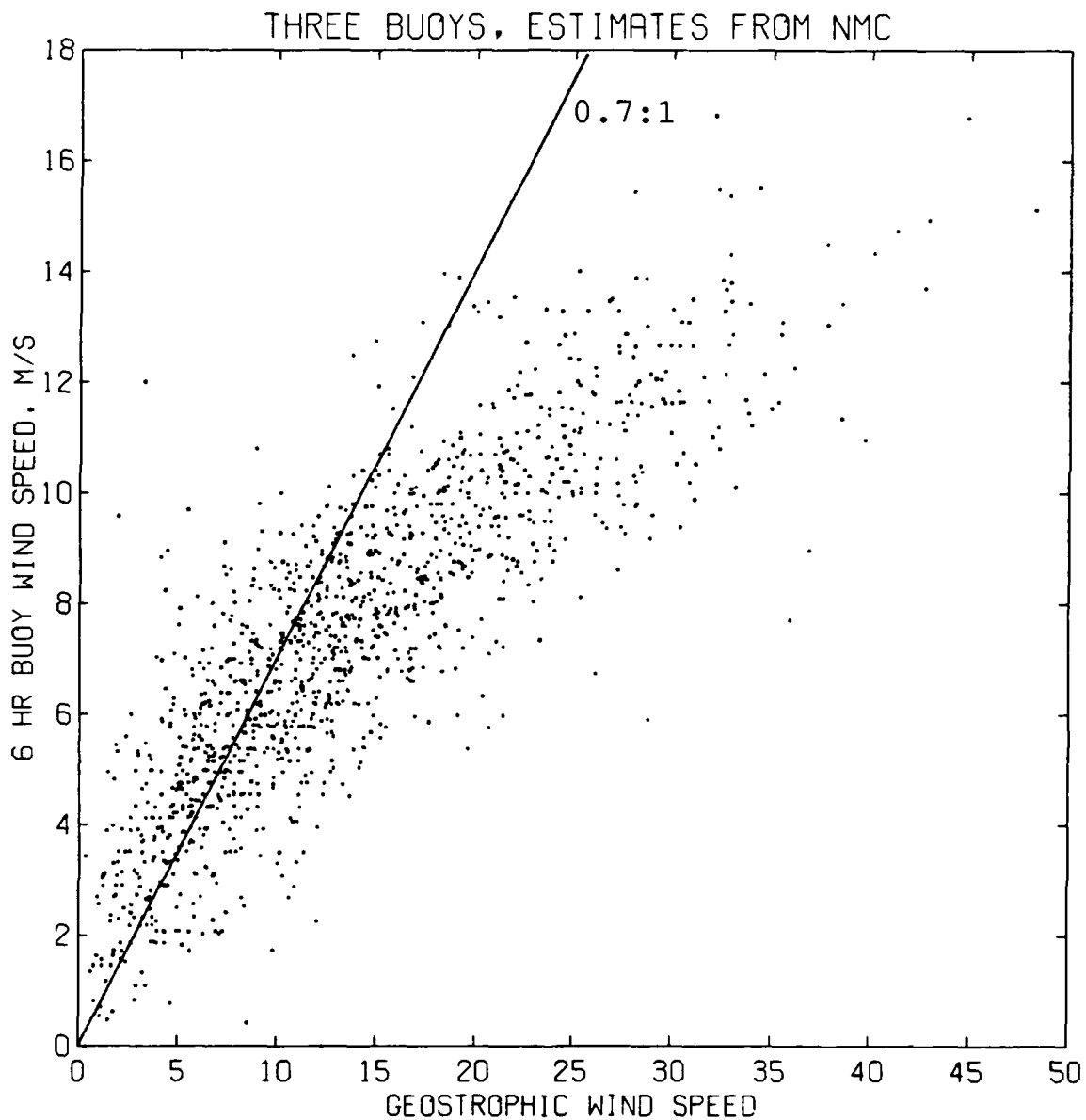


Figure 8. Scattergram of the measured wind speed (6 hour average) at all three NDBC data buoys versus the geostrophic wind from the NMC sea level pressure fields. The 0.7:1 line is added to represent a geostrophic reduction of 0.70.

Wind Speed and Both the Interpolated and the Geostrophic Wind Speed: A modest improvement in the correlations in wind speeds is obtained by using both the geostrophic and the interpolated wind speeds in a multiple regression. As stated above, the observations and Metlib are improved a little more than NMC.

Complex Correlations for the Wind Vectors: A complex correlation was calculated for the interpolated and measured wind vectors. This gives us two parameters: a reduction, R, and a turning, T. It is of the form

$$V_b = R \exp (T_i) V_i \quad (3)$$

where V_b and V_i are the complex representations of the wind vector at the buoy and from interpolation, respectively. Tables III, IV, and V show these two parameters and their uncertainties (one standard deviation). These correlations show that the observations need to be reduced by a factor of about 0.6, perhaps reflecting anemometer height differences; the directions are without a significant bias, although their uncertainty is near 20°.

Complex Correlations for the Geostrophic Wind Vector: The geostrophic reduction by this method is much lower than that found from wind speeds alone: about 0.43 for both the observations and for NMC. The lower number is typical for complex correlations because outlying points in odd directions are better accommodated by small reductions. The difference between our reduction factor and that of Marsden is all the more significant because he apparently calculated it using the complex correlation method. If both his value of 0.84 and ours of 0.43 are adjusted to 10 m, the resulting values of 0.79 and 0.46 are even more different than that obtained with the wind speed - geostrophic wind speed formulation.

The geostrophic turning angle is about 18° ($\pm 16^\circ$) for the NMC fields, similar to that obtained by Marsden, 15°. A slightly lower turning angle is found with the Metlib winds, perhaps reflecting the preconceptions of the analysts who drew the isobars while looking at the wind direction marked on the chart. In any case, the turning angle, 10°, is quite similar to that found from the objective analysis and is a mark of the skill of the analysts.

Dew Point Depression: The dew point depression is not included in the tables because it is not measured by the buoys. We do not have a good way of evaluating this parameter, but made an attempt by comparing the dew point depressions reported by *Parizeau* to those interpolated to the position of the ship from other ships in the area. The correlation was low ($R = 0.49$, $N = 87$), and the rms error of the best fit straight line was 0.67°C, a large portion of the mean dew point depression of 1.9°C. Observations from ships of opportunity were used to interpolate the dew point depression, but many ships do not report it. It is missing in the NMC interpolations.

Table V. Interpolations from Metlib grids. Correlations between 6 hour average observations (dependent) and interpolated (independent) values, 20 October through 9 December 1987.

	<u>Buoy</u> 46004
Latitude	50.9
Longitude	135.9
Number of Points	100
Pressure	
rms difference	1.18
correlation	.998
constant	4.77
gain	.996
rms error in the fit	.90
Air Temperature	
rms difference	.608
correlation	.935
constant	.38
gain	.962
rms error in the fit	.60
Air - Sea Temperature Difference	
rms difference	.63
correlation	.871
constant	-.31
gain	.91
rms error in the fit	.60
Wind Speed	
rms difference	4.70
correlation	.806
constant	2.33
gain	.471
rms error in the fit	1.62
Buoy Wind and Geostrophic Wind Speed	
correlation	.855
constant	2.99
gain	.302
rms error in the fit	1.41
Buoy Wind and Both the Interpolated and the Geostrophic Wind Speeds	
correlation	.865
constant	2.50
gain for geostrophic wind	1.39
gain for interpolated wind	.865
rms error	1.39
Complex Correlations	
Buoy Wind and Interpolated Wind	
correlation	.877
gain	.60
	(+-.16)
turning	-1°
	(+-15°)
rms error	2.74
Buoy Wind and Geostrophic Wind	
correlation	.883
gain	.42
	(+-.12)
turning	10°
	(+-16°)
rms error	2.87

VII. SPACE AND TIME RESOLUTION

The space and time resolution of the interpolated values varies from source to source. The spatial resolution is severely limited by the number of observations received. In the interpolations from observations, the mean effective distance of the ships and buoys used to determine the pressure at the Ocean Storms moorings is 370 km. The NMC grid spacing is 2.5° in both latitude and longitude, a mean resolution of roughly 200 km; the spacing on the Metlib grid is about 50 km, although the hand digitizing of the pressure fields was done on a 100 km grid. The time resolution is every 6 hours for the observations, and every 12 hours for NMC and Metlib.

A spectral analysis of the measured and the interpolated (from observations) wind speeds shows that both the variance and the coherence are concentrated at periods greater than 1 day. Figure 9 shows the spectral estimates for the measured (dashed) and the interpolated (dotted) wind speeds, along with the coherence (solid) between them, for periods from 0.5 day to 10 days. Similar results are seen for the measured and the geostrophic wind, Figure 10. This is consistent with the findings of Marsden (1987), who also found a sharp drop in the coherence at periods shorter than a day and concluded that the geostrophic wind was not a good predictor of the open ocean surface winds for periods less than 2.5 days.

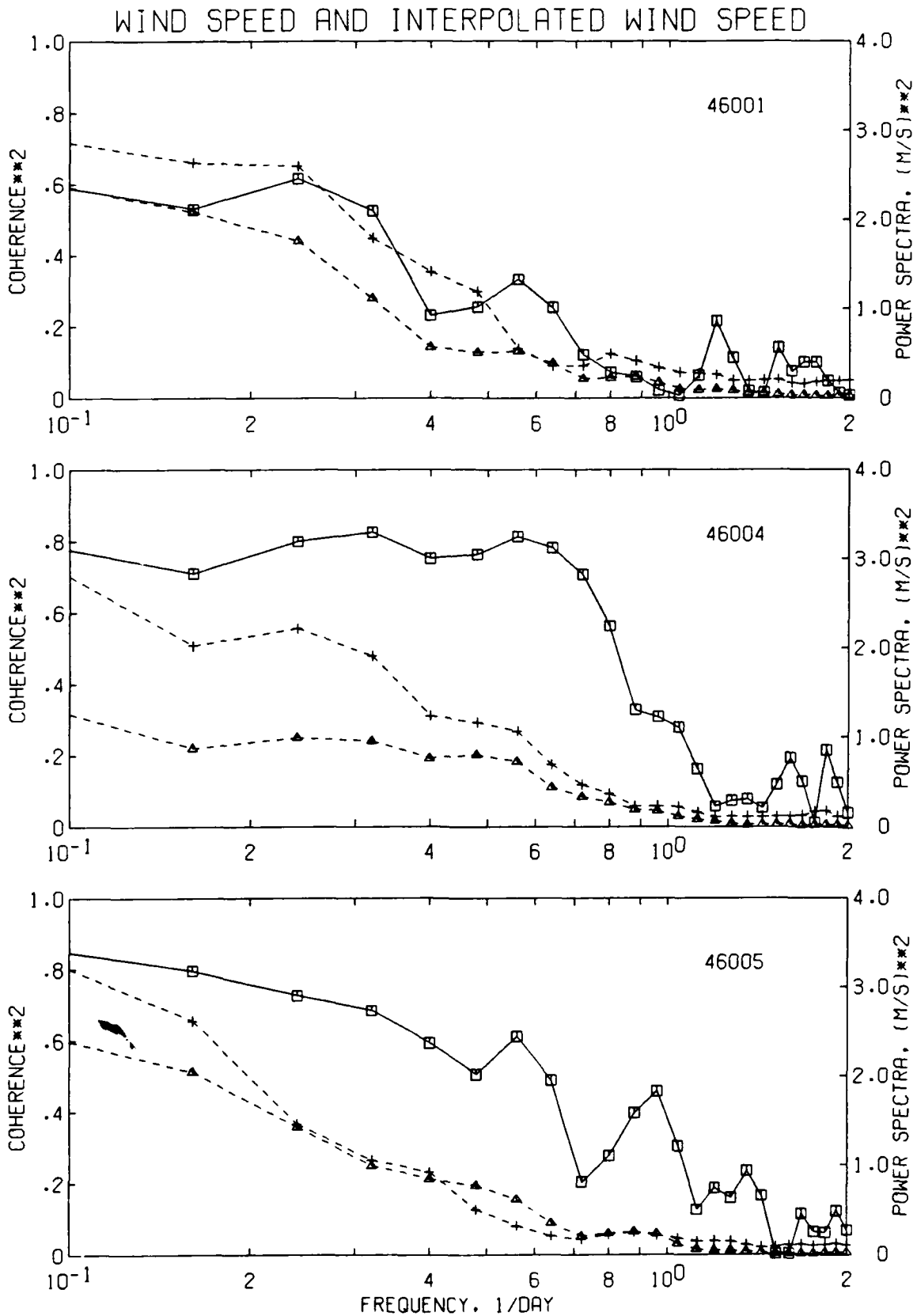


Figure 9. Power spectra and coherence for the measured wind speed and the interpolated wind speed from observations at three NDBC buoys. The coherence squared is the solid line, and the power spectra are the dashed lines; triangles denote the buoy wind speeds, and crosses denote the interpolated wind speed.

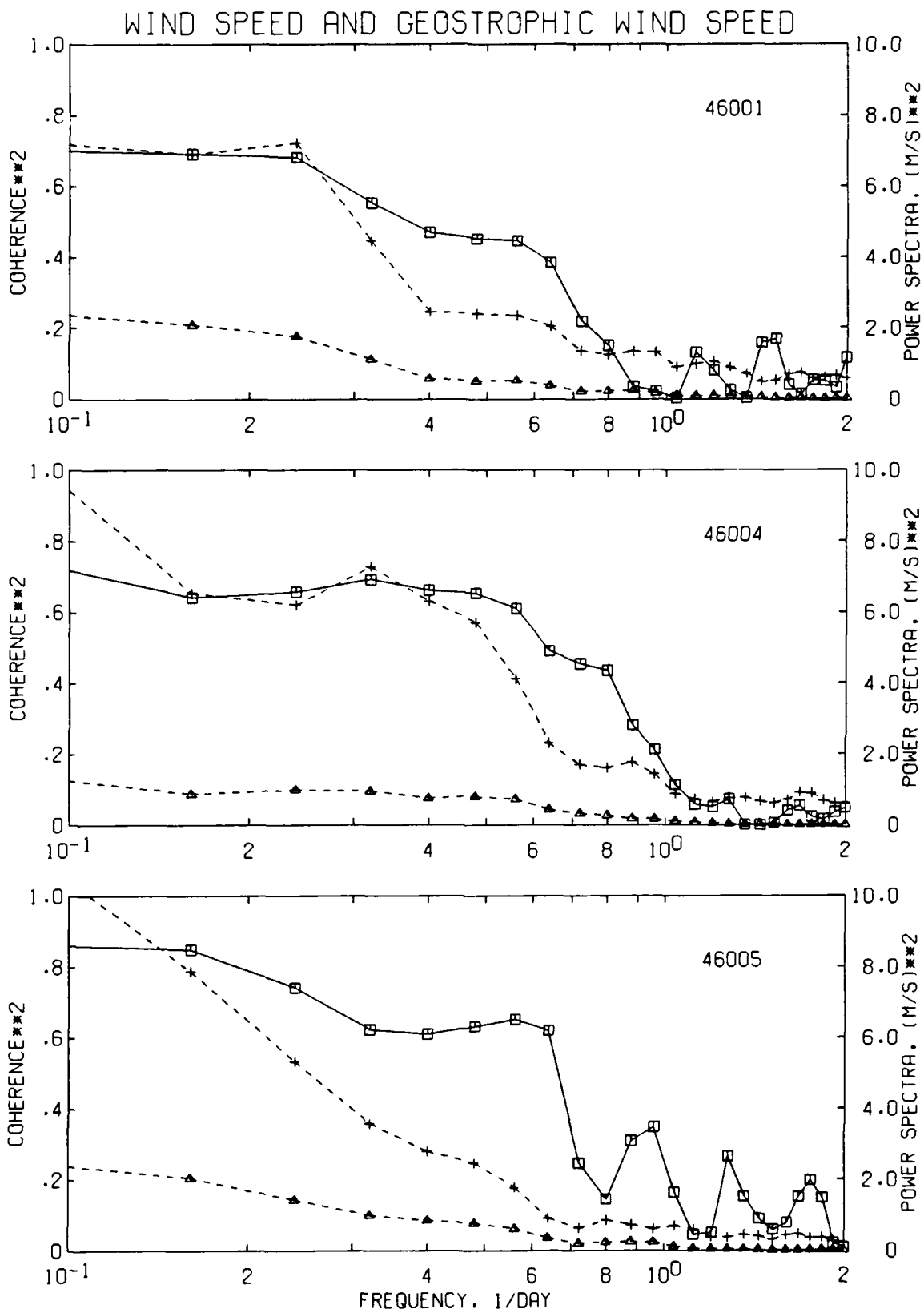


Figure 10. Power spectra and coherence for the measured wind speed and the interpolated geostrophic wind speed at the three NDBC buoys. The coherence squared is the solid line, and the power spectra are the dashed lines; triangles denote the buoy wind speed, and crosses denote the interpolated geostrophic wind speed.

VIII. AIR STRESS AND HEAT FLUX ANALYSIS

As an example of how to use the interpolated values to calculate the air stress and the heat flux, these two were calculated for the central Ocean Storms mooring for the period 20 August 1987 to 30 April 1988. The air stress was calculated using a diabatic profile with variable drag coefficient and both temperature gradient and humidity gradient corrections similar to those used in the Brown boundary layer model. The drag coefficient is taken from Kondo (1975) and is based on the 10 m wind speed adjusted for neutral stratification. The assumed profile is of the form

$$U(z) = (u_* / k) \ln [z/z_0 - \psi(z/L)]$$

where u_* is the friction velocity, k is von Kármán's constant, z_0 is the roughness length, and $\psi(z/L)$ is a stability dependent correction to the logarithmic profile. L is the Obukov length and is given by

$$L = T u_*^2 / k g T_*$$

where T is the air temperature and g is the acceleration due to gravity. T_* is defined below. The stratification correction, following Large and Pond (1982), is then

$$\psi(z/L) = -7 z/L \quad z/L > 0$$

$$\psi(z/L) = 2 \ln(1+x)/2 + \ln[(1+x^2)/2] - 2 \tan^{-1} x + \pi/2 \quad z/L < 0$$

$$x = (1 - 16z/L)^{1/4}$$

Concurrently with the wind speed profile, the temperature and humidity profiles were found:

$$T(z) = (T_*/a) \ln [z/z_t - \psi_q(z/L)]$$

$$Q(z) = (Q_*/a) \ln [z/z_q - \psi_q(z/L)]$$

where T is the potential temperature and Q is the water vapor mixing ratio. T_* and Q_* are called the friction temperature and the friction mixing ratio in analogy with u_* ; $a = 1.35$ is the ratio of the eddy diffusivities of momentum and heat. The roughness lengths for temperature and humidity, z_t and z_q , are different from that for wind speed and are based on the roughness Reynolds number as shown in Liu et al. (1979), but the stratification corrections are the same for the two.

$$\psi_q(z/L) = -7 z/L \quad z/L > 0$$

$$\psi_q(z/L) = 2 \ln [(1 + x^2)/2] \quad z/L < 0$$

$$x = (1 - 16 z/L)^{1/4}$$

From these relations and the interpolated wind speed, air-sea temperature difference, and dew point depression u_* , T_* , and Q_* were calculated in an iterative fashion until u_* changed by less than 1%. These values were then used to find the stress and heat fluxes. The wind stress, γ , the sensible heat flux, H_s , and the latent heat flux, H_l , are

$$\begin{aligned} \gamma &= \rho u_*^2 \\ H_s &= -\rho c_p T_* u_* \\ H_l &= -\rho L Q_* u_* \end{aligned}$$

where c_p is the heat capacity of air, L is the latent heat of vaporization of water, and ρ is the air density.

IX. SAMPLE DATA

Sample time series plots of the interpolated values from observations for the central Ocean Storms mooring (CO, 47.472°N, 139.263°W) are shown in Figure 11. The corrected values of wind speed, wind direction, air pressure, and air temperature are plotted for the period 20 August 1987 to 30 April 1988. The corrections are based on the values reported in Table III under "all three buoys":

$$S = 1.58 + 0.161 G + 0.352 S_i$$

$$T_{\text{air}} = -0.75 + 1.026 T_i$$

where S is the corrected wind speed, G the geostrophic wind speed, S_i the interpolated wind speed, T_{air} the corrected air temperature, and T_i the interpolated air temperature.

The air stress and sensible heat flux were calculated for the location of the central Ocean Storms mooring, CO, using the estimates of the wind speed, air-sea temperature difference, and dew point depression from the observations. Corrections were applied as shown in Table III under "all three buoys." Time series plots of the air stress and the sensible flux are shown in Figure 12. We see that the stress has a few large events, notably on 13 September, 4 October, and in early December. The sensible heat flux is also punctuated by a few large events, usually corresponding to the stress events. The large uncertainty in the air-sea temperature difference, 1.0° , means there is a large uncertainty in the heat flux. The latent heat flux is derived from the interpolated dew point depression from ships of opportunity and as such is very uncertain and has not been included. It was calculated to be about twice the sensible heat. Also plotted, in Figure 13, is the sum of the 6 hour values of the air stress and heat flux for the entire period. Again we see the episodic nature of the fluxes, but with a different perspective. In both Figures 12 and 13, October is seen as a slow month and late November and December the time of peak air stress and heat flux.

OCEAN STORMS MOORING CO. ESTIMATES FROM OBSERVATIONS

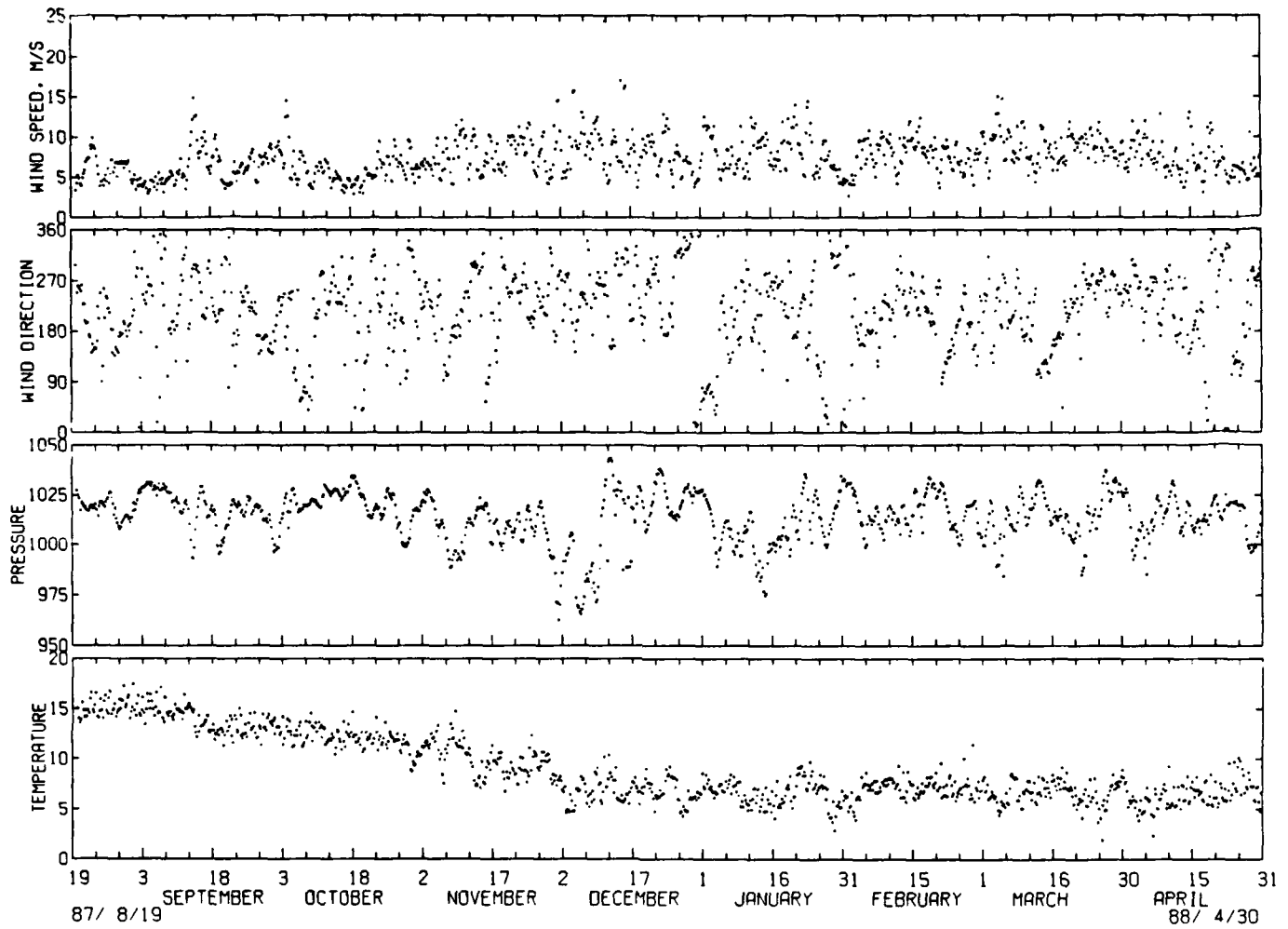


Figure 11. Time series of the estimates of the wind speed and direction, air pressure, and temperature for the central Ocean Storms mooring, CO (47.47°N, 139.26°W). The estimates are based on interpolations from observations which were corrected by the values shown in Table III under "all three buoys." There are 4 days for each tick mark.

OCEAN STORMS MOORING CO. ESTIMATES FROM OBSERVATIONS

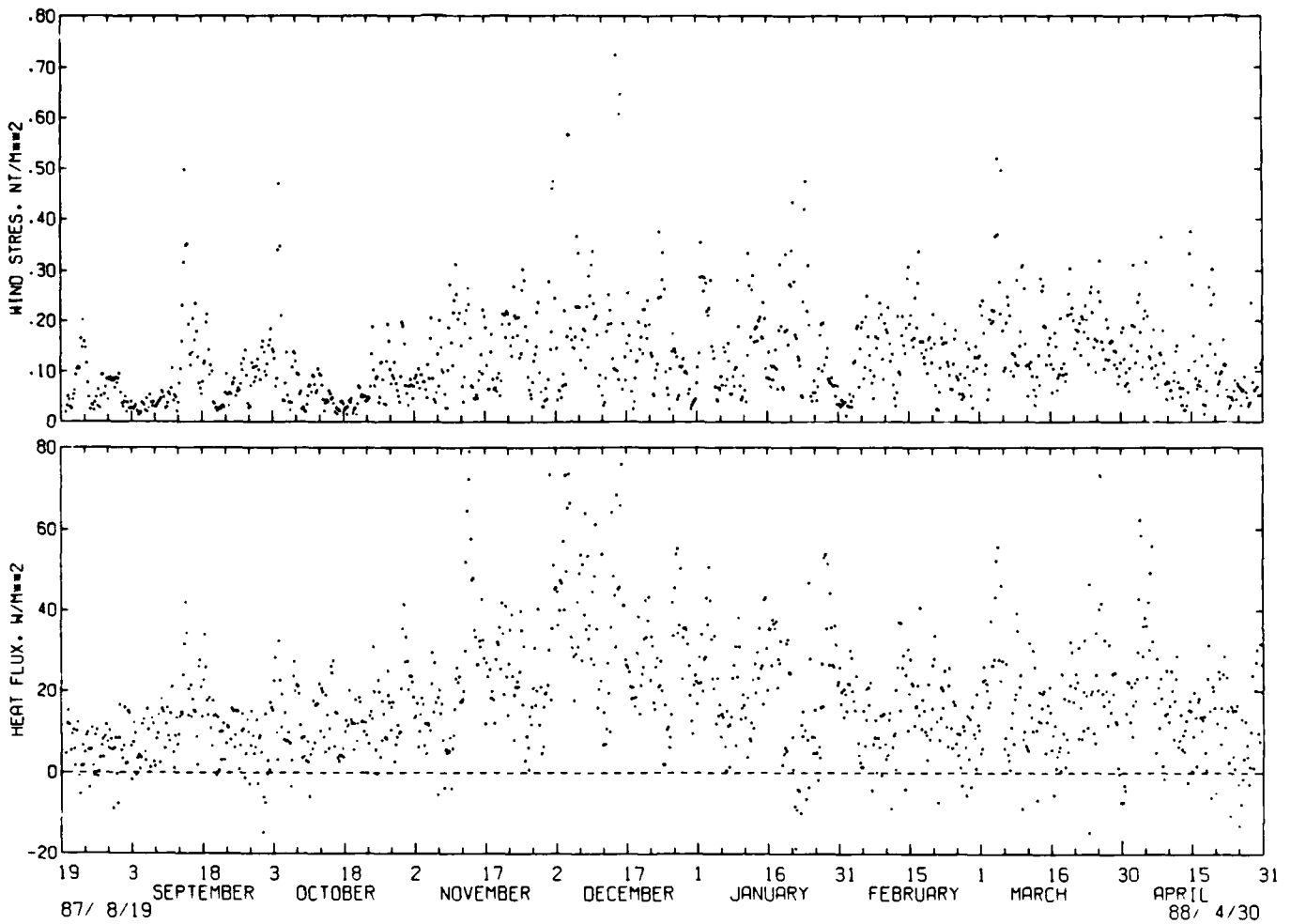


Figure 12. Time series of estimates of the stress and the sensible heat flux at the center of the Ocean Storms moored array, based on estimates of the wind speed, air-sea temperature difference, and dew point depression interpolated from the Ocean Storms data set every 6 hours.

INTEGRATED STRESS AND HEAT FLUX, CO

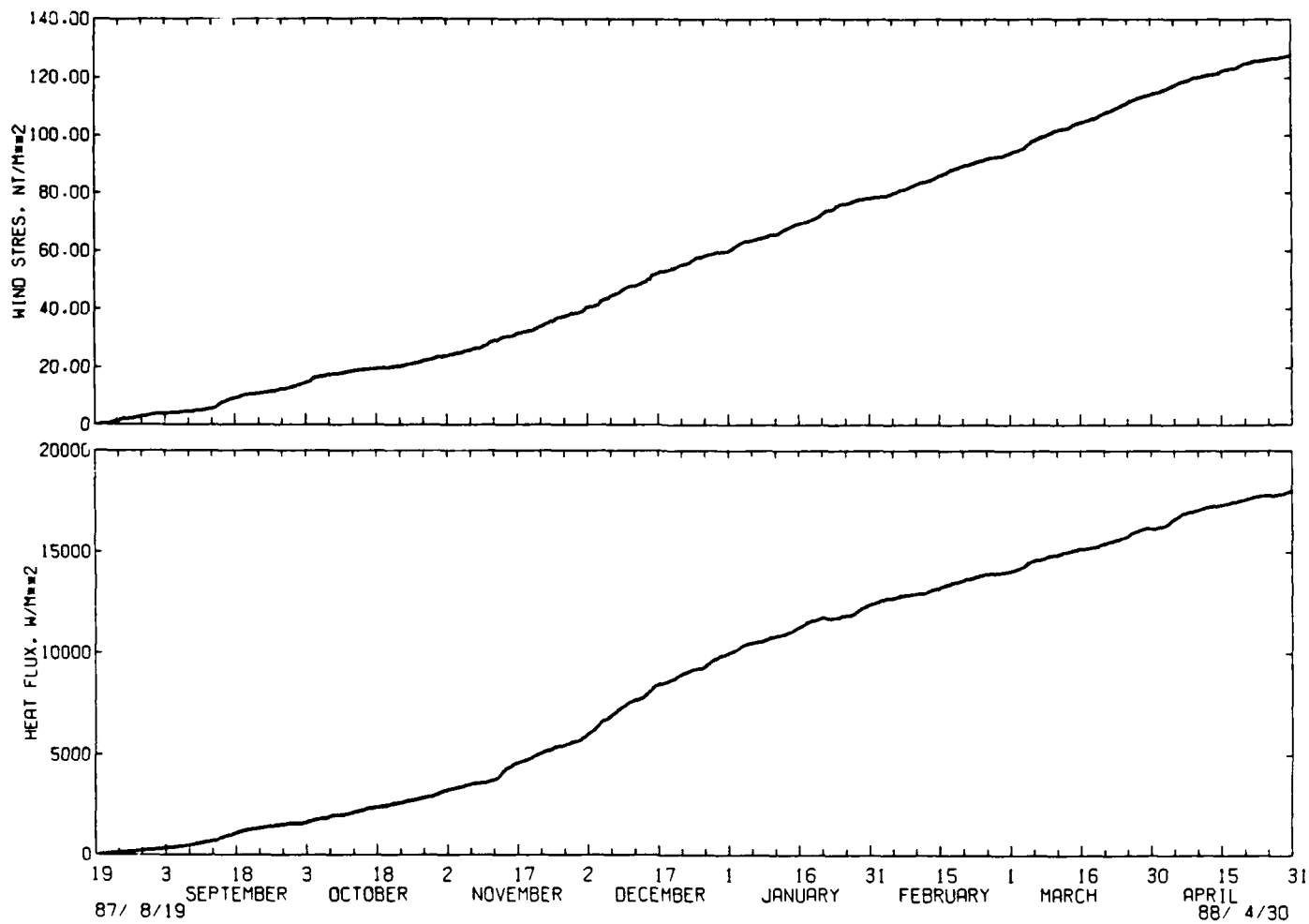


Figure 13. Time series of the sum of the air stress and the sensible heat flux shown in Figure 12.

X. RECOMMENDATIONS

The best method of using the interpolated values presented here depends on the use to be made of them. The NMC interpolations are slightly better than those based on observations or those from Metlib, and we have coverage from the beginning of the experiment until the end of May. The main drawback is the lower time resolution and the lack of air-sea temperature differences after 12 March 1988. I suggest using the corrections shown in Table IV for the combination of all three buoys in order to remove any bias that may arise from the measurement system of one particular buoy. I also suggest using the interpolated wind speed and not the combination of the interpolated wind speed and the geostrophic wind speed, since the increase in accuracy obtained by including the geostrophic wind is not very significant. Events that have a time scale of less than a day will not be well represented; if the buoys are not recording high winds accurately, the corrected interpolated wind speeds will reflect this. The recommended correction equations for the NMC interpolations are

$$\begin{aligned}\text{wind speed} &= 1.28 + 0.588 S_i \\ \text{wind direction} &= \text{NMC wind direction} \\ \text{air-sea temperature} &= -1.96 + 0.60 DT_i\end{aligned}$$

where S_i and DT_i are the interpolated wind speed and air-sea temperature, respectively. The uncertainty in the resultant wind speed will be about 1.7 m/s, in the wind direction about 15°, and in the air-sea temperature difference about 1.0°C. Wind speed and air temperature are referenced to the 5 m level; a 5% increase in the wind speed will usually be needed to adjust it to the 10 m level.

If greater time resolution is desired, bearing in mind the low coherence of the interpolated winds and the buoy winds at periods of less than a day, the interpolated observations can be used. The recommended correction equations are

$$\begin{aligned}\text{wind speed} &= 1.58 + 0.161 G + 0.352 S_i \\ \text{wind direction} &= \text{interpolated wind direction} \\ \text{air-sea temperature} &= -0.82 + 0.717 DT_i\end{aligned}$$

where G is the geostrophic wind speed. The dew point depressions interpolated from the observations should be used with great caution. The uncertainty in the resultant wind speed will be about 1.8 m/s, in the wind direction about 23°, and in the air-sea temperature difference about 1.0°C.

Acknowledgments

This work was supported by the Office of Naval Research under contract N00014-87-K-0004 with the University of Washington. Additional support in the form of computing resources was provided by the Pacific Marine Environmental Laboratory and the School of Geophysics, Georgia Institute of Technology. I would like to thank Dr. Eric D'Asaro for many useful discussions and also wish to thank Dr. D. A. Woolley, writing consultant, for editing the manuscript.

REFERENCES

- Brown, R. A., and W. T. Liu, 1982: An operational large-scale marine planetary boundary layer model. *J. Appl. Meteor.*, *21*, 261-269.
- D'Asaro, E. A., 1985: Ocean Storms, A Three-Dimensional Severe Storm, Air/Sea Interaction Experiment: Overview and Core Program. Applied Physics Laboratory, Univ. Of Wash., November 29, 1985, 39 pp.
- Gandin, L. S., 1963: The objective analysis of meteorological fields, Leningrad, 1963. English translation, Israel Program for Scientific Translations, Jerusalem, 1965.
- Kondo, J., 1975: Air-sea bulk transfer coefficients in diabatic conditions. *Bound.-Layer Meteor.*, *9*, 91-112.
- Large, W. G., and S. Pond, 1982: Sensible and latent heat flux over the ocean. *J. Phys. Oceanogr.*, *12*, 464-482.
- Liu, W., K. B. Katsaros, and J. A. Businger, 1979: Bulk parameterization of air-sea exchanges of heat and water vapor including the molecular constraints at the interface. *J. Atmos. Sci.*, *36*, 1722-1735.
- Macklin, S. A., R. L. Brown, J. Grey, R. W. Lindsay, 1984: Metlib-II - A Program Library for Calculating and Plotting Atmospheric and Oceanic Fields. NOAA Technical Memoranda ERL PMEL-54, 53 pp.
- Marsden, R. F., 1987: A comparison between geostrophic and directly measured winds over the northeast Pacific Ocean. *Atmosphere-Ocean*, *25*, 387-401.
- MWL, 1988a: North Pacific Weather Log, July, August, and September, 1987, *Mariner's Weather Log*, *32*(1), 46-53.
- MWL, 1988b: North Pacific Weather Log, October, November, and December, 1987, *Mariner's Weather Log*, *32*(2), 46-53.

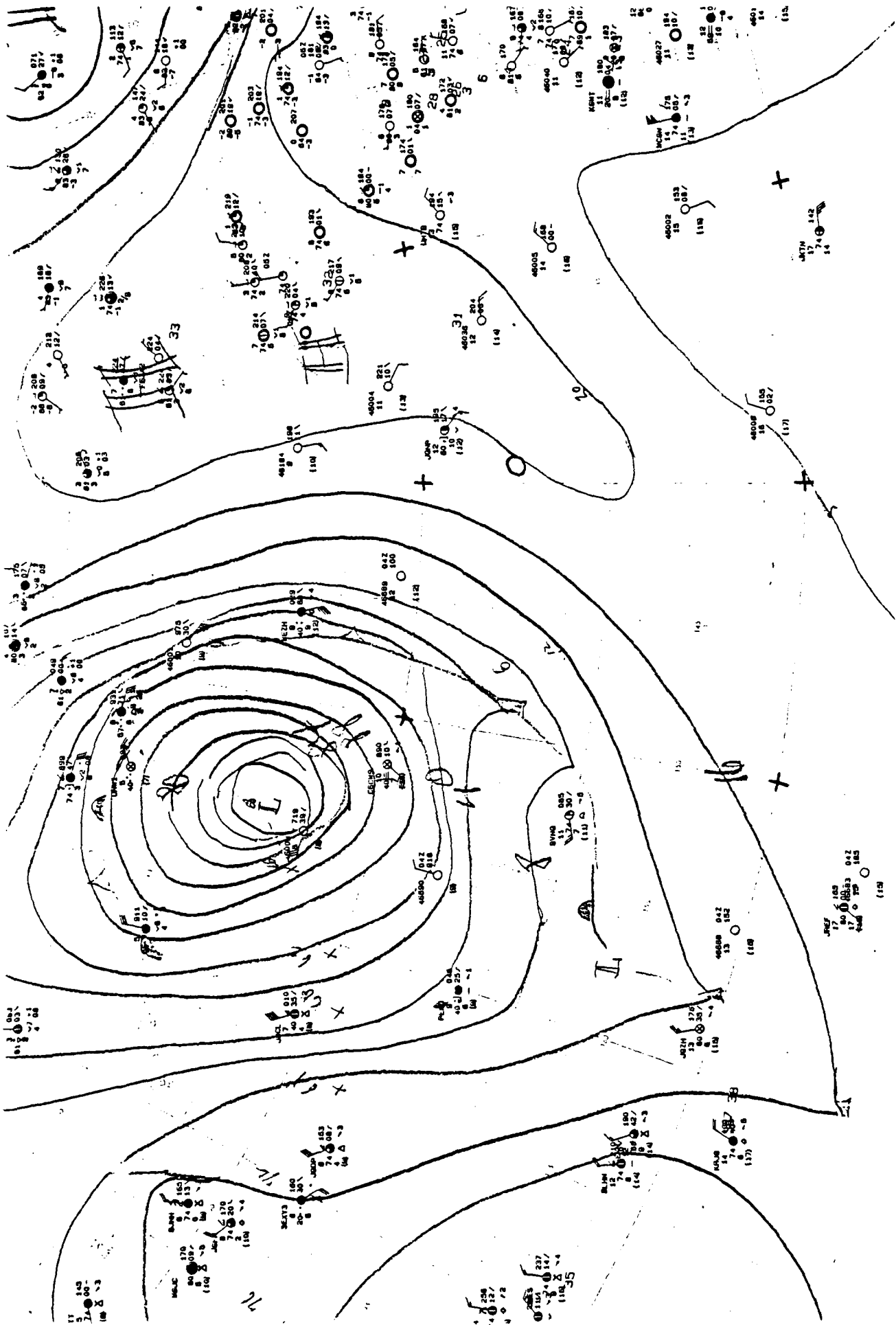
MWL, 1988c: North Pacific Weather Log, January, February, and March, 1988, *Mariner's Weather Log*, 32(3), 47-53.

NDBC, 1986: Climatic Summaries for NDBC Data Buoys. National Data Buoy Center, National Weather Service, NOAA. April 1986.

Thompson, K. R., R. F. Marsden, and D. G. Wright, 1983: Estimation of low- frequency wind stress fluctuations over the open ocean. *J. Phys. Oceanogr.*, 13, 1003-1011.

APPENDIX A

Synoptic maps analyzed by forecasters from the Canadian Atmospheric Environment Service and the Seattle Weather Service Office at the Ocean Storms Forecast Office, Sand Point, Seattle. Included are a portion of the 0600 and 1800 GMT maps for the period 20 October to 9 December 1987. The location of the Ocean Storms moorings are indicated with a small circle. Fiducial marks are at the intersections of 40° and 50°N with 130°, 140°, and 150°W.



0600 Z

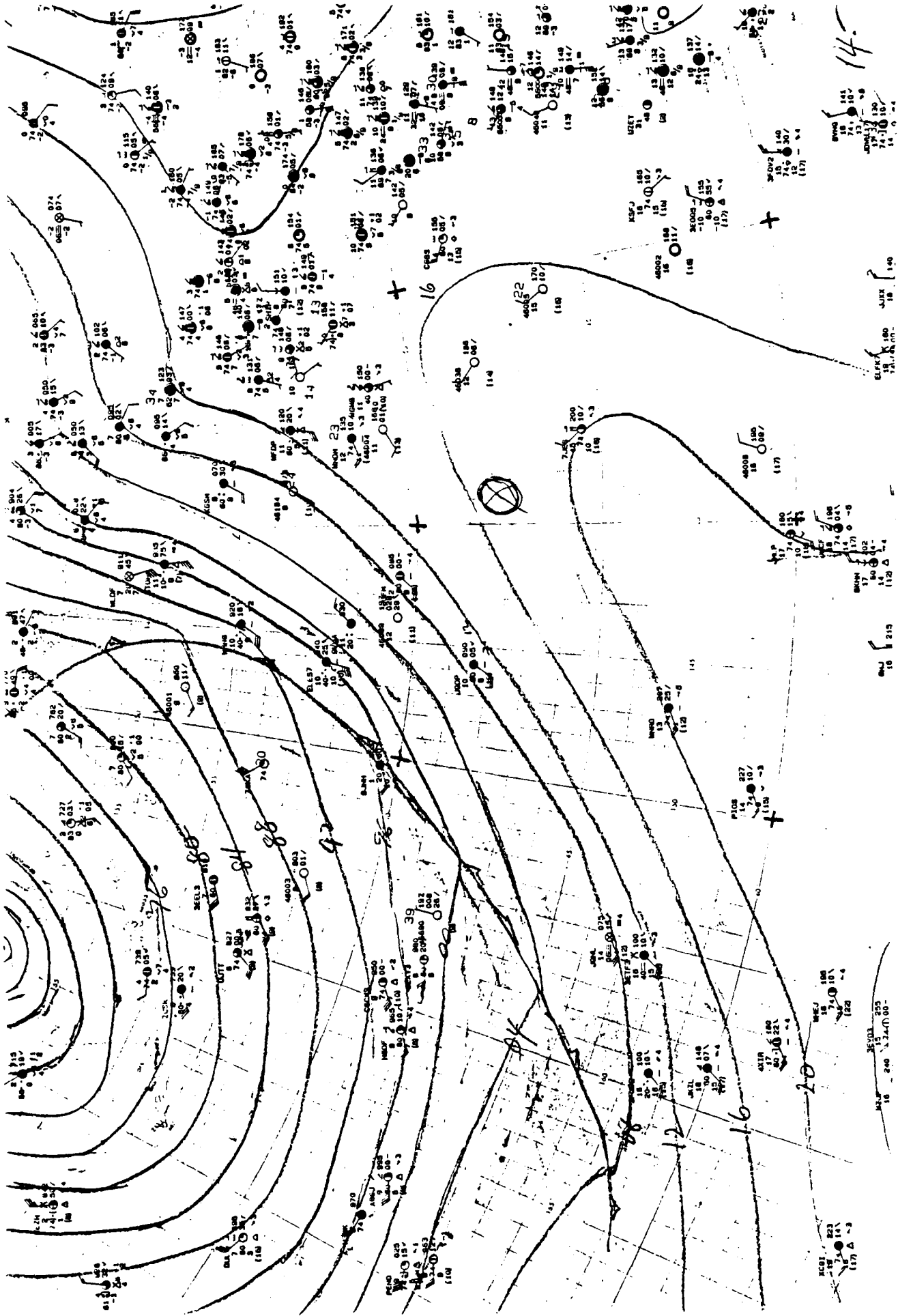
10-21-87

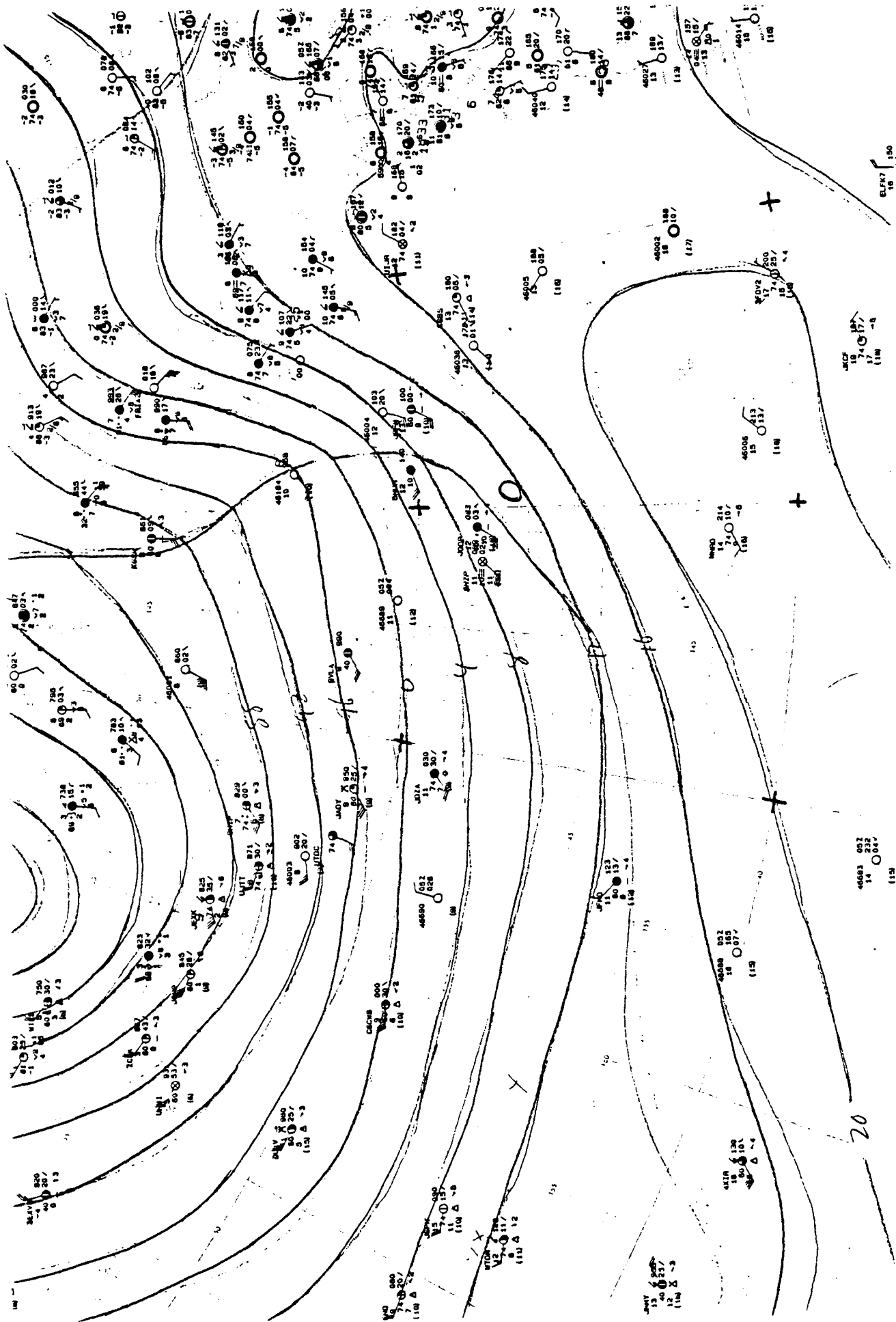
A5

A10

10-23-87

1800 Z





A11

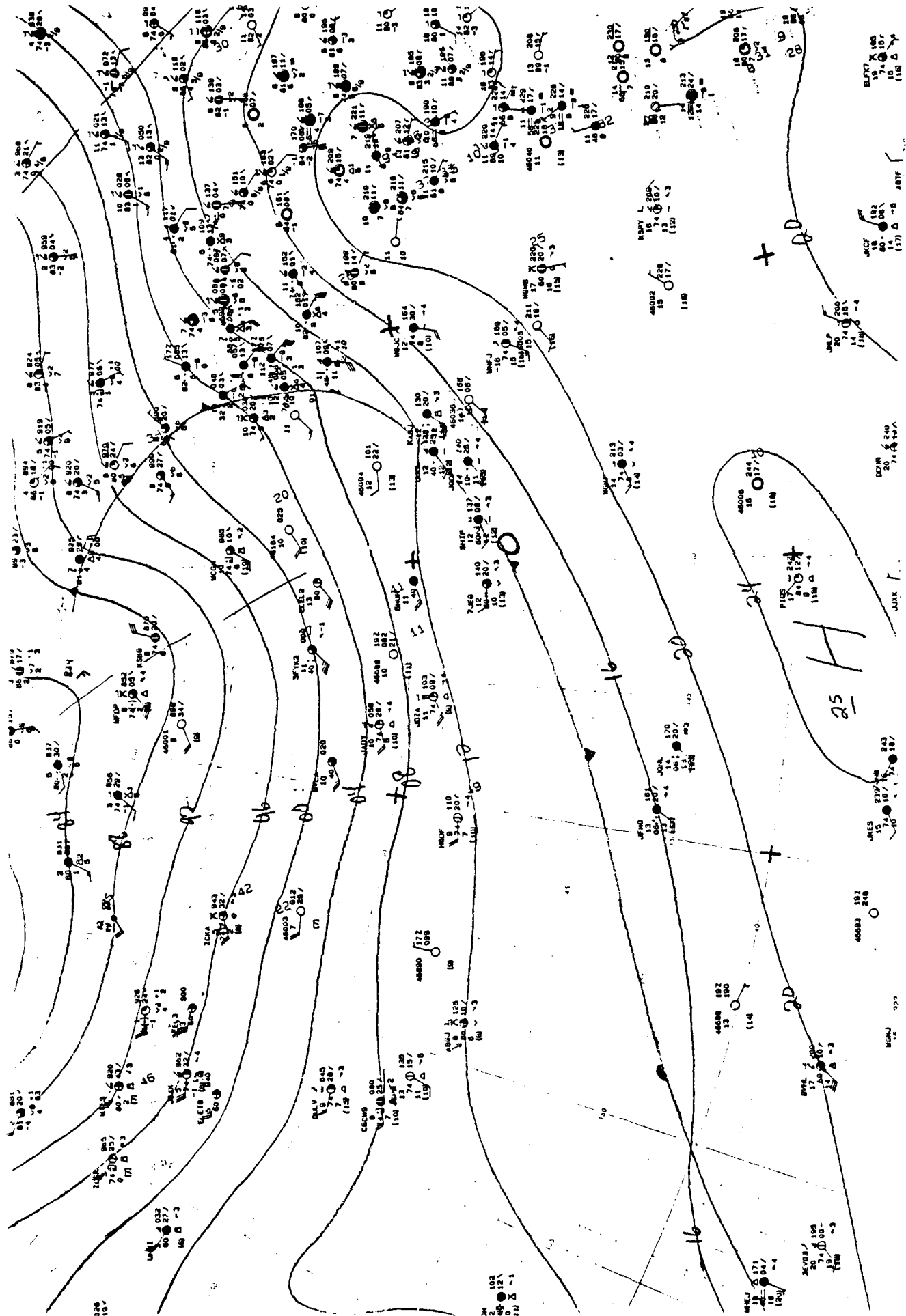
10-24-87

0600 Z

A12

10-24-87

1800 Z



25 H

16

20

22

24

26

28

30

32

34

36

38

40

42

44

46

48

50

52

54

56

58

60

62

64

66

68

70

72

74

76

78

80

82

84

86

88

90

92

94

96

98

100

102

104

106

108

110

112

114

116

118

120

122

124

126

128

130

132

134

136

138

140

142

144

146

148

150

152

154

156

158

160

162

164

166

168

170

172

174

176

178

180

182

184

186

188

190

192

194

196

198

200

202

204

206

208

210

212

214

216

218

220

222

224

226

228

230

232

234

236

238

240

242

244

246

248

250

252

254

256

258

260

262

264

266

268

270

272

274

276

278

280

282

284

286

288

290

292

294

296

298

300

302

304

306

308

310

312

314

316

318

320

322

324

326

328

330

332

334

336

338

340

342

344

346

348

350

352

354

356

358

360

362

364

366

368

370

372

374

376

378

380

382

384

386

388

390

392

394

396

398

400

402

404

406

408

410

412

414

416

418

420

422

424

426

428

430

432

434

436

438

440

442

444

446

448

450

452

454

456

458

460

462

464

466

468

470

472

474

476

478

480

482

484

486

488

490

492

494

496

498

500

502

504

506

508

510

512

514

516

518

520

522

524

526

528

530

532

534

536

538

540

542

544

546

548

550

552

554

556

558

560

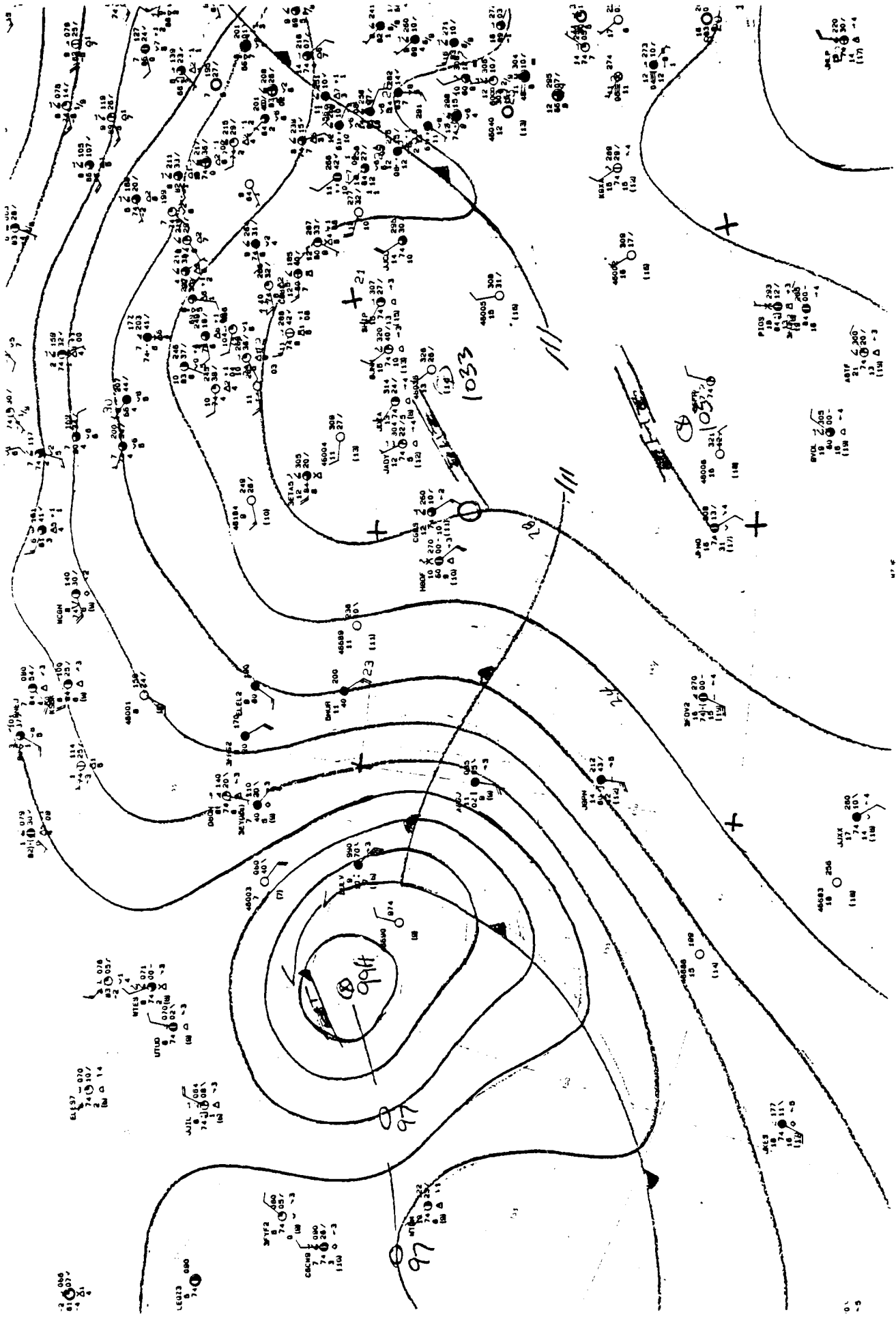
562

564

A14

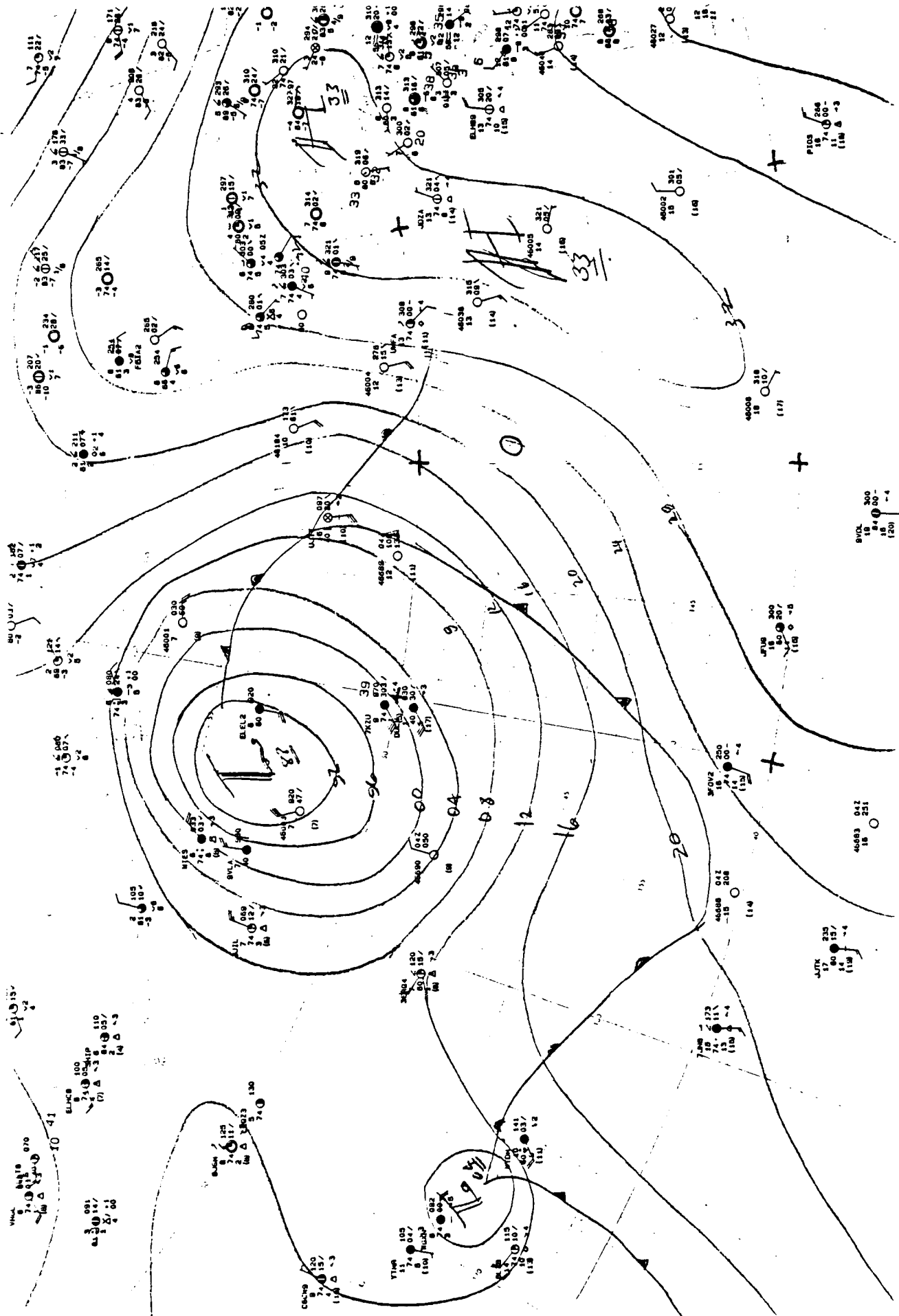
10-25-87

1800 Z



01 -5

07.6



A15

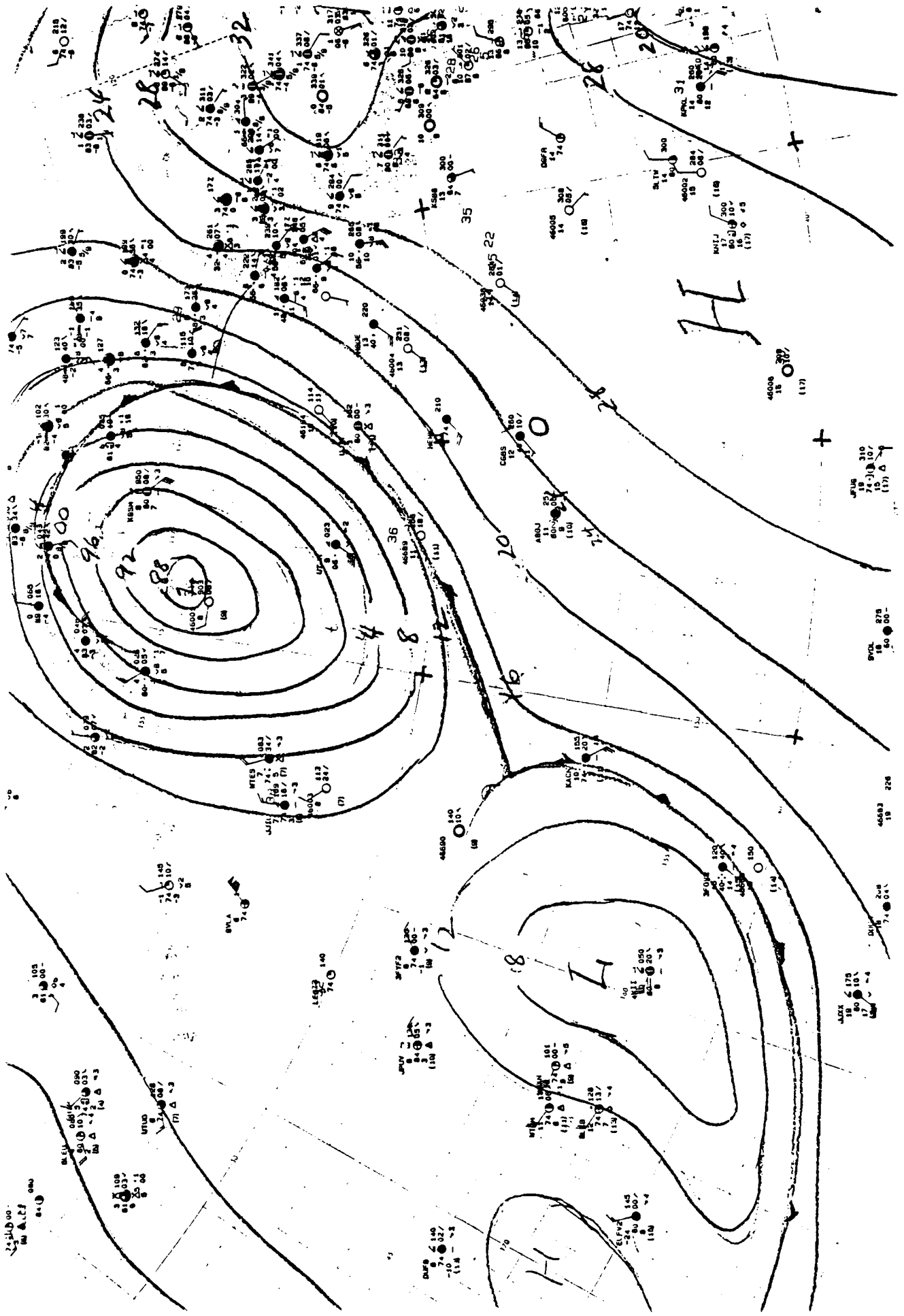
10-26-87

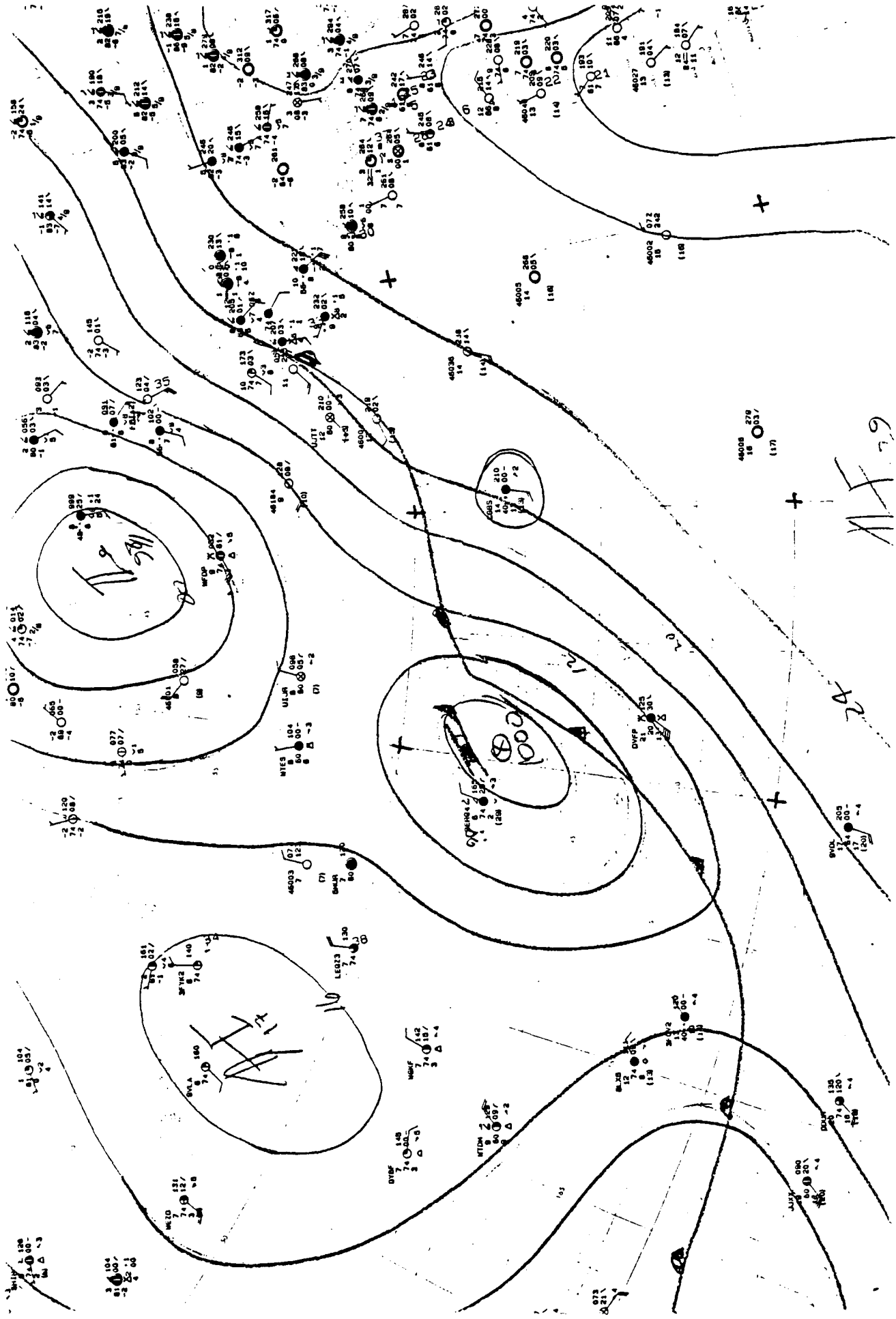
0600 Z

A16

10-26-87

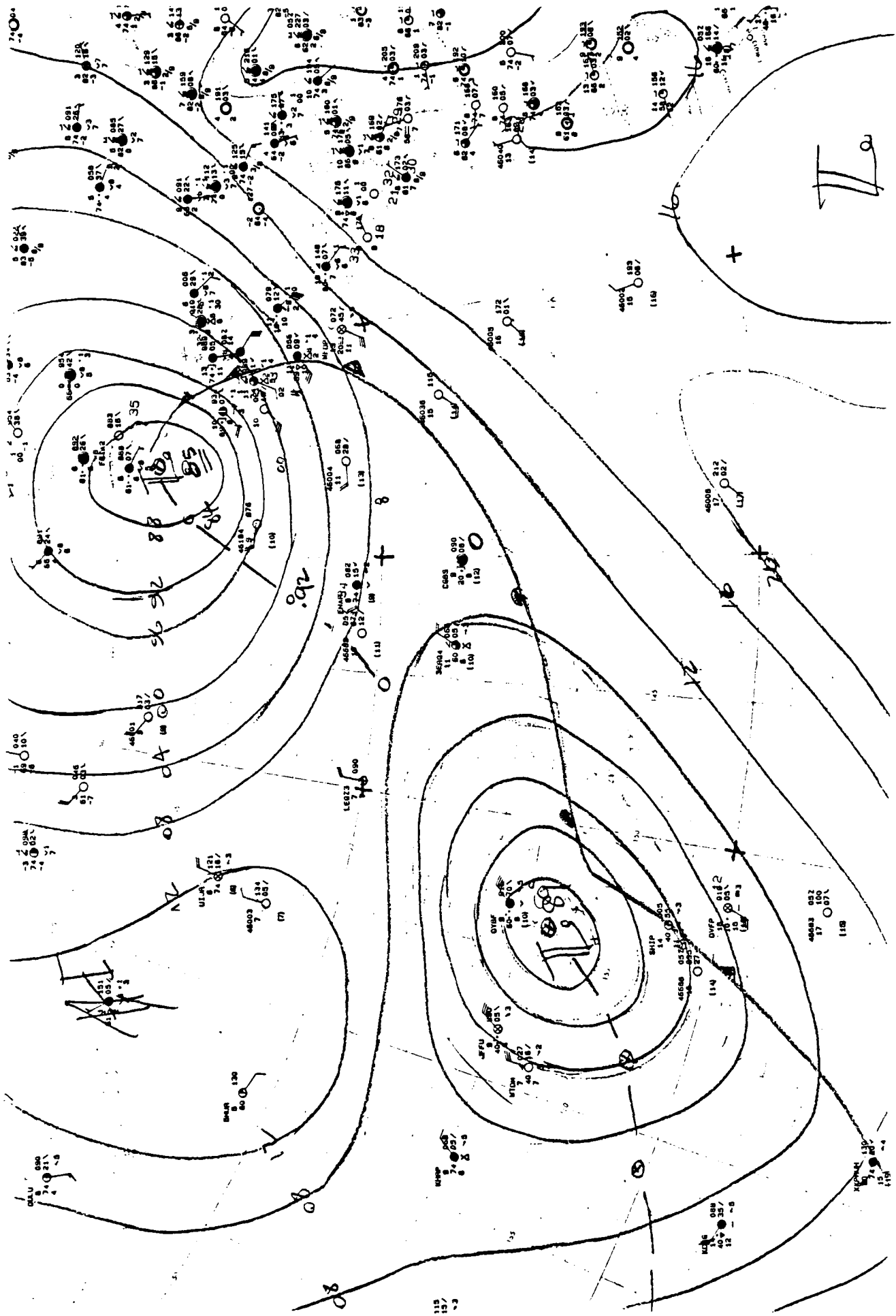
1800 Z





AF 29

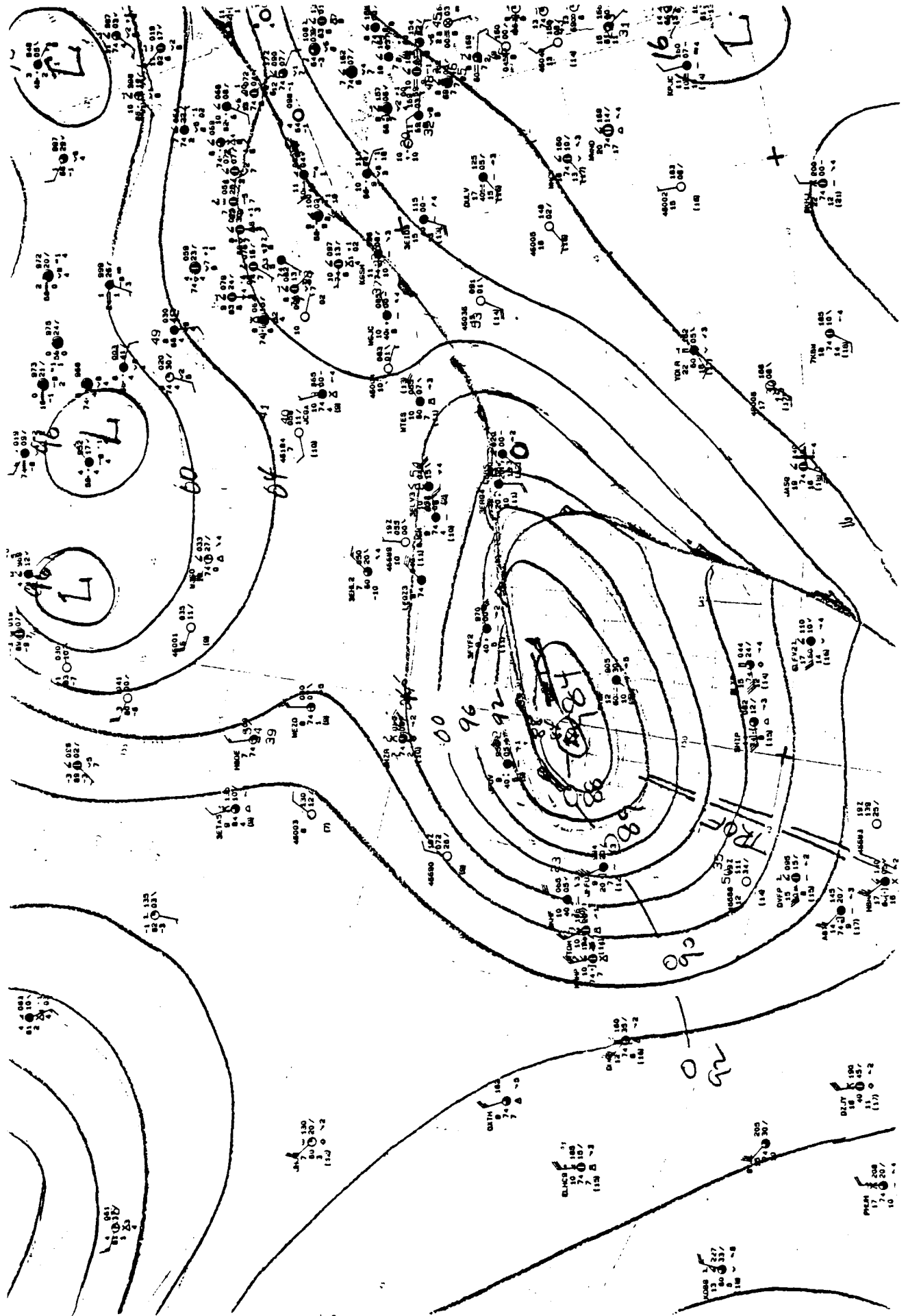
1000



A20

10-28-87

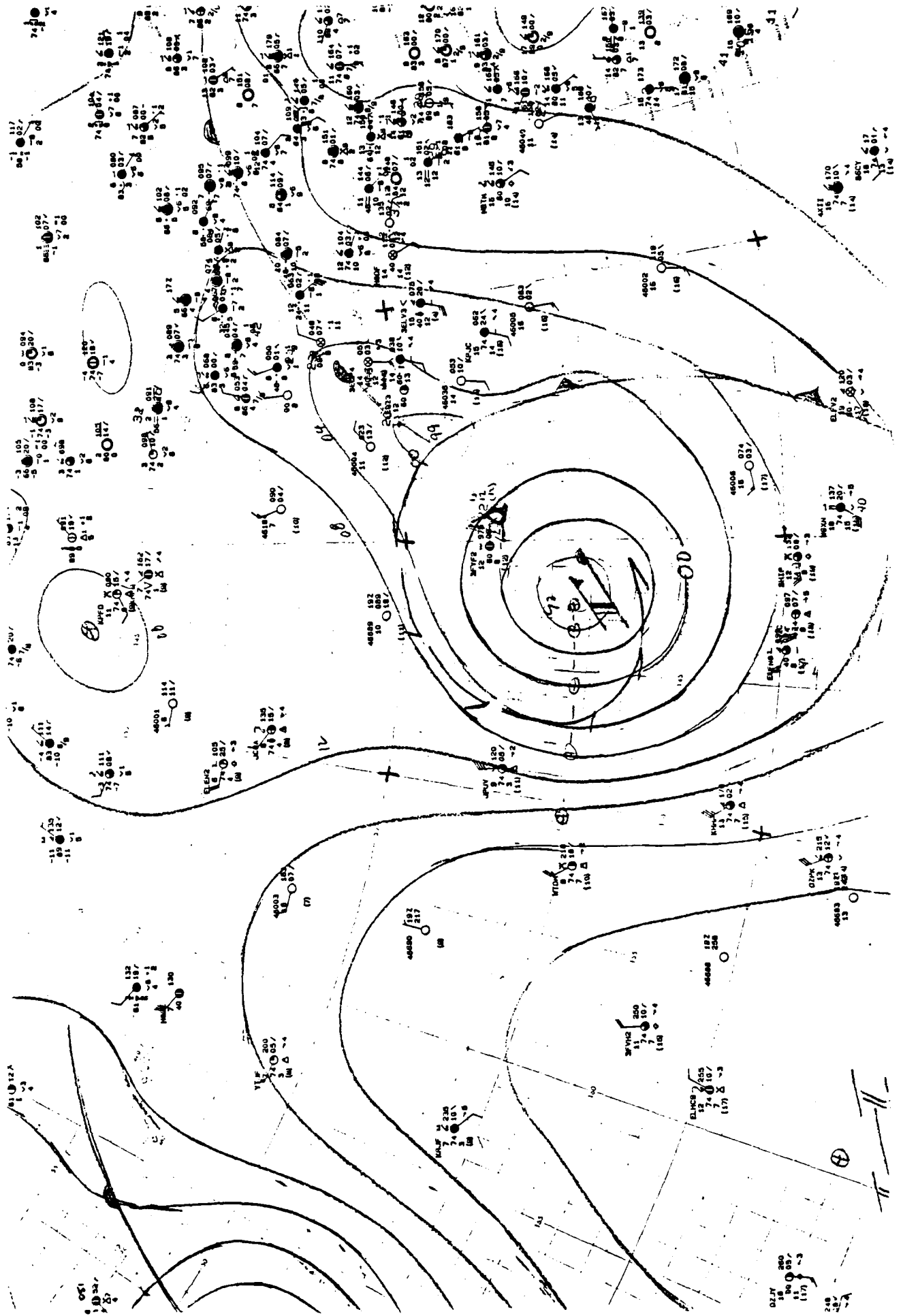
1800 Z

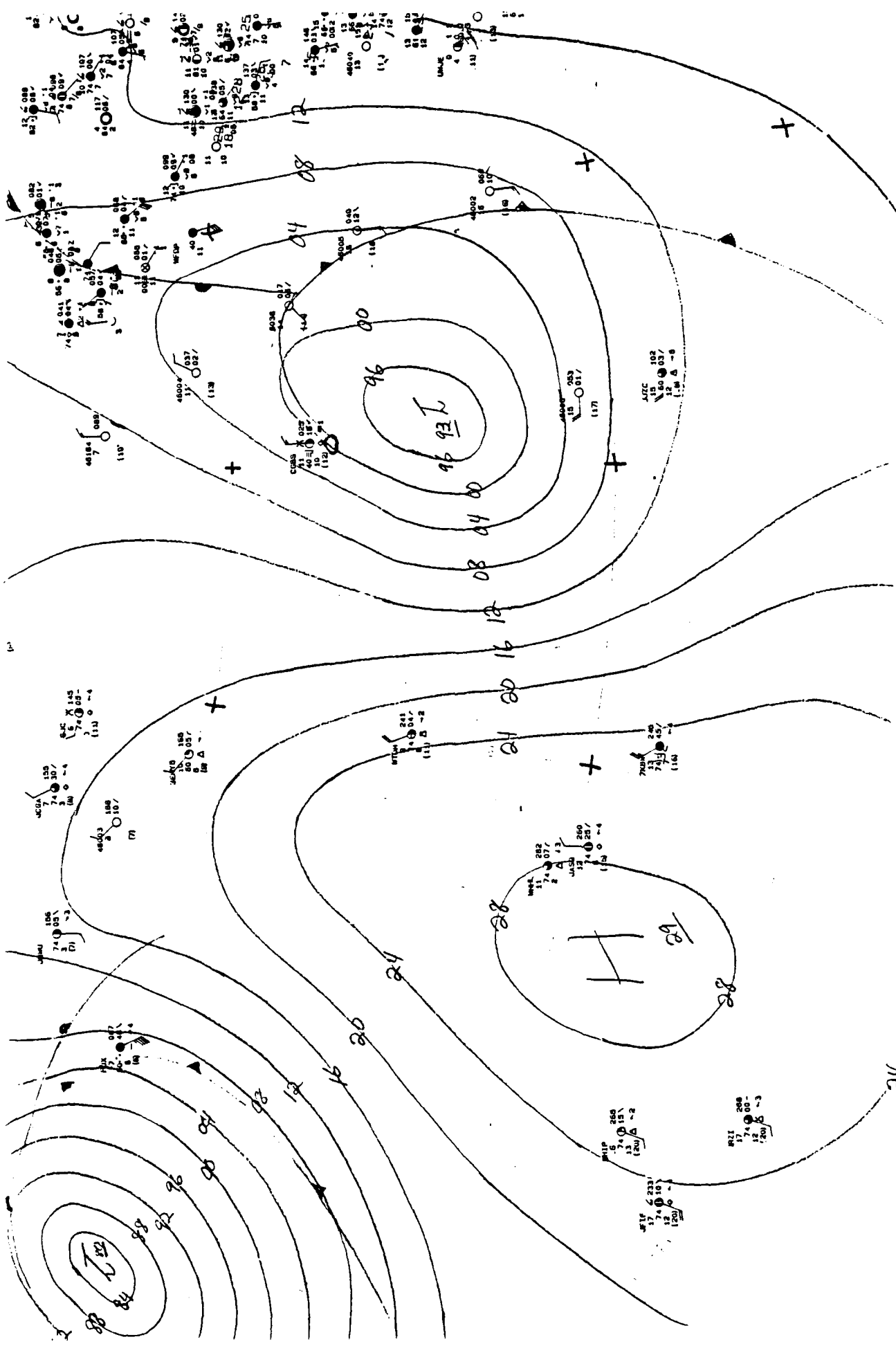


A22

10-29-87

1800 Z

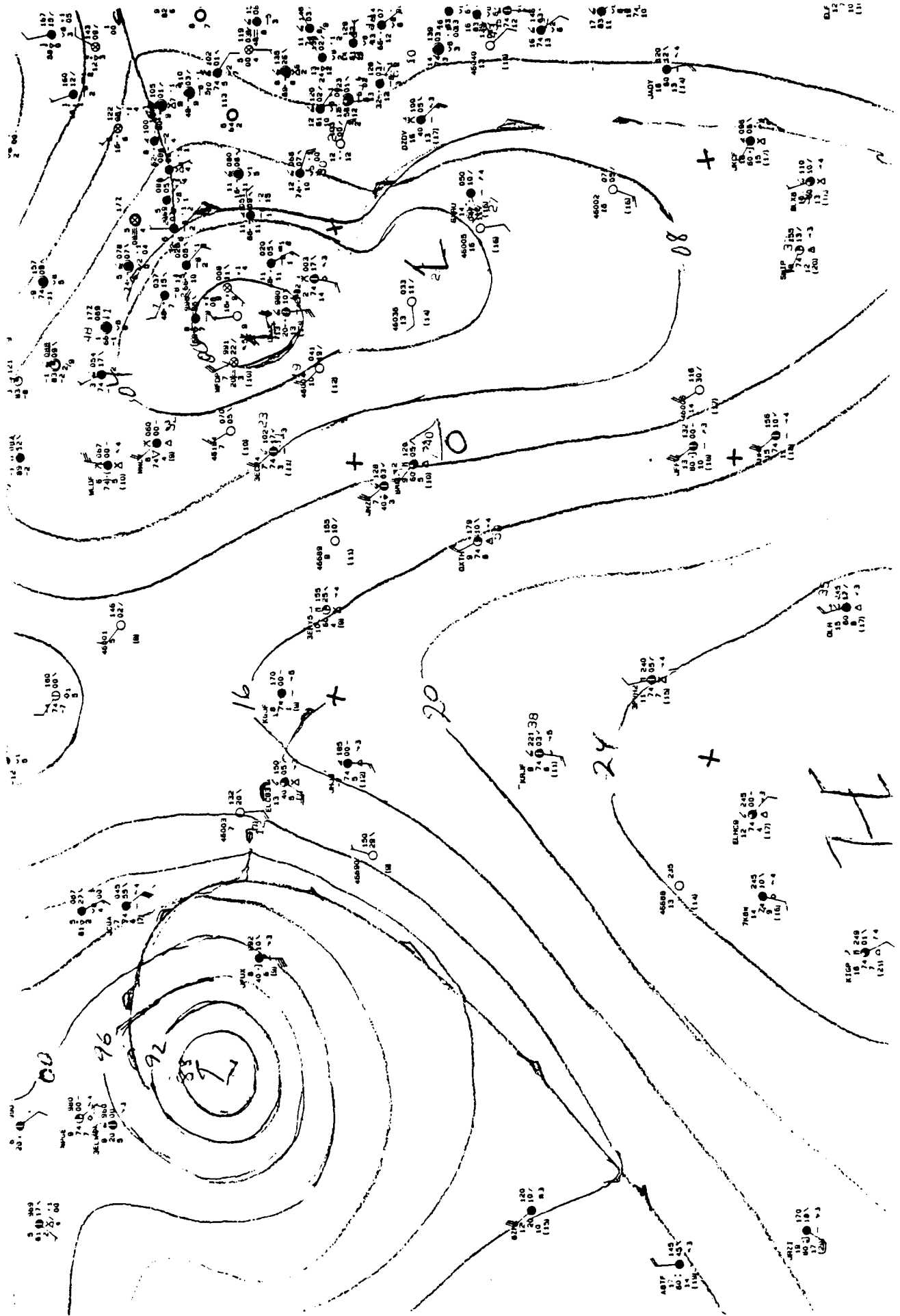


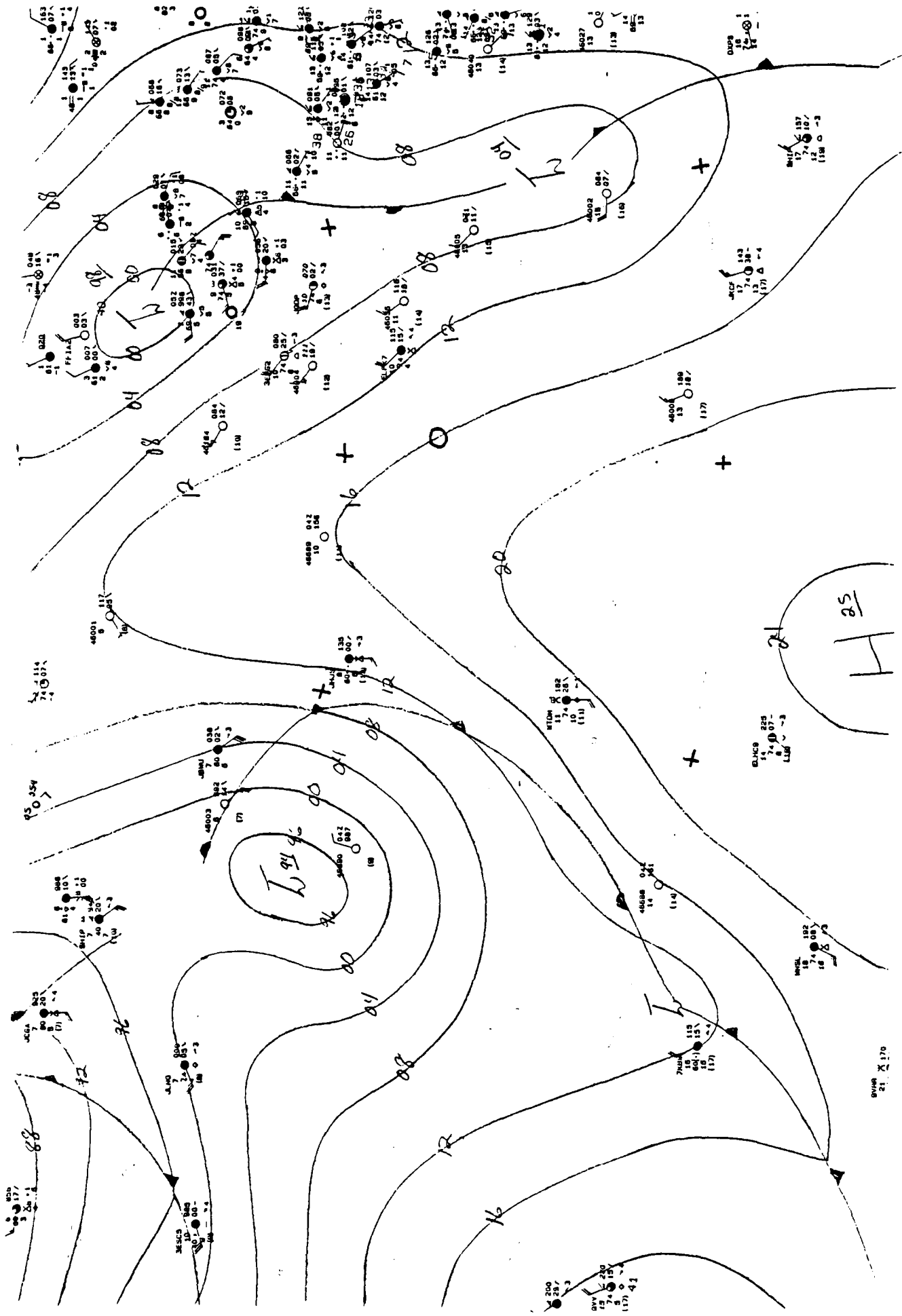


A24

10-30-87

1800 Z





A25

10-31-87

0600 Z

8170
21

ELUCR 223
14 7.4 107-
15 16 18 7.3

200
257
0.4
15 7.4 15
16 18 7.3
(17) 4.2

4508 0.2
14 14
(1.4)

182
18 7.4 108
16 18 7.3

WIDM 182
15 7.4 28
16 18
(1.1)

7.0 0.7

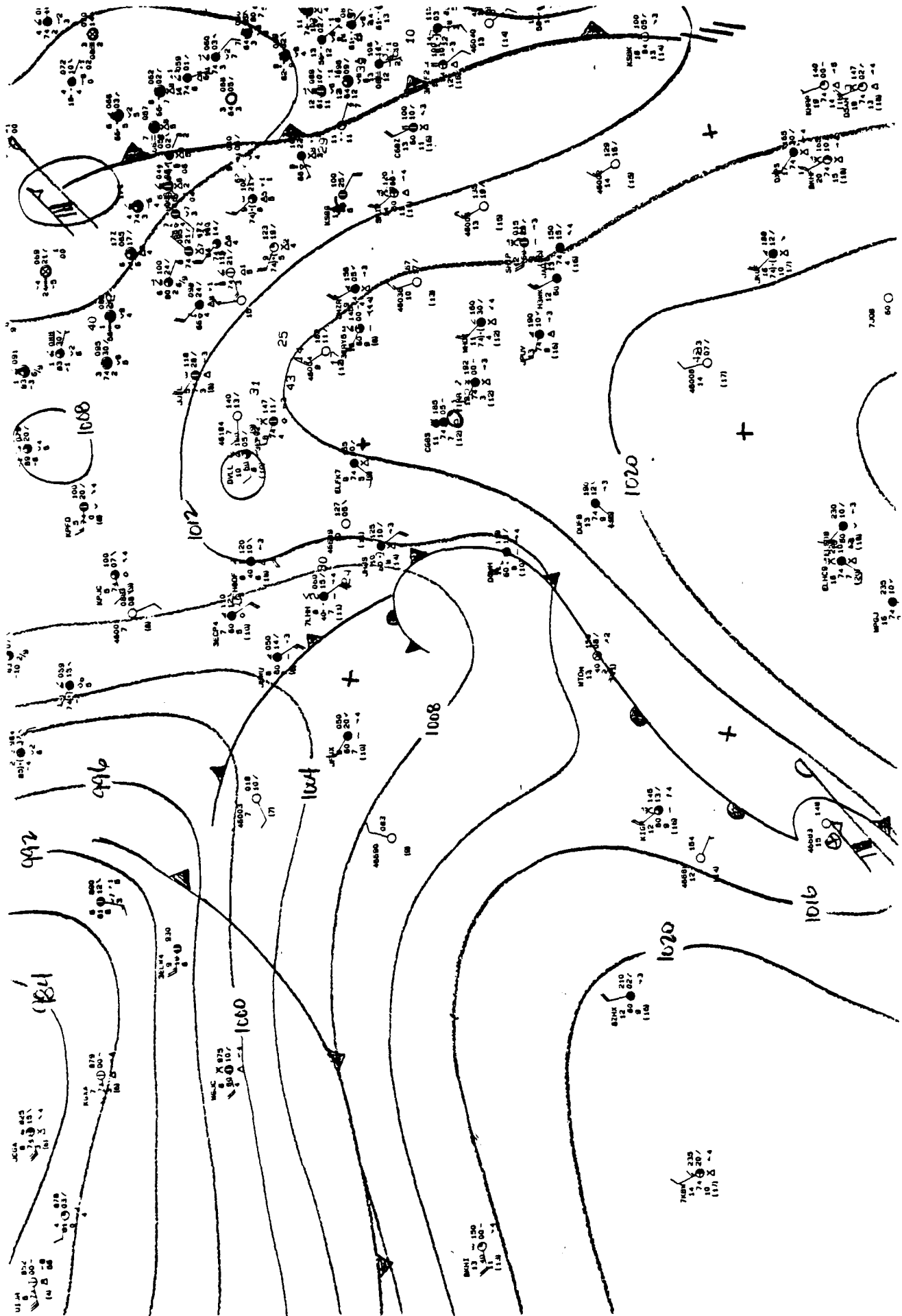
95.354

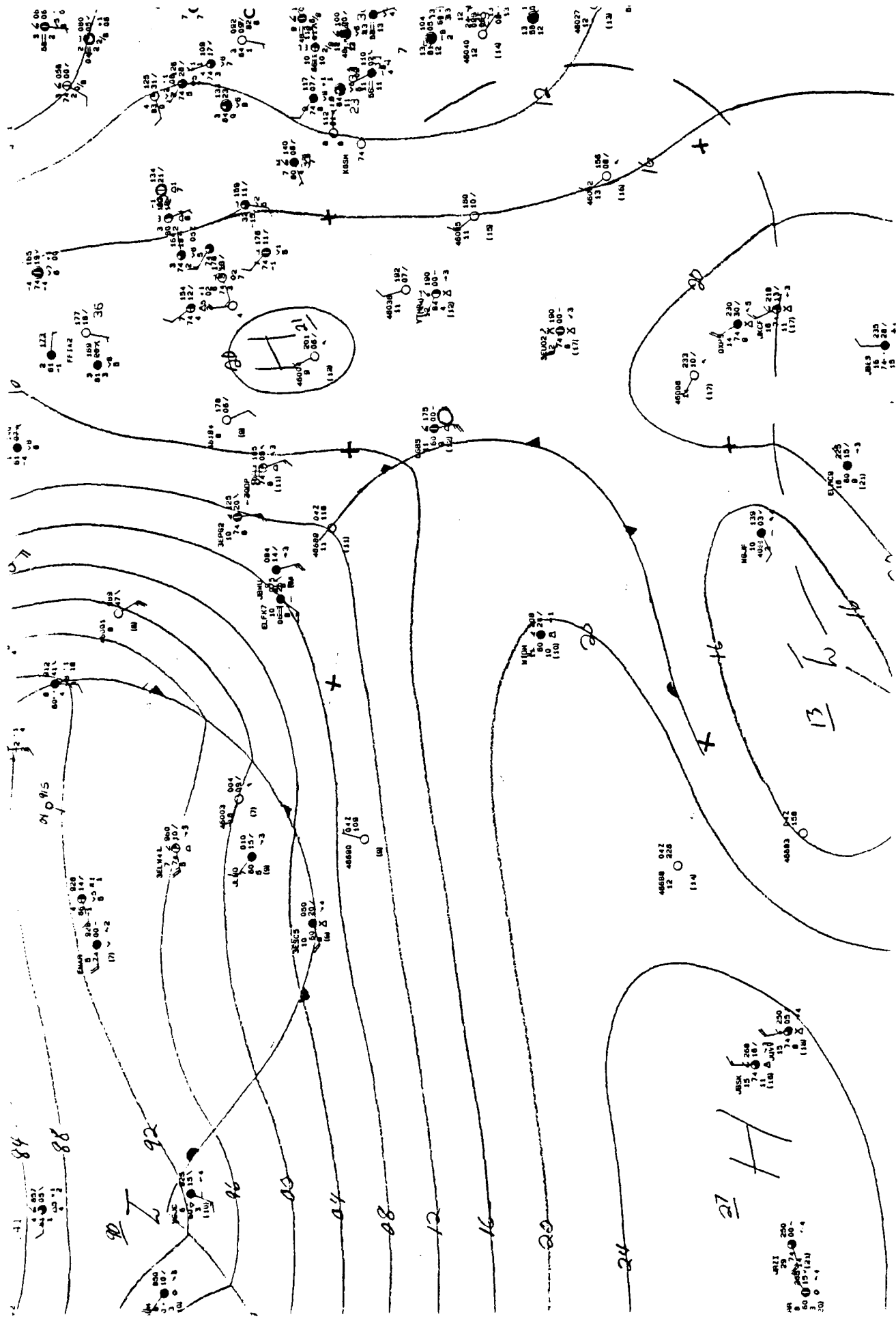
0.48
10 10
11 11
12 12
13 13
14 14
15 15
16 16
17 17
18 18
19 19
20 20
21 21
22 22
23 23
24 24
25 25
26 26
27 27
28 28
29 29
30 30
31 31
32 32
33 33
34 34
35 35
36 36
37 37
38 38
39 39
40 40
41 41
42 42
43 43
44 44
45 45
46 46
47 47
48 48
49 49
50 50
51 51
52 52
53 53
54 54
55 55
56 56
57 57
58 58
59 59
60 60
61 61
62 62
63 63
64 64
65 65
66 66
67 67
68 68
69 69
70 70
71 71
72 72
73 73
74 74
75 75
76 76
77 77
78 78
79 79
80 80
81 81
82 82
83 83
84 84
85 85
86 86
87 87
88 88
89 89
90 90
91 91
92 92
93 93
94 94
95 95
96 96
97 97
98 98
99 99
100 100

A26

10-31-87

1800 Z

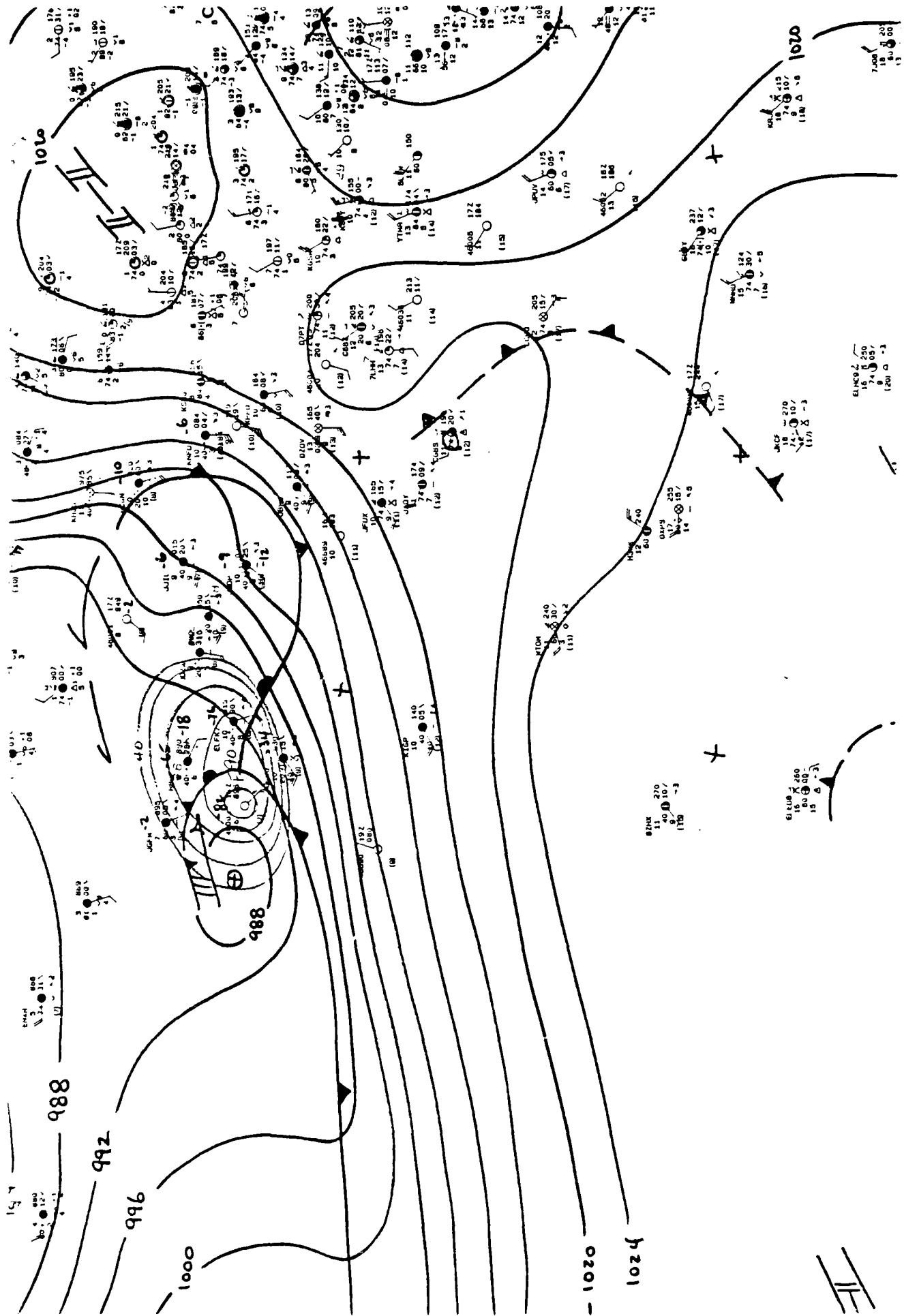


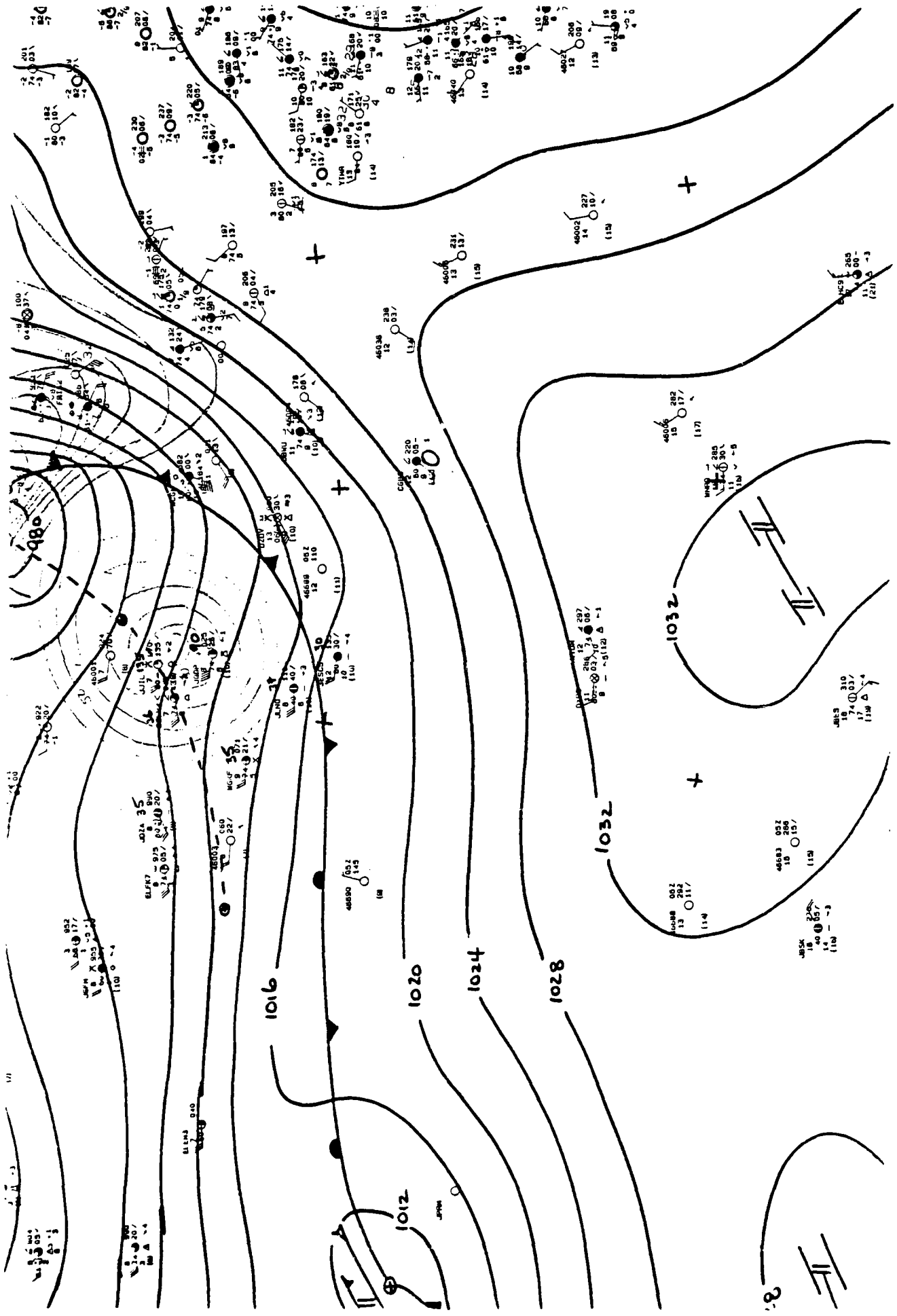


0600 Z

11-01-87

A27





0600 Z

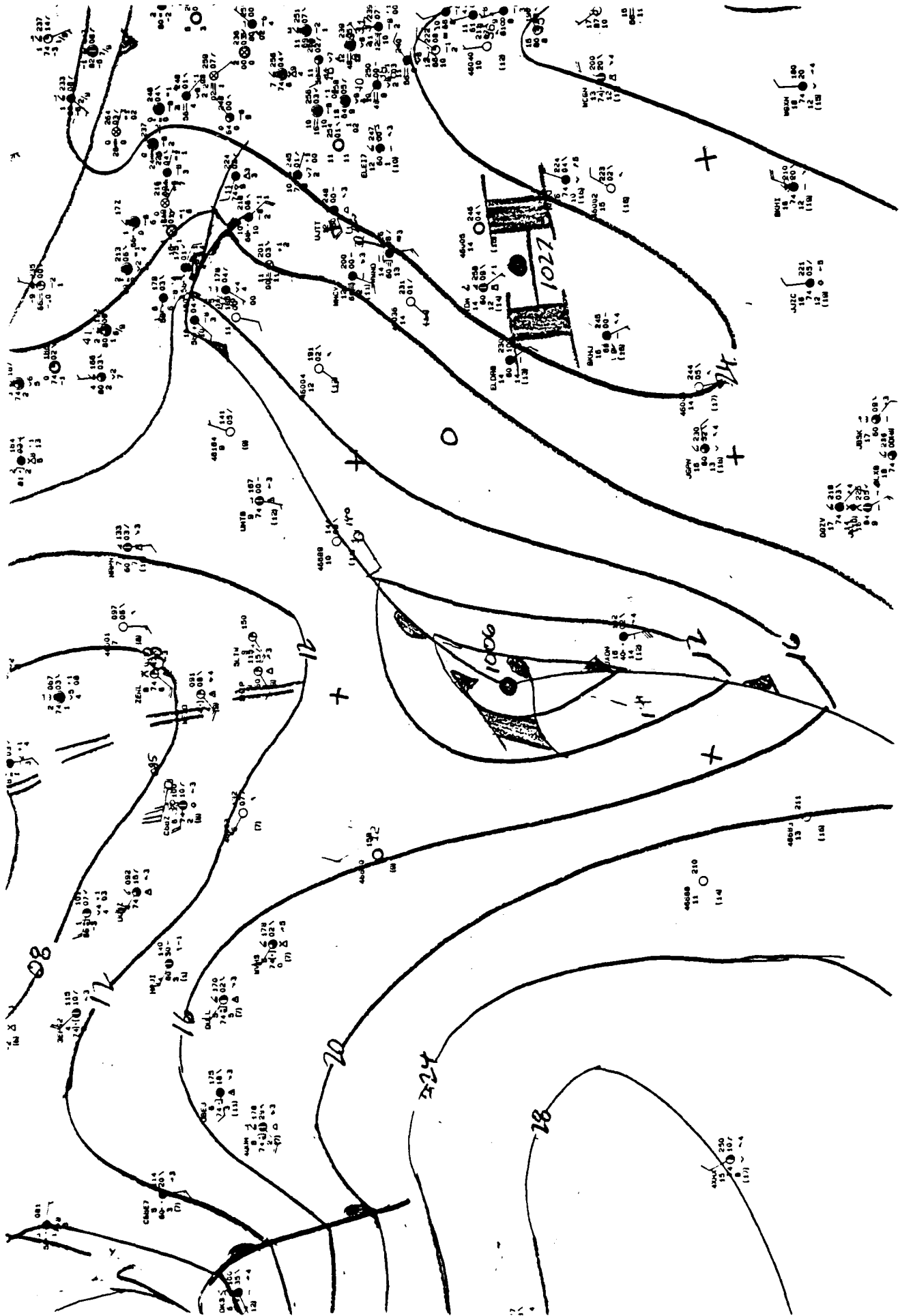
11-02-87

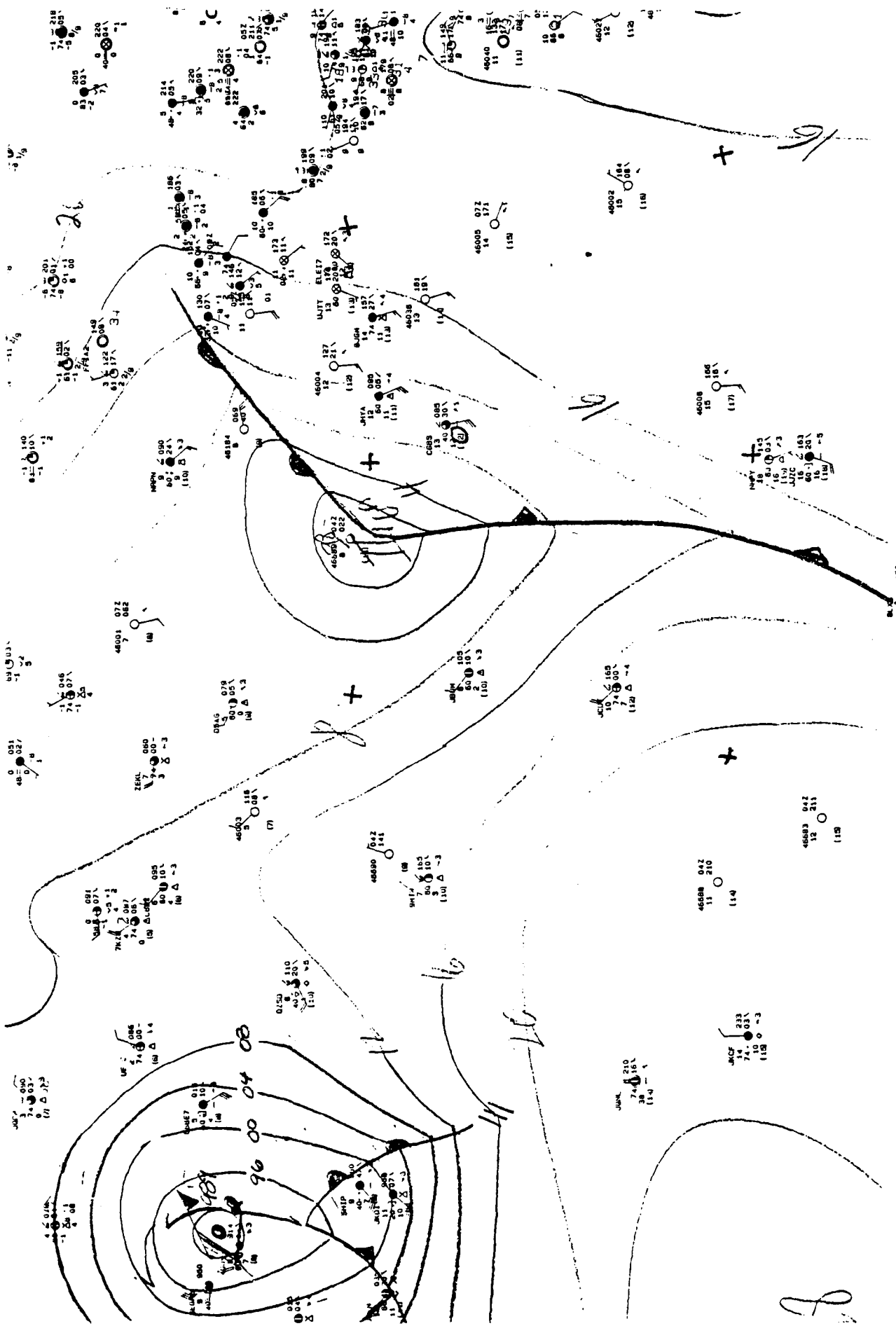
A29

A34

11-04-87

1800 Z

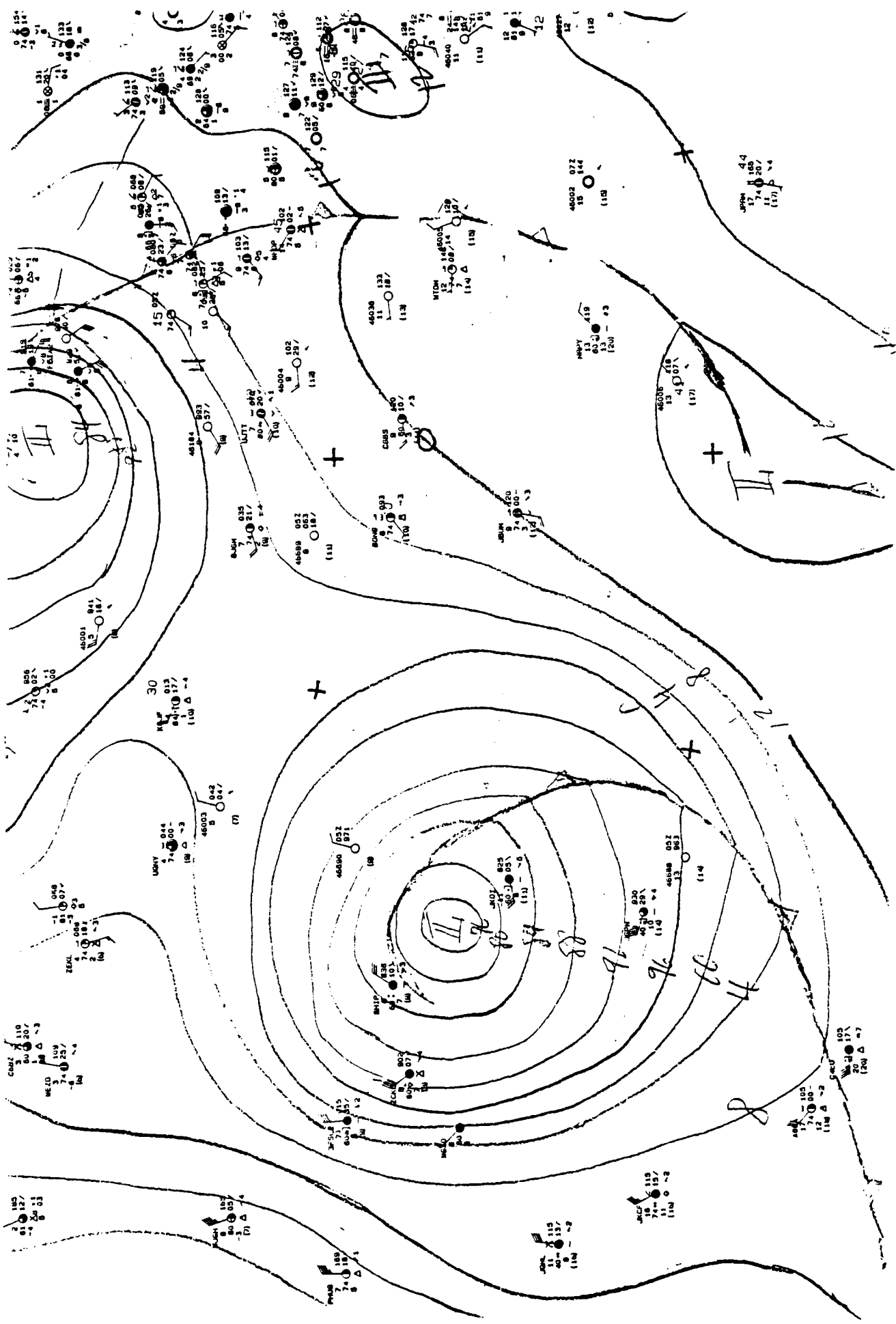




0600 Z

11-05-87

A35



A37

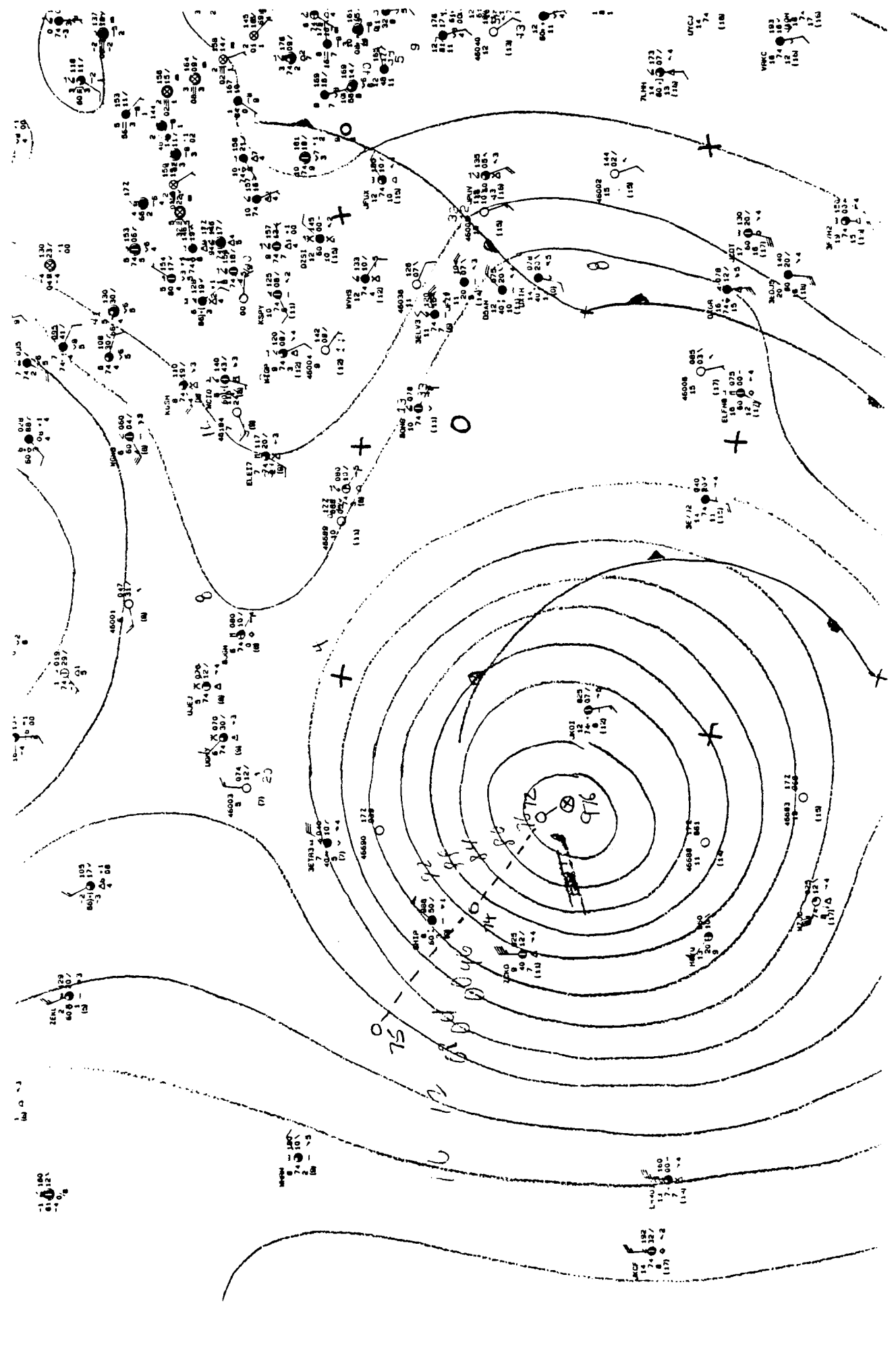
11-06-87

0600 Z

A38

11-06-87

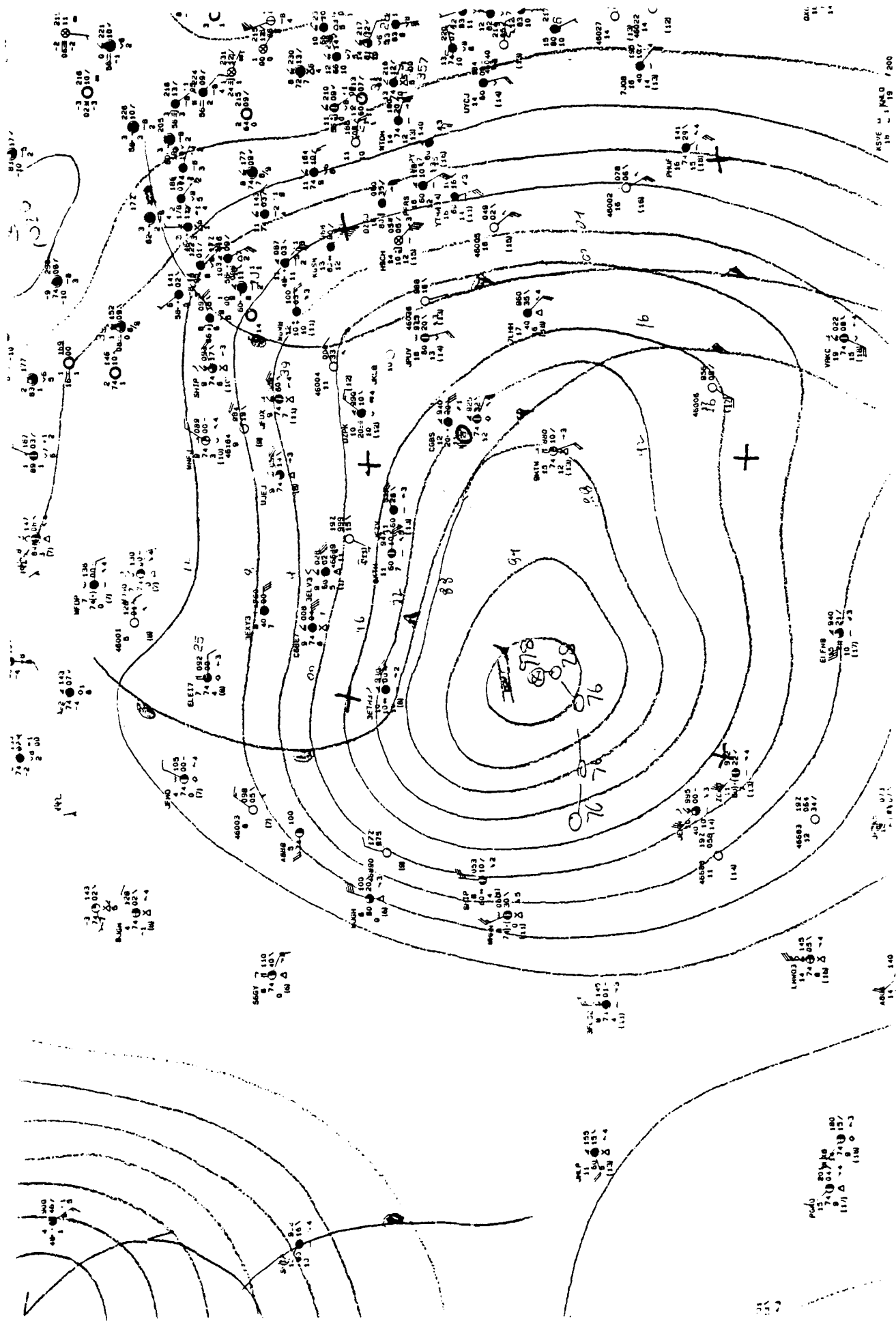
1800 Z



A40

11-07-87

1800 Z



KSVE M KNO / 200

ABN 140

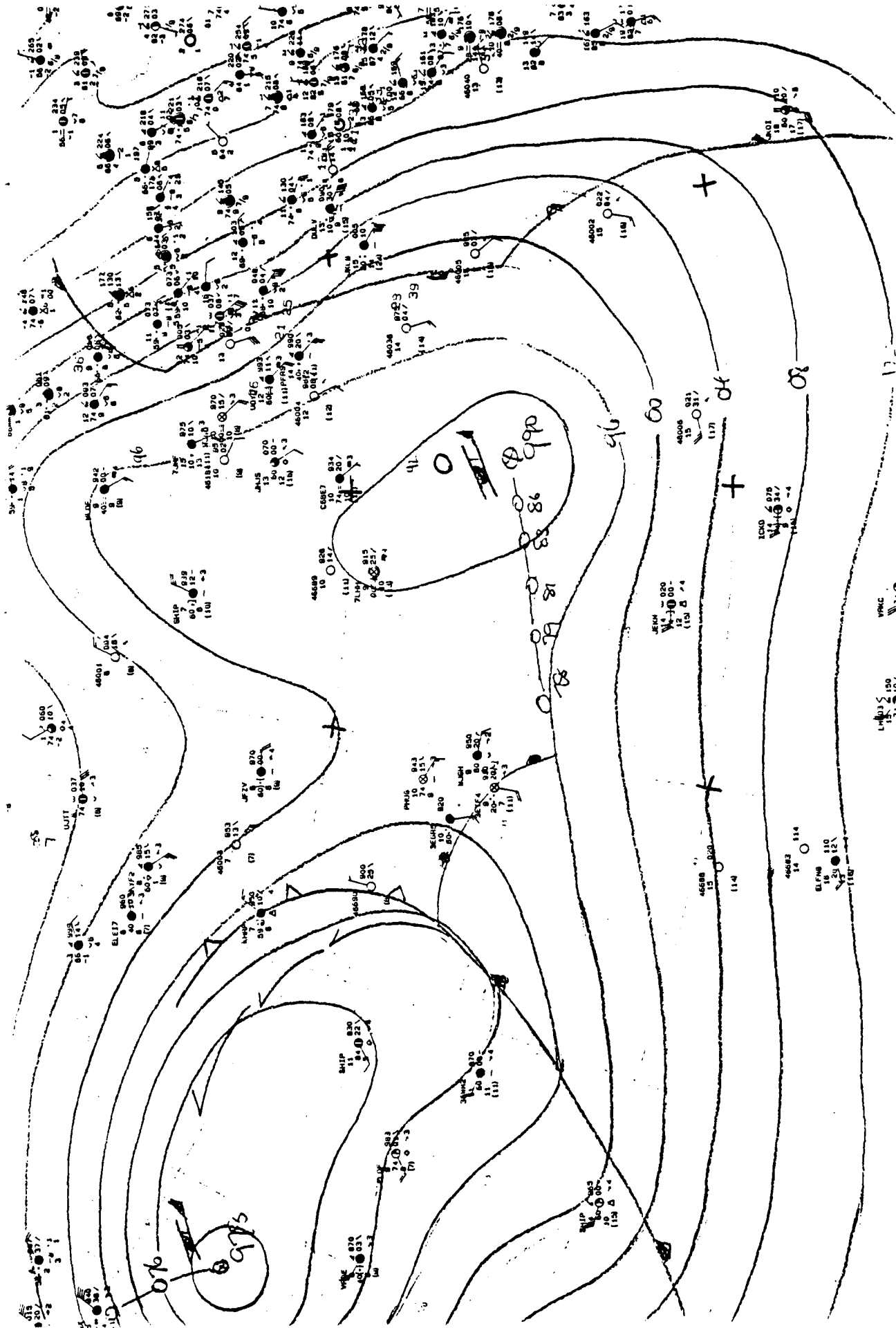
110

110

A42

11-08-87

1800 Z



46015 150
11 107

46015 114
11 110
11 112

46015 114

46015 114

46015 114

46015 114

46015 114

46015 114

46015 114

46015 114

46015 114

46015 114

46015 114

46015 114

46015 114

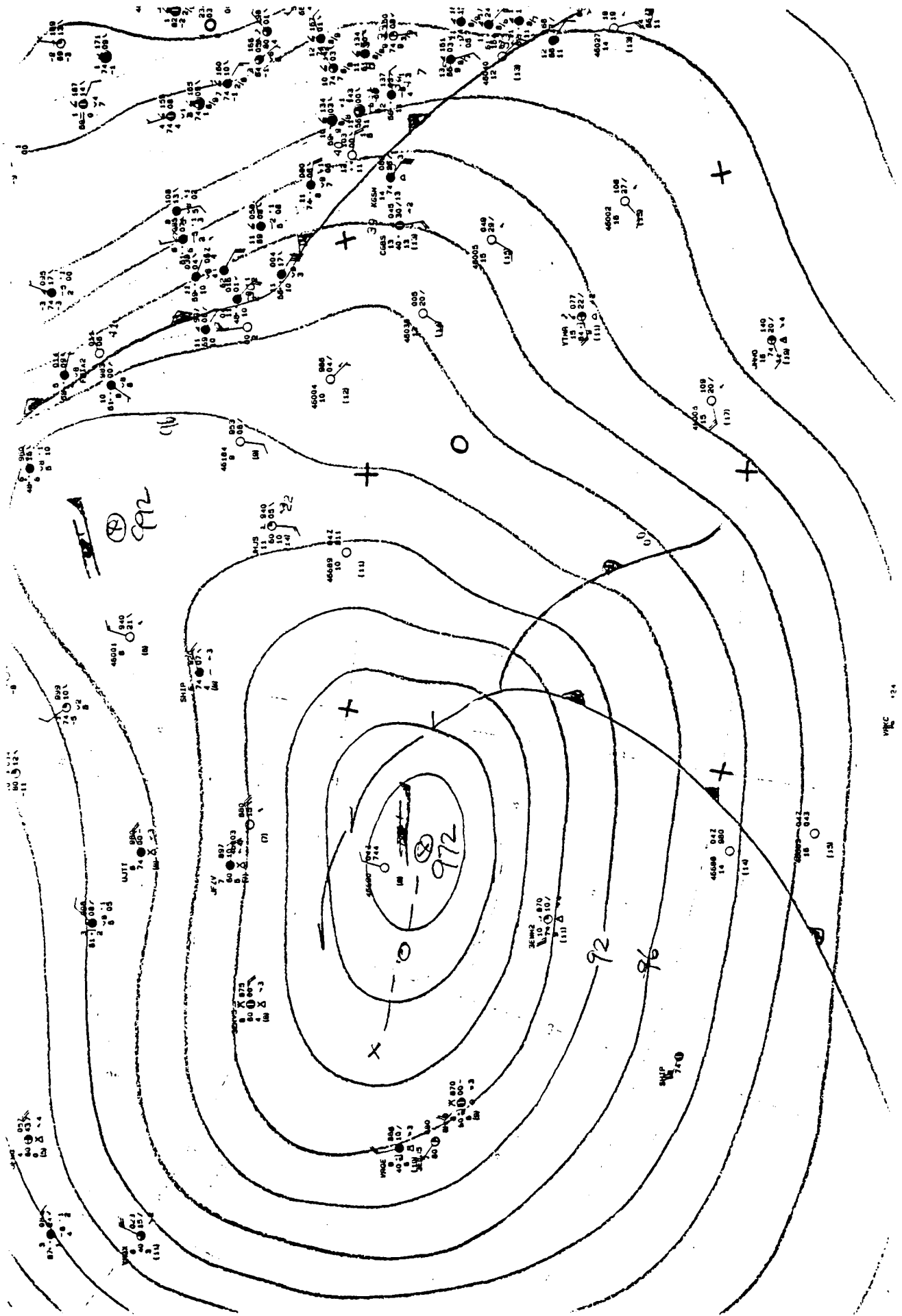
46015 114

46015 114

46015 114

46015 114

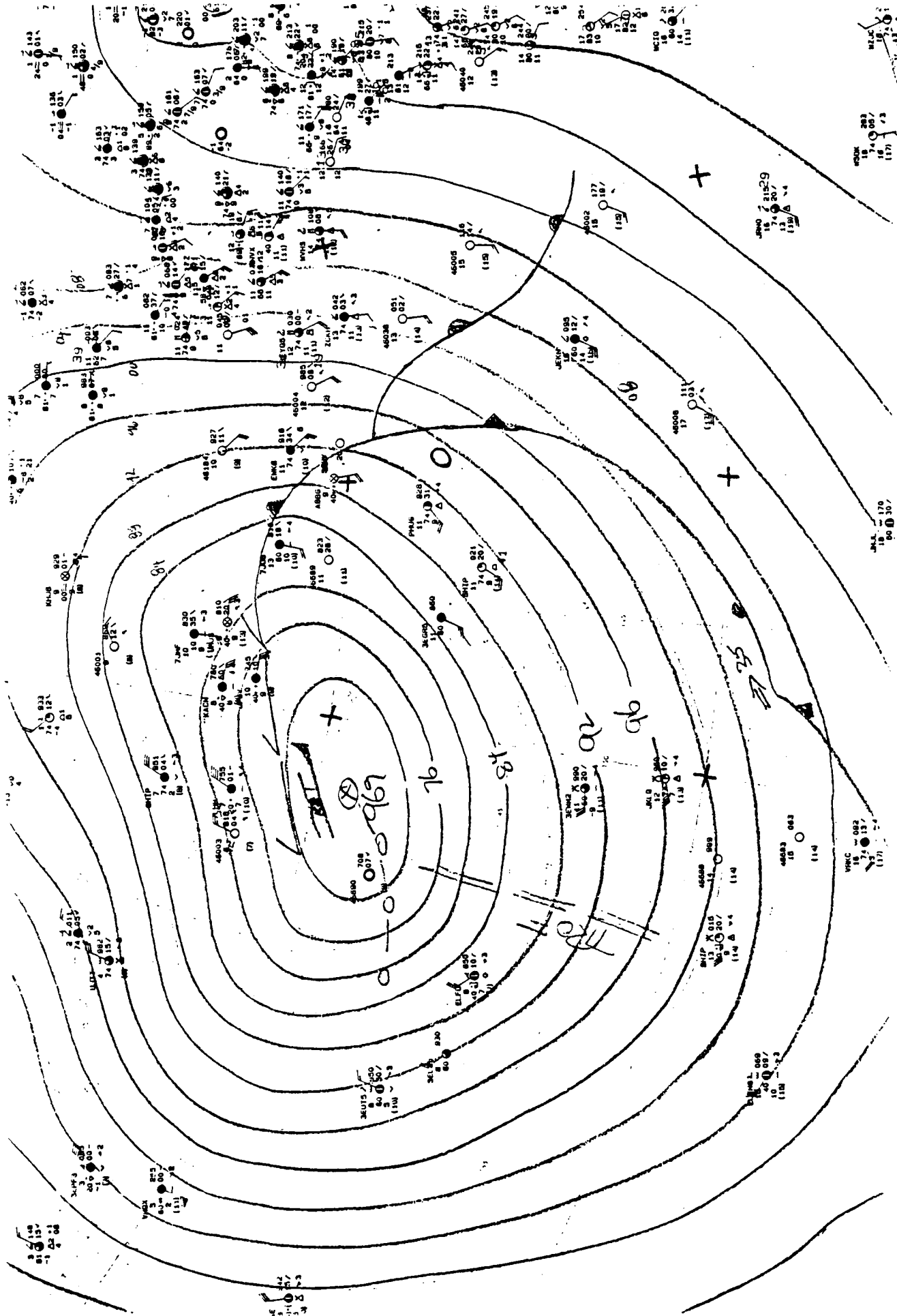
46015 114

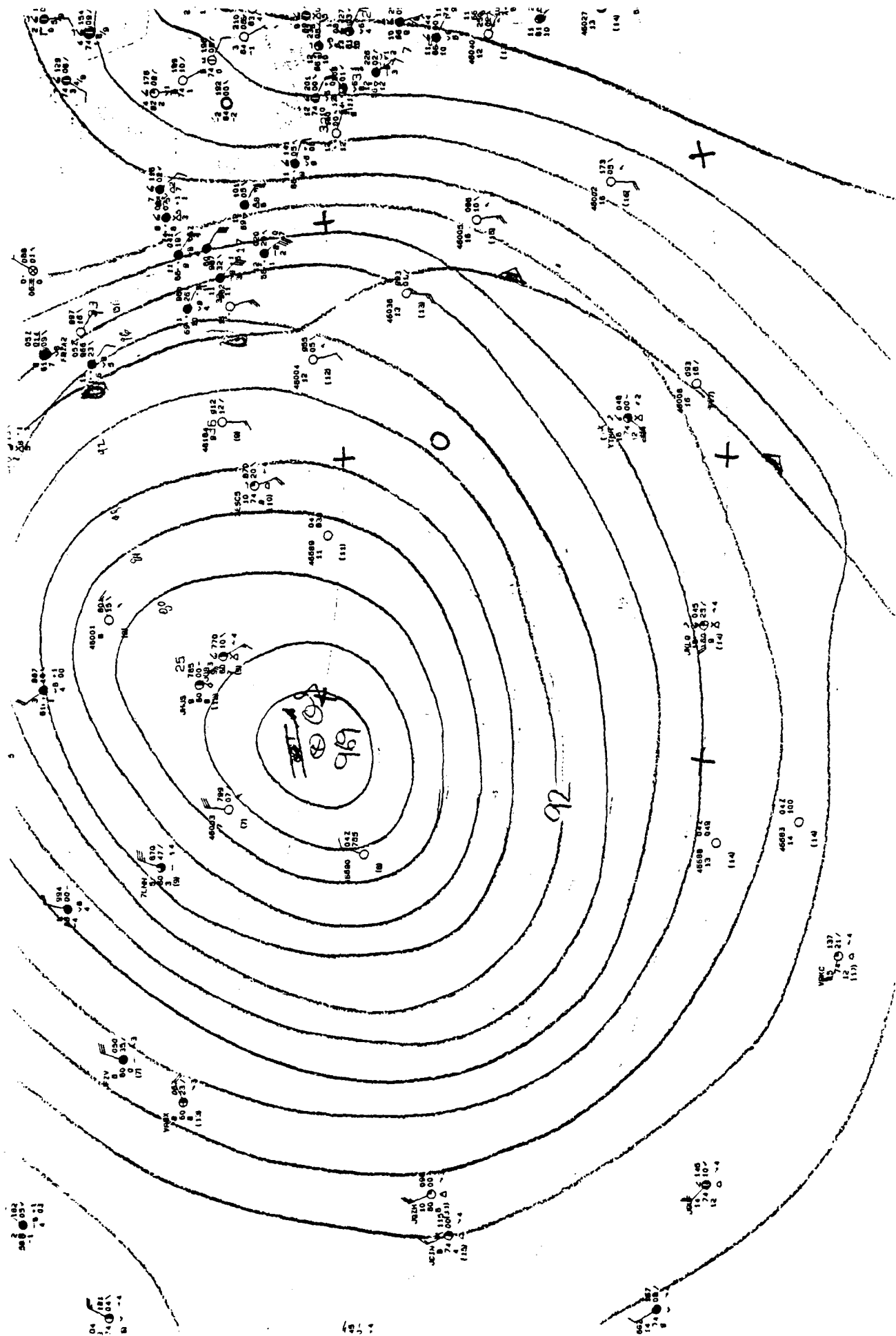


A44

11-09-87

1800 Z





0600 Z

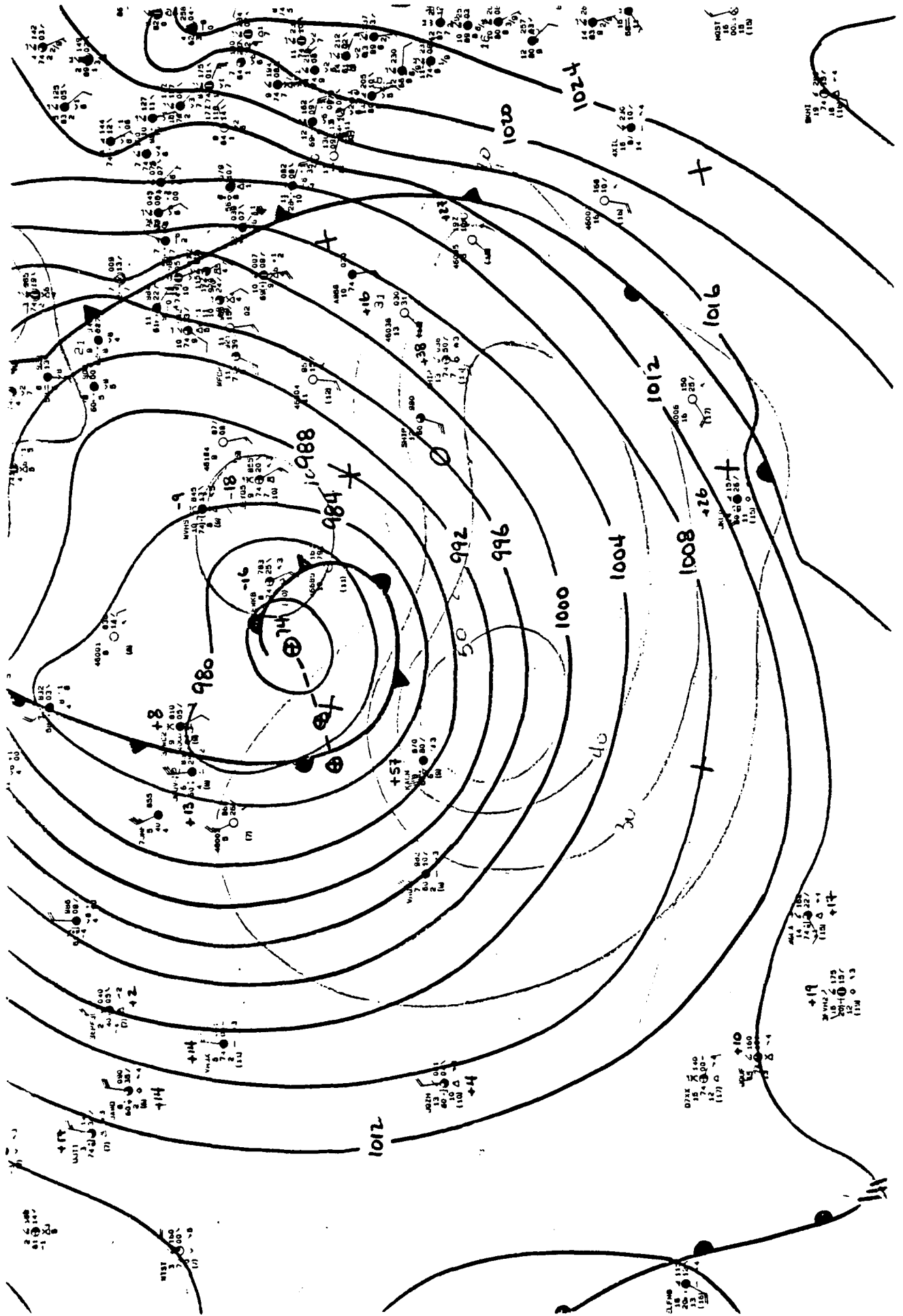
11-10-87

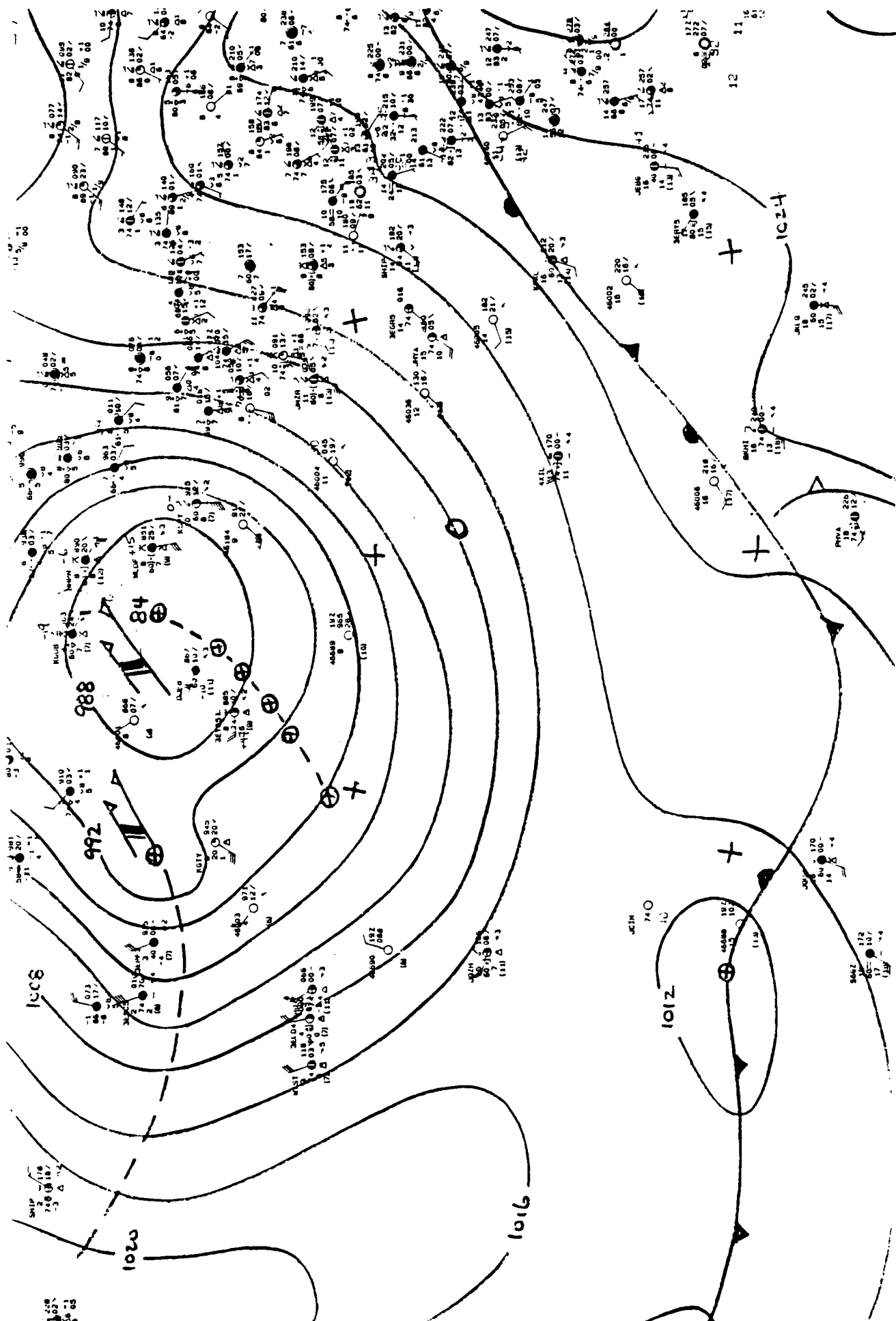
A45

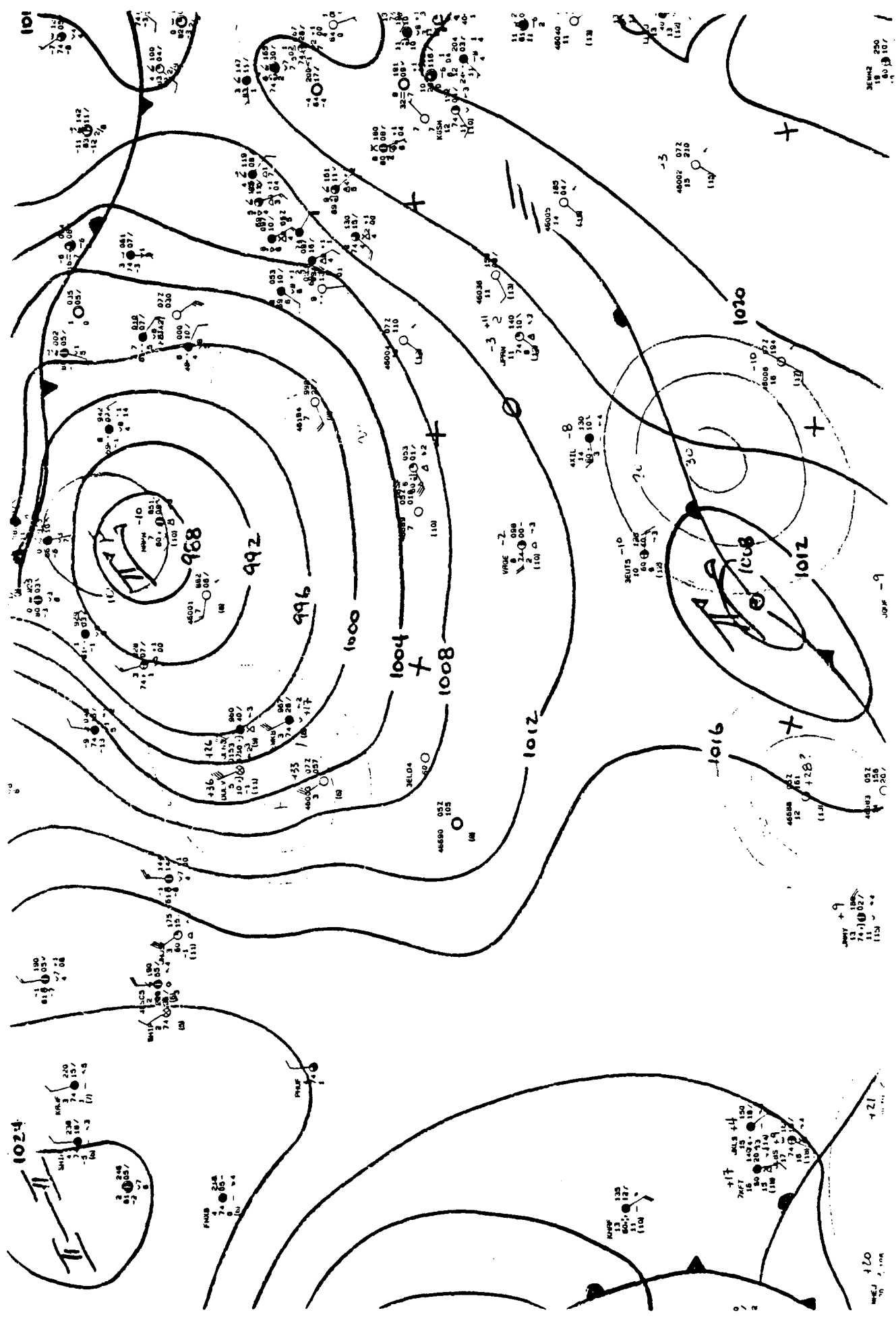
A46

11-10-87

1800 Z



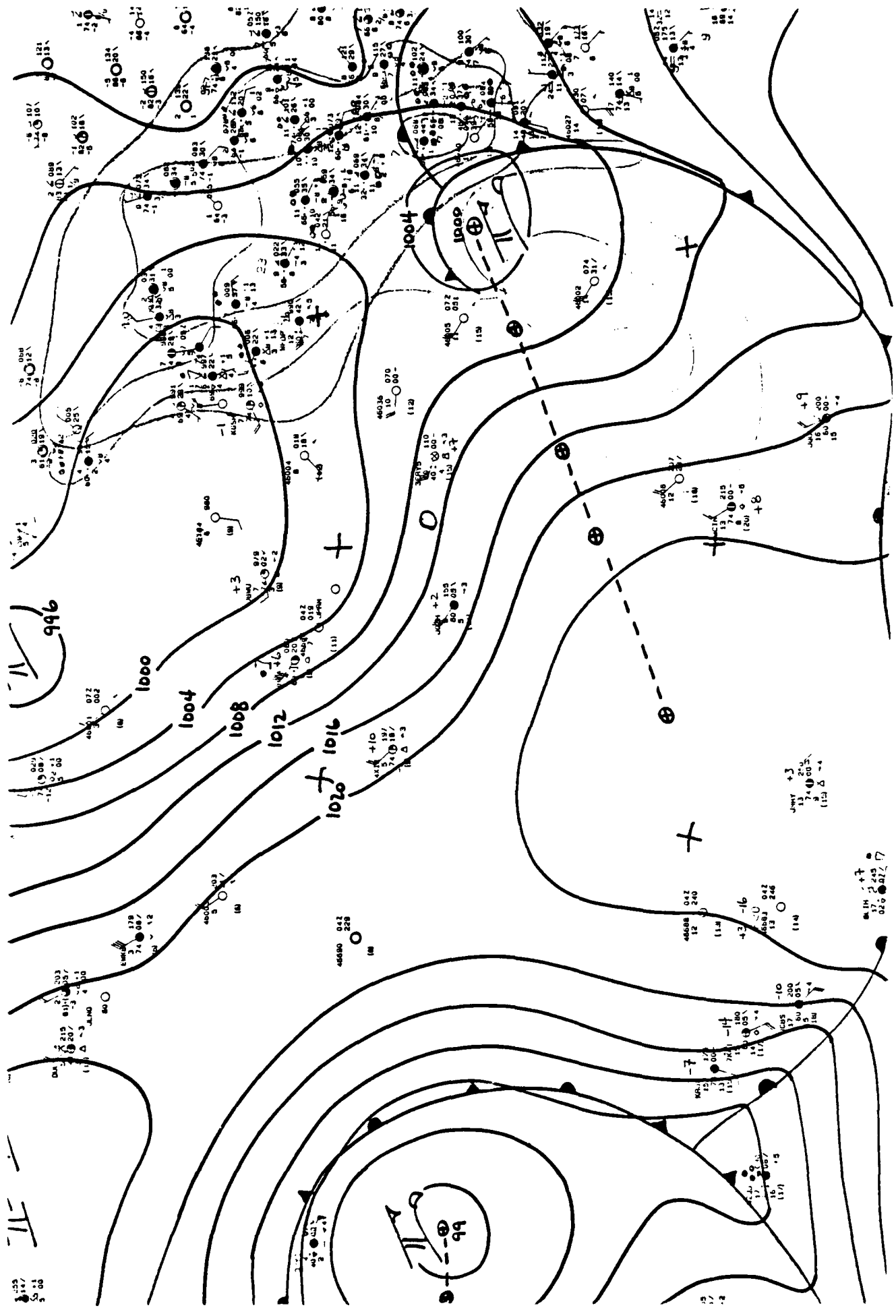


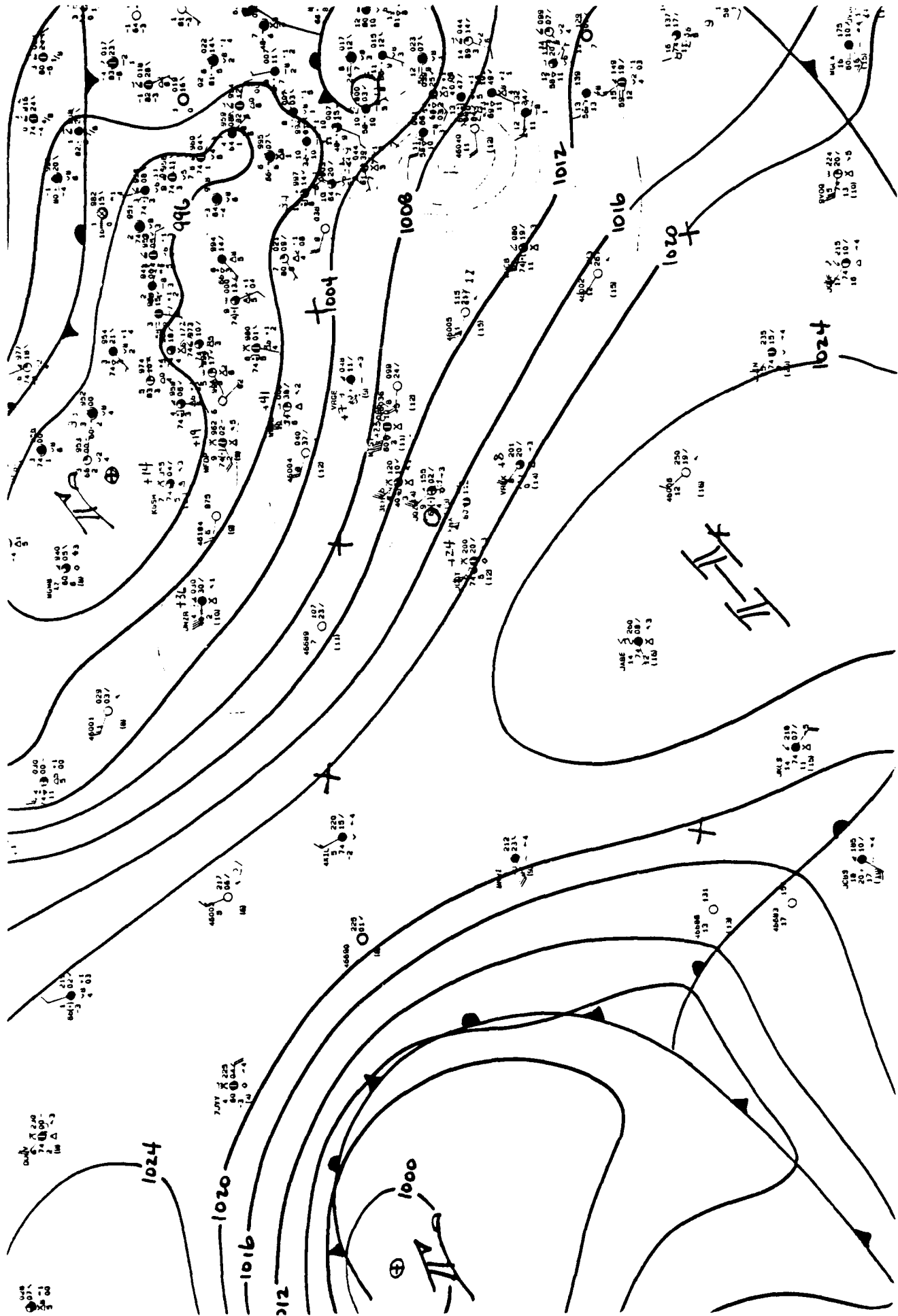


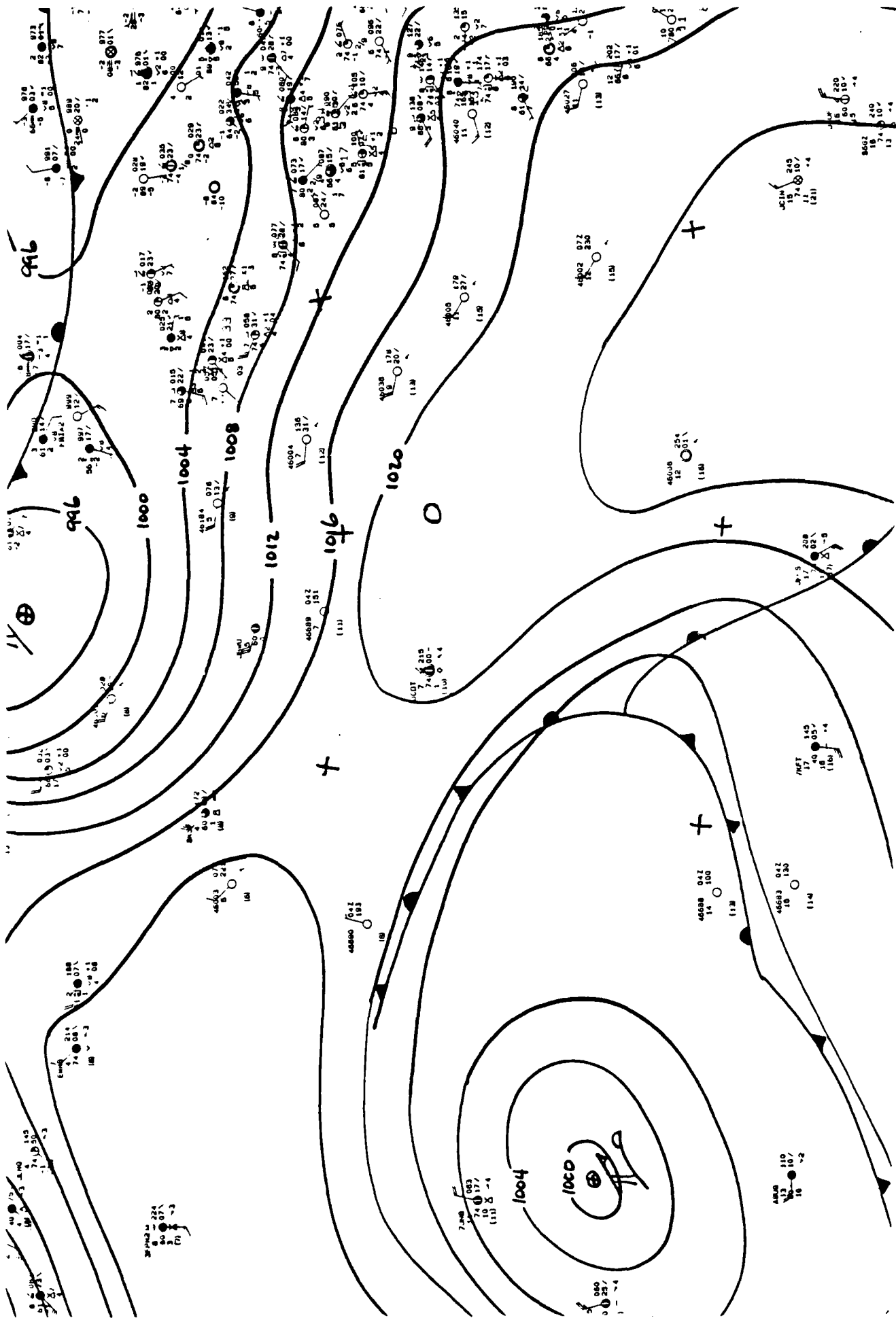
A49

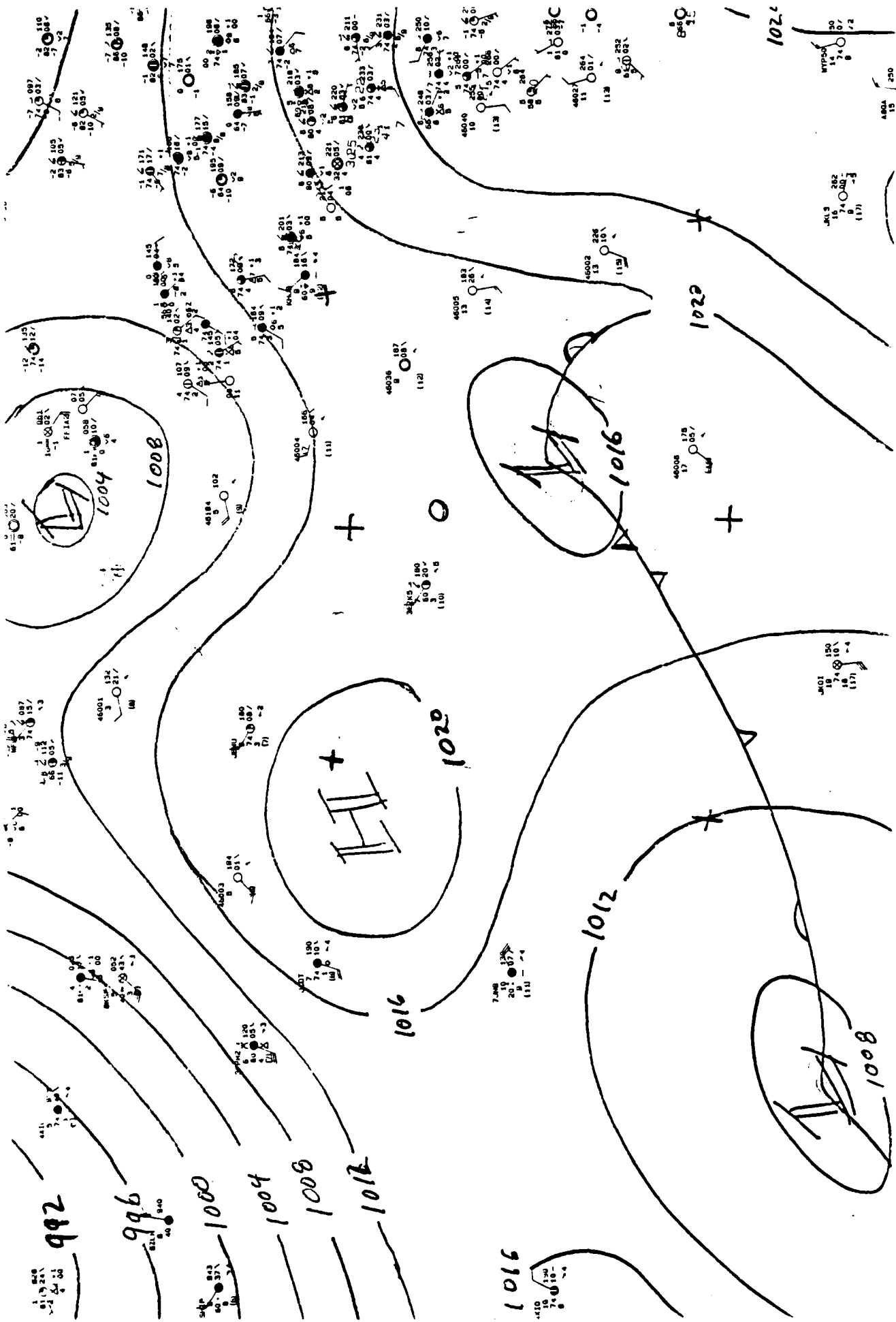
11-12-87

0600 Z





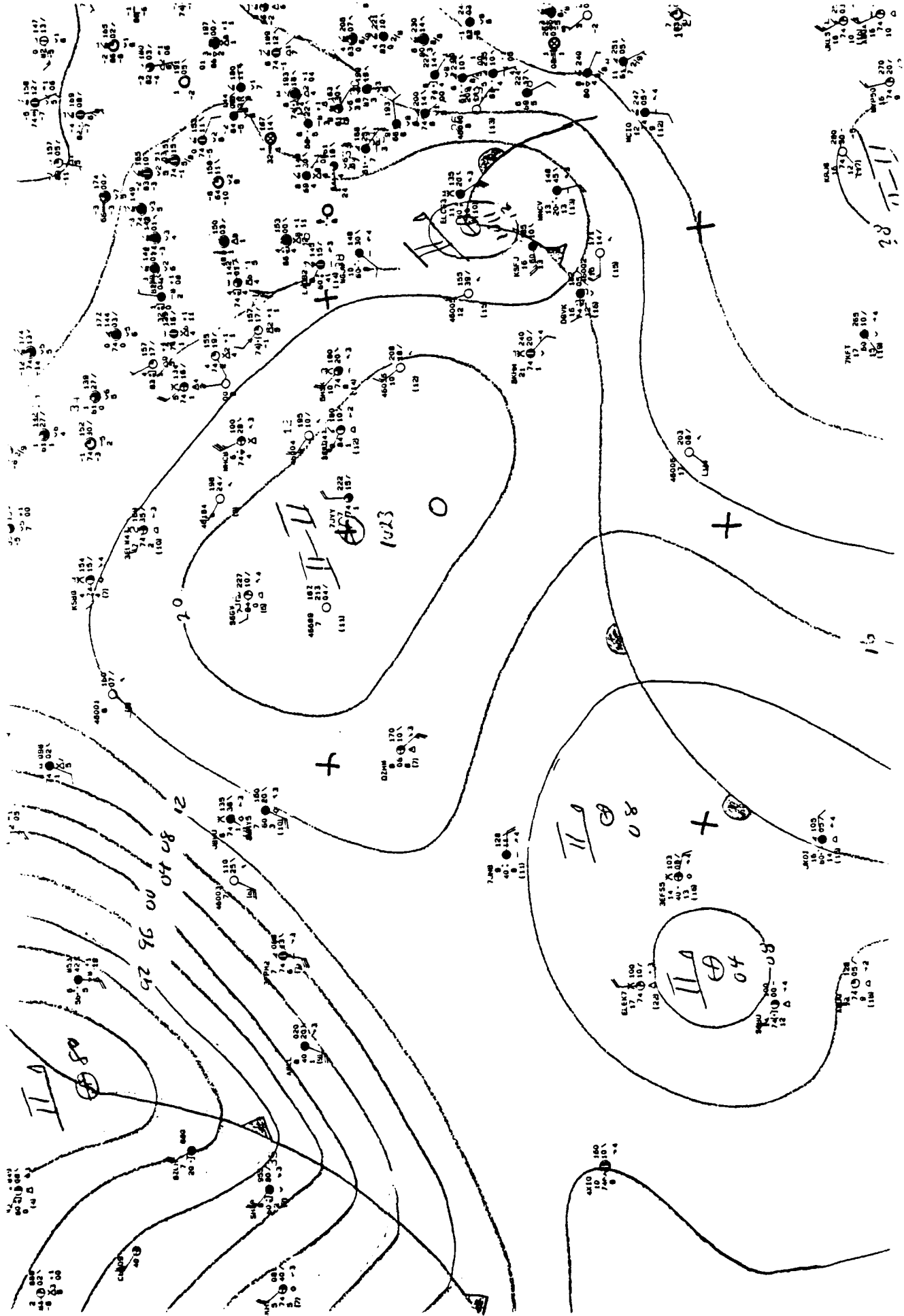


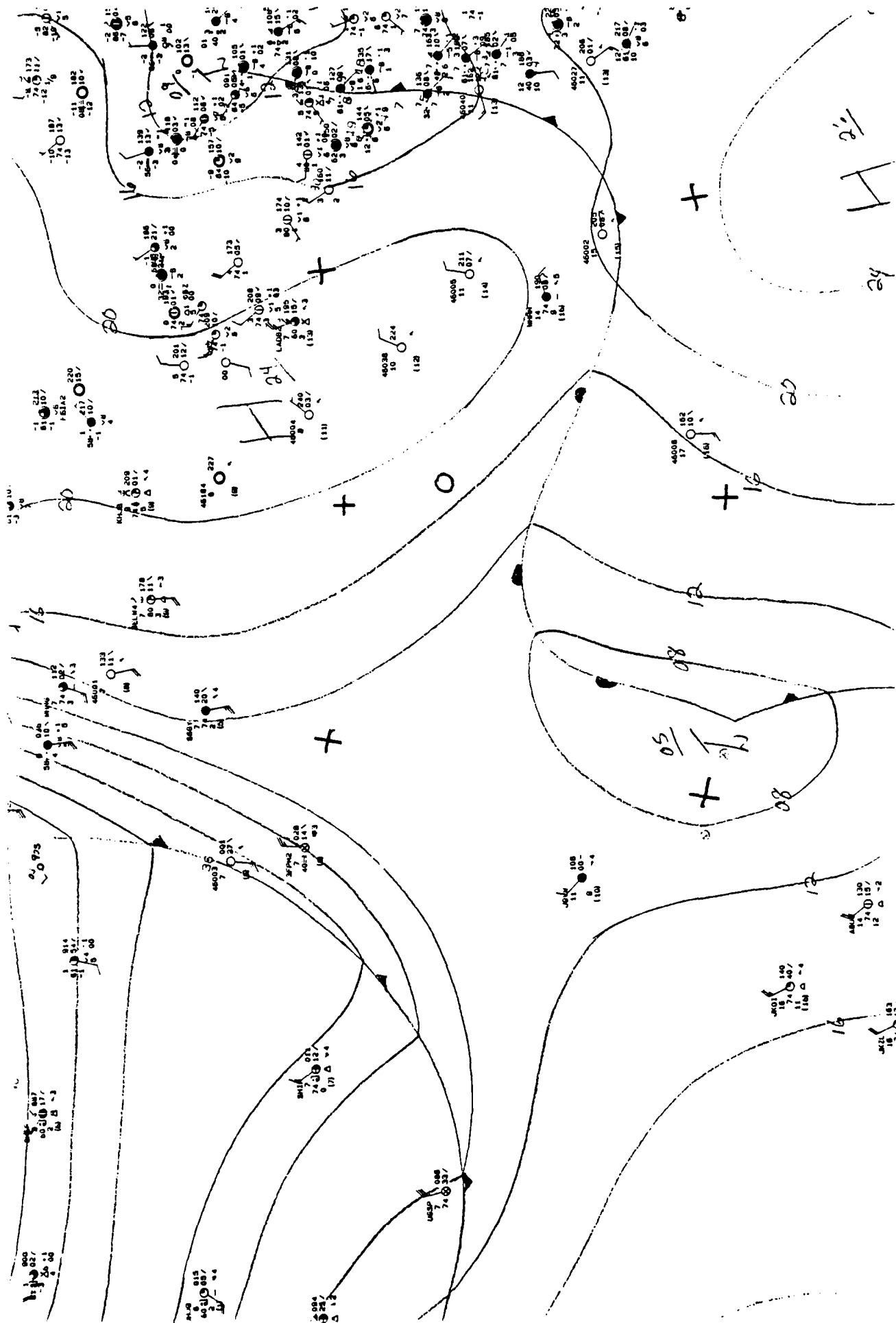


A56

11-15-87

1800 Z

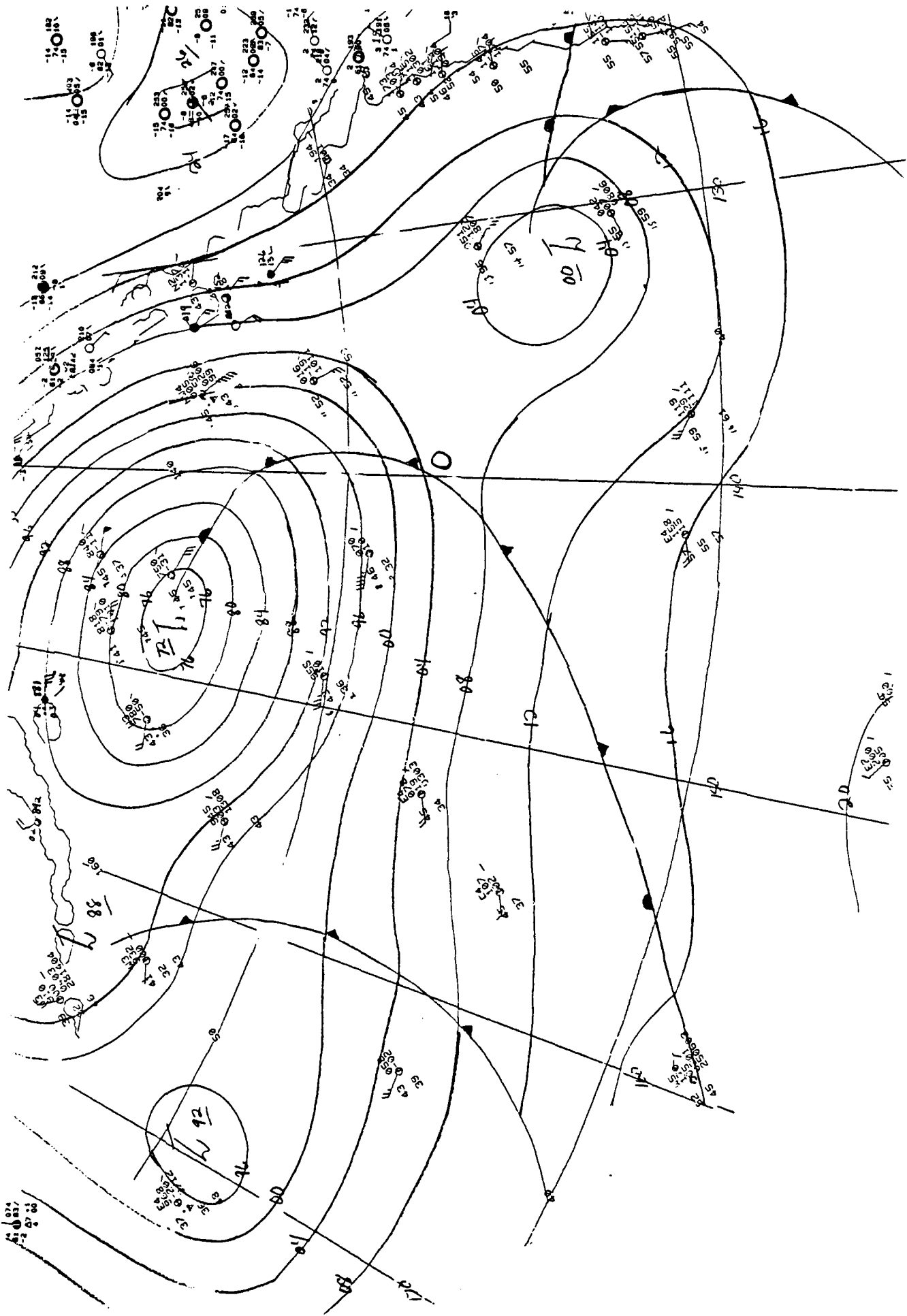




0600 Z

11-16-87

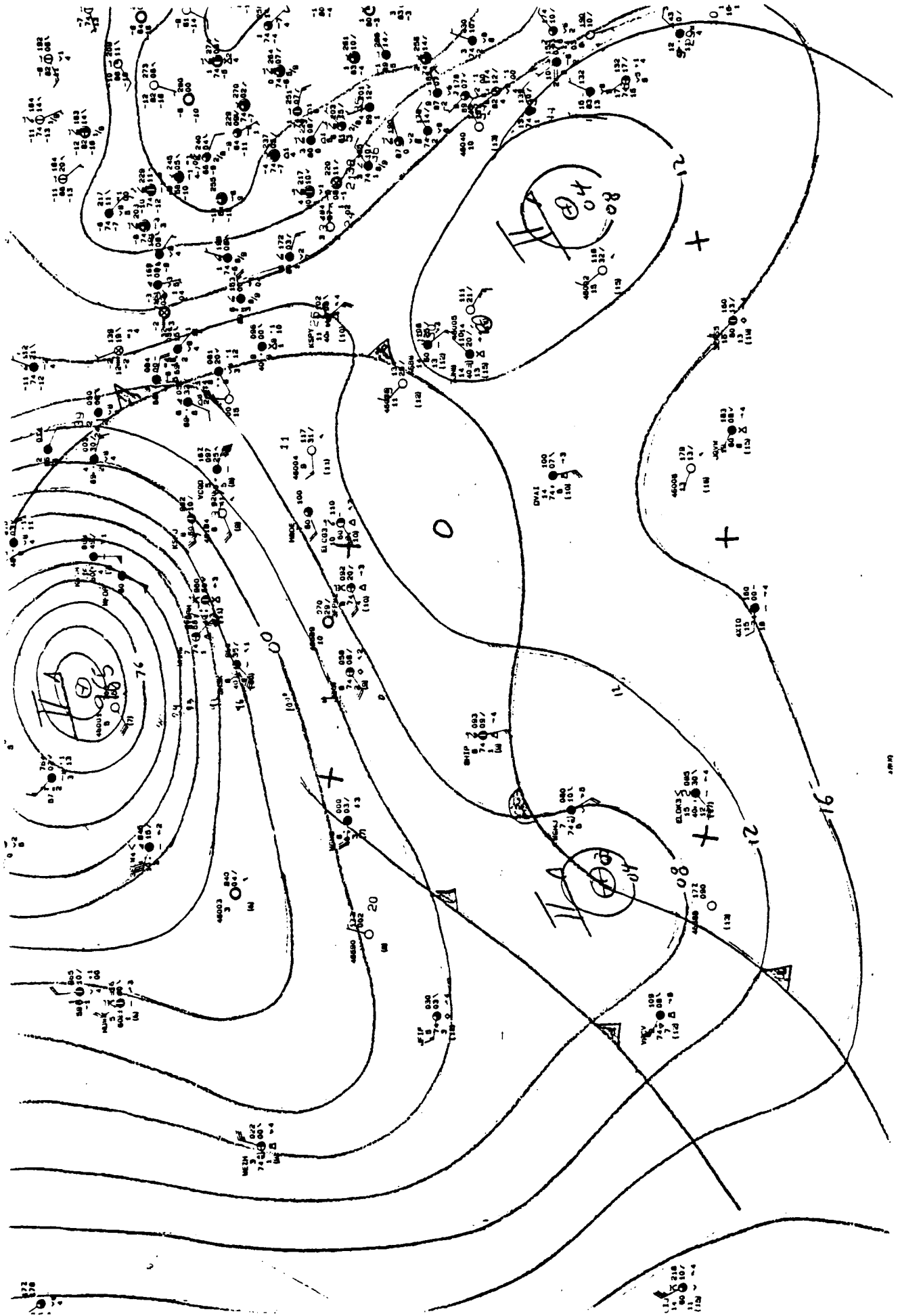
A57



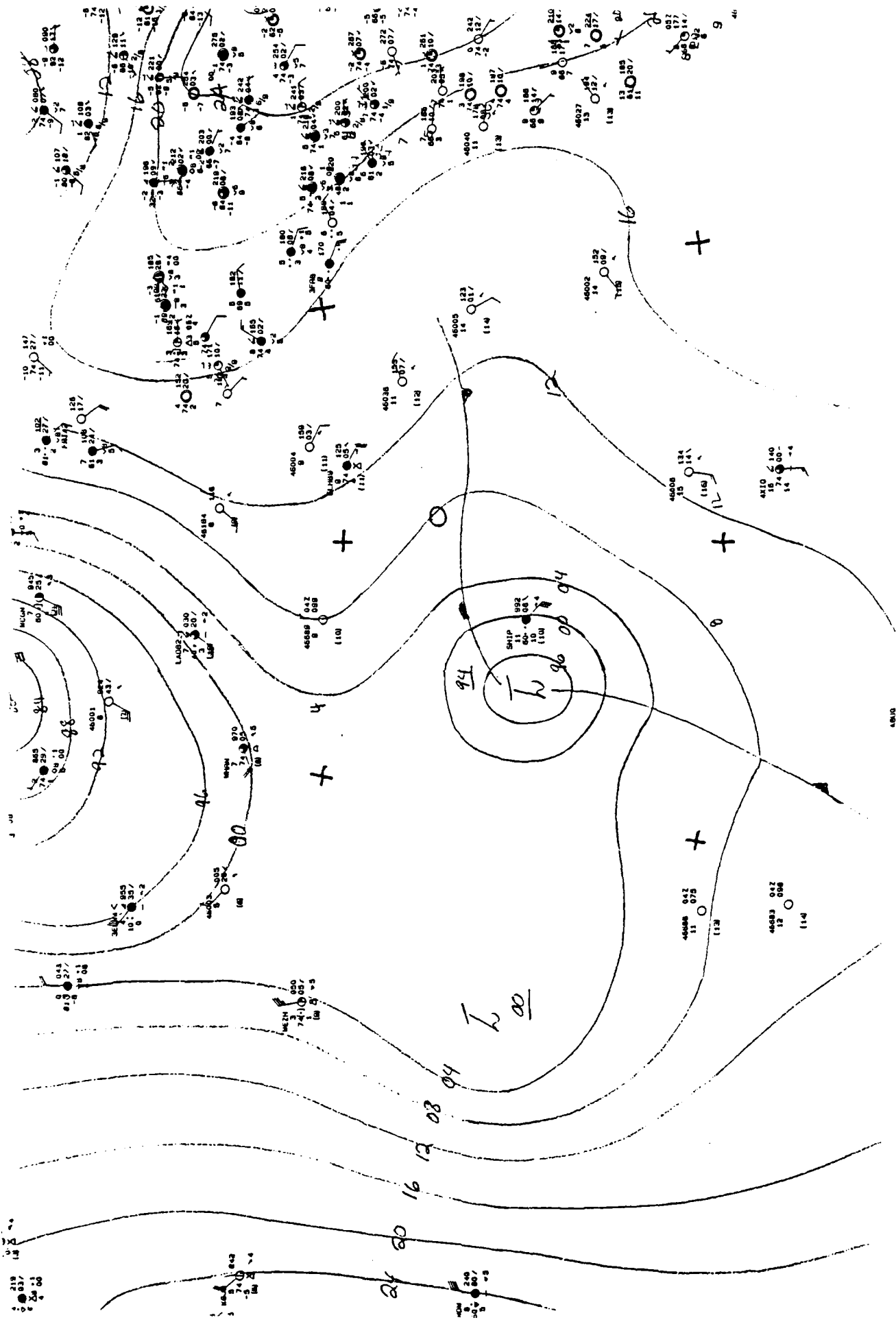
A60

11-17-87

1800 Z



AMIN



A61

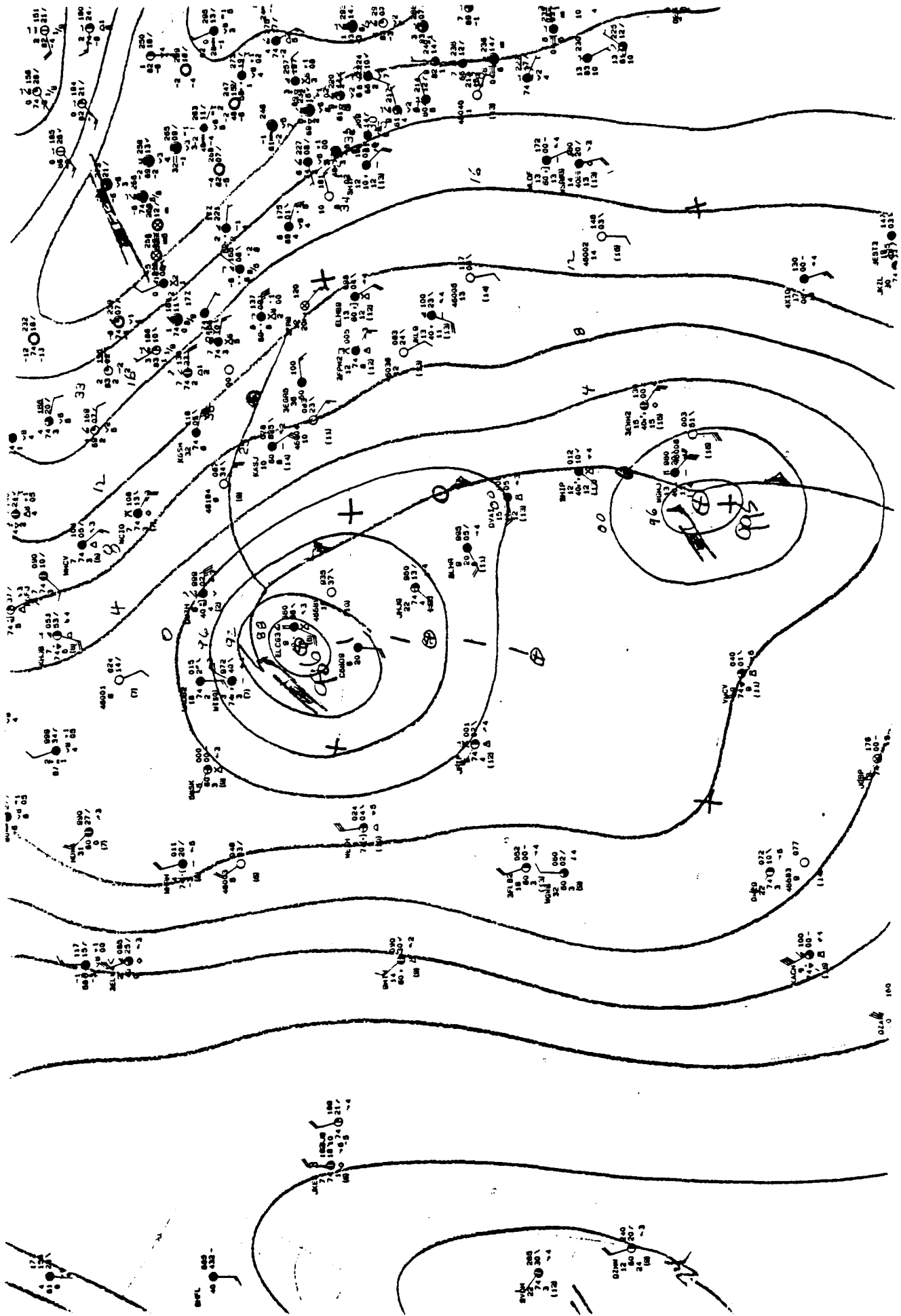
11-18-87

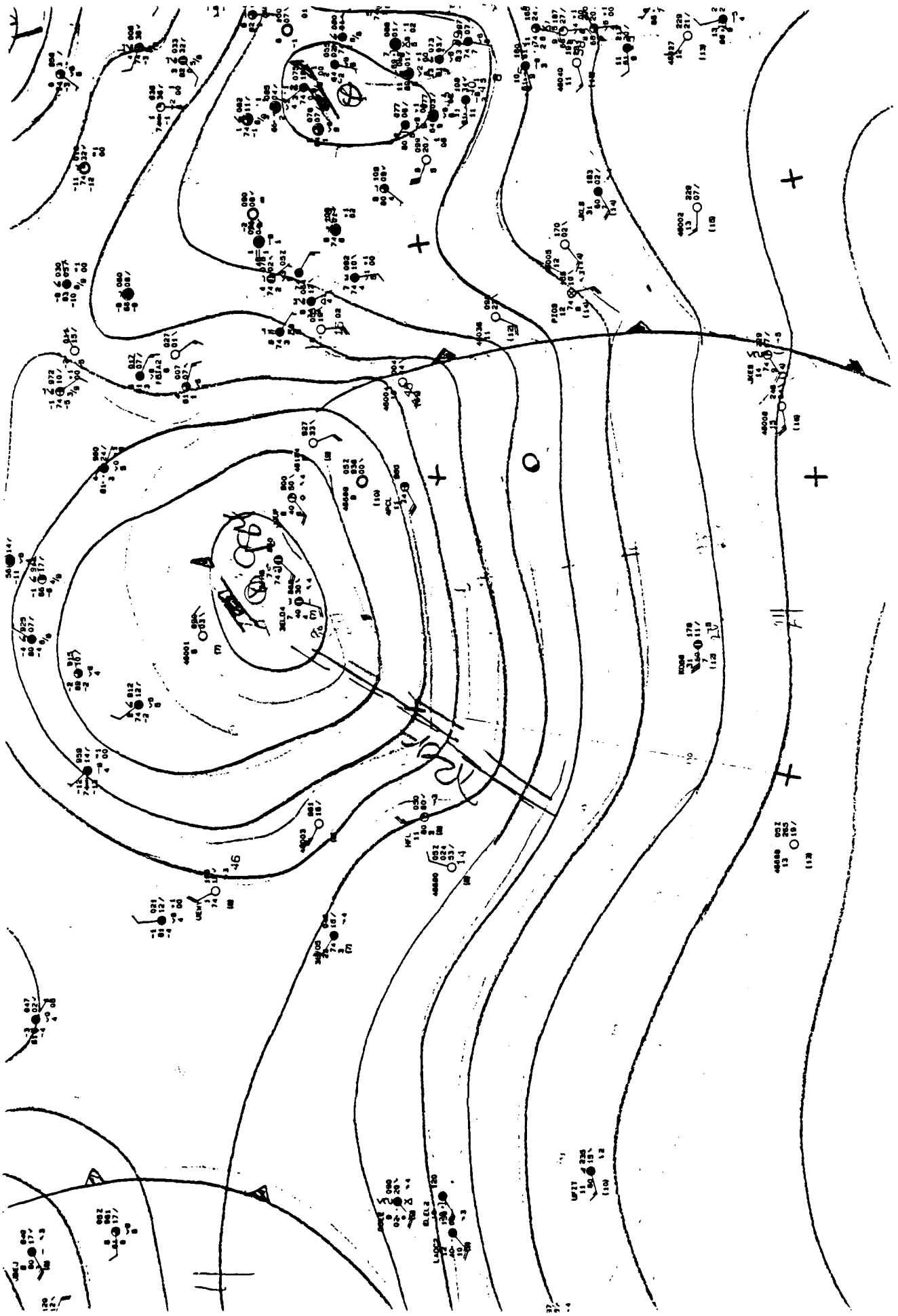
0600 Z

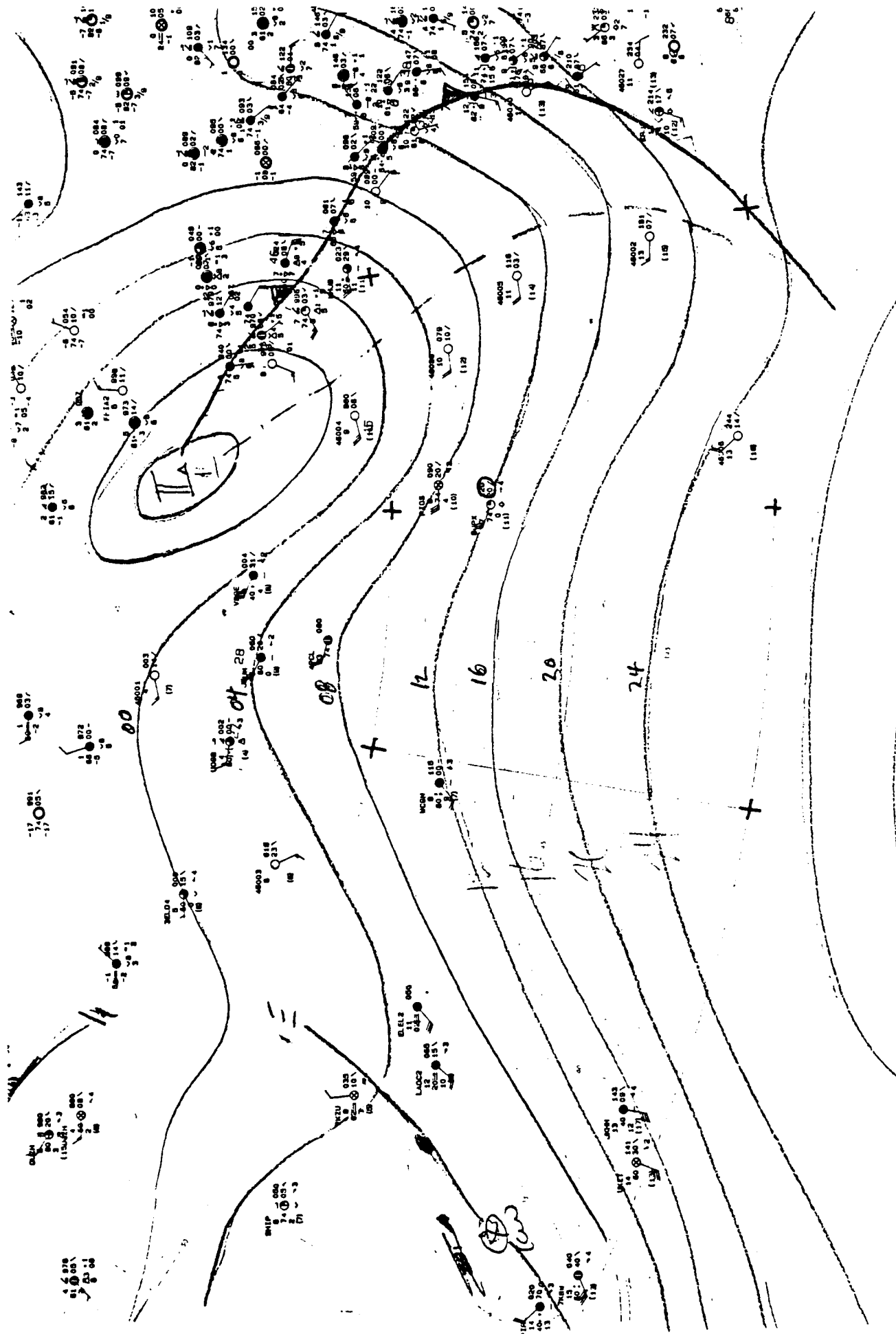
A62

11-18-87

1800 Z



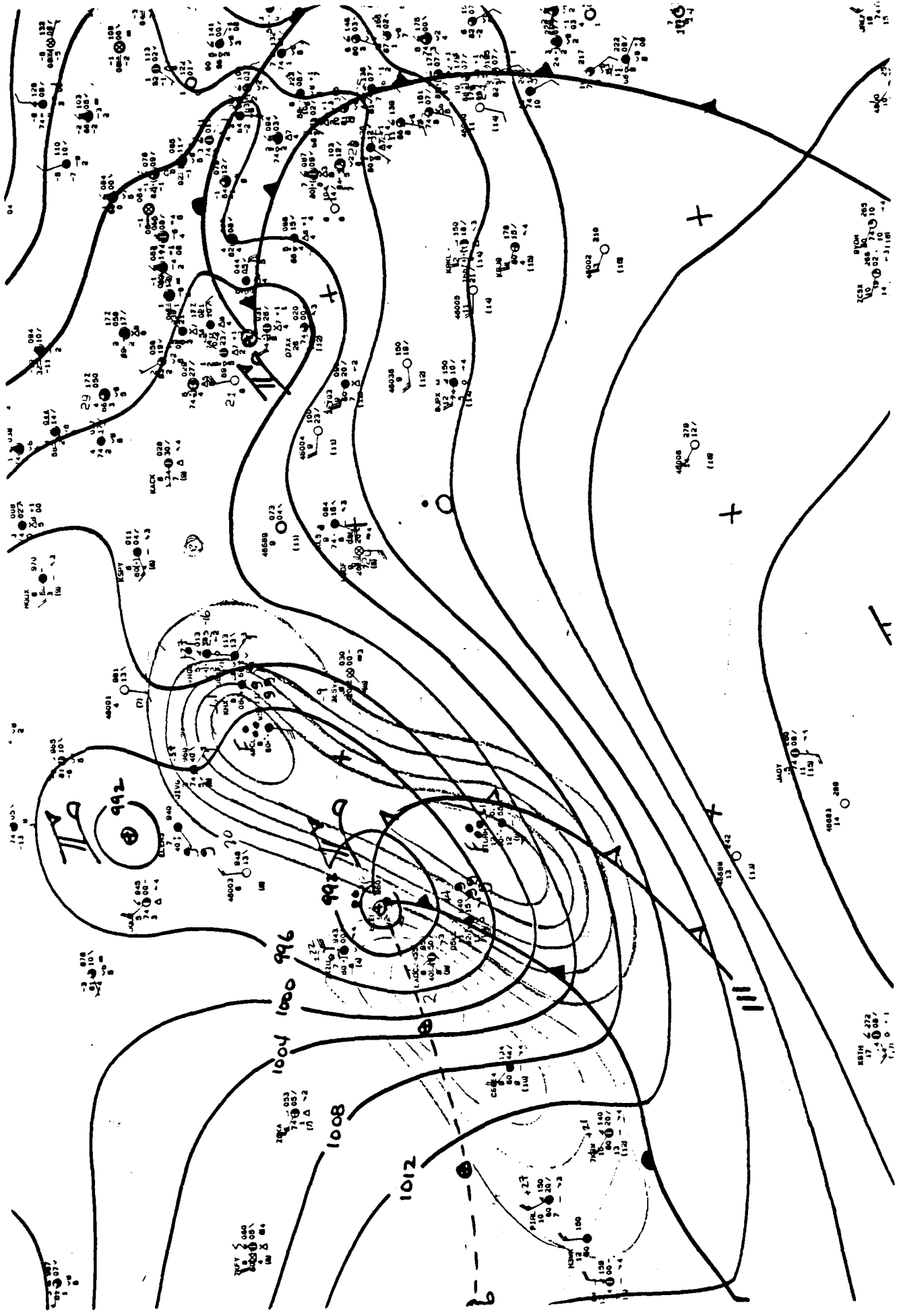


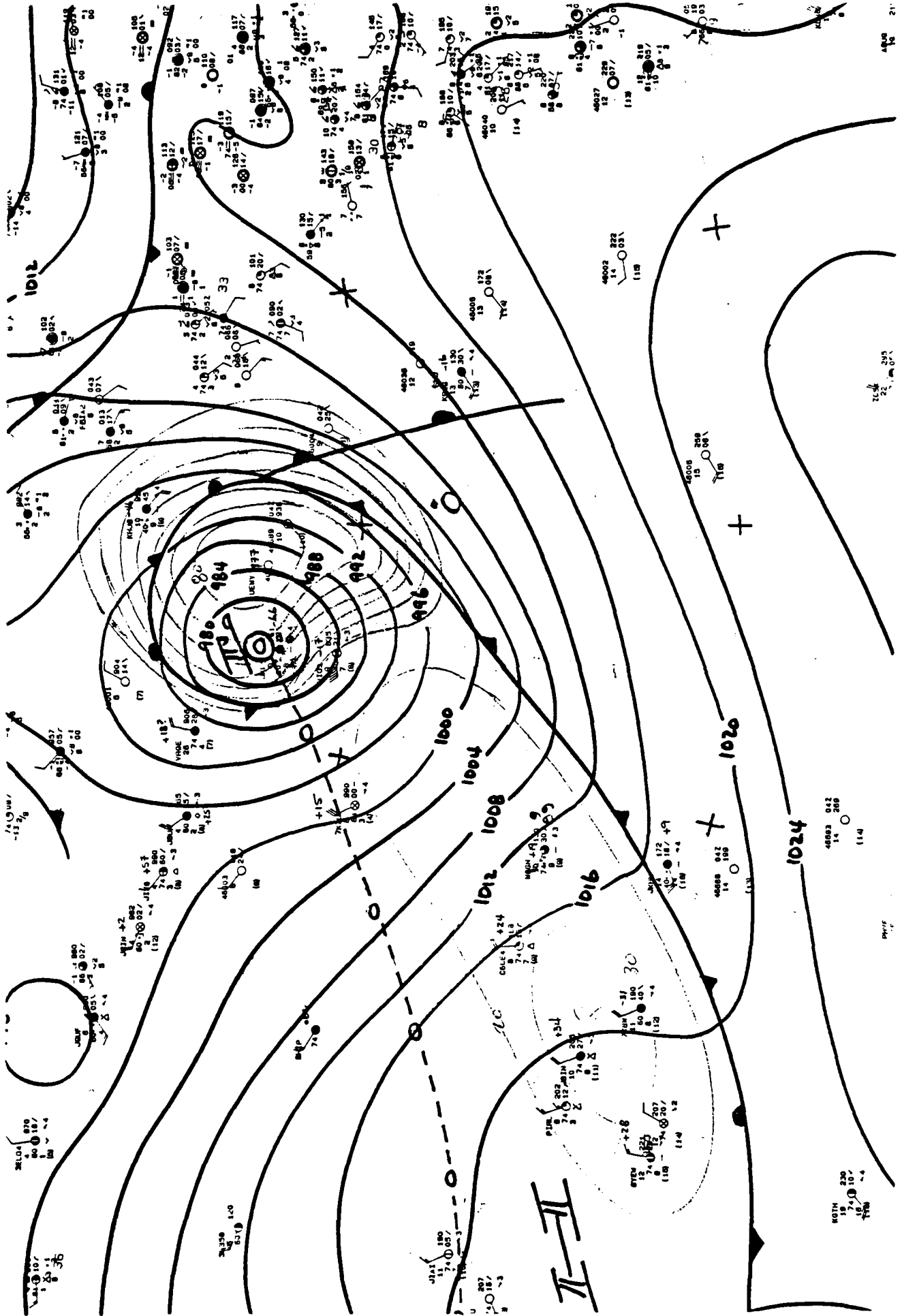


A68

11-22-87

1800 Z

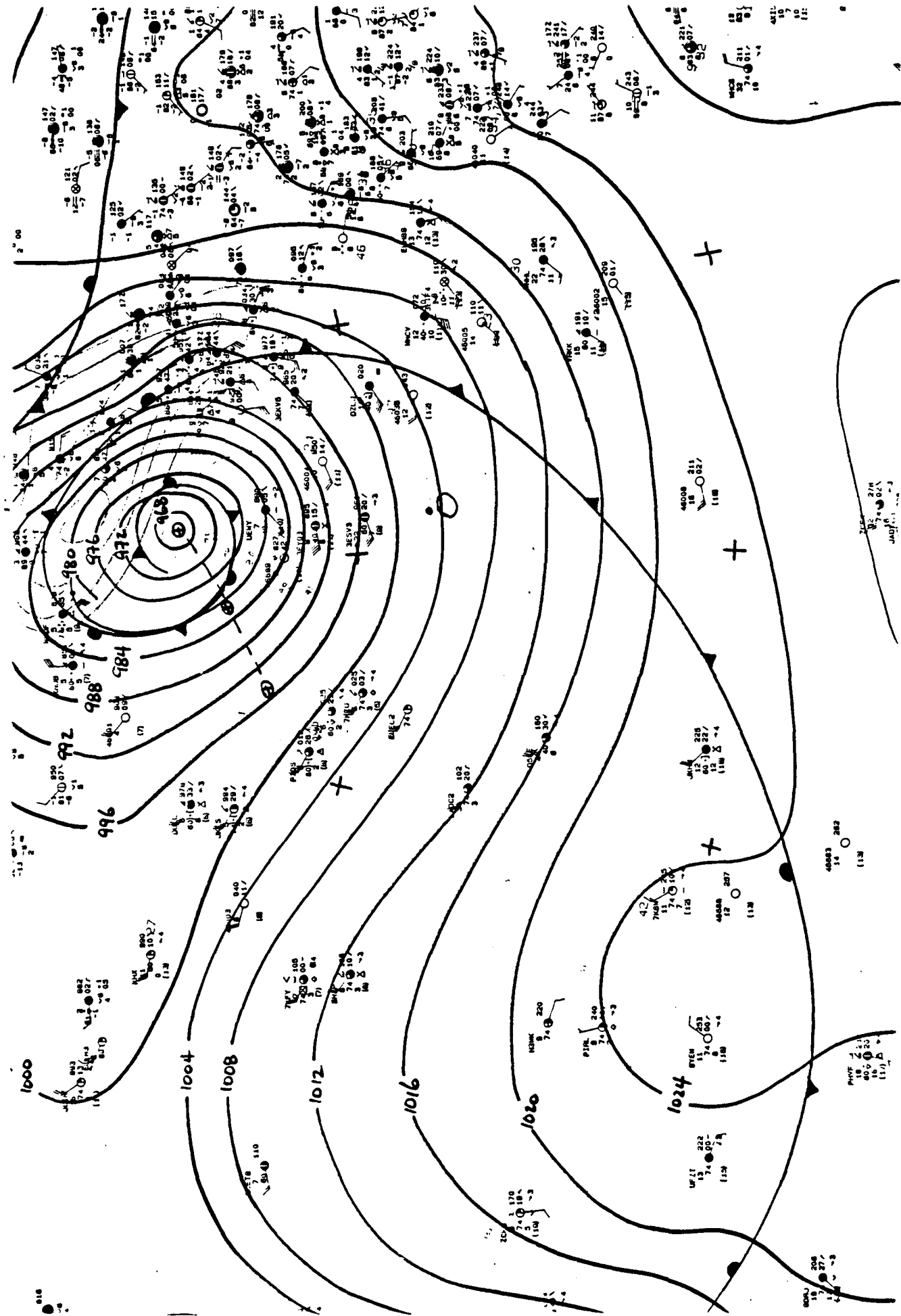


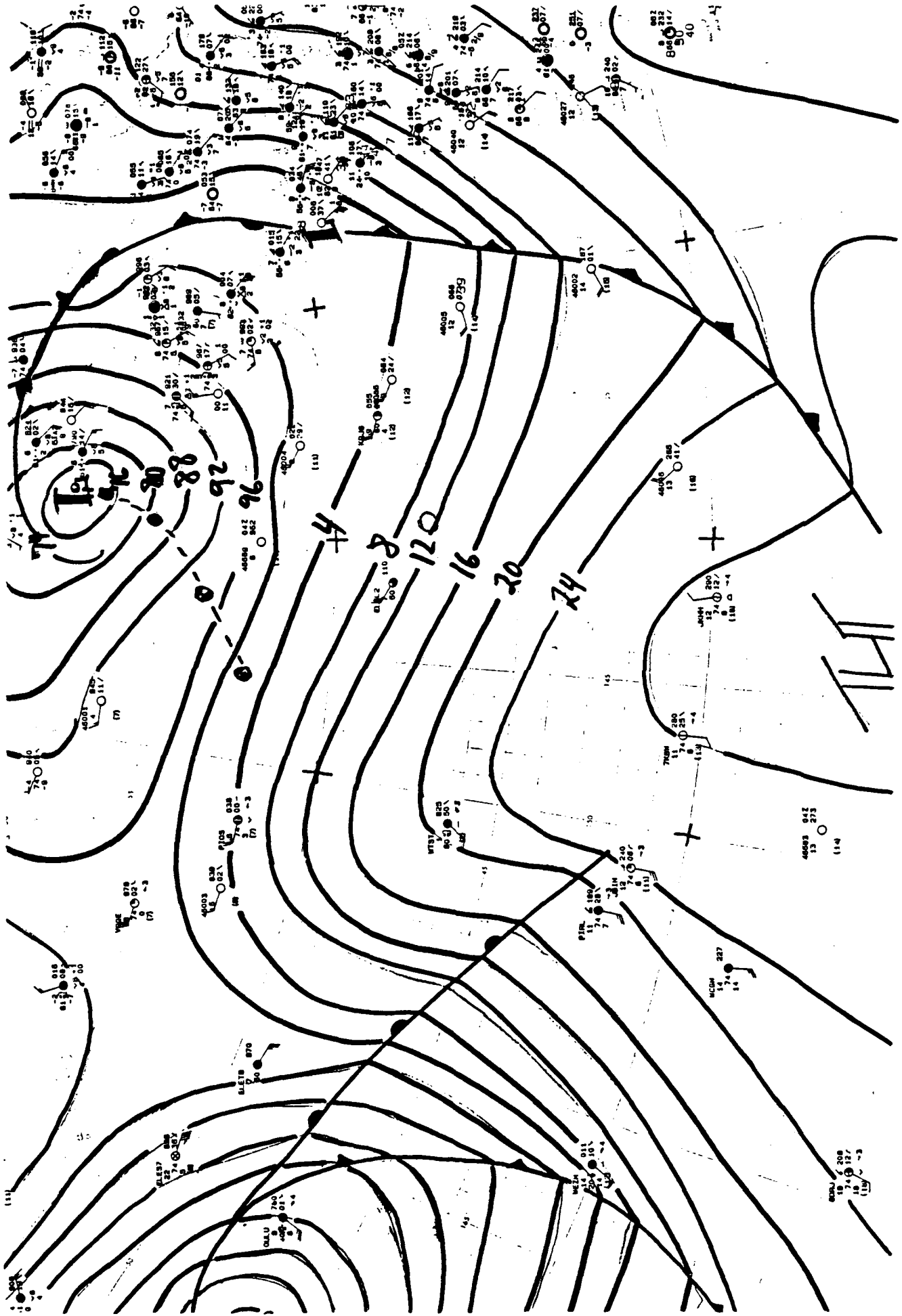


1800 Z

11-23-87

A70

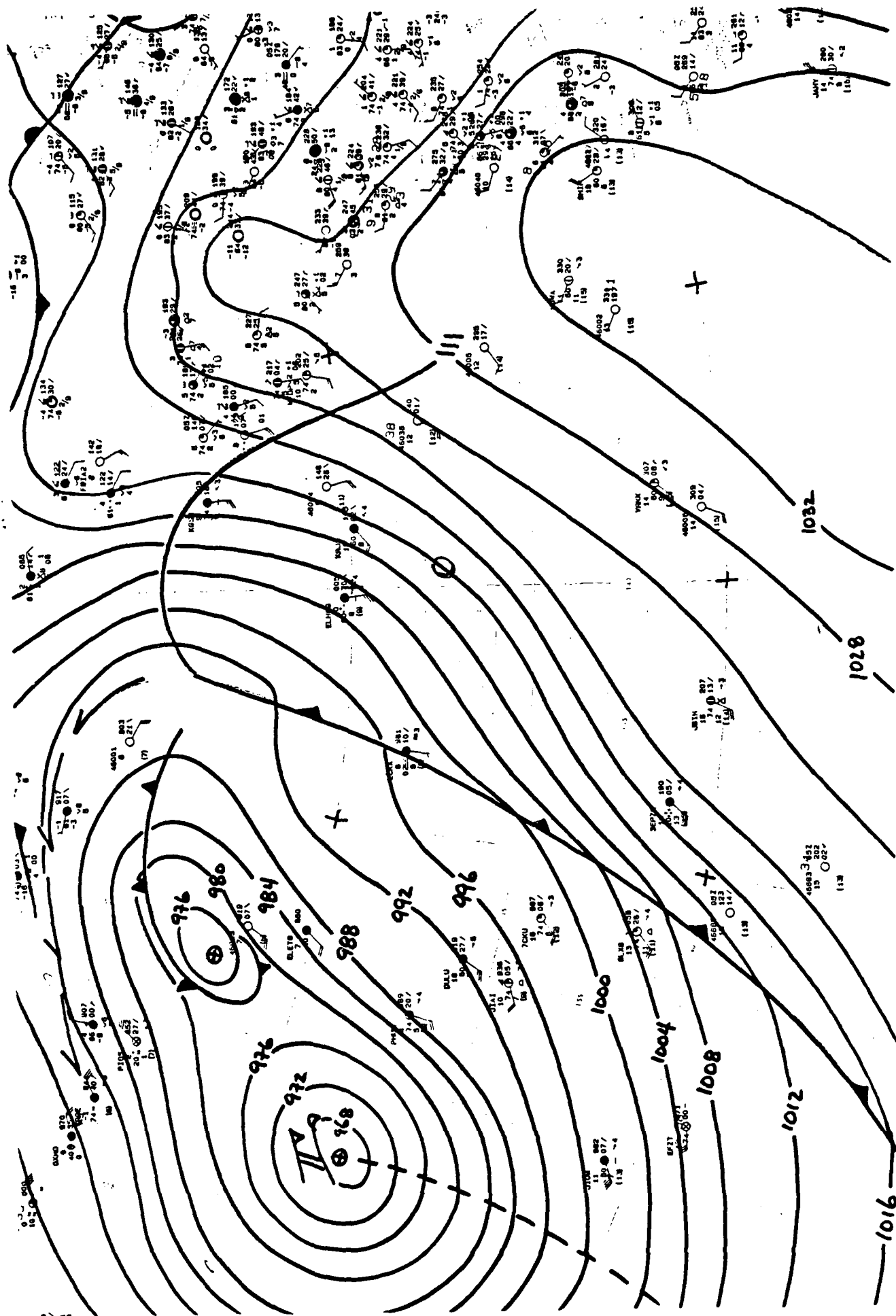




A71

11-24-87

0600 Z



0600 Z

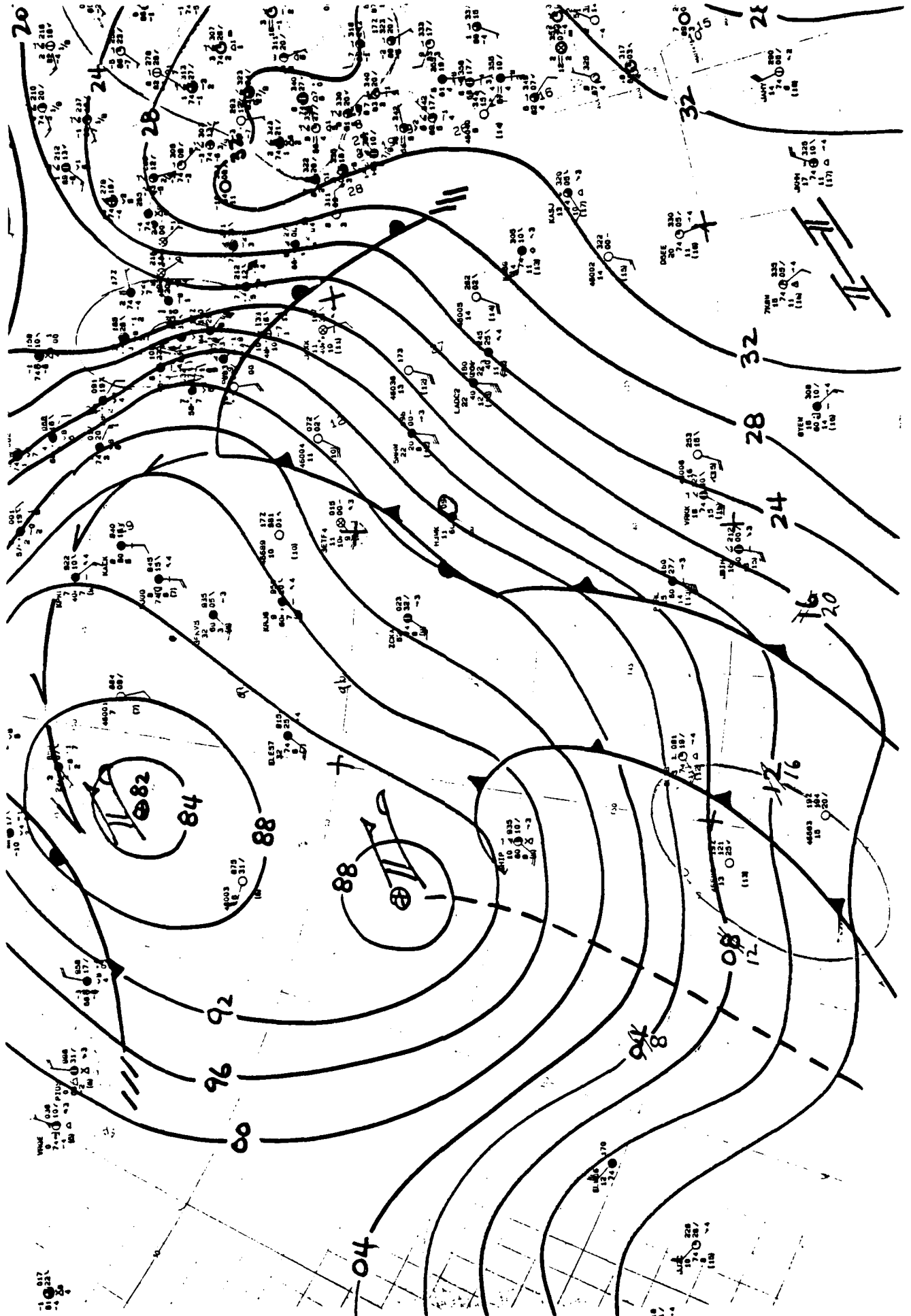
11-25-87

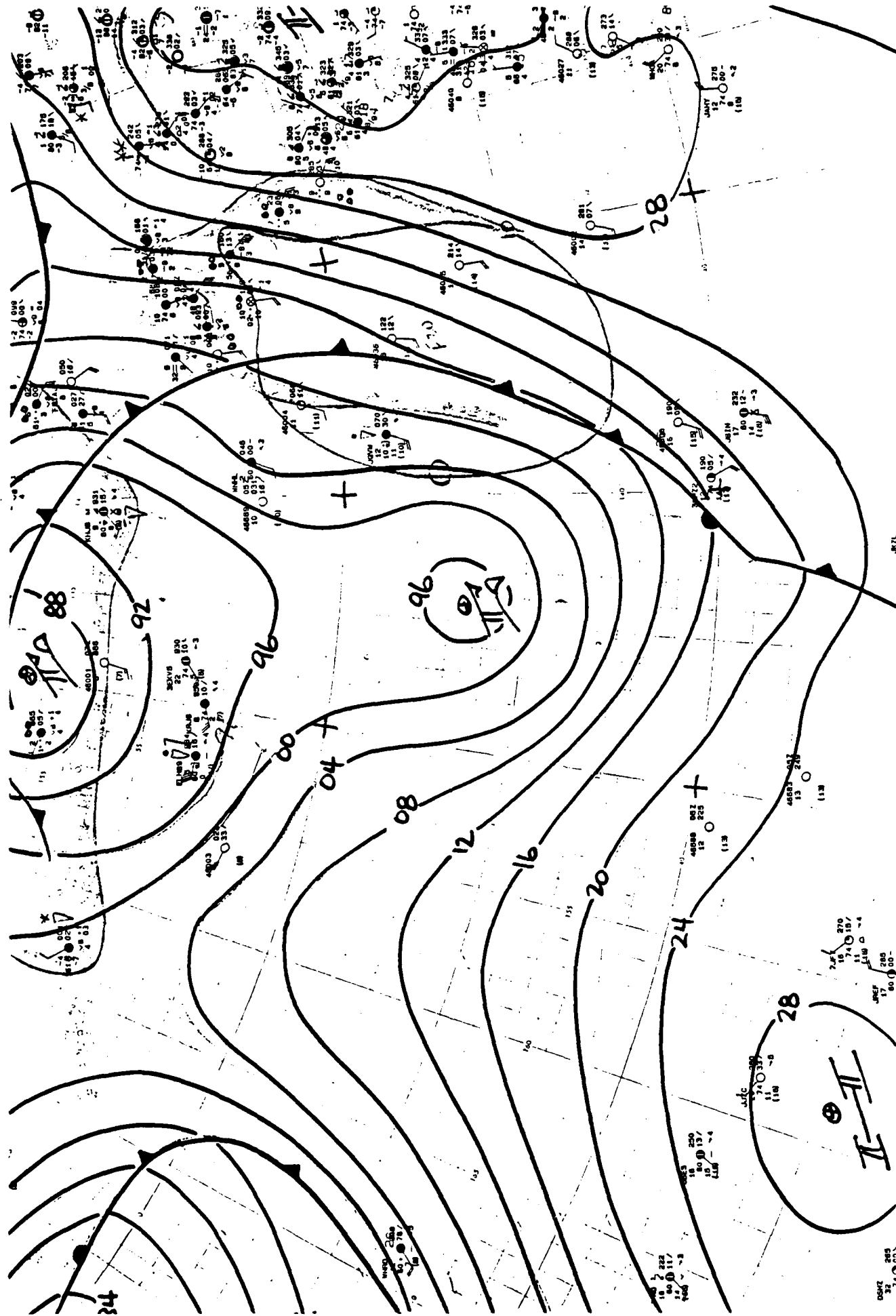
A73

A74

11-25-87

1800 Z





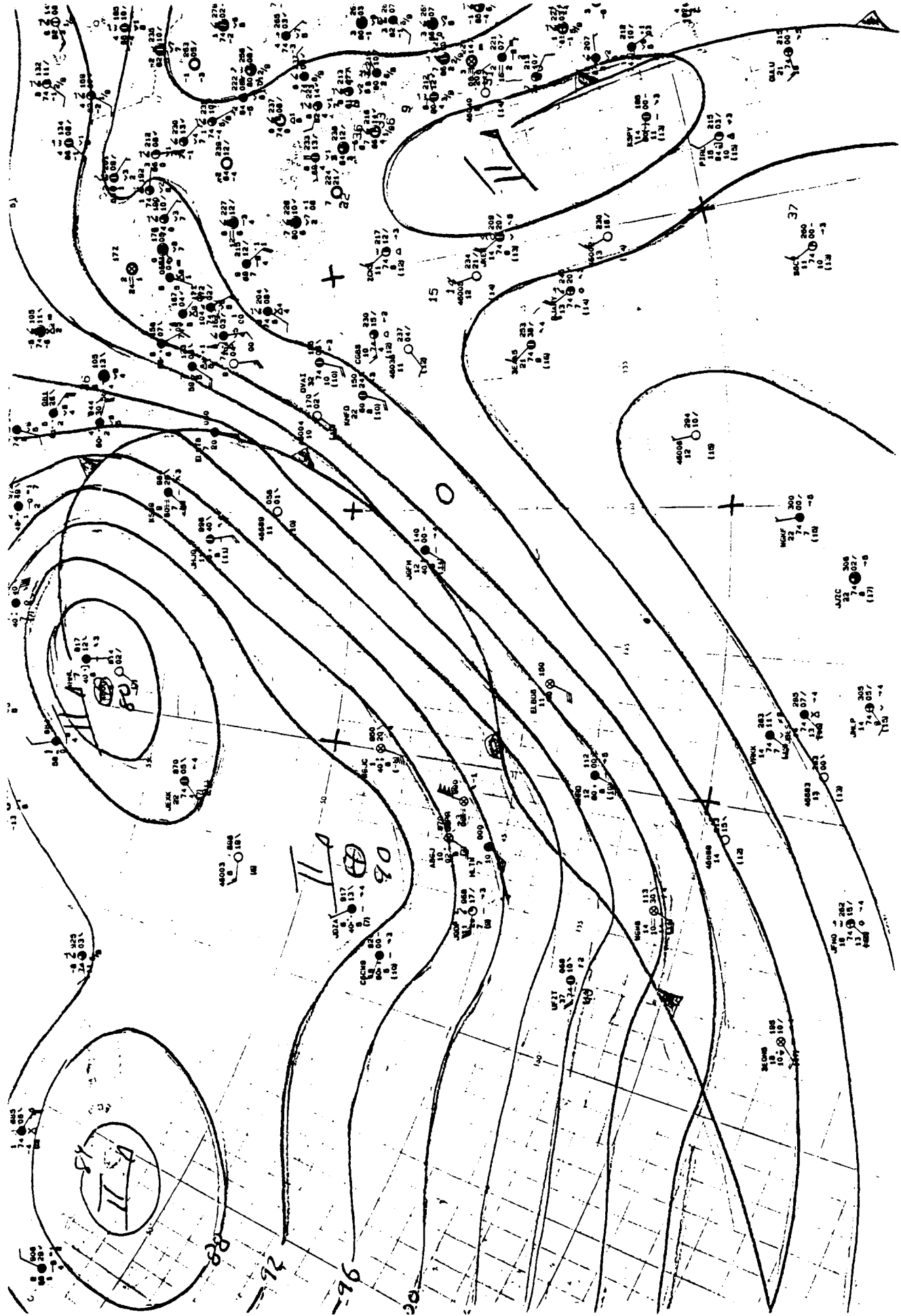
0600 Z

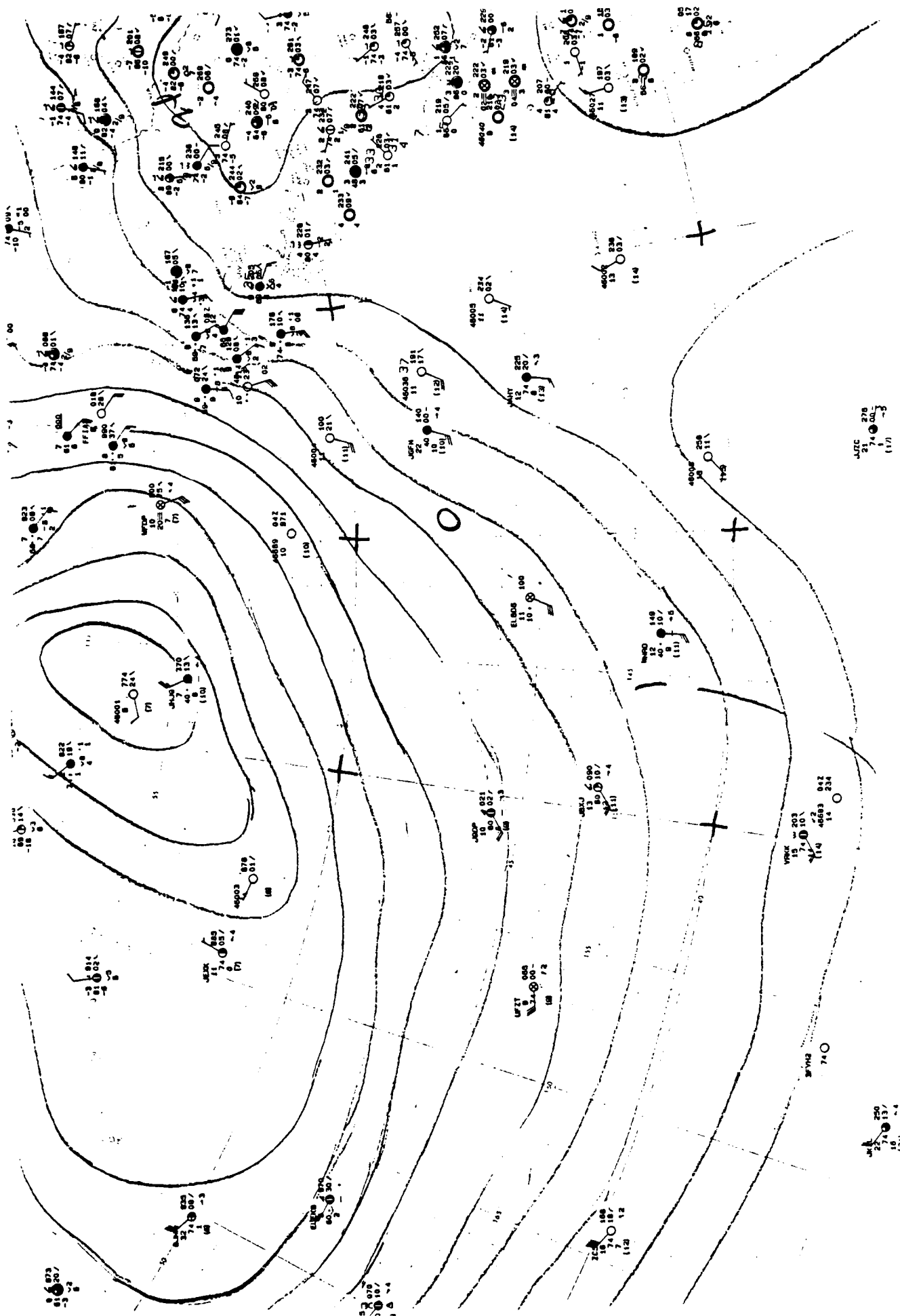
11-26-87

A75

JRTL

0607 283
31 0000-





A79

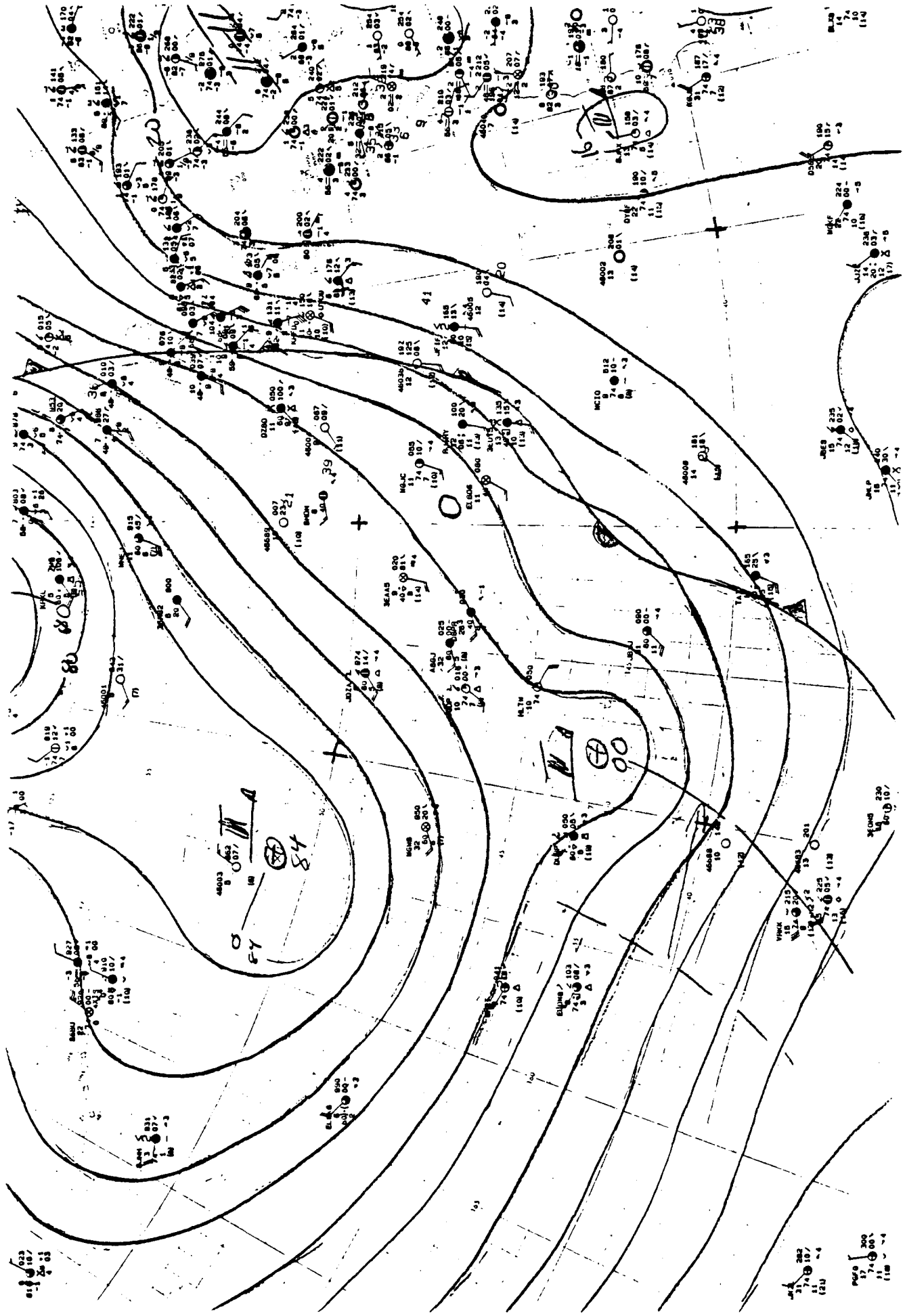
11-28-87

0600 Z

A80

11-28-87

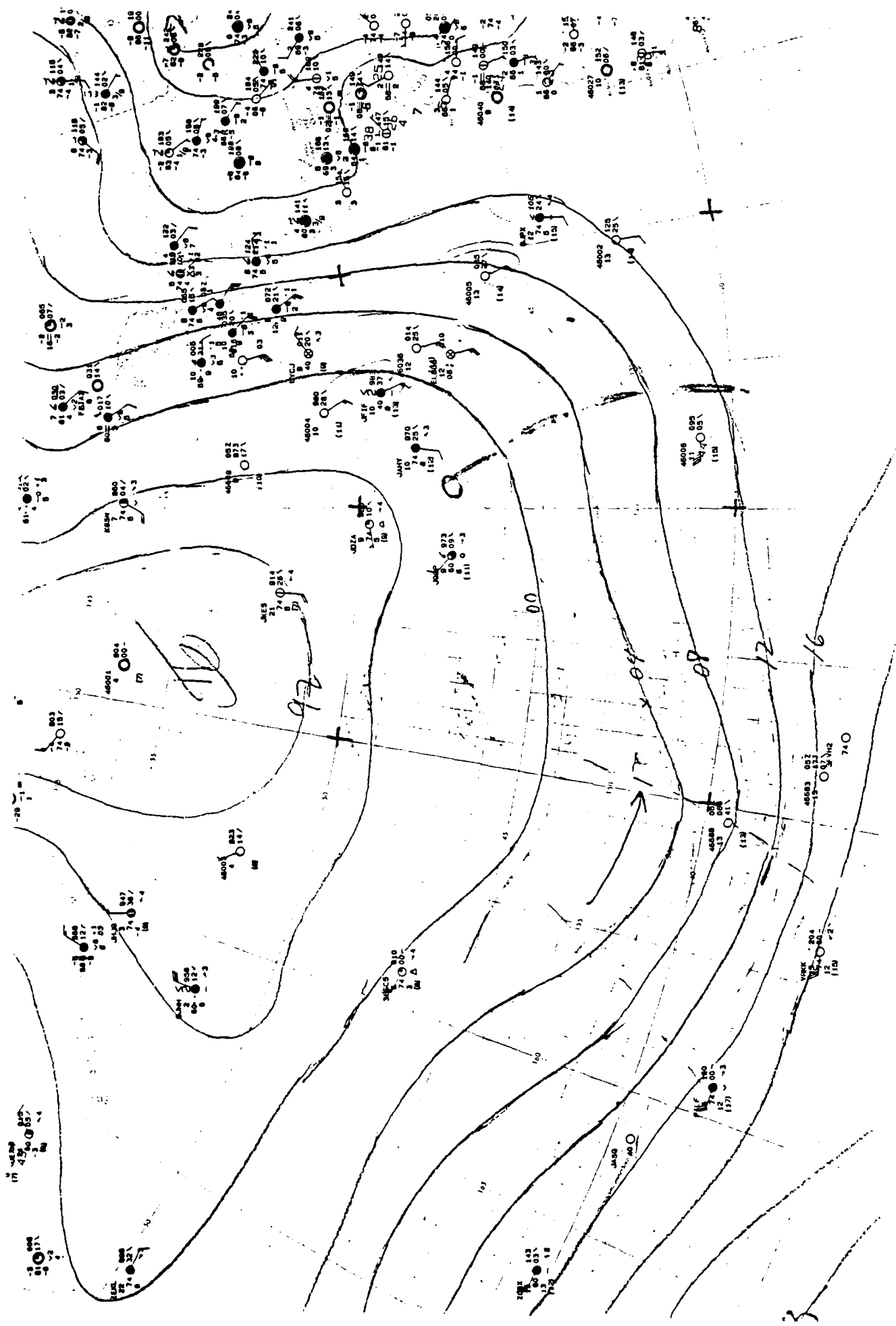
1800 Z



023
107
110

282
107
110

300
107
110



A81

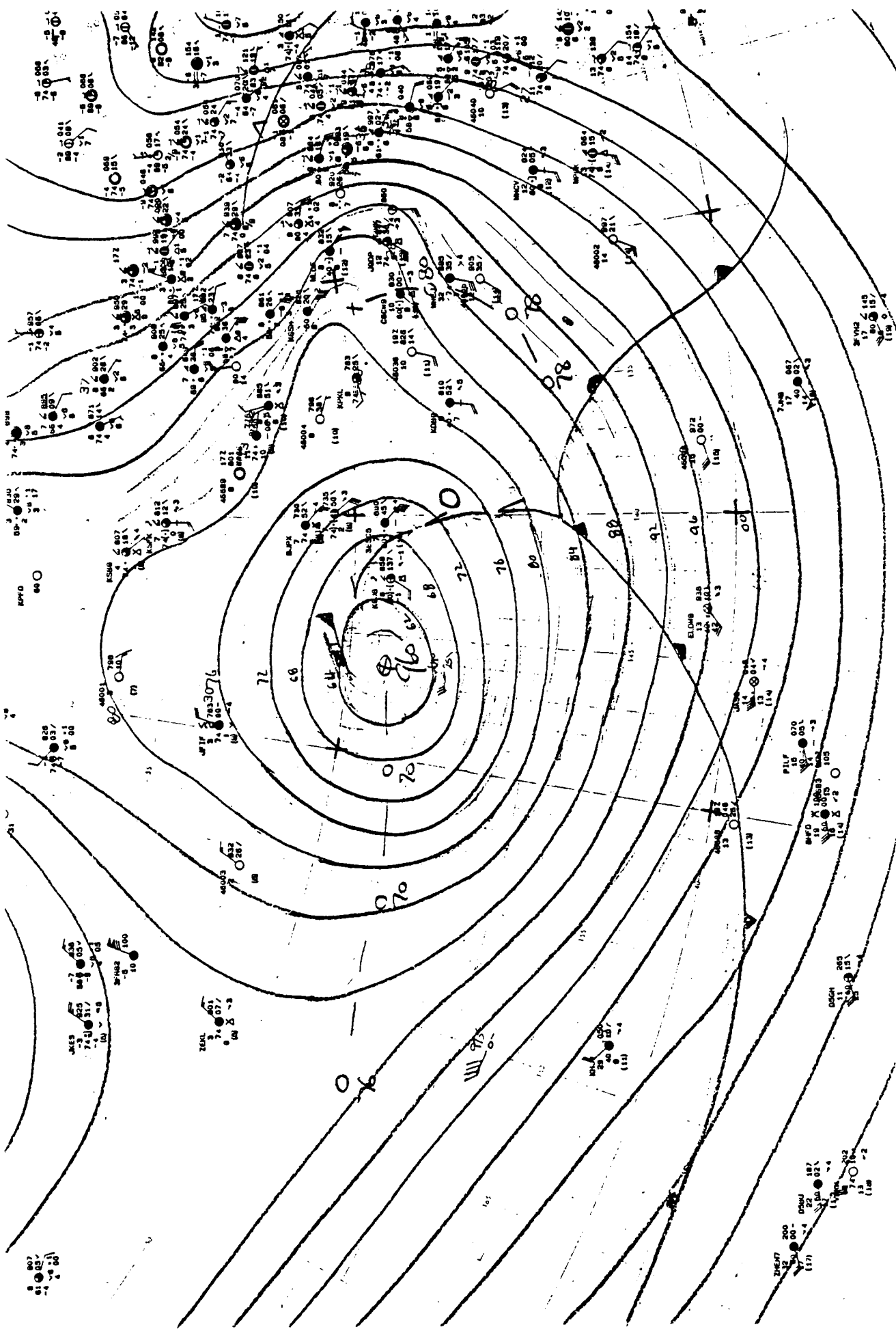
11-29-87

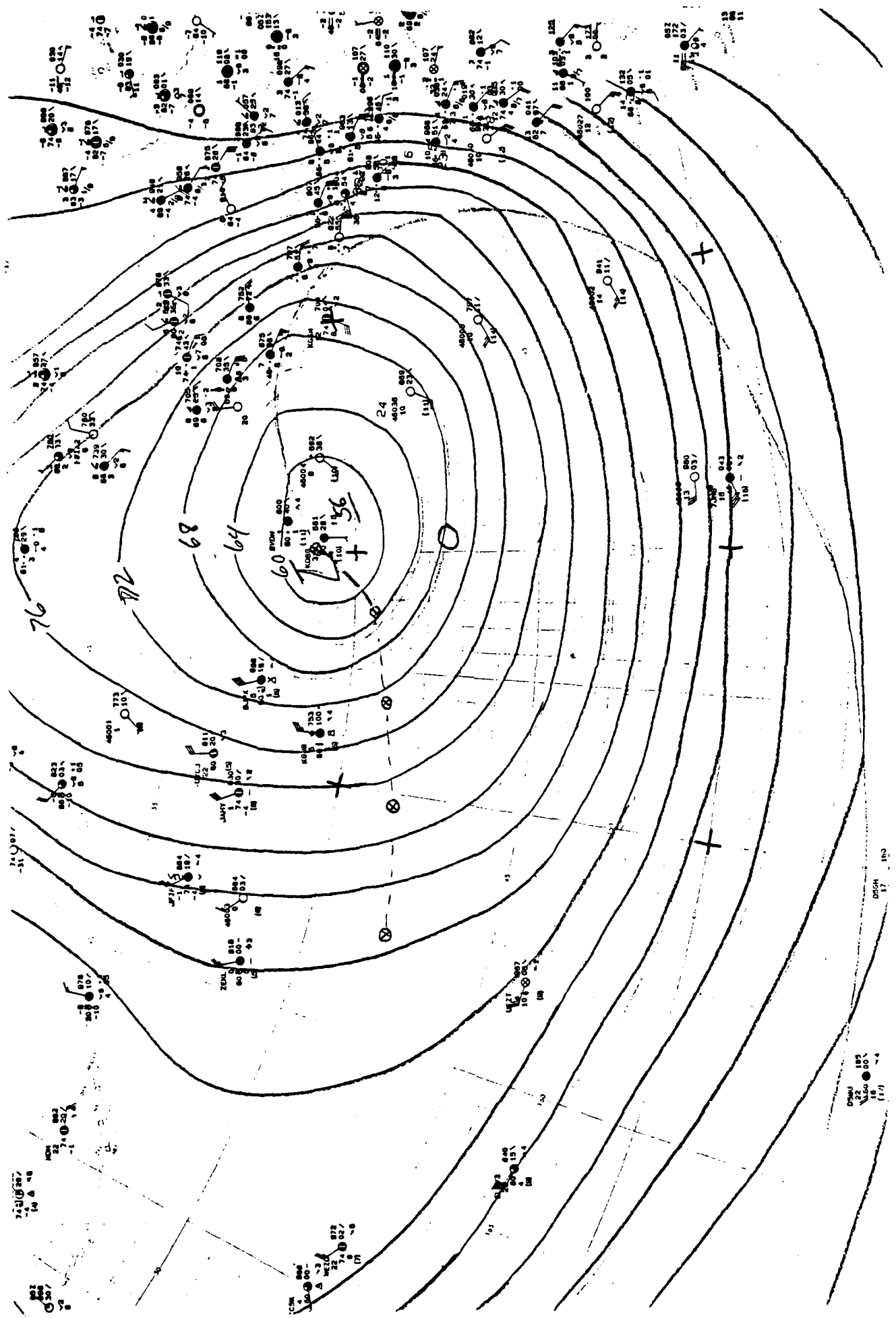
0600 Z

A84

11-30-87

1800 Z





DRAWN 185
 22 JUN 60
 (1/1)

DEGN 17
 180

A85

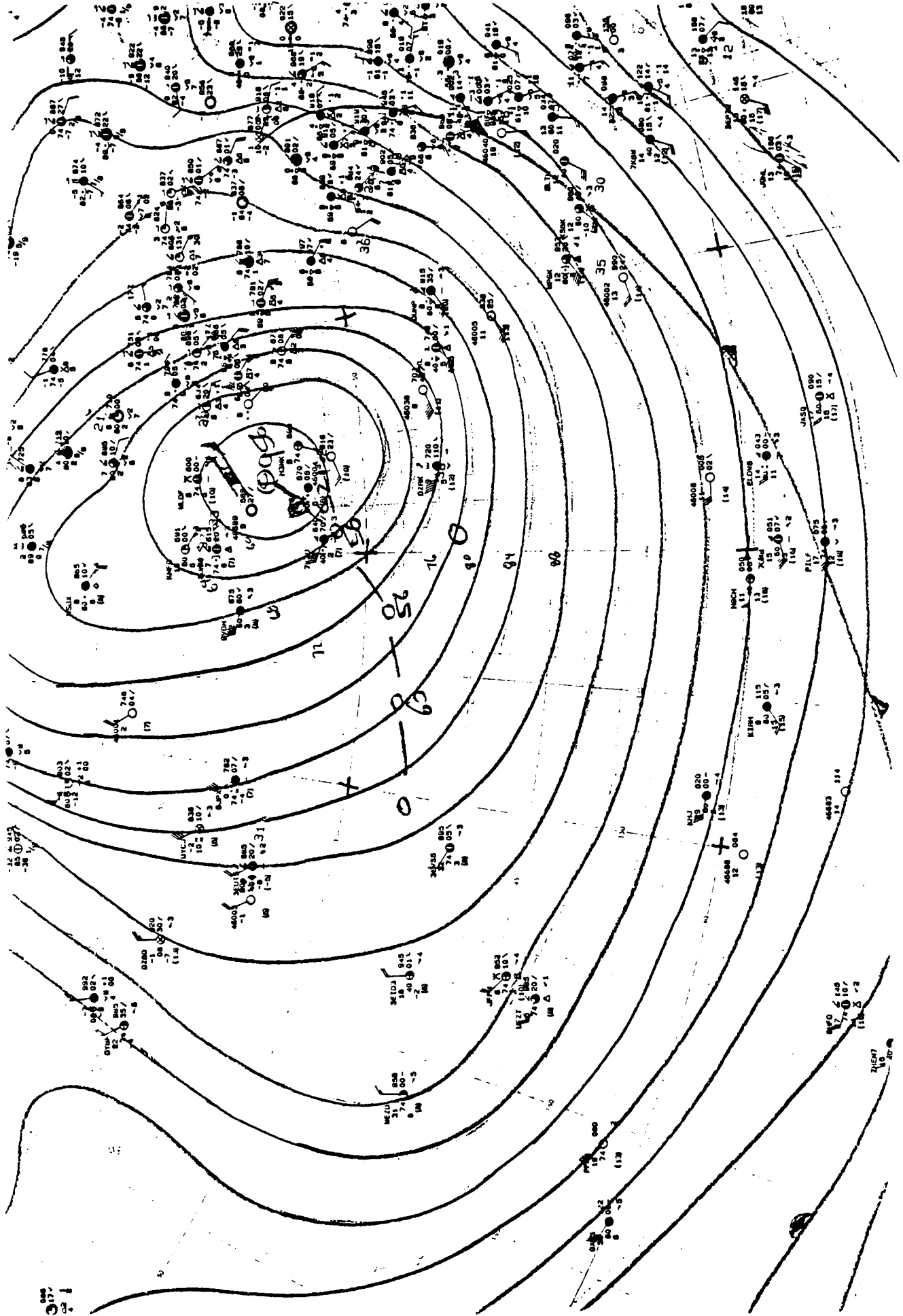
12-01-87

0600 Z

1800 Z

12-01-87

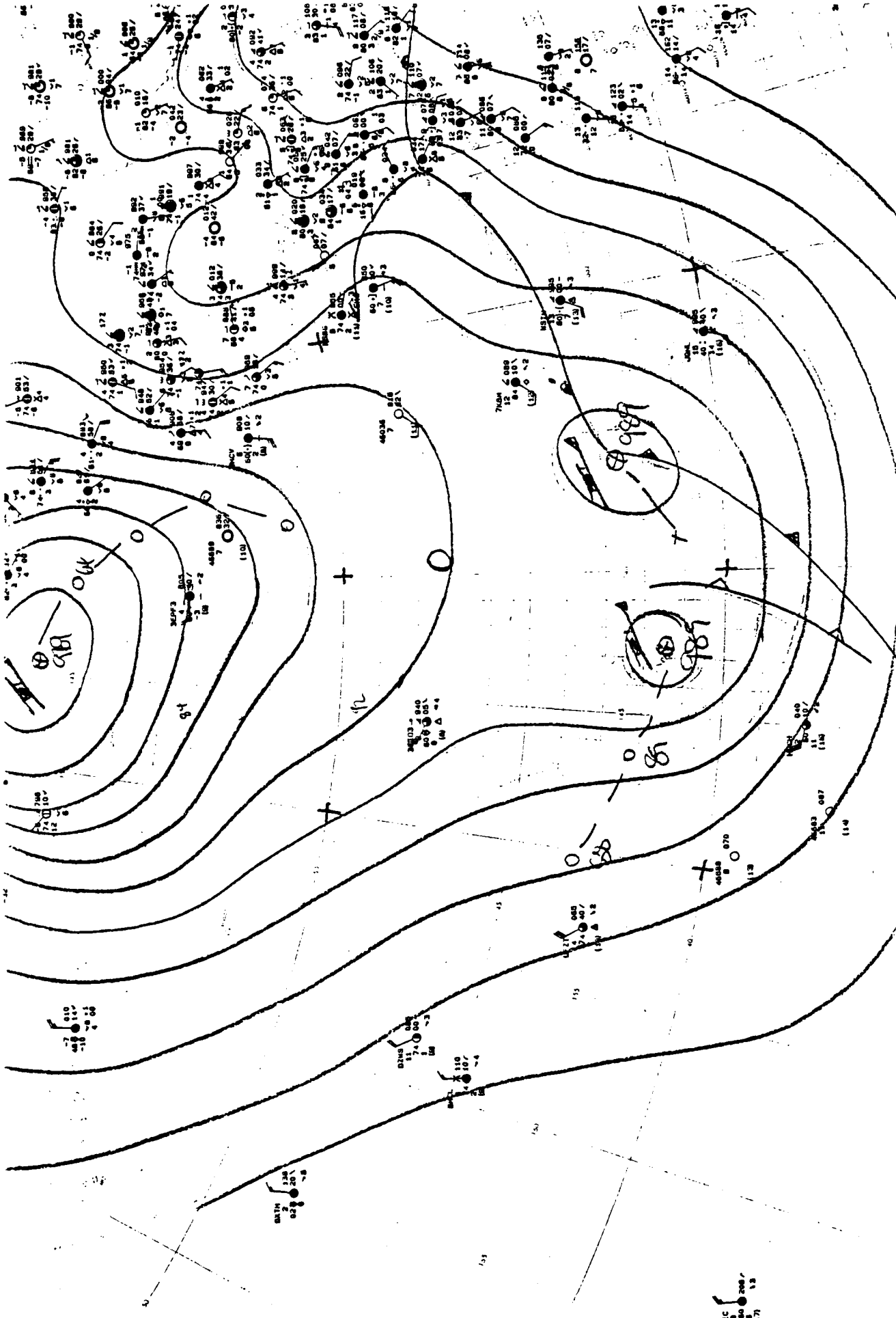
A86



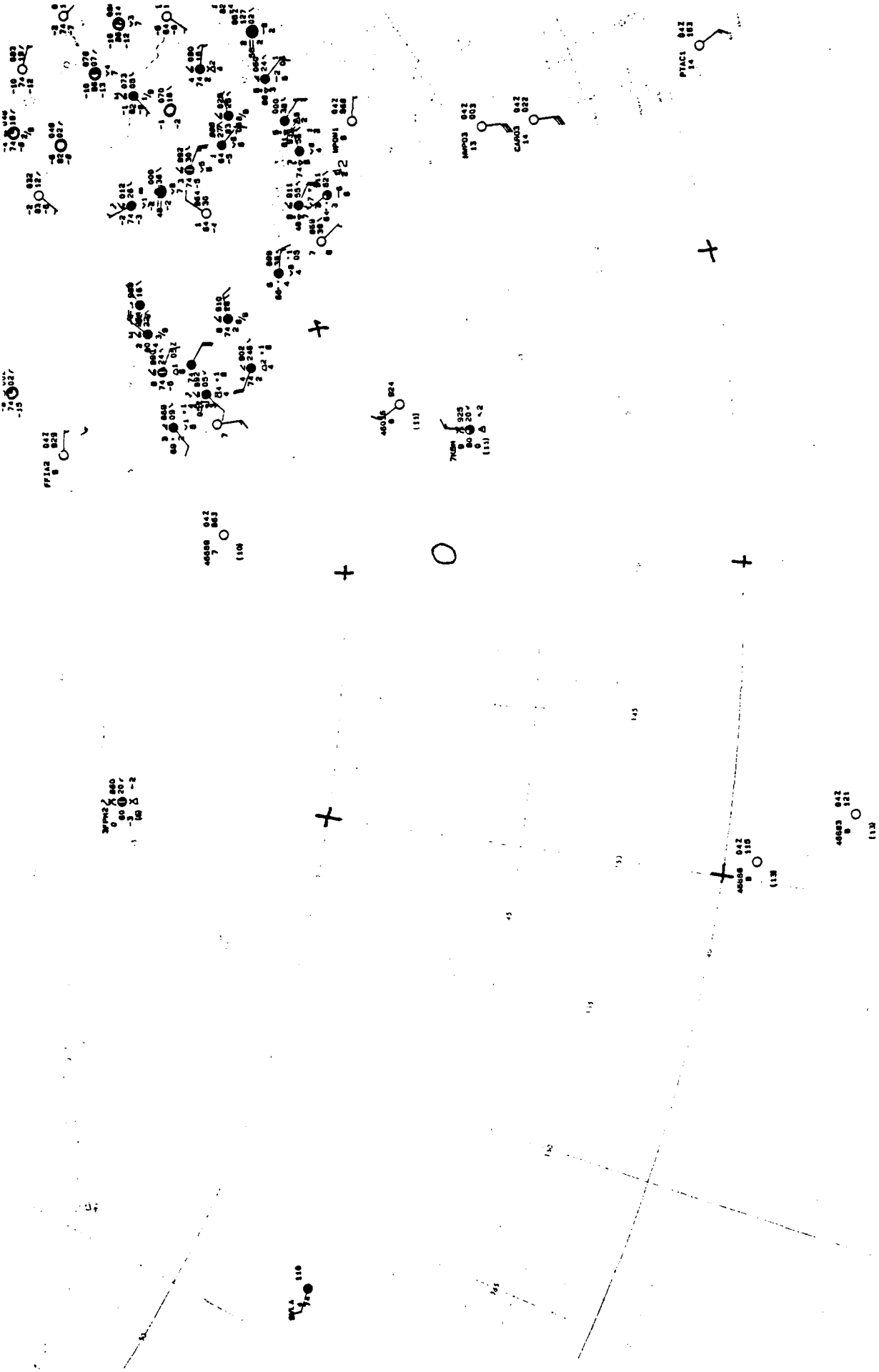
A88

12-02-87

1800 Z



MC
171
172
173



0600 Z

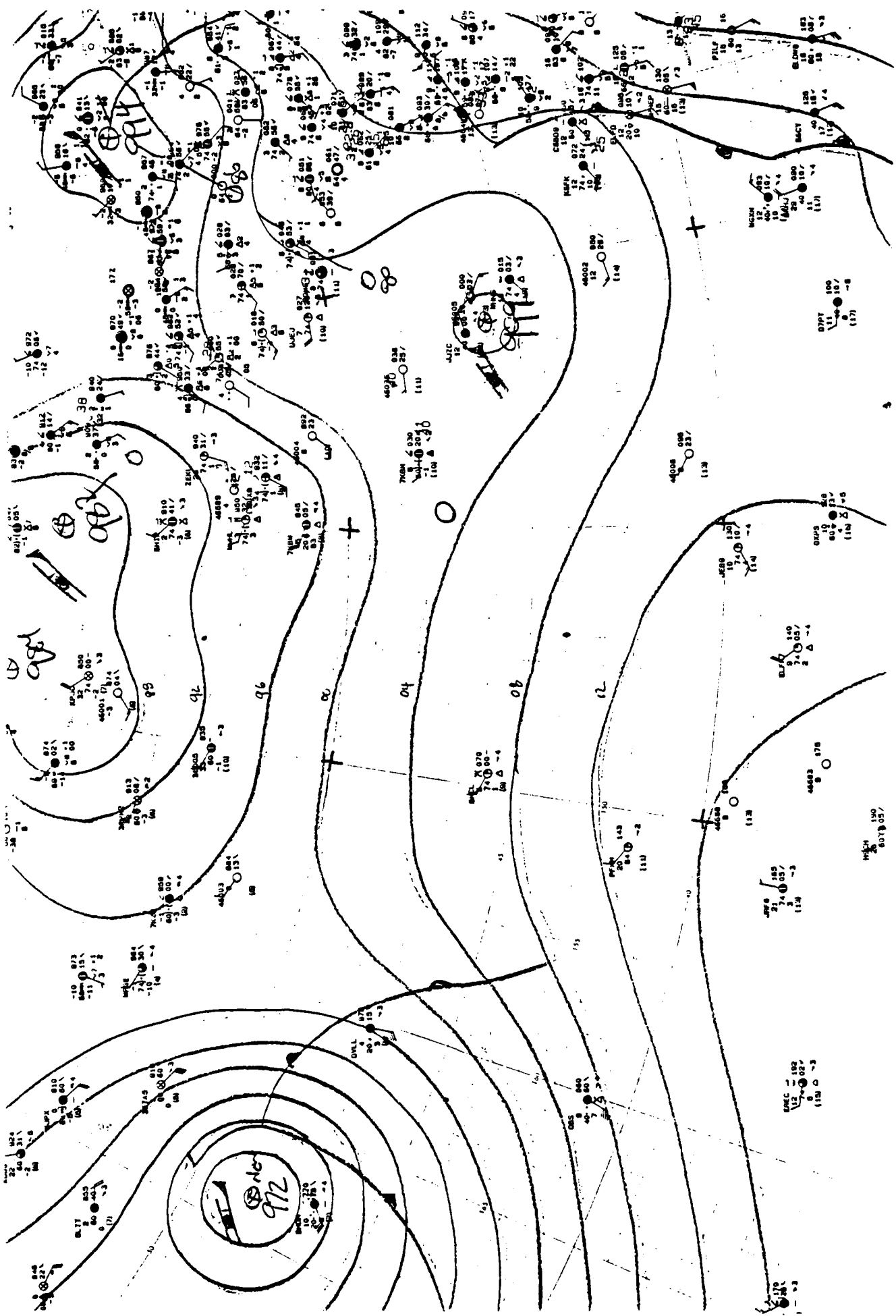
12-03-87

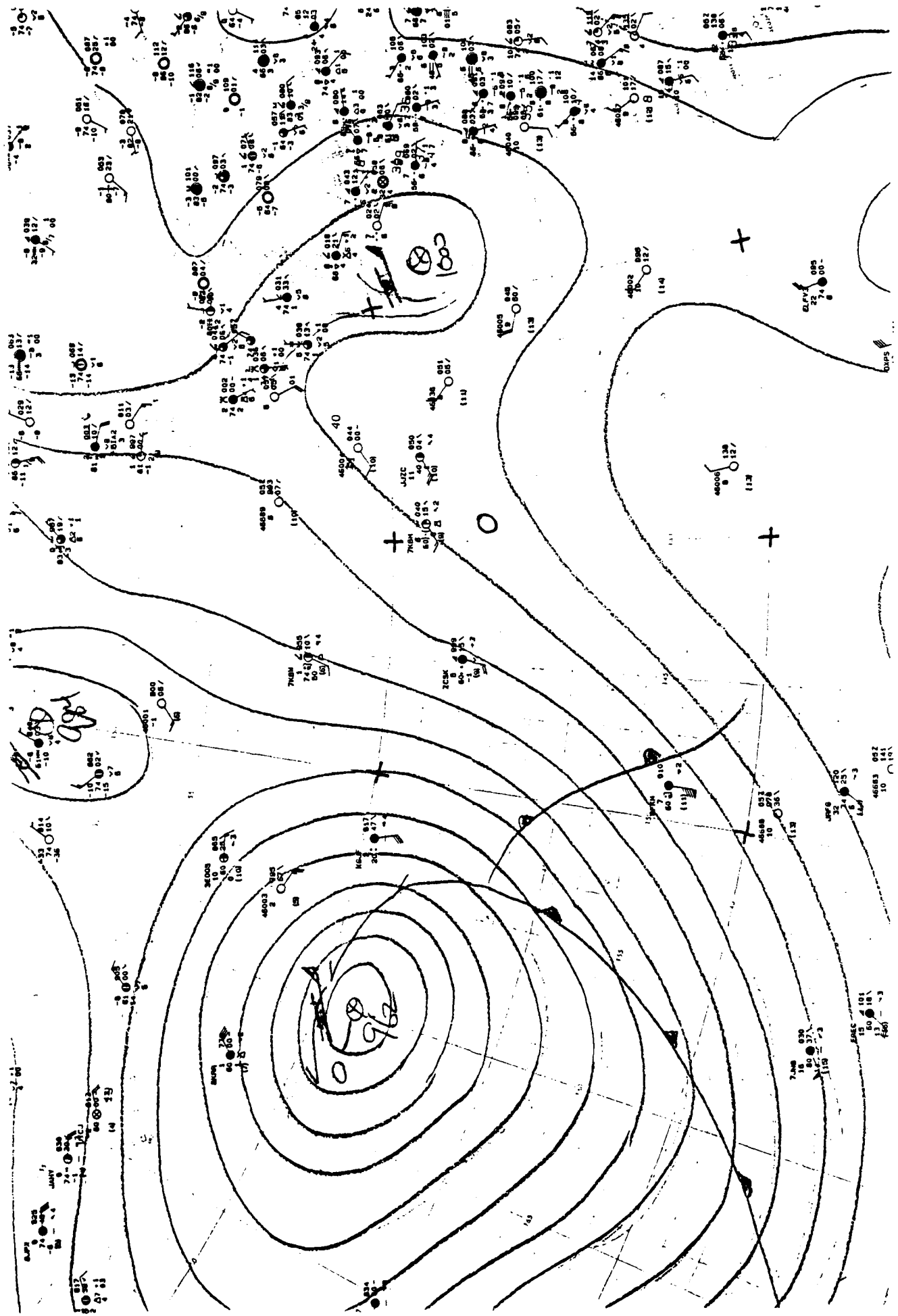
A89

A90

12-03-87

1800 Z





A91

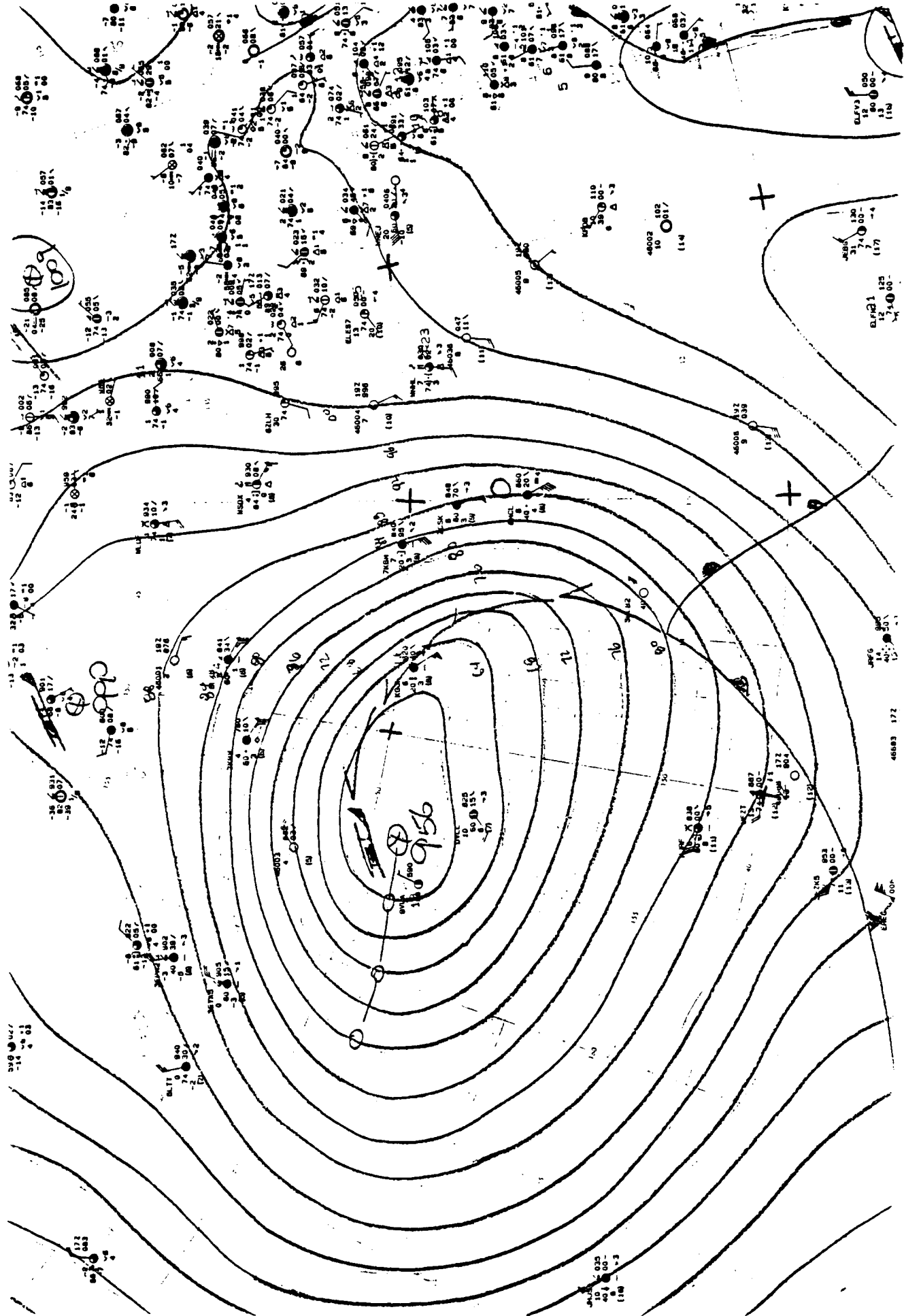
12-04-87

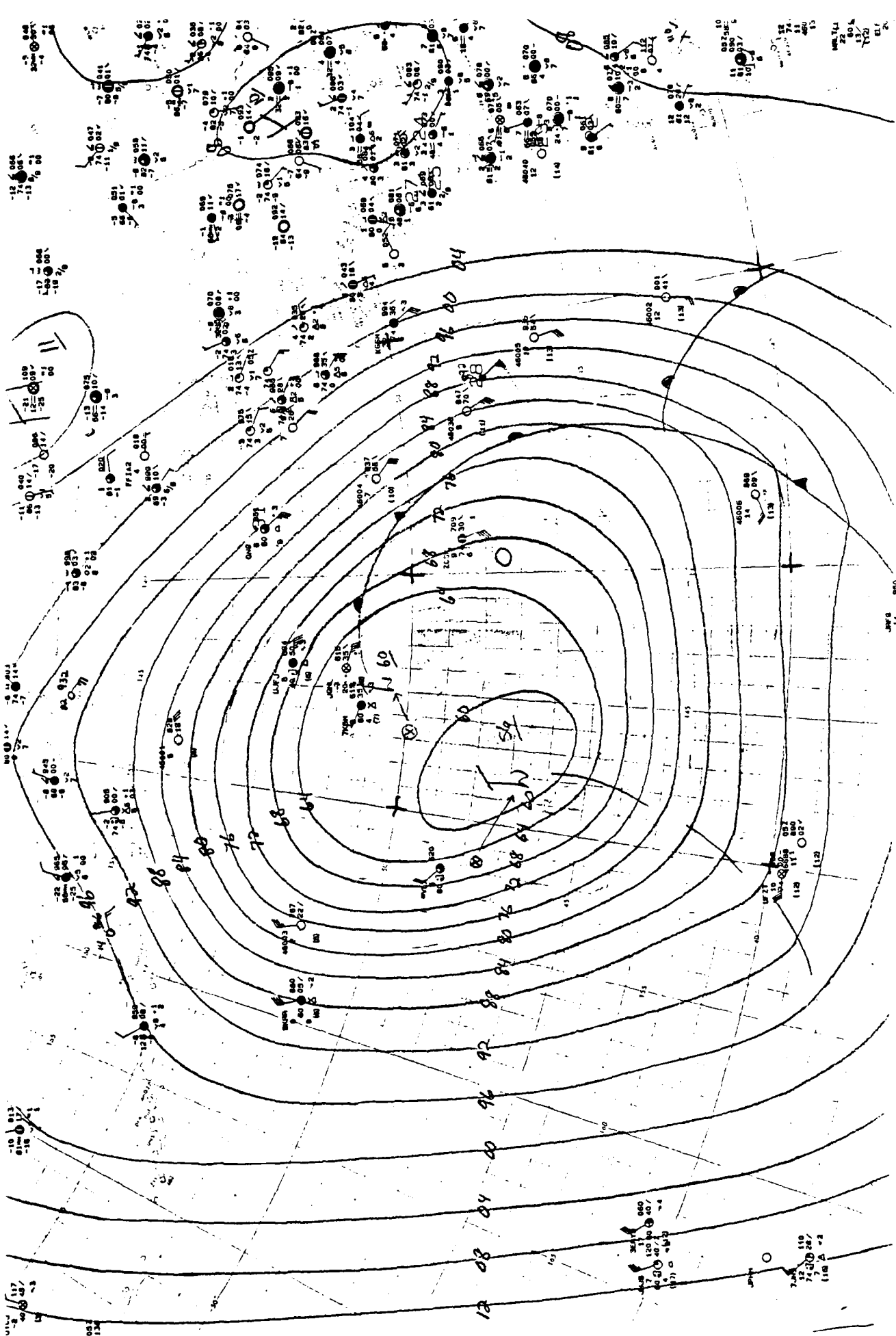
0600 Z

A92

12-04-87

1800 Z

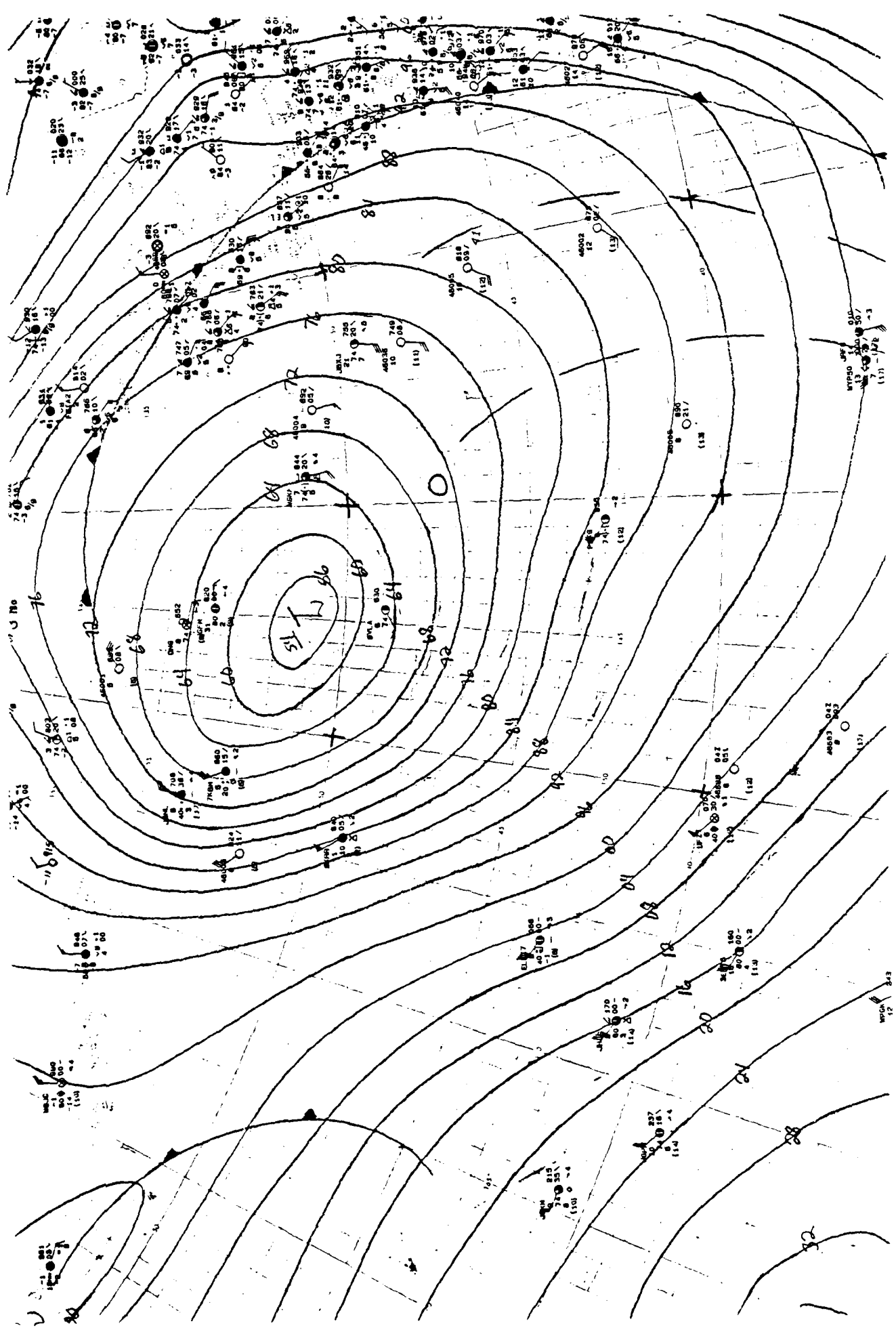




0600 Z

12-05-87

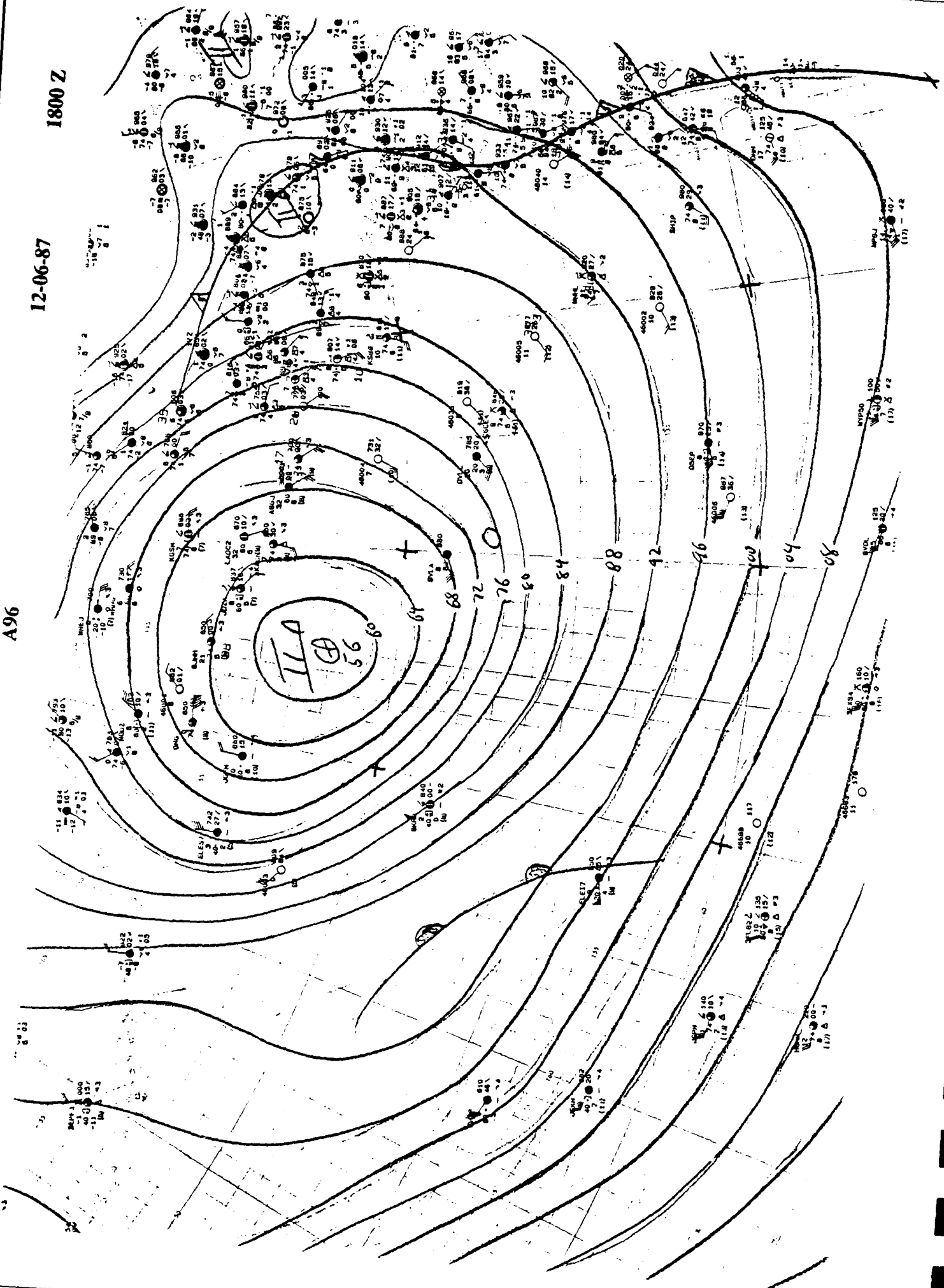
A93

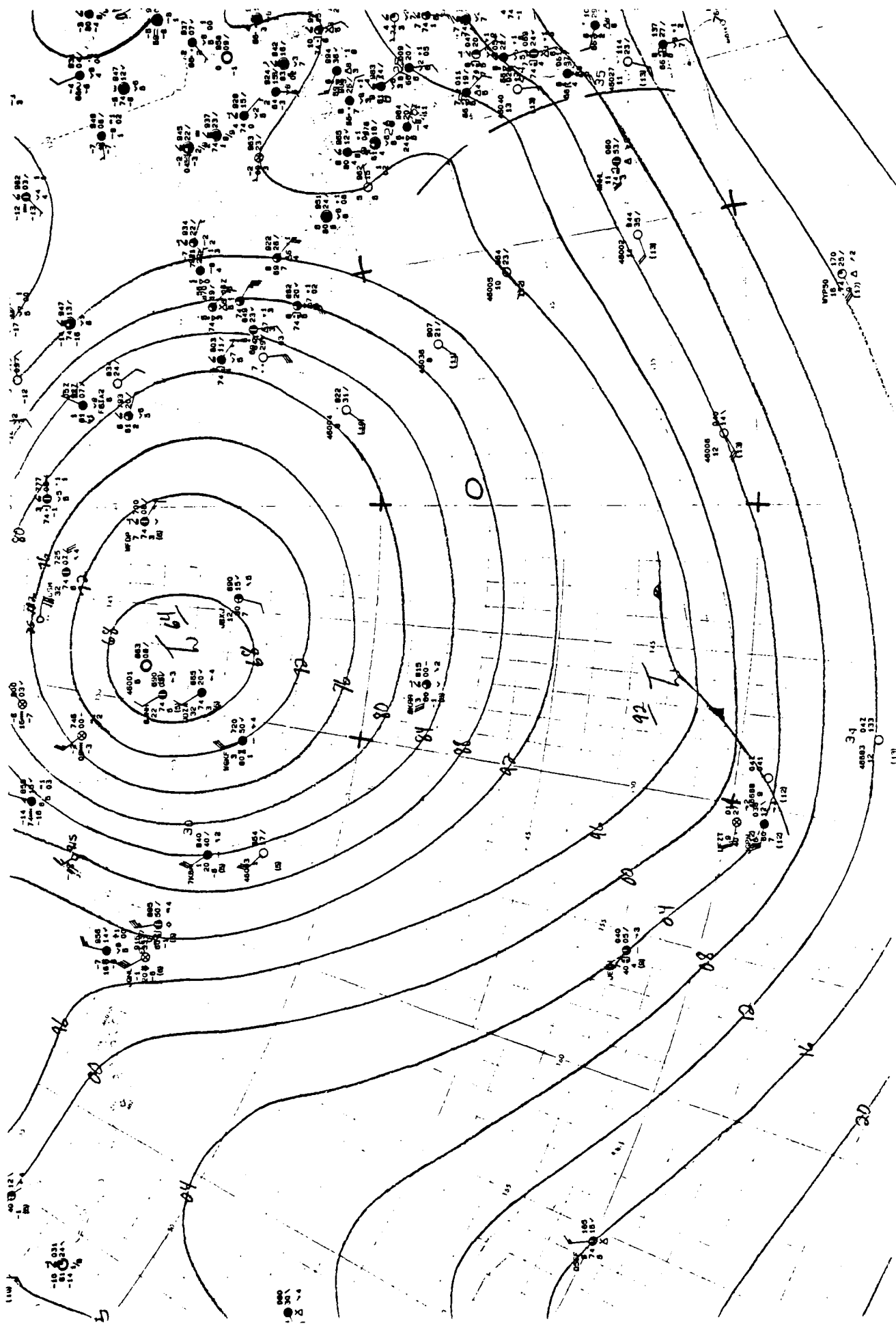


A96

12-06-87

1800 Z





0600 Z

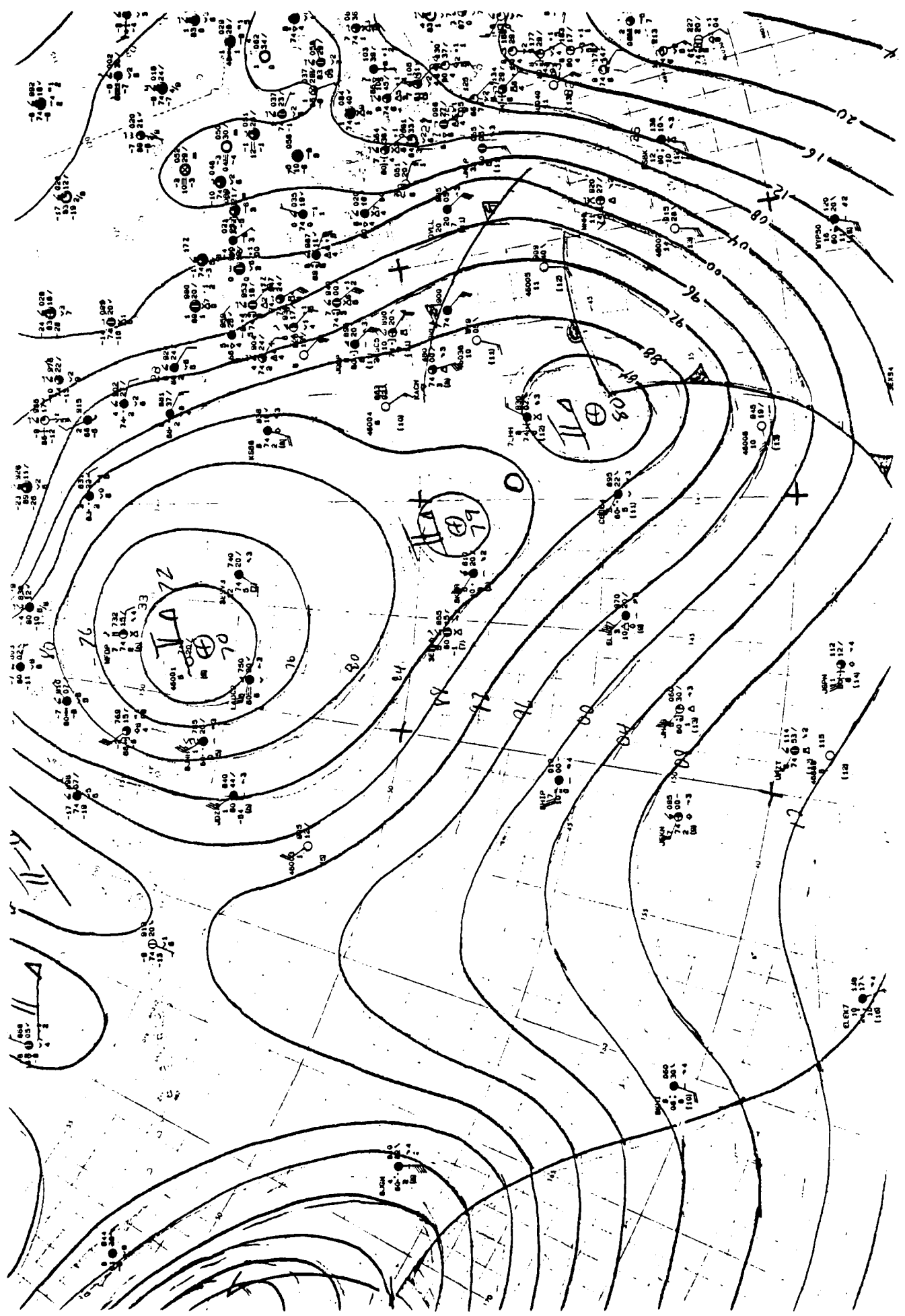
12-07-87

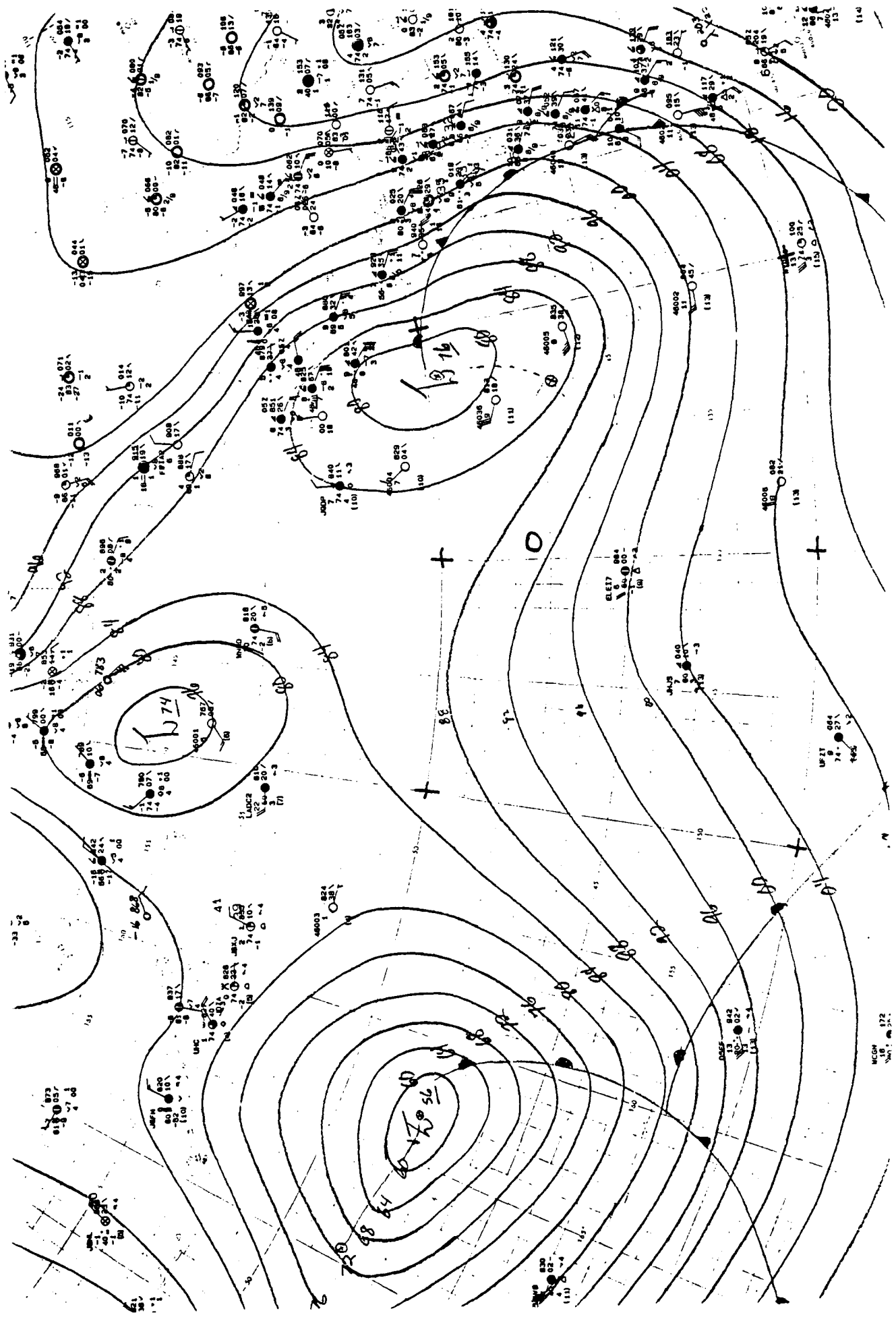
A97

1800 Z

12-07-87

A98



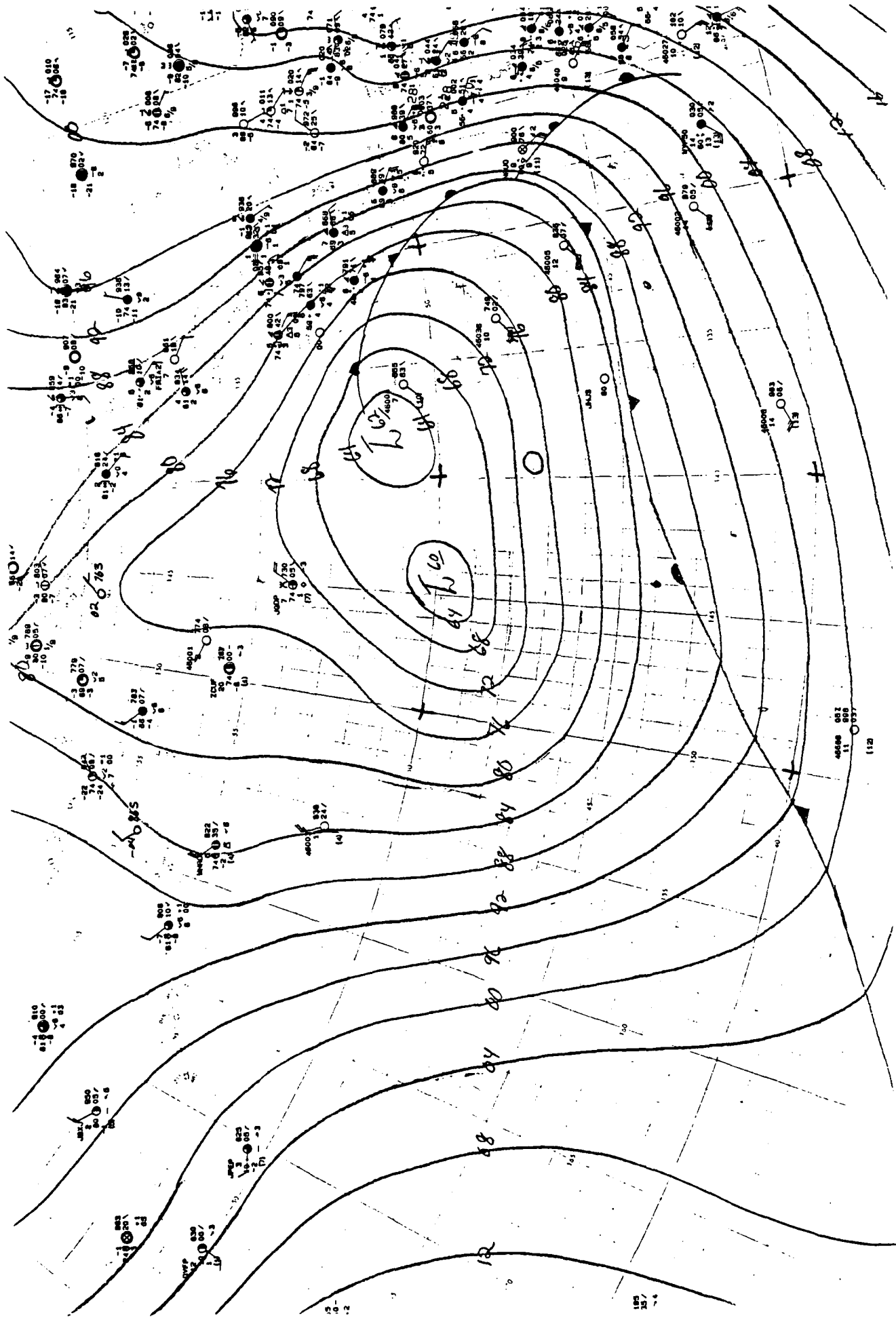


0600 Z

12-08-87

A99

MOON 172
18 18 31.5



0600 Z

12-09-87

A101

APPENDIX B

Ocean Storms Surface Meteorology Data Tape

The data tape is nine track, unlabeled, 6250 BPI, and ASCII coded, with 80 characters per record and 4800 characters per block. The 18 files on the tape are

1. Ocean Storms marine observations, 1987 (60065 records)
2. Ocean Storms marine observations, 1988 (34430 records)

Interpolated values for selected locations

3. From observations, Ocean Storms moored array, nine stations, 20 August 1987 to 30 April 1988 (JD 232.0 to 486.75, 27540 records)
4. From NMC, Ocean Storms moored array, nine stations, 20 August 1987 to 31 May 1988 (JD 232.0 to 517.5, 14931 records)
5. From observations, thermistor buoys, 1 October to 31 December 1987 (JD 274.25 to 365.75, 5205 records)
6. From NMC, thermistor buoys, 1 October to 31 December 1987 (JD 274.25 to 365.75, 2550 records)
7. From observations, Lagrangian drifters, 1 October 1987 to 30 April 1988 (JD 274.25 to 486.75, 103140 records)
8. From NMC, Lagrangian drifters, 1 October 1987 to 31 May 1988 (JD 274.5 to 517.5, 57177 records)

Metlib fields

9.	Sea level pressure, mb	type code 8,	4580 records
10.	Air temperature, °C	16	"
11.	Air-sea temperature difference, °C	30	"
12.	Dew point depression, °C	18	"
13.	Wind speed, U component, cm/s	486	"
14.	Wind speed, V, cm/s	496	"
15.	Wind stress, U, dyne/cm ²	506	"

16.	Wind stress, V, dyne/cm ²	516	"
17.	Sensible heat flux, mW/cm ²	536	"
18.	Latent heat flux, mW/cm ²	546	"

The format for each type of file is outlined below.

Observations

The variables included and the format used are listed in Table B-1, and a small sample of the file is shown in Table B-2.

Interpolated values

The variables included in the data files are summarized in Table B-3, and a small sample of the files is shown in Table B-4. The time is in days from the start of 1987. The wind speed is interpolated from the reported wind speeds, while the direction is derived from interpolated wind components. The air pressure was interpolated to nine separate locations on a nine point grid with 1 km spacing in order to allow the calculation of the geostrophic wind and the curl and the divergence of values derived from the geostrophic wind. The grid is parallel to 140°W and is a polar stereographic projection true at 60°N. The difference between the center point and each grid point is in the array; P(5) is the center point and is always equal to zero; the central pressure is recorded separately as PRES. The geostrophic wind components are

$$G_u = -G_{\text{cnst}} * (P(2) - P(8)) / 2$$

$$G_v = G_{\text{cnst}} * (P(6) - P(4)) / 2$$

$$G_{\text{cnst}} = 539.2 * (1 + \sin 60^\circ) / (1 + \sin \theta) / \sin \theta$$

where θ is the latitude. The expression for finding the geostrophic wind directions is

$$\text{DIR} = 50 - \text{long.} - \tan^{-1} (G_v / G_u)$$

The data in each interpolated file are in chronological order—taken every 6 hours for those based on the observations and every 12 hours for those based on the NMC grid point data. All the buoys are grouped together in random order. There are scattered missing times in the NMC data, and there are no air-sea temperature differences available after 12 March 1988.

Table B-1. Variables and format of the marine observations data set.

Variable	Format	Notes
Station id	A7	ships call sign or buoy number
Time: month, day hour, minute	4I2	GMT
Latitude, ° N	F6.2	decimal degrees
Longitude, ° W	F6.2	"
Pressure, mb	F6.1	"
Wind direction, ° true	I4	"
Wind speed, m/s	F5.1	"
Wind indicator	I1	1 = measured, 2 = estimated
Air temperature, °C	F5.1	"
Water temperature, °C	F5.1	"
Wave period, sec	I3	"
Wave height, m	F4.1	"
Dev pt temperature, °C	F5.1	"
Visibility, VV	A3	WMO code
Significant weather, WW	A2	"
Cloud cover, N	A1	"
Cloud height, h	A1	"
Cloud group, N _h C _L C _M C _H	A4	"
Source code	A1	blank = Prime, A = TD1129

The format is

(A7, 4I2, 2F6.2, F6.1, I4, F5.1, I1, 2F5.1, I3, F4.1, F5.1, A3, A2, 2A1, A4, A1)

Missing values are coded as -99.0

Table B-2. Sample of marine observations file.

4XLR	820	0	0	40.20134.701025.0	360	10.32	17.0	17.0	-99.0	6	3.0	14.0	97022	818600A
D5EE	820	0	0	40.60129.601020.5	10	14.41	16.0	17.0		4	3.0	15.5	97402	8488--A
46022	820	0	0	40.80124.501018.1	20	3.11	13.5	12.5		8	1.5	-99.0		A
MARK	820	0	0	40.80126.401019.0	30	7.21	14.4	13.3		4	1.0	13.3	98	8584--A
A80G	820	0	0	40.80136.601027.0	20	6.71	23.0	12.5		4	1.5	20.0	97022	767820A
46006	820	0	0	40.80137.601027.1	20	6.21	15.5	16.6		8	1.5	-99.0		A
7KBW	820	0	0	40.90139.201027.0	360	6.21	20.5	17.0		4	.5	14.0	98	82849-A
WGKN	820	0	0	41.20135.901025.8	360	9.31	18.3	-99.0		4	.5	14.3	98022	8485--A
JADY	820	0	0	41.60140.501028.2	100	5.21	16.0	17.4		4	.5	13.5	98	534461A
46027	820	0	0	41.80124.401019.4	340	3.11	11.8	11.7		8	1.0	-99.0		A
WYR751	820	0	0	42.30152.201026.0	110	7.72	20.0	18.5		4	1.5	17.0	98	747400A
46002	820	0	0	42.50130.401021.5	350	8.21	14.9	16.3		6	1.5	-99.0		A
3EF55	820	0	0	42.50151.301027.0	160	4.61	22.5	22.0		4	1.5	20.3	98021	54434-A
WTEA	820	0	0	42.70126.701019.5	30	5.21	15.2	14.3		4	.5	14.7	97502	8374--A

Table B-3. Variables in the interpolated data files.

- Station id
- Julian date from start of 1987
- Latitude (degrees north)
- Longitude (degrees west)
- Wind speed, m/s, interpolated from the reported wind speeds with no corrections for observation heights.
- Wind direction, degrees clockwise from north, from direction, based on interpolated u and v components
- Air temperature, °C for observations, °K for NMC
- Air - sea temperature difference, °C, interpolated as such
- Dew point depression, °C
- Pressure, mb (PRES))
- Pressure array, 9 values of P-PRES on a 1 kilometer grid:
 - P(1) P(2) P(3)
 - P(4) P(5) P(6)
 - P(7) P(8) P(9) (P(5) = 0)
- Estimate of the interpolation error, wind speed, m/s
 - " air temperature, °C
 - " air-sea temperature difference °C
 - " dew point depression, °C
 - " pressure
- Weighted distance to the stations used for interpolation, kilometers
- Total number of stations available
- Number of pressure points dropped in error checking

The format is
(A7,F7.2,2F8.3,6F7.2,/,9F8.6,6F7.2,2I5)

Table B-4. Sample of the interpolated data files.

```

46061 274.25 48.603 140.115 10.55 140.07 13.50 1.47 1.14 995.70
-.018732 .006817 .032393-.025534 .000000 .025562-.032339-.006819 .018729
.97 .65 .50 .52 1.67 389.48 59 0
46061 274.50 48.600 140.084 8.62 179.56 12.61 -.36 .50 996.37
-.034237-.010652 .012969-.023584 .000000 .023619-.012900 .010683 .034302
.77 .56 .42 .46 1.04 295.51 48 0
46063 274.50 48.580 139.285 8.97 177.08 12.90 -.27 .51 998.55
-.027854-.006220 .015433-.021618 .000000 .021636-.015389 .006212 .027832
.72 .55 .42 .46 .96 231.18 48 0
46063 274.75 48.597 139.297 8.41 164.38 13.38 1.11 .92 996.27
-.022610-.002630 .017376-.019970 .000000 .019995-.017321 .002638 .022623
.70 .50 .41 .41 .89 266.07 92 0
46061 274.75 48.603 140.100 7.90 164.65 12.93 .67 .90 995.76
-.020141-.002649 .014856-.017475 .000000 .017487-.014810 .002647 .020117
.75 .51 .38 .40 1.02 314.61 92 0
  
```

Metlib Fields

There are 51 days, or 102 fields, for each variable. Each field may be read with the Fortran statements

```
        DIMENSION A(19,25), IA(19,25)
        READ (1, 10) IYR, MNTH, IDAY, IHR, ITYPE, IM, JM
10     FORMAT ( 7I5 )
        READ (1, 20) ((IA(I,J),I=1,IM),J=1,JM)
20     FORMAT ( 10I7 )
        DO 100 I = 1, IM
            DO 100 J = 1, JM
                A(I,J) = IA(I,J) / 100.0
100    CONTINUE
```

where IYR, MNTH, IDAY, and IHR are the GMT date and time of the field, ITYPE is the variable type code, and IM and JM are the dimensions of the field (IM is always 19; JM is 19 or 25).

On 3 December at 0600 GMT no data were available at the Ocean Storms Forecast Office for map analysis; dummy fields are included for that time and they should be ignored.

The arrays start in the lower left corner of the grid and proceed from left to right across the bottom, then continue with the next line up, and finally end in the top right corner. The four corners of the large grid are located at

54.45°N 144.51°W, 54.14°N 131.03°W

44.31°N 143.43°W, 44.09°N 133.16°W.

The relation for determining the latitude and longitude of a grid point I,J is

$$GI = 7 - I$$

$$GJ = 101 - J$$

$$LAT = 90 - 2 * \tan^{-1} (\text{SQRT}(GI**2+GJ**2) / 237.777)$$

$$LONG = 140 + \tan^{-1} (GI/GJ)$$

The U and V components are relative to the grid; the relation for determining the speed and direction of the wind is

$$\text{SPD} = \text{SQRT}(U^{**2} + V^{**2})$$

$$\text{DIR} = 50 - \text{LONG} - \tan^{-1}(V/U)$$

where the DIR is the direction from which the wind is blowing. Note that the wind, stress, and heat flux are in cgs units.

Unclassified

SECURITY CLASSIFICATION OF THIS PAGE

REPORT DOCUMENTATION PAGE				Form Approved OMB No 0704-0188	
1a REPORT SECURITY CLASSIFICATION Unclassified		1b RESTRICTIVE MARKINGS ----			
2a SECURITY CLASSIFICATION AUTHORITY ----		3 DISTRIBUTION / AVAILABILITY OF REPORT ----			
2b DECLASSIFICATION / DOWNGRADING SCHEDULE ----					
4 PERFORMING ORGANIZATION REPORT NUMBER(S) APL-UW TR 8823		5 MONITORING ORGANIZATION REPORT NUMBER(S)			
6a NAME OF PERFORMING ORGANIZATION Applied Physics Laboratory University of Washington		6b OFFICE SYMBOL (if applicable)	7a NAME OF MONITORING ORGANIZATION		
6c ADDRESS (City, State, and ZIP Code) 1013 NE 40th Street Seattle, WA 98105-6698		7b ADDRESS (City, State, and ZIP Code)			
8a NAME OF FUNDING / SPONSORING ORGANIZATION Office of Naval Research, Dept. of the Navy		8b OFFICE SYMBOL (if applicable)	9 PROCUREMENT INSTRUMENT IDENTIFICATION NUMBER N00014-87-K-0004		
8c ADDRESS (City, State, and ZIP Code) 800 North Quincy Street Arlington, VA 22217-5000		10 SOURCE OF FUNDING NUMBERS			
		PROGRAM ELEMENT NO	PROJECT NO	TASK NO	WORK UNIT ACCESSION NO
11 TITLE (Include Security Classification) Surface Meteorology during Ocean Storms Field Program (U)					
12 PERSONAL AUTHOR(S) Ronald W. Lindsay					
13a TYPE OF REPORT Technical		13b TIME COVERED FROM Aug '87 TO Apr '88	14 DATE OF REPORT (Year, Month, Day) October 1988		15 PAGE COUNT 164
16 SUPPLEMENTARY NOTATION					
17 COSATI CODES			18 SUBJECT TERMS (Continue on reverse if necessary and identify by block number)		
FIELD	GROUP	SUB-GROUP			
04	02		meteorology; Ocean Storms		
19 ABSTRACT (Continue on reverse if necessary and identify by block number)					
<p>A summary of the meteorological conditions in the Gulf of Alaska during the Ocean Storms experiment is presented along with a data set of the surface meteorological observations by ships of opportunity and National Data Buoy Center buoys. An optimal interpolation procedure is described and used with the surface observations to interpolate air pressure, wind speed and direction, air temperature, air-sea temperature difference, and dew point depression. Separate interpolations are made using the National Meteorological Center 2.5 degree grids and digitized versions of hand analyses made during the experiment. Extensive comparisons are made between these three data sets and the observations at three NDBC buoys. These are used to assess the accuracy of the interpolated fields and to suggest optimal ways to use them to compute surface winds, temperatures, and fluxes. The hand analyzed synoptic charts of the surface meteorology are included. The air stress</p>					
20 DISTRIBUTION / AVAILABILITY OF ABSTRACT <input checked="" type="checkbox"/> UNCLASSIFIED/UNLIMITED <input type="checkbox"/> SAME AS RPT <input type="checkbox"/> DTIC USERS			21 ABSTRACT SECURITY CLASSIFICATION Unclassified		
22a NAME OF RESPONSIBLE INDIVIDUAL Eric A. D'Asaro		22b TELEPHONE (Include Area Code) (206) 545-2982		22c OFFICE SYMBOL	

Unclassified

SECURITY CLASSIFICATION OF THIS PAGE

19. Abstract (continued)

and sensible heat flux are presented for the position of the Ocean Storms moorings. A data tape containing all the observations, interpolations, and fields is described.